THE PROCEEDINGS OF
THE PHYSICAL SOCIETY

VOL. 50, PART 2 *March* 1, 1938 NO. 278

THE RATE OF VISCOUS FLOW OF METALS: PART 1, TIN

BY L. C. TYTE, B.SC., PH.D., F.INST.P.,
Ballistics Directorate, Research Department, Woolwich

Received 5 *October* 1937. *Read in title* 26 *November* 1937

ABSTRACT. A description is given of a new method of determining the dependence of the rate of viscous flow of metals on the deforming force and its variation with temperature. The measurements were made by means of an optical lever system, and the effect of changes in length produced by possible temperature fluctuations in the furnace were eliminated by the use of a second wire as a support for the lever.

It has been found that, for tin, for very small extensions the velocity of viscous flow v can be considered independent of time, but is connected with the stretching load P by an exponential relation for any given temperature and with the absolute temperature T by an exponential relation for any given load. Different relationships of the form

$$v = \delta e^{\beta PT - \alpha P + \gamma T},$$

where α, β, γ and δ are constants, have been obtained, from the {flow, load} curves, for the rates of flow of tin for glide in one and two directions respectively, and the relations are probably of the type

$$v = K\{e^{\beta (P+P_0)(T-T_0)} - 1\},$$

where K, β, P_0 and T_0 are constants. Evidence has been obtained in support of the view that the temperature of the allotropic modification from β to γ tin takes place at 203° C. and not at 161° C. The loads for transition from single to double glide and the breaking loads have been shown to be connected with the corresponding temperatures by a hyperbolic expression. Finally, the behaviour of the tin wire has been shown to be in general agreement with the results obtained from single crystals.

§ 1. INTRODUCTION

When a metal is strained beyond the elastic limit, deformations take place which are a function of time. Of late years this phenomenon has been the subject of extensive researches embracing both engineering-scale creep experiments and the study of glide in single crystals. This work has been fully discussed in recent books(1, 2, 3, 4).

The present research was undertaken, at the suggestion of Prof. Lees, to investigate the viscous part of the flow in metal wires, over a large range of loads, from air-temperatures to the melting-points of the materials. The experiments were commenced on tin, which shows all the plastic phenomena at ordinary temperatures and has the lowest melting-point of the metals easily obtainable in the form of wire.

§ 2. EXPERIMENTAL METHOD

As the metal wires were to be maintained at a uniform temperature over a wide temperature range the apparatus had to be compact, and wires 5 cm. in length were used. They were suspended in a vertical furnace, whose temperature was measured by thermocouples. Two wires were employed, one under constant load acted as standard, thereby eliminating errors due to thermal expansion and small fluctuations of temperature, while the other was subjected to various loads, the extension causing a tilting of an arm, supported by the wires, which was in turn measured by an optical lever system.

For the small loads used, the percentage elongation and diminution of cross section of the wires were too small to make it necessary to take the latter into account. With larger loads the decrease of cross section was not uniform, but local thinning occurred. The present experiments were therefore performed under constant load, provided by a scale pan and ordinary weights.

§ 3. DETAILS OF THE APPARATUS

The complete apparatus is shown in figure 1, details of it being as follows.

The furnace. This consisted of an alundum tube *A*, on which the heating coil was wound. It was surrounded by lagging *B*, and enclosed in a sheet iron jacket *C*, the ends being closed with slabs of sindanyo *D*, which were bolted together by steel stays *E*, the ends of which served as terminals for the furnace winding. The whole was supported on stout iron legs *F*. The top of the furnace, above the apparatus, was filled with a plug of asbestos wool and covered with a sindanyo cap. An iron tube (see below) fitted into the interior of the furnace and with the outer iron jacket *C*, acted as isothermal surfaces which helped to maintain uniformity of temperature along the axis of the furnace. The heating current was taken from the 240 volt mains, and measured by an ammeter, small fluctuations being adjusted by means of the resistances in series with the furnace.

Methods of supporting the wires. The ends of the wires were gripped in a pair of steel jaws *G*, which could be screwed together, one of them being bolted to a square bar of sindanyo *H*. This refractory material which is easy to work, has a fairly high tensile strength and a low thermal conductivity, which helped to diminish losses from the ends of the wires. These bars, supporting the wires, were themselves fastened, side by side, by passing them through holes in a disc of steel *J*, being kept in position by small steel pins *K* passed through the bars. This steel plate rested on three pegs projecting from the inner walls of an iron tube *L*, which fitted closely into the furnace. The bottom of the tube was bolted to a disc of sindanyo *M*, having a rectangular hole cut in its centre, through which the bars attached to the lower ends of the wires passed. The disc also acted as a screen to prevent direct radiation from the furnace to the mirror system. It was supported by three brass legs *N* with adjustable feet, so that the apparatus could be levelled to let the wires hang vertically. Thus the wires were supported in the middle portion of the furnace, symmetrically about its axis, and maintained at the same uniform temperature along their length. The lower ends of the wires were gripped in the same way and supported sindanyo bars *O*, which projected below the disc. Strips of steel were bolted to the bottom ends of the bars, and in turn carried steel tables *P* to support the mirror system. A hook was attached to the experimental wire and passes through a hole in the bench to support the scale pan and an applied load.

The mirror system. A mirror *Q* was attached at an angle of 60° to the bottom of a U-shaped piece *R*, balancing weights being placed on the other ends. On the under side of the U piece there were two pairs of hardened steel knife-edges, which rested on the tables *P*. The table on the experimental wire had a notch cut in its surface into which one pair of the knife-edges fitted, while the table on the standard wire was left smooth. The presence of the knife-edges on the mirror arm ensured the constancy of the distance between them and eliminated any effect which might have been caused by the wires moving nearer together or farther apart, while the notch on the table of the experimental wire kept the mirror in the same position and no transverse motion of the mirror was caused by the tilt.

The mirror reflected light from an illuminated scale into a telescope, where the scale deflection was observed.

Let e be the extension of the wire of length L, and b the distance between the knife-edges of the mirror arm, which is thus tilted through an angle ϕ given by

$$e/b = \tan\phi = \phi,$$

assuming the angle to be small. The beam of light from the scale reflected into the telescope moves through an angle 2ϕ, which, if δ is the scale deflection and λ the distance of the mirror from the scale, is given by

$$\delta/\lambda = \tan 2\phi = 2\phi$$
$$= 2e/b$$

and ,

$$e = \delta b/2\lambda.$$

Now $b = 0{\cdot}990$ cm. and $\lambda = 273{\cdot}9$ cm., therefore a scale deflection δ of 1 cm. means an extension of the specimen of $e = 0{\cdot}001807$ cm. The specimen is of length 5 cm. and as the scale reading can be determined to 0·01 cm., the apparatus is capable of recording changes as small as 0·0000036 cm. per cm. length, or approximately four parts in a million.

§4. MEASUREMENT OF TEMPERATURE

Thermocouples and method of mounting. Two stout thermocouples *T*, of 22 s.w.g. Hoskin's alloy wire (chromel and alumel), with junctions on the axis were used to measure the temperature of the furnace in the near neighbourhood of the wire. The junctions were formed by silver solder. The leads were mounted in silica twin-bore tubes *S*, which were encased in thin brass tubing to give them greater strength. They passed down the inside of the steel tube and out through the sindanyo slab to the cold junction, being insulated by glass tubing.

The cold junction. This consisted of a short length of brass tube, about 4 cm. in diameter, which had its bottom plugged up with a wooden block. The tube was filled with mercury and closed with a cork, through which passed four small glass tubes, immersed in the mercury, whose temperature was given by an accurate mercury-in-glass thermometer. The small glass tubes were filled with mercury, and the leads of the thermocouples rested in them, along with the copper leads from the potentiometer, used to measure the e.m.f. generated. The brass tube was covered with baize to prevent heating by radiation from the furnace.

Calibration of thermocouples. The e.m.f. of the thermocouples was balanced in the usual way against a standard cell, an ionization potentiometer by Tinsley being used. The two thermocouples were found to give almost identical readings at the various fixed points employed in the calibration, as shown in the following table 1.

Table 1. Cold-junction temperature, 20·0° C.

Fixed point	Temperature (° C.)	E.m.f. (mv.)	
		Thermocouple 1	Thermocouple 2
M.p. ice	0·0	−0·78	−0·78
B.p. water	100·0	3·21	3·21
B.p. aniline	184·1	6·56	6·56
M.p. tin	231·9	8·50	8·49
M.p. cadmium	320·9	12·26	12·26
M.p. sulphur	444·3	17·53	17·53

§ 5. CONDUCT OF EXPERIMENT

Before an experiment, the specimen of wire was suspended in the furnace, with a load of 200 g. on its lower end to keep it taut, and heated to 200° C. It was allowed to remain at this temperature for a few minutes and then slowly cooled in the furnace. Portions of the wire were fastened in the steel jaws, which were placed exactly at either end of a steel standard of length, thus ensuring that the wires were always the same known length (4·99 cm.). The apparatus was then set up and the furnace heated up to approximately the desired temperature, when the current was reduced to a value which would maintain the furnace temperature constant at the required value. It was found that variations of temperature along the specimen, or due to current fluctuations, were never more than 1 or 2 per cent.

After the temperature had remained steady for some time the experiment was commenced. The scale pan was placed on the hook, and the immediate deflection was observed in the telescope. Scale readings were then taken at 2 min. intervals, until the rate of increase of length with time became constant. The load was then increased, and the experiment repeated, and so on until the rate of extension became so great that it was impossible to take further observations, or, in some cases, till the wire broke. It was found that the rate of flow soon fell to a constant value, and usually readings over a period of 15–20 min. were taken for each load. By taking comparatively short time periods, the value of the flow was obtained without any appreciable reduction in cross-sectional area, which occurs over long periods.

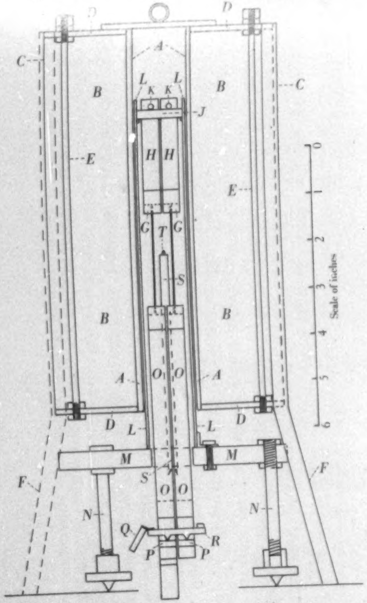
D
D
C
C
A
B
B
L
L
K
K
J
E
E
H
H
G
T
G
S
B
B
A
O
O
A
D
D
L
L
M
M
S
O
O
F
F
N
N
Q
R
P
P
Scale of inches
0
1
2
3
4
5
6

Figure 1. Diagram of apparatus.

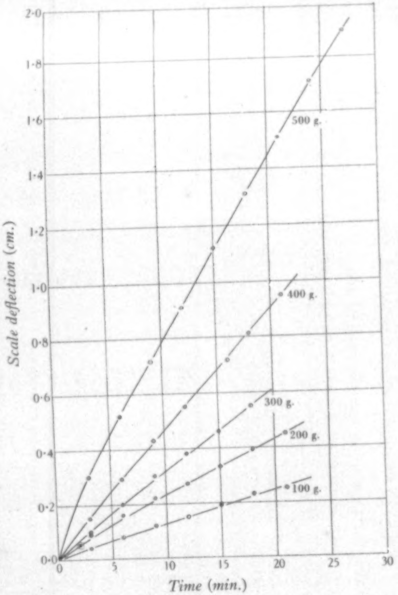

Figure 2. {Extension, time} curves at 101·8° c. for loads of 100 to 500 g.

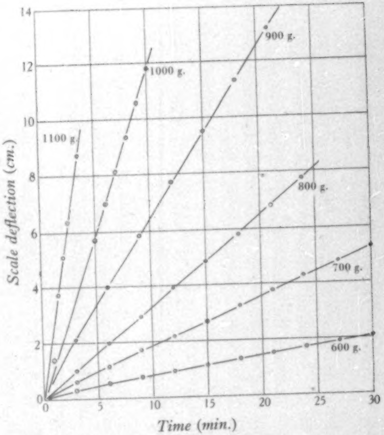

Figure 3. {Extension, time} curves at 101·8° c. for loads of 600 to 1100 g.

It was not considered necessary to anneal the wire, before the experiment with the new load, since Shoji(5) obtained the same values for the final flow of his wires in the two cases, when between increases of load he had (i) unloaded the wire and annealed it at the same temperature as before the commencement of the experiment, and (ii) only unloaded the wire for a period of 10 hours.

§ 6. EXPERIMENTAL RESULTS

Experiments have been performed from air-temperatures up to 200° c. at intervals of approximately 25° c., the increments of load used being 100 g., except in the case of the experiments carried out at 200° c. when 50 g. stages were used to increase the number of possible observations. The material used was white tin wire of no. 16 s.w.g. and density 7·291 g./cm^3.

At lower temperatures it was found that a load could be applied to the wires without causing visible viscous flow, but as soon as a certain value of the load was exceeded a small but definite flow was obtained, the rate of flow increasing rapidly

Table 2. Experiment performed at 102° c. The furnace was heated by a current of 1·5 amp., which was reduced to 1·0 amp.

Load (g.)	Scale reading (cm.)	Initial deflection (cm.)	Subsequent deflection (cm.)	Time	Time interval (min.)	Cold-junction temperature (° c.)	E.m.f. (mv.)
	15·79			11 h. 27 m.			
200	15·65	0·14		27	0		
	15·56		0·09	30	3		3·20 (1)
	15·49		0·16	33	6		3·18 (2)
	15·43		0·22	36	9		
	15·38		0·27	39	12	22·0	
	15·32		0·33	42	15		3·20 (1)
	15·26		0·39	45	18		3·18 (2)
	15·20		0·45	48	21		
300	15·04	0·16		48	0		3·19 (1)
	14·94		0·10	51	3		
	14·84		0·20	54	6		3·18 (2)
	14·74		0·30	57	9		
	14·66		0·38	12 0	12		3·19 (1)
	14·58		0·46	3	15	22·2	
	14·49		0·55	6	18		3·17 (2)
	16·00			2 24			
900	15·52			24	0		
	13·90		2·10	27	3		
	12·04		3·96	30	6		3·22 (1)
	10·16		5·84	33	9		3·20 (2)
	8·30		7·70	36	12	22·9	
	6·50		9·50	39	15		3·20 (2)
	4·70		11·30	42	18		3·22 (1)
	2·82		13·18	45	21	23·0	

Mean temperature of the cold junction	22·5° c.
Mean e.m.f. of thermocouple 1	3·20 mv.
Mean e.m.f. of thermocouple 2	3·18 mv.
Mean e.m.f. of thermocouples	3·19 mv.
Mean e.m.f. of thermocouples, corrected for cold junction at 20·0° c.	3·28 mv.
Mean temperature of specimen (from calibration curve)	102° c.

with further increase of load. It was also noticed that with increase of temperature this necessary initial load decreased in value until at 223° C. the wire collapsed merely under the weight of the sindanyo bar attached to it, i.e. a load of 51 g.

The three definite types of extension were obtained, namely: (*a*) the immediate extension on loading; (*b*) the initial flow, which gradually died out; and (*c*) the elongation which continued at a constant rate. Since the apparatus was designed to measure small changes in length, for heavy loads the initial extension was too large to be measured, and special arrangements would have to be made if accurate measurements of this quantity were required. Naturally, some measure of the initial flow can be obtained from the {extension, time} curve for each load, but since this effect depends very largely on the previous history and treatment of the specimen, and further, like the immediate extension, is an additive effect, the method of experiment was not suitable for giving values on which great reliance could be placed. However, the rate of constant flow is a factor which is quite independent of previous loads to which the material may have been subjected, and for given temperature conditions is solely dependent on the stress. Moreover, the method adopted has the advantage in that, as the load is applied in stages, the initial flow phenomena also take place in stages, and thus for any given load their effect becomes negligible much more rapidly than it would for the same load applied to an unstrained wire. Table 2 gives an abstract from a typical set of experiments performed at 102° C.

Table 3

Experimental temperature (° C.)		19	50	79	102	129	158	182	207
Load on wire (g.)	Stress (kg./cm.^{2})	Rate of extension (10^{-8} cm./sec. per cm.)							
150	7·4								22·9
200	9·9								62·0
250	12·3			6·02	8·13	15·1	19·3	44·0	141
300	14·8								556
350	17·3			7·53	12·0	24·1	36·1	82·0	1658
450	22·2	1·08	3·67	10·1	18·1	40·4	63·8	158	
550	27·2	1·39	4·94	15·1	26·8	66·8	114	419	
650	32·1	1·99	6·87	19·3	39·8	105	223	1687	
750	37·0	2·71	9·89	28·1	63·2	193	548	5902	
850	42·0	3·74	12·7	39·1	104	386	1440		
950	46·9	4·93	16·5	55·4	193	819			
1050	51·8	6·45	21·0	86·1	370				
1150	56·8	8·43	26·6	155	723				
1250	61·7	11·2	34·0	281	1481				
1350	66·6	15·0	51·8	524					
1450	71·6	19·9	77·1	904					
1550	76·5	25·9	117	1566					
1650	81·5	35·7	176	3011					
1750	86·4	51·2	269	4909					
1850	91·3	76·8	440						
1950	96·2	112	939						
2050	101·2	162	1192						
2150	106·1	229							
2250	111·1	324							
2350	116·0	495							
2450	121·0	668							
2550	125·9	940							
2650	130·8	1379							

The general type of {extension, time} curves obtained is shown in figures 2 and 3 for the experiment at 102° C., with time as abscissa and the extension, in scale divisions, as ordinate. The curves illustrate the way in which the higher rate of flow soon falls to the steady constant value given by the linear portion of the curve. They also serve to indicate the increase in the final rate of flow with increase of stressing force, but this point is more clearly demonstrated in figure 4.

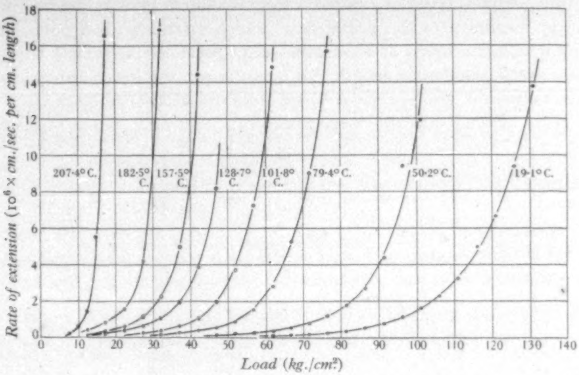

Figure 4. Curves showing relationship between the rate of extension and load for different temperatures.

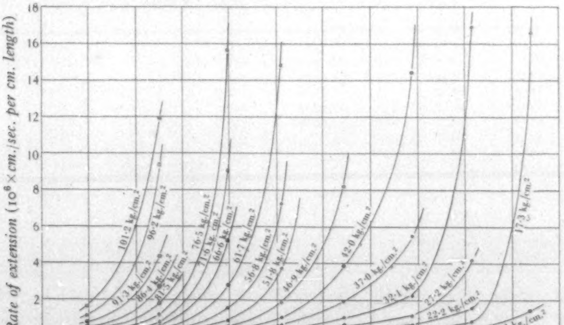

Figure 5. Curves showing the relationship between the rate of extension and temperature for different loads.

The diameter of each specimen was measured, but it was found that the deviation of each specimen from the mean value was so small that the mean value was used for calculating the original cross-sectional area and the stress per unit area for any given load.

The values of the load (g.) applied, the stress (kg./cm.^{2}) and the rate of viscous flow (cm./sec. per cm. length) given by the linear portions of the {extension, time} curves are given for each of the temperatures, and are shown in figures 4 and 5. In figure 4 the loads are abscissae, and the rates of flow are ordinates, the curves being drawn for each temperature investigated. These curves are in agreement with those of previous workers and show the initial gradual increase of the rate of flow with load, the subsequent more rapid increasing rate of flow and the final rapid rate ultimately producing rupture.

In figure 5 temperatures are abscissae and the rates of flow are ordinates, the curves being drawn for constant load. They are similar to the {rate-of-flow, load} curves, but show noticeable irregularities at the higher temperatures.

It can be seen from the {rate-of-flow, load} curves at small loads that the least load P_E necessary to cause flow cannot be determined graphically.

§ 7. THE RELATION BETWEEN THE VELOCITY OF FLOW AND LOAD

The {velocity-of-flow, load} curves at constant temperature appear to be of the form

$$\text{velocity of flow} \propto e^{n\,(\text{load})},$$

where n is a constant, and plotting $\log_e$ (velocity of flow) against load gave straight lines as shown in figure 6, where $\log_e v$ are ordinates and loads P abscissae, hence

$$\log_e v = \log_e A + BP.$$

For a definite value of the load, depending on the temperature, the slope of the curves (with the exception of the experiment performed at 207° C.) undergo a sudden change, thus the curve really consists of two intersecting straight lines.

The values of the slopes B and the intercepts $\log_e A$, from which the constants A are calculated, are given in table 4, for both the slopes of the straight lines, together with the transition loads for each temperature examined.

Table 4

Temp. (° C.)	First slope			Second slope			Transition load (kg./cm.^{2})
	$B\,.\,10^2$	$\log_e A$	$A\,.\,10^9$	$B\,.\,10^2$	$\log_e A$	$A\,.\,10^{10}$	
19	5·9	−19·64	2·95	7·45	−20·90	8·39	80·3
50	5·7	−18·33	10·95	9·0	−20·53	12·12	65·9
79	6·6	−17·55	23·95	11·1	−19·65	29·38	47·9
102	8·4	−17·43	26·84	13·5	−19·49	34·18	40·2
129	11·1	−17·21	33·46	14·9	−18·68	76·92	35·8
158	11·9	−16·90	45·76	18·7	−18·97	57·99	30·4
182	13·0	−16·25	88·07	27·3	−19·79	25·43	24·6
207	44·8	−18·74	7·29	—	—	—	—

In figure 7 the values of B (for the first and second slopes) are plotted as ordinates against the temperature as abscissae. The resulting curves for each slope are straight lines, the line for the first slope holding up to the 207° C. value and the second line being true up to the 182° C. value.

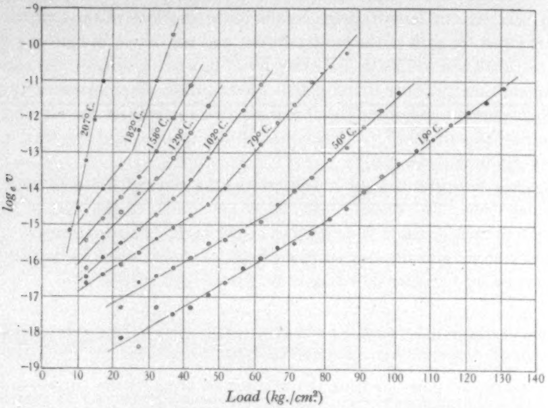

Figure 6. Curves relating $\log_e v$ with load for different temperatures.

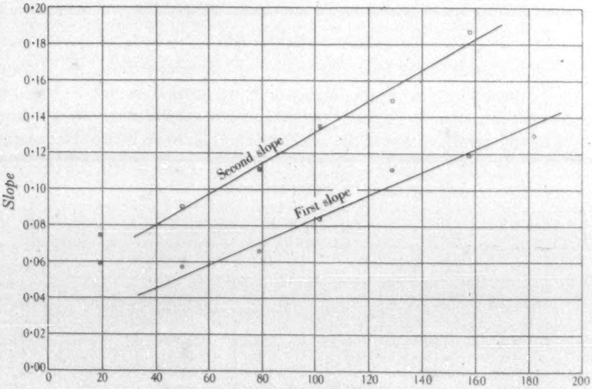

Figure 7. Curves relating the slope B of the $\{\log_e v, P\}$ curves with temperature.

These lines can be represented by the equation

$$B = \alpha + \beta T,$$

where T is the temperature measured in degrees absolute and α and β are constants.

The values of B for 19° C. are considerably off the lines. The allotropic modification from α to β tin occurring at 18° C. (see below) and the consequent doubt as to whether the tin at 19° C. is in the same condition as at the higher temperatures, justifies their omission in evaluating the constants given in table 5.

Table 5

	First slope	Second slope
α	$-0{\cdot}155$	$-0{\cdot}187$
β	$6{\cdot}42.10^{-4}$	$8{\cdot}54.10^{-4}$

Hence, designating B_1 and B_2 as the first and second slopes, we have the values

$$B_1 = 6{\cdot}42.10^{-4} - 0{\cdot}155$$

and

$$B_2 = 8{\cdot}54.10^{-4} - 0{\cdot}187.$$

A straight-line plot was not obtained between A and T, but on plotting $\log_e A$ against the temperature, a linear relation was found to hold, as shown in figure 8.

The 19° C. point was considerably off the first slope line and was again neglected. The corresponding point on the second slope line was well on the curve and included in the evaluation of the constants in the equation

$$\log_e A = \gamma T + \log_e \delta$$

given in table 6.

Table 6

	First slope	Second slope
γ	$0{\cdot}0124$	$0{\cdot}0164$
$\log_e \delta$	$-22{\cdot}126$	$-25{\cdot}658$
δ	$2{\cdot}46.10^{-10}$	$7{\cdot}19.10^{-12}$

Hence

$$A_1 = 2{\cdot}46.10^{-10}\, e^{0{\cdot}0124T}$$

and

$$A_2 = 7{\cdot}19.10^{-12}\, e^{0{\cdot}0164T}.$$

Thus the rate of flow taking place on the first series of slopes can be expressed by the formula

$$v_1 = 2{\cdot}46.10^{-10}.e^{0{\cdot}0124T}.e^{(6{\cdot}42.10^{-4}T-0{\cdot}155)\,P},$$

and on the second series of slopes by

$$v_2 = 7{\cdot}19.10^{-12}.e^{0{\cdot}0164T}.e^{(8{\cdot}54.10^{-4}T-0{\cdot}187)\,P}.$$

§ 8. THE RELATION BETWEEN THE VELOCITY OF FLOW AND TEMPERATURE

Similarly, an investigation of the velocity of flow at constant pressure-temperature data gave the relationship

$$v = A'\,e^{B'T}.$$

In figure 9, $\log_e v$ is plotted as ordinate against T as abscissa, a series of straight lines being obtained. As there are many more constant-load curves and correspondingly fewer points for each curve, the determination of the slope and intercept cannot be made with great accuracy, but yield results of interest. In figure 9 the lines for which there are sufficient data have been drawn in thickly, with dotted lines to indicate the probable path of those curves for which there is inadequate information.

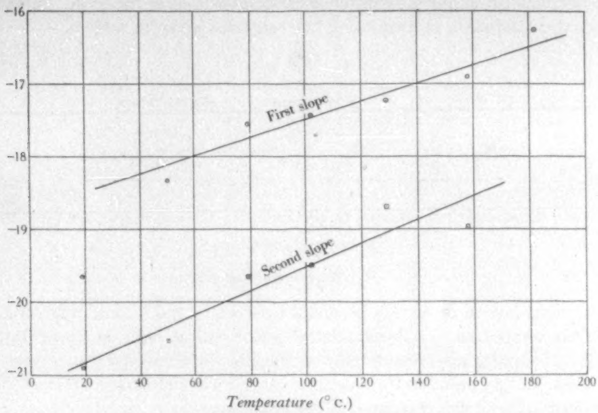

Figure 8. Curves relating the logarithm of the intercept of the $\{\log_e v, P\}$ curves with temperature.

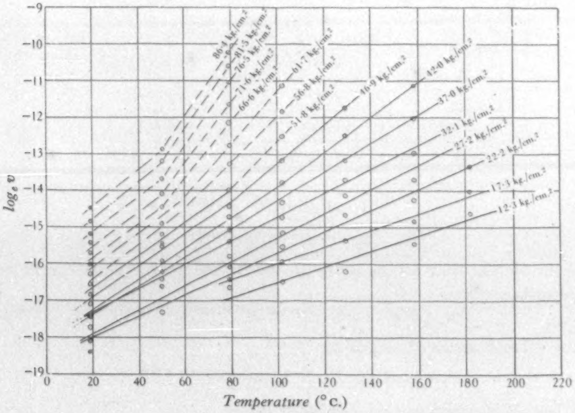

Figure 9. Curves relating $\log_e v$ and temperature for different loads.

Moreover, for some of the readings taken at the higher temperatures, there is some doubt as to the continuity of the curves owing to the allotropic modification which occurs from β to γ tin. The points at 19° C. for small loads, like the points for the same temperature in figures 7 and 8, lie off their proper curves, but they have not been neglected in this case.

The values of the constants for the second slope corresponding to loads of 56·8 kg./cm.² and upwards can only be considered as indications of the order, being obtained from two points.

In figure 10, values of B' are plotted as ordinates against the corresponding loads as abscissae. It is clear that they fall into two groups, which must be considered as evidence that the $\{\log_e v, T\}$ curves, like the $\{\log_e v, P\}$ curves, change their slope, in this case, at a definite critical temperature—a fact only suggested by the middle-load curves in figure 9. From figure 10 straight-line plots are obtained, the curves representing well the range of slopes whose values it was possible to obtain. If the linear relation is represented by the equation

$$B' = \gamma' + \beta' P,$$

where β' and γ' are constants, the values shown in table 7 are obtained.

Table 7

	First slope	Second slope
β'	$6{\cdot}77 . 10^{-4}$	$9{\cdot}91 . 10^{-4}$
γ'	0·0124	0·0104

Hence, if B_1' and B_2' are first and second slopes, they can be written

$$B_1' = 6{\cdot}77 . 10^{-4} P + 0{\cdot}0124,$$
$$B_2' = 9{\cdot}91 . 10^{-4} P + 0{\cdot}0104.$$

As before, the $\{A', P\}$ plots do not give straight lines, but the linear relation holds for the $\{\log_e A', P\}$ curves, which are given in figure 11, $\log_e A'$ being plotted as ordinate and P as abscissa. The values again divide up into two sets, corresponding to the first and second slopes, and the points lie quite well on the straight lines, which can be represented by the equation

$$\log_e A' = \alpha' P + \log_e \delta',$$

the values of the constants being given in the following table 8.

Table 8

	First slope	Second slope
α'	− 0·164	− 0·242
$\log_e \delta'$	− 22·219	− 23·041
δ'	$2{\cdot}24 . 10^{-10}$	$9{\cdot}85 . 10^{-11}$

Hence $$A_1' = 2{\cdot}24 . 10^{-10}\, e^{-0{\cdot}164P}$$
and $$A_2' = 9{\cdot}85 . 10^{-11}\, e^{-0{\cdot}242P}.$$

Thus the rate of flow taking place on the first series of slopes can be represented by the formula

$$v_1 = 2{\cdot}24 \,.\, 10^{-10}\, e^{-0{\cdot}164P}\, e^{(6{\cdot}77 \,.\, 10^{-4}P + 0{\cdot}0124)\,T},$$

and on the second series of slopes by

$$v_2 = 9{\cdot}85 \,.\, 10^{-11}\, e^{-0{\cdot}242P}\, e^{(9{\cdot}91 \,.\, 10^{-4}P + 0{\cdot}0104)\,T}.$$

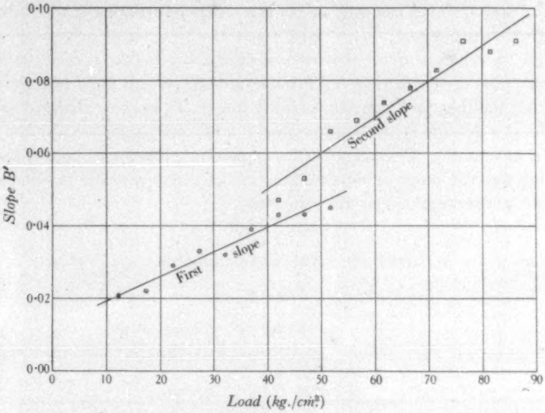

Figure 10. Curves relating the slope B' of the $\{\log_e v, T\}$ curves with load.

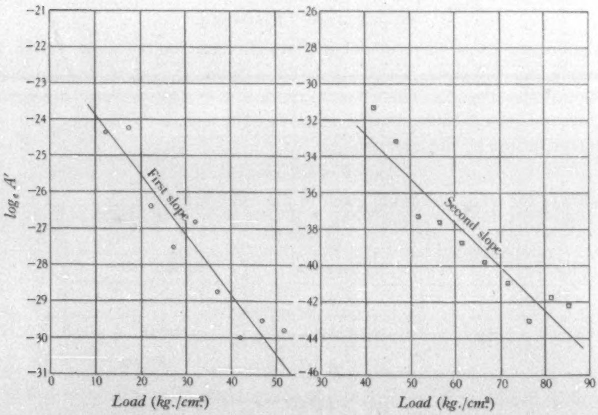

Figure 11. Curves relating the logarithm of the intercept A' of the $\{\log_e v, T\}$ curves with load.

§ 9. EMPIRICAL REPRESENTATION OF RESULTS

Expressions for v have been obtained from both the $\{\log_e v, P\}$ and the $\{\log_e v, T\}$ series of curves and they show, independently, that for any given temperature and load the value of the resulting rate of flow is given by a formula of the type

$$v = \delta e^{\beta PT - \alpha P + \gamma T}.$$

The values of the constants calculated from the different curves are given in table 9.

Table 9

		δ	β	α	γ
First slope	$\{\log_e v, P\}$ curves	$2{\cdot}46 . 10^{-10}$	$6{\cdot}42 . 10^{-4}$	$0{\cdot}155$	$1{\cdot}24 . 10^{-2}$
	$\{\log_e v, T\}$ curves	$2{\cdot}24 . 10^{-10}$	$6{\cdot}77 . 10^{-4}$	$0{\cdot}164$	$1{\cdot}24 . 10^{-2}$
Second slope	$\{\log_e v, P\}$ curves	$7{\cdot}19 . 10^{-12}$	$8{\cdot}54 . 10^{-4}$	$0{\cdot}187$	$1{\cdot}64 . 10^{-2}$
	$\{\log_e v, T\}$ curves	$9{\cdot}85 . 10^{-11}$	$9{\cdot}91 . 10^{-4}$	$0{\cdot}242$	$1{\cdot}04 . 10^{-2}$

The agreement between the numerical values of the constants is excellent for the first slope and quite good for the second slope, the values for which cannot be calculated with much accuracy from the available data for the $\{\log_e v, T\}$ curves.

The empirical equation can be written in the form

$$v = Ke^{\beta\,(P+P_0)\,(T-T_0)},$$

where K, P_0 and T_0 are new constants given by

$$P_0 = \gamma/\beta,$$
$$T_0 = \alpha/\beta,$$
$$K = \delta e^{\alpha\gamma/\beta}.$$

These constants T_0 and P_0 possess a definite physical significance; T_0 is the temperature below which the particular type of flow concerned cannot occur, and P_0 is the corresponding critical load, which, being positive, shows that the temperature is the essential condition for plastic flow, as once the critical value is exceeded, viscous flow will occur for the smallest load applied. It is to be noted that this temperature is below the $\alpha - \beta$ modification temperature, which implies that β tin always satisfies the condition for plastic flow.

These constants, calculated from the values given by the $\{\log_e v, P\}$ curves only, are given in table 10.

Table 10

	P_0, viz. γ/β (kg./cm.^{2})	T_0, viz. α/β	$\beta . 10^4$	$\alpha\gamma/\beta$	$\delta e^{\alpha\gamma/\beta}$
First slope	19·3	241° K.	6·42	2·99	$4{\cdot}89 . 10^{-9}$
Second slope	19·2	219° K.	8·54	3·59	$2{\cdot}60 . 10^{-10}$

Hence the empirical equations are, for the first slope

$$v=4{\cdot}89\,.\,10^{-9}\exp\{6{\cdot}42\,.\,10^{-4}\,(P+19{\cdot}3)\,(T-241)\}\ \text{cm./sec. per cm. length,}$$

and for the second slope

$$v=2{\cdot}60\,.\,10^{-10}\exp\{8{\cdot}54\,.\,10^{-4}\,(P+19{\cdot}2)\,(T-219)\}\ \text{cm./sec. per cm. length.}$$

To make v equal to 0 for the critical values the expression must be written

$$v=K\,\{e^{\beta\,(P+P_0)\,(T-T_0)}-1\},$$

but that this is only a formal requirement is shown by the comparison of certain values of $\exp\{\beta\,(P+P_0)\,(T-T_0)\}$ with unity as shown in table 11.

Table 11

P (kg./cm.²)	T (° K.)	$\exp\{\beta\,(P+P_0)\,(T-T_0)\}$	
0	293	$1{\cdot}9$	First slope
70	293	$2{\cdot}0\,.\,10$	
0	450	$1{\cdot}3\,.\,10$	
20	450	$2{\cdot}0\,.\,10^2$	
90	293	$1{\cdot}0\,.\,10^3$	Second slope
30	450	$1{\cdot}6\,.\,10^4$	

This demonstrates clearly that the unity term plays a negligible part for the larger values of P and T. Calculating the rate of flow for $P=22{\cdot}2$ kg./cm.² and $T=292°$ K. (the lowest velocity of flow observed) the value

$$v=1{\cdot}9\,.\,10^{-8}\ \text{cm./sec. per cm. length}$$

is obtained, when the unity term is neglected, and

$$v=1{\cdot}4\,.\,10^{-8}\ \text{cm./sec. per cm. length}$$

when it is taken into account. The difference is $0{\cdot}5\,.\,10^{-8}$ cm./sec. per cm. length and as the apparatus is only sensitive to changes per unit length of 4 in 10^6, there can be no possibility of distinguishing between the two cases.

The experimental results and empirical expressions only hold for tin in the β, tetragonal form, deviations from the relations occurring for the higher temperatures where γ or rhombic tin is being examined.

§ 10. THE ALLOTROPIC MODIFICATION OF TIN

Tin can exist in three allotropic modifications, α (grey) cubic tin, β (white) tetragonal tin, and γ rhombic tin. The temperature at which the change from α to β tin occurs was found by Cohen(6) to be 18° C. The $\beta\rightarrow\gamma$ modification temperature seems to be known with less certainty; Degens(7) and Werner(8) gave 161° C., but Smits and de Leeuw(9) gave 202·8° C. From experiments on the velocity of effusion at 500 kg./cm.² Tammann(10) found a modification point at 203° C. and Jaenecke(11), who investigated the modification under pressure, also considered that the value obtained by Degens and Werner was unsuitable.

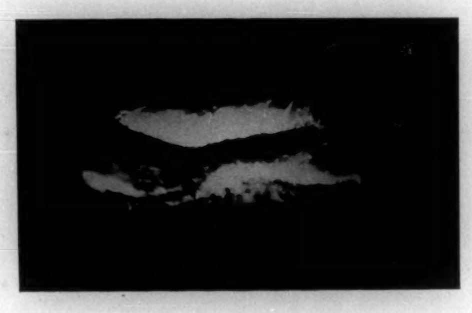

Figure 12*a*. Wire stretched at 182° C.

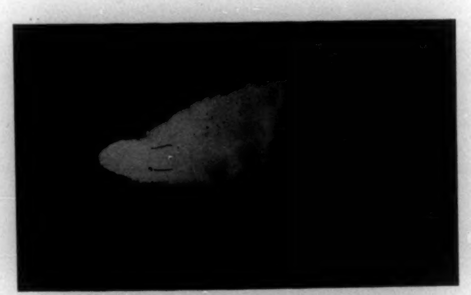

Figure 12*b*. Wire stretched at 207° C.

To face page 168

It will be noticed that all the $\{\log_e v, P\}$ curves consist of two intersecting straight lines with the exception of that for 207° c., which is a single straight line. From the points of intersection it would seem probable that the modification temperature lies between 182° c. and 207° c. A striking confirmation is offered by the examination of the fractures of the wires at these two temperatures. A photograph of the break at 182° c. is given in figure 12*a* on the plate. It shows the twofold nature of the specimen just before fracture and demonstrates that it is due to double glide in two different directions. The specimen at 207° c., shown in figure 12*b* on the plate, exhibits, however, a clean chisel-like fracture, where glide has obviously been occurring in one direction only. Thus it seems certain that the higher temperature is the true one for the allotropic modification.

§ 11. THE RELATION BETWEEN THE TRANSITION AND BREAKING LOADS AND TEMPERATURE

It has already been noticed that the curves plotted between $\log_e v$ and P and $\log_e v$ and T both change their slope at definite critical values. As the values for the $\{\log_e v, T\}$ curves cannot be considered very reliable, the $\{\log_e v, P\}$ curves have been used to obtain the values of the transition loads and temperatures shown in table 12. In addition, the values of the maximum stress used have been tabulated; these correspond approximately to the breaking load of the wire.

Table 12

Temperature (° c.)	Temperature (° K.)	Transition load P_{12} (kg./cm.^{2})	Breaking load P_B (kg./cm.^{2})
19	292	80·3	130·8
50	323	65·9	101·2
79	352	47·9	86·4
102	375	40·2	61·7
129	402	35·8	46·9
158	431	30·4	42·0
182	456	24·6	37·0
207	480	—	17·3

In figure 13 the transition loads P_{12} and breaking loads P_B are plotted as ordinates against the temperatures, in degrees absolute, as abscissae. Both the resulting curves are hyperbolic in form and suggest that

$$(P+P_c)(T-T_c)=C.$$

A point (P_0, T_0) was taken on the curve and the new variables p and t were obtained, where $p=P-P_0$ and $t=T-T_0$, the equation reducing to

$$\frac{t}{p}=-\frac{t}{P_0+P_c}-\frac{T_0-T_c}{P_0+P_c},$$

and t/p can be plotted against t, giving straight-line plots as shown in figure 14. The values of the critical constants P_c and T_c obtained from the slopes and intercepts of these curves are given in the following table 13, together with the values of the constant C.

Table 13

	P_c (kg./cm^2)	T_c (° K.)	C
Transition-load curve	19·5	161	$1{\cdot}30 . 10^4$
Breaking-load curve	41·2	174	$2{\cdot}20 . 10^4$

Hence it is seen that the loads necessary for the transition from the first slope to the second, or for breaking, decrease with increase of temperature in a regular manner.

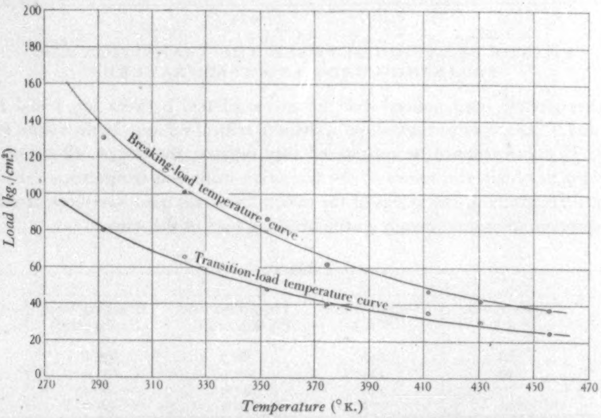

Figure 13. Curves relating critical loads with corresponding temperatures.

The {breaking-load, temperature} curve is in general agreement with the results obtained by Ingall$^{(12)}$, who has investigated the relation between the tensile strength and temperature for copper, silver, nickel and some alloys. He found that it could be expressed, up to a critical inflection temperature, by a straight line which changes direction at any temperature at which allotropic or phase change may take place, and then, for higher temperatures, by a curved line which may exist in two or more portions. Up to the critical temperature the fracture takes place across both grain and grain boundaries, and there was an indication that above it fracture takes place along the boundaries only.

The curved portion of the curve for higher temperatures represents the stages where breaking is due to gliding along the glide planes of the crystals, the actual fracture occurring at some point where local thinning takes place owing to some fault or irregularity. The hyperbolic relation between the breaking load and temperature for tin has already been given, and the constant T_c, viz. 174° K.,

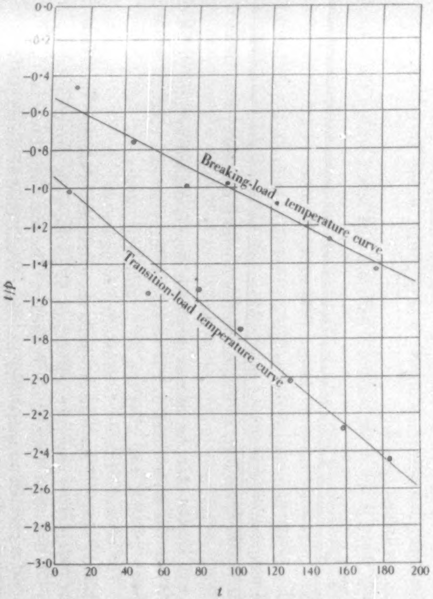

Figure 14. Curves relating t/p with t.

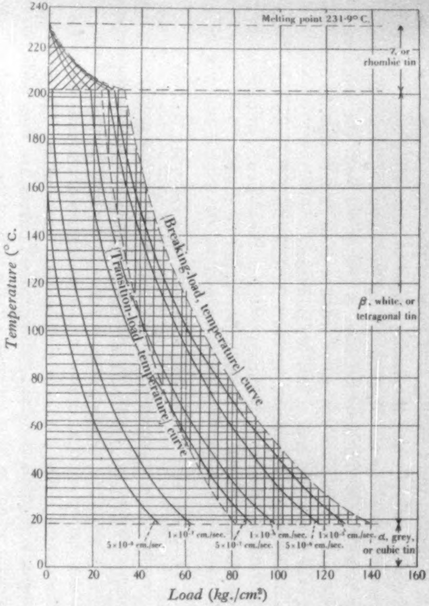

Figure 15. Graphical representation of results.

would give the critical inflection temperature if there were no allotropic modification at 18° C. However, the breaking load must increase with decrease of temperature, until a stage is reached where the load required to cause glide is also large enough to cause fracture across the metal grains, giving the critical inflection temperature and the new stage where the breaking load is connected with the temperature by a linear relation and fracture can occur without glide; a fact that Andrade observed in some experiments on lead at low temperatures.

It is unfortunate that a curve between the least load P_E necessary to start flow and temperature could not be obtained owing to the difficulty of measuring P_E, but it is probable that a similar hyperbolic law would be obeyed.

§ 12. GRAPHICAL REPRESENTATION OF THE RESULTS

The results can be represented qualitatively by the simple graphical representation, shown in figure 15. Loads are plotted as abscissae and temperatures as ordinates, the temperature modifications being indicated by horizontal lines. {Load, temperature} curves are then drawn for certain values of the rate of extension, and are discontinuous at the $\beta \rightarrow \gamma$ tin modification temperature. The {breaking-load, temperature} and {transition-load, temperature} curves are then added as dotted lines. Thus for all points lying above and to the right of the {breaking-load, temperature} curve immediate fracture occurs. The area to the left of the {breaking-load, temperature} curve can be divided up into three portions; (i) the γ tin area, where glide occurs in one direction only, shown by cross-hatching; (ii) the β tin area between the breaking-load and transition-load curves, where glide occurs in two directions, shown by double hatching; and (iii) the β tin area to the left of the {transition-load, temperature} curve, where glide occurs in one direction only, shown by horizontal hatching.

Finally there is the α tin region, which has not fallen within the scope of the present work.

§ 13. THEORY

It has already been stated that when a metal wire is subjected to the necessary load and temperature conditions its extension can be considered to consist of three parts, the elastic extension, an initial extension which dies away with time, and the viscous flow.

It is well known that the viscous or plastic flow is caused by glide of the crystal planes. White tin crystallizes in the tetragonal bipyramidal class, of space group D_{4h}^{19}; axis $a = 5{\cdot}818$ A. and $c = 3{\cdot}174$ A.(13), and four atoms are contained in each element. The crystal structure is illustrated in figure 16.

Mark and Polanyi(14) have investigated the extension of single β tin crystals. They found the [001], [101] and [111] directions to be the glide directions and observed that they did not occur with equal frequency. The least usual was [111], which was never found at normal temperatures and only in one case of a wire stretched at high temperature for which the glide occurred in the [001] direction when stretched cold. In each case the glide plane was {110}. Of the fifteen cases examined, the direction

[001] occurs in eleven, [101] in three and [111] in one only. The glide planes found were the {100} and {110} planes, the latter being by eight cases to three the more frequent.

The examination of single crystals of β tin was repeated by Obinata and Schmid(15). They confirmed the earlier result that the important translation systems were the [001] direction in either the {100} or {110} planes. In rare cases, glide was observed in the [101] direction in either the {101} or {121} planes. These four glide systems were found at each of the temperatures (20°, 100° and 200°) examined, but no evidence of glide in the [111] direction was observed. It is interesting to note that no structural change was indicated by the X-ray photographs taken at 200° C., which is in line with the conclusion above that the allotropic modification temperature is above 200° C.

This gives a satisfactory explanation of the phenomena observed during the present work. Starting from zero load, any increment will produce elastic extension only until the load exceeds the elastic limit, which is dependent on the temperature, and in some cases is exceeded by the least load applied. When the elastic limit is exceeded glide occurs along the direction [001], the glide planes being either {100} or {110}, whichever is more favourably oriented to the direction of stress. This continues, the rate of flow increasing with load and temperature as has been described above, until a second critical load temperature condition is reached, when glide occurs in the [101] direction as well, the glide plane being either {101} or {121} and hence causes the definite large change in the rate of increase of flow with load and temperature as observed.

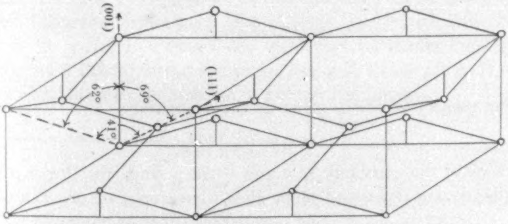

Figure 16. Diagram showing crystal structure of white tin.

Now the distance between atoms in the [001] direction is 3·17 A. and the angle between the [001] and [101] directions 61° 23′; hence the distance between atoms in the [101] direction is 6·63 A. There is experimental evidence that the direction of greatest atomic density is usually the direction of glide, and it would appear to be safe to generalize that the probability of a direction of glide is a function of the atomic density in that direction. Let us now assume that the flowability in any direction, for given temperature and load conditions, is also proportional to the atomic density in that direction, i.e. inversely proportional to the distance apart of the atoms.

Hence the flowability in the [001] direction can be written as $f(P, T)/d_{[001]}$ and in the [101] direction as $f(P, T)/d_{[101]}$, where $f(P, T)$ is a function of the temperature and load conditions. For single glide the flowability F_s in the direction of load can be written as $k.f(P, T)/d_{[001]}$, where k is a constant depending on the orientation of the [001] direction to the direction of loading.

Taylor[16] has shown that double glide can be expressed as the sum of the separate single glides without simultaneous glide. Thus for double glide the flowability F_d in the direction of loading is

$$k.f(P, T)\left\{\frac{1}{d_{[001]}}+\frac{\cos 61^\circ}{d_{[101]}}\right\},$$

61° being the angle between the [001] and [101] directions. Hence the ratio of flowability for double and single glide can be expressed as

$$\begin{aligned}\frac{F_d}{F_s}&=\frac{k.f(P, T)\left\{\frac{1}{d_{[001]}}+\frac{\cos 61^\circ}{d_{[101]}}\right\}}{k.f(P, T)\left\{\frac{1}{d_{[001]}}\right\}}\\&=1+\frac{d_{[001]}}{d_{[101]}}\cos 61^\circ\\&=1{\cdot}23.\end{aligned}$$

Now the velocity of flow is given by the expression

$$v=\delta e^{\beta PT-\alpha P+\gamma T},$$

and the ratios of the constants α, β and γ taken from the $\{\log_e v, P\}$ curves for double glide (second slope) and single glide (first slope) are given in table 14.

Table 14

	Second slope	First slope	Ratio
α	0·187	0·155	1·21
β	$8{\cdot}54.10^{-4}$	$6{\cdot}42.10^{-4}$	1·33
γ	$1{\cdot}64.10^{-2}$	$1{\cdot}24.10^{-2}$	1·32

The agreement of these values with the calculated figure of 1·23 gives support to the hypothesis made above and illustrates the value of single crystal data in the interpretation of results obtained for the behaviour of a mass of crystals in a wire.

§ 14. SUMMARY OF RESULTS

(i) For very small extensions the velocity of viscous flow can be considered to be independent of time, but it is connected with the stretching load by an exponential relation for any given temperature and with the temperature by an exponential relation for any given load.

(ii) The exponential relations

$$v_1 = 2{\cdot}46\,.\,10^{-10}\, e^{0{\cdot}0124T}\, e^{(6{\cdot}42\,.\,10^{-4}T - 0{\cdot}155)\,P},$$

$$v_2 = 7{\cdot}19\,.\,10^{-12}\, e^{0{\cdot}0164T}\, e^{(8{\cdot}54\,.\,10^{-4}T - 0{\cdot}187)\,P}$$

have been obtained, from the {flow, load} curves, for the rates of flow of tin for glide in one and two directions respectively, and the relation is probably of the form

$$v = K\,\{e^{\beta\,(P+P_0)\,(T-T_0)} - 1\}.$$

(iii) Evidence has been obtained in support of the view that the temperature of the allotropic modification from β to γ tin takes place at 203° C. and not at 161° C.

(iv) The transition and breaking loads have been shown to be connected with the corresponding temperatures by a hyperbolic expression.

(v) The behaviour of the tin wire has been shown to be in general agreement with the results obtained for single crystals.

§ 15. ACKNOWLEDGEMENT

I am indebted to Prof. C. H. Lees for facilities for carrying out this investigation in the Physical Laboratories of Queen Mary College, and for his interest and suggestions during its progress. I desire also to express my thanks for a grant from H.M. Department of Scientific and Industrial Research and to Dr A. D. Crow and the Ordnance Committee for permission to publish this paper.

REFERENCES

(1) ELAM, C. F. (MRS TIPPER). *Distortion of Metal Crystals.* (Oxford, 1935.)
(2) *First Report on viscosity and plasticity of the Committee for the Study of Viscosity of the Academy of Sciences at Amsterdam* (1935).
(3) TAPSELL, H. J. *Creep of Metals.* (Oxford, 1931.)
(4) Section by Ewald on the mechanical structure of solids in *The Physics of Solids and Fluids* (Blackie, 1930; second edition, 1937).
(5) SHOJI. *Sci. Pap. Inst. Phys. Chem. Res., Tokyo*, Nos. 57 and 58.
(6) COHEN. *Z. Phys. Chem.* **63**, 625 (1908).
(7) DEGENS. *Z. Anorg. Chem.* **63**, 207 (1909).
(8) WERNER. *Z. Anorg. Chem.* **83**, 275 (1913).
(9) SMITS and DE LEEUW. *Versl. gewone Vergad. Akad. Amst.* **21**, 661 (1912).
(10) TAMMANN. *Schmelzen und Kristallisieren* (1903). Liepzig.
(11) JAENECKE. *Z. Phys. Chem.* **90**, 265, 280, 296, 313 (1915).
(12) INGALL. *J. Inst. Met.* **30**, 2, 171; **32**, 4; **34**, 171.
(13) WESTGREN and PHRAGMÉN. *Z. Anorg. Chem.* **75**, 80 (1928).
(14) MARK and POLANYI. *Z. Phys.* **18**, 75 (1923).
(15) OBINATA and SCHMID. *Z. Phys.* **82**, 224 (1933).
(16) TAYLOR. *Proc. Roy. Soc.* A, **116**, 39 (1927).

DISCUSSION

For discussion see page 311.

AN IMPEDANCE MAGNETOMETER

By E. P. HARRISON, Ph.D., F.R.S.E., F.Inst.P.
and H. ROWE, B.Sc.

Received 6 *July* 1937. *Read in title* 26 *November* 1937

ABSTRACT. A magnetometer for measuring local variations of magnetic field uses the fact that the impedance of a nickel-iron wire of high permeability varies with the axial component of the magnetic field in which the wire is placed.

---

§ 1. GENERAL DESCRIPTION

It is sometimes desired to effect a magnetic survey of a laboratory, building or locality throughout which the normal magnetic field of the earth is modified by the presence of masses of iron such as girders, water pipes or tanks. The instrument described in this paper has been found very convenient for the purpose, and although it deals with vertical components only it would not be difficult to extend its scope to the measurement of any two horizontal components. The apparatus possesses a wide range of sensitivity and has the advantage that direct readings can be taken as quickly as the instrument can be moved from place to place, without fresh adjustment.

The action of the device depends on the fact that if a high-permeability nickel-iron wire is carrying alternating current its impedance is affected by a change in the axial component of the magnetic field in which the wire is placed(1, 2). Under the correct conditions this change of impedance, which is mainly in the resistance component, may be as large as 20 per cent for a field-change of 0·2 gauss; thus there exists here a relation between field and impedance obviously capable of being used in a practical instrument. In outline, the method of using this relation is to place the nickel-iron wire in one arm of an a.-c. bridge which is balanced when the wire is fixed in a constant magnetic field. A change in this field alters the impedance of the wire and upsets the balance of the bridge, producing an alternating current in the detector arm. This current is passed through a low-pass filter to eliminate harmonics, amplified, rectified, and applied to a d.-c. microammeter. The output rectification circuit is of special type and enables a central-zero microammeter to be used, increase of field deflecting the pointer to one side of the zero and decrease of field deflecting it to the other side.

Sensitivity can be quickly and easily adjusted between wide limits; for instance between 1000 $\gamma./\mu$a.* and 2 $\gamma./\mu$a., although at the highest sensitivities, as is natural, special precautions have to be adopted to achieve reliable readings. In fact, at a sensitivity approaching $2\,\gamma./\mu$a., the instrument becomes suitable only for use at a fixed station for recording variations in the earth's field. The various items forming the complete circuit will now be described in detail.

---

* 1 $\gamma. = 10^{-5}$ gauss.

§ 2. DETAILS OF CONSTRUCTION

The nickel-iron wire. This is of mumetal 26 s.w.g., 9 in. long. It is straightened by passing a current through it when under tension; it is then annealed in hydrogen at 1000° c. for half an hour, and cooled with the furnace. The wire is mounted in a groove on an ebonite strip *a*, figure 1. One end is soldered to a terminal *b* and the other connected to an insulated terminal *c* by means of a small copper spiral. This arrangement has been found necessary in order to avoid setting up strains in the wire.

The wire and its ebonite support, together with the terminals, are mounted on a ¼-in. brass strip *d*, and a cover plate *e* of ebonite serves to protect the wire from injury. The groove is machined in the ebonite base plate so that the wire lies accurately parallel to the sides of the supporting brass block. The whole system is then supported by thread from a point at one end so that the wire hangs vertically under gravity. A small bob, not shown in figure 1 but attached to the lower end of the block, dips below the surface of heavy oil in a receptacle suitably mounted, and serves to damp critically the swings of the wire and its mounting when the apparatus is carried from place to place.

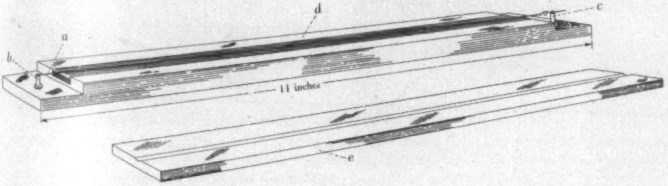

Figure 1.

The bridge. A Maxwell inductance-resistance bridge having equal ratio arms, is used with the following components; it is shown in figure 2. *a*, *a* are ratio coils of manganin each of resistance 2·34 Ω., wound non-inductively. *b* is a fixed inductance of about 30 turns of 22 s.w.g. copper wire wound on a paxolin cylinder 5·5 cm. diameter. Its inductance at 500 c./sec. is about 48 μH. *c* is the mounted indicating wire of effective resistance 1·1 Ω. and inductance 103 μH. at 500 c./sec. *d* is a manganin non-inductive resistance for temperature-compensation, of value 0·6 Ω. *e* is a variable inductance consisting of two pairs of coils mounted on the ends of two arms rotating on a common axis. The effective resistance of these coils is 0·72 Ω. and the inductance can be varied between the limits 99 and 167 μH. at 500 c./sec. *f* is a rheostat consisting of a circular bare 16-gauge German silver wire mounted on the rim of an ebonite disk 1¼ cm. thick and 15 cm. in radius.

A radial arm carried on a spindle through the centre of the disk makes sliding contact with the circular wire. Resistance can be varied by this means through 0·18 Ω.

It will be realized that this forms a somewhat critical bridge, and in making it up care must be taken to measure and adjust the components accurately before assembly. In order to allow additional latitude for magnetic field much below or much above those for which this bridge is adjusted, three terminals *g*, *h*, *k*, figure 2, are provided, which enable a short length of manganin wire to be inserted in either arm of the bridge. Normally the three terminals are connected by a strip of copper. Since the bridge and, in particular, the nickel-iron wire, possesses a rather large temperature coefficient of effective resistance,* some measure of compensation has been adopted by including a non-inductive manganin coil *d* in one of the arms.

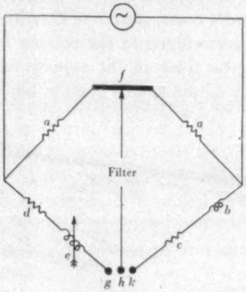

Figure 2.

Further reduction in the effects of temperature has been achieved by mounting the whole bridge in a cork-lagged box which has the additional advantage of forming a very convenient mounting for the nickel-iron wire with its damping system, and for the circular rheostat and the variable inductance. The last two are fitted with spindles and knobs for adjusting purposes, which project outside the lagged box.†

The oscillator. In all measurements involving the peculiar magnetic properties of nickel-iron alloys it is desirable to use alternating current of pure sine-wave form. A simple type of two-valve oscillator working at a fixed frequency is used in the present apparatus. The theoretical diagram is given in figure 3. A tuned anode coil is choke-capacity-coupled in the oscillatory valve circuit and the grid coil is connected via a grid condenser and grid leak. Under these conditions and with a Mullard PM2DX valve with 120 v. anode voltage, the anode current consumption is less than 1 ma. The anode coil is tuned to 500 c./sec. The output coil also is tuned to the fixed frequency of 500 c./sec. and loosely coupled to the anode and grid coils. This ensures harmonic-free alternating current being fed to the output valve, a Mullard PM2A. The output transformer T of this valve is designed with three output windings. Two are equal in magnitude and supply power at 0·5 v. to the special rectifier-detector which is described below. The third winding supplies 30 ma. to the bridge circuit. The three coils, anode, grid, and output, are enclosed in a sealed tin box in order to be completely screened and prevent pick-up in the bridge amplifier.

---

* The coefficient of the nickel-iron decreases as the field increases; typical values are 0·00306 in zero field, 0·00303 in 0·2 gauss and 0·00211 in 1·0 gauss.

† For a periodic temperature wave of amplitude 4° c. and period 12 hr., the time lag produced by the box is about 6 hr.

The filter. Since the ferromagnetic wire when carrying alternating current will cause harmonics to be generated, it is necessary to connect a suitable filter in the detector arm of the bridge between the bridge and amplifier. In practice the harmonics generated are of sufficient magnitude to cause overloading of the amplifier. The filter used is of low-pass type and is terminated by a 300-Ω. resistance, figure 3. A suitable matching transformer connects the 2-Ω. bridge to the filter to match the 300-Ω. terminating resistance. The degree of amplification obtainable can be controlled by the step-up ratio of a transformer connecting the filter to the amplifier.

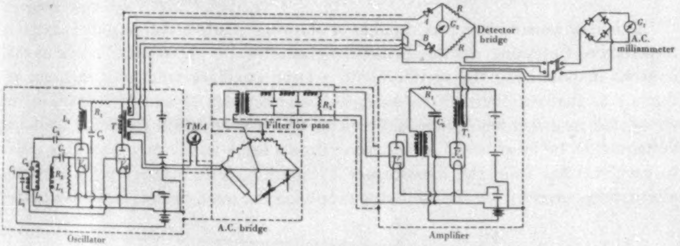

Figure 3. All leads between screened boxes in screened sleeving.

V_1, PM2DX, V_2, PM2A, V_3, PM1A, V_4, PM2A; L_1, 6400 turns, L_2, 6400 turns, L_3, 5000 turns, on 1-in. inner diameter, 1-in. depth, 36 S.W.G., D.S.C., L_4, A.F. choke; R_1, 10,000 Ω., R_2, 0·5 MΩ., R_3, 300 Ω., R, 75 Ω.; C_1, 0·01 μF., C_2, 4 μF., C_3, 0·05 μF., C_4, 0·05 μF., C_5, 2 μF.; T, output transformer of oscillator; T_1, 13·1 step-down transformer; A, B, Westinghouse 5-ma. CuO rectifiers; TMA, thermal milliammeter; G_2, d.-c. microammeter.

The bridge amplifier. This is a straight two-valve transformer-coupled amplifier using a PM1A valve for the first stage and a PM2A valve for the output stage, figure 3. It is supplied with its own h.t. and l.t. current to prevent interaction with the oscillator. A 3·5 : 1 step-up transformer couples the two stages and the first valve is suitably decoupled by 10,000-Ω. anode resistance and 1-μF. by-pass condenser. The first valve is run at zero grid bias while bias for the output can be supplied either by battery or automatically from a 300-Ω. resistance connected in the h.t. negative lead. The output transformer has a 13 : 1 step-down ratio to match the output to the special rectifier detector.

The indicating meters. The output from the amplifier can be measured by one of two alternative methods. The secondary of the output transformer, T_1, is connected via a double-pole double-throw switch to two different types of measuring instrument. For rough results and to obtain an approximate balance of the a.-c. bridge the output is connected to a commercial rectifier-type a.-c. milliammeter, G_1, figure 3. This instrument possesses two main disadvantages; it is very insensitive in the zero region, and it will not distinguish between positive and negative outputs from an a.-c. bridge. To overcome these disadvantages, a second type of instrument, the detector bridge described in full below, is connected to the other terminals of the switch and is used in conjunction with a d.-c. central-zero microammeter G_2. In practice, an approximate balance is first obtained with the a.-c. milliammeter as detector, after which the detector bridge is switched into the circuit for the final balancing operation.

§ 3. THE RECTIFIER DETECTOR BRIDGE

This instrument, which is capable of showing positive and negative changes in impedance, functions on the principle given by C. H. Walter⁽³⁾. The method consists in polarizing the rectifier with a large auxiliary voltage of the same frequency as that supplied to the bridge. Two rectifiers A and B, figure 4 (*a*), are connected in a rectifier bridge network to which is supplied the small alternating voltage e; to be measured. At the same time a large auxiliary voltage E is applied to each rectifier from the transformer T, figure 3. The primary of T is fed with alternating current from the oscillator supplying the main bridge, and two secondary windings supply voltages in antiphase to the rectifiers A and B. Action is similar to that of the Cosens⁽⁴⁾ a.-c. bridge detector which uses valves instead of copper-oxide rectifiers. Thus a voltage $(E+e)$ acts on one rectifier and a voltage $(-E+e)$ on the other. The corresponding rectified currents pass through two equal resistances R across which a d.-c. ammeter G is connected. Since, for voltages well above the threshold value, the characteristic curve of the rectifier is approximately linear, the current through the meter is proportional to the difference between the amplitudes of the vectors $(E+e)$ and $(-E+e)$.

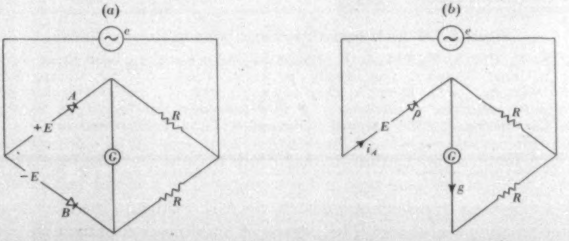

Figure 4. Rectifier detector. e is the out-of-balance e.m.f. from the detector arm of the main bridge. E and $-E$ are the applied polarizing e.m.fs. from windings on the input transformer T.

Referring to figure 4 (*a*), let E be the voltage applied to rectifier A and $-E$ that applied to rectifier B, and let e be the voltage to be detected.

Assume that a positive half-wave of E is acting in arm A and let i be the instantaneous current in that arm. Since a positive half-wave is in arm A, a negative half-wave of E will be in arm B. But the rectifier B has infinite resistance to negative half-waves. The circuit thus reduces to that of figure 4 (*b*). Let ρ be the resistance of the rectifier and i_A the current through it. Then

$$i_A = \frac{E+e}{\rho+Z}$$

where Z is the resistance of G and R in series-parallel, so that

$$Z = \frac{R(R+G)}{2R+G}.$$

For the rectifier A let $E = E_0 \sin \omega t$ and $e = e_0 \sin(\omega t + \alpha)$, where α is the phase-difference between E and e. Then

$$i_A = \frac{1}{\rho+Z}\left[E_0 \sin \omega t + e_0 \sin(\omega t + \alpha)\right]$$

when $0 < \omega t < \pi$, and $i_A = 0$ when $\pi < \omega t < 2\pi$, since in this case $\rho = \infty$.

Putting I_A for the mean value of i_A over a cycle, and writing $\theta = \omega t$, we have

$$I_A = \frac{1}{2\pi}\left[\frac{1}{\rho+Z}\int_0^{\pi}\{E_0 + e_0 \cos\alpha\}\sin\theta\, d\theta + \int_0^{\pi} e_0 \sin\theta \cos\theta\, d\theta + \int_{\pi}^{2\pi}(0)\, d\theta\right]$$

$$= \frac{1}{\pi(\rho+Z)}\left[E_0 + e_0 \cos\alpha\right].$$

Similarly for the mean current I_B of rectifier B, remembering the antiphase sign for E, we have

$$I_B = \frac{1}{\pi(\rho+Z)}\left[-E_0 + e_0 \cos\alpha\right].$$

Therefore

$$I_A + I_B = \frac{2e_0 \cos\alpha}{\pi(\rho+Z)} \qquad \text{......(1)}.$$

With reference again to figure 4 (*a*), when the current I_A is flowing in the arm A no current is flowing in the arm B, and vice versa; therefore the total current g in the meter is given by

$$g = \frac{R}{2R+G}(I_A + I_B)$$

$$= \frac{2e_0 R \cos\alpha}{\pi(2R+G)(Z+\rho)} = \frac{2e_0 R \cos\alpha}{\pi\left[\rho(2R+G) + R(R+G)\right]}.$$

For g to be a maximum we have $dg/dR = 0$, or

$$[2\pi e_0 \cos\alpha]\left[\rho(2R+G) + R(R+G)\right] = [2Re_0 \cos\alpha]\,\pi(2\rho + 2R + G)$$

giving

$$R = \sqrt{(G\rho)} \qquad \text{......(2)}.$$

It is seen from equation (1) that the difference in amplitude between the vectors $(E+e)$ and $(-E+e)$ is proportional to $2e_0 \cos\alpha$, and this is proportional to the current through the meter. Thus the deflection of the d.-c. meter G_2 is independent of the magnitude of E, which merely serves to increase the efficiency of the rectifier. Moreover the deflection changes sign when the direction of the voltage e is reversed which is exactly what is required in the present application. The value of R for maximum sensitivity is given by equation (2).

As it is unlikely that two identical rectifiers can be obtained commercially, adjustable resistances must be provided so that zero meter deflection may correspond to zero input in the detecting arm of the main bridge. A simple way of effecting this adjustment is indicated in figure 5, where a variable resistance r, small compared with R, is connected in the circuit as shown. With zero value of the input e, the slider contact of r is adjusted until the meter reads zero.

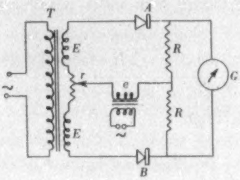

Figure 5.

In the instrument being described the value of ρ was 40 Ω., while G was 140 Ω., so that R is made equal to $\sqrt{(40 \times 140)}$, or 75 Ω.

As has been mentioned on p. 179, the transformer T is supplied with two extra secondary windings having equal numbers of turns such that $E=0\cdot5$ v. In the construction of the detector bridge the windings were adjusted to render the use of the resistance r unnecessary.

§ 4. THE INPUT CURRENT

It has been shown(1, 2) that the effective resistance of high-permeability nickel-iron wire varies with the value of the current supplied to the wire and in fact has a maximum value, at any particular frequency, corresponding to a current named the "optimum current". It is clearly of advantage to use this optimum current in the instrument now being described, since not only is the slope of the {resistance, field} curve and therefore the sensitivity greatest under these conditions, but working on the flat maximum ensures that small and unavoidable variations in current shall have the least effect possible on the impedance.

Since the measured optimum current for the wire used, at a frequency of 500 c./sec. is 22 ma., scrutiny of the bridge values given on p. 177 and in figure 2 shows that the input from the oscillator must be kept at 29 ma. This is adjusted on the meter *TMA*, figure 3, by means of a small rheostat not shown in the figure.

§ 5. THE SENSITIVITY OF THE APPARATUS

The sensitivity of the magnetometer is defined as the field-change expressed in gauss for 1 μa. on the indicating d.-c. ammeter. To measure this the lagged box containing vertical wire and bridge was placed between two horizontal (Helmholtz) coils sufficiently large to provide a uniform field throughout the space occupied by the wire. The bridge having been balanced by adjustment of f and e, figure 2, a known current is passed in the Helmholtz coils; the deflection on the meter G_2, figure 3, corresponding to a known field produced by the coils gives the sensitivity of the magnetometer.

For convenience in subsequent use a single coil, of diameter 30 cm. was fixed to the top of the box so that its centre was vertically above the point of suspension of the hanging nickel-iron wire. When a current is passed through this coil the deflection on the meter forms a measure of the sensitivity as determined in the large coils. The scale of the indicating meter was shown to be linear in respect to vertical field by measurements made in the Helmholtz coils.

Sensitivity can be varied by introducing a transformer between filter and amplifier. For the lower sensitivity ranges of the order of 100 $\gamma./\mu$a. no transformer is used, and this is the arrangement given in figure 3. For higher ranges from 100 $\gamma./\mu$a. up to 1 or 2 $\gamma./\mu$a. transformers of increasing ratio up to 1 : 60 may be used. A certain variation in sensitivity can also be achieved by varying the voltage supplied to the amplifier.

§ 6. ASSEMBLY FOR A SURVEY

For use during a magnetic survey, the box containing bridge and hanging wire is mounted, together with filter, amplifier unit and batteries on a wooden stretcher which may conveniently be provided with non-magnetic tyred wheels. Alternatively, the stretcher fitted with legs may be carried from place to place by two bearers. Owing to the critical damping of the hanging wire, readings of the microammeter may be taken as quickly as 1 or 2 sec. after the stretcher has been set down. If the optimum current is maintained, sensitivity does not change; it may, however, readily be checked at any time by means of the auxiliary calibrating coil.

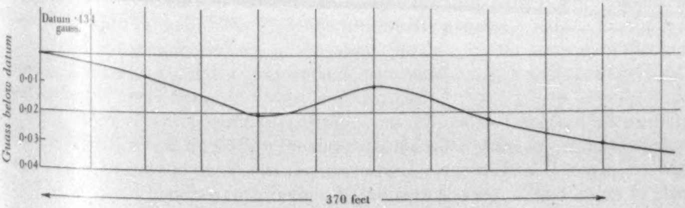

Figure 6. Survey of vertical force.

The result of a survey of vertical field made with this instrument is given in figure 6 as an example. The region explored contained large masses of iron scattered about at various distances from the line of survey and readings were taken to the nearest 2 μa. which was equivalent to 100 γ. This line was independently surveyed by a different method on a different day and the results of the two surveys agreed to 0·5 per cent.

The impedance instrument was taken four or five times over the line of survey and always returned to its zero reading at the selected datum point. The readings along the line were in agreement among themselves within $\pm 100\ \gamma$.

§ 7. ACKNOWLEDGEMENTS

Our thanks are due to Dr J. H. Powell for taking the survey shown in figure 6, and to Mr W. Day and Mr Cousins for valuable assistance during the construction of the instrument. We are indebted to the Admiralty for permission to publish this paper.

REFERENCES

(1) Harrison, Turney and Rowe. *Nature, Lond.*, **135**, 961 (1935).
(2) Harrison, Turney, Rowe and Gollop. *Proc. Roy. Soc.* **157**, 891 (1936).
(3) Walter, C. H. *Z. Tech. Phys.* **13**, 363 (1932).
(4) Cosens. *Proc. Phys. Soc.* **46**, 818 (1934).

THE APPLICATION OF THE ABSORPTION METHOD TO THE DETERMINATION OF THE UPPER LIMITS OF CONTINUOUS β-RAY SPECTRA

By E. E. WIDDOWSON and F. C. CHAMPION

Communicated by Prof. C. D. Ellis, 7 December 1937

ABSTRACT. (1) An objective method of treating absorption data is devised for obtaining the most reliable value for the upper limit of continuous β-ray spectra. (2) The effect of geometrical conditions, of change of source-intensity, and of source-thickness on the absorption curve and on the apparent upper limit is discussed. (3) Feather's empirical equation connecting range and energy of β rays is corrected in accordance with more recent determinations. The corrected equation is $R=0\cdot536E-0\cdot165$. (4) The method is applied to absorption curves obtained for the β rays emitted from Mg^{27}, Si^{31} and As^{76}. The values $0\cdot885\pm0\cdot068$ g./cm.^{2}, $0\cdot571\pm0\cdot047$ g./cm.^{2} and $1\cdot400\pm0\cdot024$ g./cm.^{2} are in good agreement with the values obtained by other methods.

§ 1. INTRODUCTION

The absorption method for the determination of the upper limit of continuous β-ray spectra has the advantages of being rapid and experimentally simple, and of permitting the use of fairly weak sources. Unlike the methods of magnetic focusing and of the expansion chamber, the absorption method gives little information concerning the spectrum itself; but for the naturally occurring radioactive elements it has been found to give satisfactory values of the upper limit(1, 2). The intensities of induced radioactive elements formed with the aid of naturally occurring radioactive elements are usually extremely small. Doubt has been expressed as to the validity of the results obtained by the absorption method for such weak sources, and several workers have noticed that it appears to give low values for the upper limits(3).

The object of the present investigation was to devise a method of treating absorption data which would give the most reliable value of the upper limit obtainable from them, and to test the method on various β-ray spectra. The method was applied to results obtained with radium E and with thorium C and found to give values for the end points agreeing with the average values of recent determinations by other methods. The β-ray spectra of Mg^{27}, Si^{31} and As^{76} were next examined and the method was again shown to be satisfactory.

It is interesting to examine the application of the expansion chamber method to a typical source such as Si^{31} which was used in the present absorption experiments. If a standard expansion chamber had been used under conditions conducive to the production of reliable β-ray tracks(4), then allowing for the decay of the source, about 1000 photographs would have been required for a reasonable chance of observing a single track. Assuming that photographs may be obtained at the rate of one per minute, this would occupy about 15 hr. The present work on Si^{31}, carried out by the absorption method, occupied about 80 hr. Hence by applying the expansion chamber to sources of the same strength for the same time, a total of six tracks would have been obtained. It would clearly be impossible to deduce an end point from such limited data, whereas the value for the end point obtained from the absorption data in this case is accurate to ± 10 per cent. An increase in the strength of the source, while increasing the efficiency of the cloud-chamber work, would also be accompanied by an increase in the accuracy of the value obtained had the absorption method been used. The general conclusion is that, provided an absorption apparatus has been carefully calibrated in the manner described later, the value obtained for the end point is at least as good as that obtained by a reasonable number of expansion-chamber photographs.

§ 2. DETERMINATION OF THE UPPER LIMIT FROM THE ABSORPTION CURVE

The absorption curve of the β rays emitted from a radioactive substance represents very approximately the integral of the spectrum from the high-energy end. This is by no means accurately true, so the spectrum itself cannot be obtained by differentiating the absorption curve. Both curves, however, approach the energy axis tangentially at the upper limit, although the straggling which results from the absorption process produces a more marked tailing off in the case of the absorption curve. With weak sources, such as occur with induced radioactive elements, this tailing off is increased, for to obtain sufficient intensity (1) a large solid angle must be subtended at the source by the detector, whereupon an exceptionally large proportion of the β particles fail to traverse the absorbing foils in an approximately normal direction; and (2) the source itself must be of considerable thickness. Neither of these factors is at all appreciable under conditions commonly used hitherto, that is, with small surface deposits of naturally occurring radioactive elements and flat absorbing foils.

The usual procedure for determining the upper limit from the absorption curve has been to plot the relative ionization or number of counts against thickness of absorber. The limit is then taken as the range corresponding to the point at which the curve becomes flat as estimated by eye. With strong sources subtending a small solid angle at the detector, the uncertainty introduced by visual estimation may not be large, but this method must always be subjective, and no reliable estimate of the error involved can be obtained. In cases where the weakness of the source introduces large statistical errors, the visual method is much less satisfactory. A visual estimate of the upper limit from absorption curves obtained with weak sources under the present experimental conditions gave results which were far too low.

An alternative method which has been used by some workers is to plot the logarithm of the intensity against the thickness of the absorber and to take as the upper limit the thickness at which the resulting linear curve cuts the ordinate corresponding to the natural leak or background of the measuring-apparatus. Now it is clear that for β particles which themselves possess a finite upper energy limit, there must be a corresponding upper limit to the absorption curve. This curve, therefore, should not be represented by an exponential function which approaches the range-axis OX asymptotically and which has no finite upper limit.

On the other hand, a curve represented by $y = \sum_n a_n (x_0 - x)^n$, where a_n is a constant and x_0 is the thickness of absorber corresponding to the upper limit, would appear to be satisfactory. Now the factors producing the absorption curve are very complex, and some empirical expression must be adopted. The present aim is to produce the simplest possible formula which will give a correct value for the end point x_0. We have found that a single term of the above polynomial is sufficient, the value of n being determined by the type of source and the arrangement of the apparatus. With weak thick sources of radium E, thorium C, Mg^{27}, Si^{31} and As^{76}, separated from the counter by a thin cellophane wall, very nearly the whole range was operative. Under these conditions $n = 4$ gave satisfactory values for the end points. With other radium E sources separated from the counter by a thick glass wall, so that less than one half of the range was operative, $n = 3$ gave more satisfactory results. That a single term in the expression $y = \sum_n a_n (x_0 - x)^n$ expresses

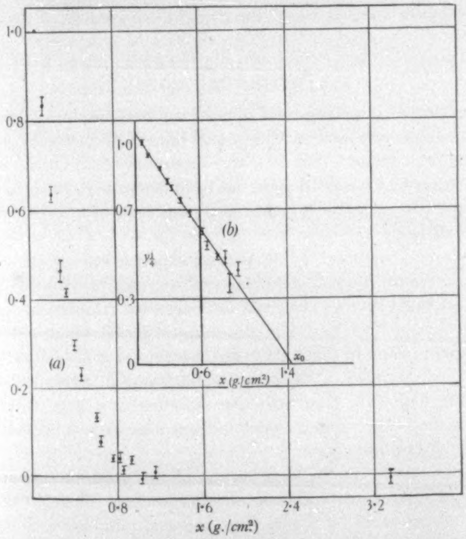

Figure 1 (*a*) and (*b*).

the experimental results satisfactorily is fortunate, since it allows of a simple calculation of the standard deviations to be made. The latter include, of course, only the errors due to chance fluctuations in the rate of emission of the β particles. Their importance lies in the fact that they give a foundation for comparing the accuracy of different results obtained by the same method. The calculations are carried out in the appendix, pp. 193–5.

As typical of the results, figure 1 (*a*) shows the absorption curve for As^{76}, and figure 1 (*b*) the corresponding linear relation between $y^{\frac{1}{2}}$ and x. The vertical lines drawn through the points give the values of the standard deviations, and the upper limit is given by the value x_0 where the straight line cuts the X axis.

§ 3. DEPENDENCE OF THE APPARENT UPPER LIMIT ON EXPERIMENTAL CONDITIONS

The dependence of the apparent upper limit on experimental conditions does not affect the result obtained for the upper limit if the value of n for the given apparatus has been found—that is, if the apparatus has been calibrated with the aid of a β-ray emitter whose end point has been determined by some other method. The variation of the apparent upper limit is, however, of a certain general interest and is discussed below.

(*a*) *Geometrical conditions.* In the present experiments a single-tube counter of aluminium, 0·15 mm. thick, 5 cm. long and 1·5 cm. in diameter was used vertically. The activated sources consisted of concentric cylinders about 2 mm. thick and placed around the counter. The absorbing material, which was in the form of aluminium tubing, could be placed between the counter and the surrounding source. The solid angle subtended by the counter at a point on the source was as large as $4\pi/5$. The straggling of the β particles was therefore very large, and for this reason alone some method other than a visual one was necessary in estimating the upper limit from the absorption curve.

The general results on the dependence of the apparent upper limit on the geometrical conditions agree with those of other workers. Thus Fermi and others(5), in their preliminary study of β rays from induced radioactive elements, mention that to allow for the geometrical conditions (which were the same as those adopted by the present writers) they applied a correction of about 20 per cent to the apparent values which they found for the mean energy of the β rays. Similarly, Baschwitz(6) found a variation in the upper limit of radium E when the effective intensity of a source was altered by means of variable apertures in contact with the detecting ionization chamber. On the other hand, no appreciable variation occurred when the aperture was kept constant but different areas of the source were used. It is clear that a large variation is made in the solid angle in the former case but not in the latter.

(*b*) *Use of a thick source.* Since in order to obtain sufficient intensity the sources of the induced radioactive elements were required in the form of thick cylinders, the calibrating sources of radium E and thorium C were made up in a similar manner. A layer of plaster of Paris about 2 mm. thick, situated between two concentric cylinders (the outer of ebonite and the inner of thin cellophane), was set with water to which a few drops of an acid solution of radium (D+E+F) or thorium (B+C+etc.) had been added. The three elements Mg^{27}, Si^{31} and As^{76} were produced by neutrons emitted either from a radon-beryllium source of strength up to 60 mC. or from a radium-beryllium source containing 50 mg. of radium in 2-mg. needles. The source and the activated element were surrounded with paraffin wax in the usual manner. To obtain Mg^{27}, aluminium tubes 1 mm. thick were used, while for the production of Si^{31} and As^{76}, amorphous phosphorus and arsenic were used in powder form and contained in hollow cylindrical vessels with inner walls of thin cellophane, leaving a layer of powder about 2 mm. thick. The satisfactory application of a single term with n equal to 4 to the absorption curves obtained with the widely varying radioactive elements examined here would indicate that the sources need be of only approximately the same geometrical thickness. Ideally, for sources to be of the same effective thickness, their actual thicknesses (g./cm.²) would have to be adjusted in accordance with the unknown energy-distribution of their β rays.

(*c*) *Variation with source intensity.* The sources used in the present experiments varied considerably in intensity from one to another, and it was desirable to examine the effect, if any, of a variation in source-intensity on the apparent value of the upper limit. Measurements were therefore carried out with sources of radium E of different intensities, contained in cylinders with inner walls of glass, but under the previous geometrical conditions. With such sources, only the latter part of the range is operative and it was found that a single term of the absorption formula, corresponding to $n = 3$, gave values for the upper limit in best agreement with the accepted value. The results with four sources of different intensities are shown in table 1.

Table 1

Source	Intensity with 0·275 g./cm.² of absorber	Upper limit (g./cm.²)	Error (standard deviation)
1	101	0·477	0·016
2	58	0·479	0·019
3	11	0·489	0·029
4	1	0·424	0·078

The second column gives the relative intensities of the sources with 0·275 g./cm.² of absorber already interposed. The third column contains the corresponding values of the upper limit, while the last column contains a measure of the accuracy expressed in terms of the standard deviation and calculated from the formulae developed in the appendix. It will be observed that, within the limits of error, no consistent variation of the measured upper limit occurs as the intensity of the source is altered. Similar negative results for radium E were obtained by Baschwitz and for Si^{31} by Newson(7).

§4. RESULTS, AND DISCUSSION OF RESULTS

Our measurements of the absorption of the β particles emitted by radium E, thorium C, Mg^{27}, Si^{31} and As^{76} (two sources) are given in table 2. In column 3, for thorium C, Si^{31} and As^{76}, which have half-value periods of some hours, Y is expressed as the ratio of the number of counts observed to the number which would have been observed had no absorber been present. Expressing Y in this manner as an intensity-ratio allows of the combination of results obtained with sources of different initial intensities. In deducing Y, suitable correction has of course been made for the decay of the source and for the presence of a background count.

For Mg^{27}, which has a half-life of only a few minutes, the intensity-ratio was taken as the ratio of the number of counts with absorber present for the period 1 to 7 minutes to the number of counts without absorber during the period 7·5 to 16·5 minutes. This choice gives an intensity-ratio of about unity for zero absorber.

For radium E, the decay of which was negligible during the time taken by the experiments, the intensity was obtained directly from the number of counts in a given time.

The quantity y plotted in figure 1 is the difference $(Y - Y_0)$, where Y_0 is the effective background count given by the ordinate of the absorption curve after it has become horizontal. These points are discussed more fully in the appendix, pp. 193–5.

In table 3, column 2 contains the values of the upper limits obtained from the intercept on the X axis when $y^{\frac{1}{2}}$ is plotted against x. Column 3 contains the corresponding values of the standard deviations of the upper limits, calculated with the aid of the formulae developed in the appendix. Column 4 gives the percentage value of the standard deviation. In column 5 the upper limits have been converted from g./cm.^{2} to MV. by making use of Feather's empirical equation(14),

$$R = aE + b, \quad (E > 0{\cdot}7 \text{ MV.}),$$

where R is the range in g./cm.^{2}, E is the corresponding energy in MV., and a and b are constants. The equation is based on the maximum ranges and the upper limits of the β-ray spectra of thorium C, radium E and radium C as determined by other methods. A number of recent determinations have been made for radium E; from the mean of the more reliable values*, namely 1·18, a straight line fitted by the method of least squares gives

$$R = 0{\cdot}536E - 0{\cdot}165.$$

Upper limits determined directly from the experimental data have been used instead of those obtained from extrapolation of a Konopinski-Uhlenbeck plot(20), since the latter usually gives much higher values and it is doubtful if it is a true representation of the spectrum in the region of the upper limit. Columns 6, 7 and 8 contain respectively the values for the upper limits obtained by others, the initials of the corresponding workers and the methods used by them.

Table 2

Source	x (g./cm^2)	Y	Standard deviation of Y
Radium E	0·048	20·70	1·08
	0·119	7·55	0·85
	0·189	1·98	0·58
	0·240	0·61	0·33
	0·309	0·03	0·39
	0·431	−0·57	0·44
	0·517	−0·54	0·39
	0·636	−0·36	0·44
	0·815	−0·50	0·38
Thorium C	0·048	1·000	—
	0·233	0·384	0·0109
	0·306	0·268	0·0067
	0·500	0·070	0·0060
	0·636	0·062	0·0047
	0·760	0·023	0·0019
	0·815	0·021	0·0010
	1·548	0·021	0·0014
Mg^{27}	0·041	1·092	0·092
	0·081	0·789	0·051
	0·138	0·663	0·029
	0·213	0·411	0·030
	0·281	0·275	0·046
	0·351	0·186	0·026
	0·418	0·086	0·015
	0·473	0·007	0·027
	0·543	−0·019	0·043
	0·632	0·036	0·049
	0·681	−0·004	0·039
	0·797	−0·089	0·087
	1·036	0·007	0·026
Si^{31}	0·051	1·000	—
	0·092	0·862	0·050
	0·119	0·540	0·034
	0·167	0·386	0·023
	0·229	0·178	0·021
	0·292	0·053	0·015
	0·354	0·033	0·018
	0·435	−0·015	0·024
	0·505	−0·012	0·019
	0·600	−0·006	0·023
	0·697	−0·008	0·013
As^{76} (1)	0·051	1·000	—
	0·119	0·832	0·015
	0·238	0·633	0·012
	0·305	0·462	0·018
	0·354	0·413	0·007
	0·435	0·296	0·006
	0·505	0·221	0·012
	0·613	0·130	0·005
	0·675	0·073	0·003
	0·772	0·047	0·004
	0·841	0·044	0·009
	0·897	0·011	0·003
	0·943	0·029	0·005
	1·033	−0·004	0·007
	1·171	0·006	0·012
	3·3 Pb	−0·006	0·008
As^{76} (2)	0·048	1·000	—
	0·308	0·460	0·0114
	0·500	0·308	0·0084
	0·636	0·130	0·0057
	0·760	0·008	0·0129
	0·815	−0·018	0·0010
	1·074	−0·018	0·0016
	1·548	−0·013	0·0014

Table 3

Element	Upper limit (g./cm.^{2})	Standard deviation of limit	Standard deviation (per cent)	Upper limit (MV.)	Upper limit, other workers	Name	Method
Radium E	0·458	0·064	14	1·16	0·475 g./cm.^{2}	N. F.(1)	Absorption
					1·18 MV.	Mean*	Expansion chambe and magnetic focusing
Thorium C	1·023	0·028	2·8	2·22	0·98 g./cm.^{2}	J. A. C.(8)	Absorption
					2·18 MV.	R. W. G.(9)	Magnetic focusing
					2·25 MV.	W. J. H.(10)	Magnetic focusing
Mg^{27}	0·885	0·065	7·4	1·96	0·95 g./cm.^{2}	M. C. H.(11)	Absorption
Si^{31}	0·571	0·047	8·3	1·37	1·50 MV.	H. W. N.(7)	Absorption
					1·44 MV.	H. W. N.	Weak source
					1·8 MV.	K., R. and P.(12)	Expansion chamb
As^{76} (1)	1·454	0·048	3·3	3·02	3·4 MV. ($K-U$)	B. and M.(13)	Expansion chamb
As^{76} (2)	1·384	0·029	2·2	2·89	2·4 MV. (spectrum ends)	B. and M.	Expansion chamb
As^{76} (1) and (2)	1·400	0·024	1·7	2·92	—	—	—

Comparing columns 5 and 6, we observe a general agreement between the values for the upper limits obtained by the present method and the mean of the values given by other methods. Considering first the results for radium E, we may note that a very weak source was used, so that the possible error in the upper limit was large. However, within the limits of this error the agreement is quite satisfactory. With thorium C, considerably stronger sources were used and the standard deviation of the upper limit is only about 3 per cent. In spite of the fact that strong γ rays are present and that the spectrum is a composite one, the value for the upper limit agrees well with that given by other workers. Indeed, the method seems to be applicable whether or not γ rays are emitted, for in addition, of the remaining elements, Mg^{27} and As^{76} emit γ rays while Si^{31} does not.

The agreement shown in columns 5 and 6 for Mg^{27} is just within the limit of error. It is possible that the true value of the upper limit is slightly below that given by Henderson, who applied the logarithmic method to his absorption data. He had the advantage, however, of a strong source, and small-solid-angle conditions were used.

Several determinations have been made for Si^{31}. Thus Kurie, Richardson and Paxton using an expansion chamber found a value 1·85 MV. from their experimental results, although a Konopinski-Uhlenbeck extrapolation gave 2·05 MV. Even the former value is somewhat above the highest value deducible from our results. We find better agreement with the values obtained by Newson, who used the absorption method and two strong sources. The stronger of the two sources gave the higher value for the upper limit but no great significance can be attached to the difference as it is almost within his experimental error.

---

* The value used is the mean of the values obtained by Champion(4), Alichanian(15), Lecoin(16), Lyman(17), Langer and Whitaker(18), and O'Conor(19).

In the present investigation, two determinations have been made for As^{76}, one with an earlier apparatus and a background count of 4 per minute and the second with a later apparatus giving a background of 15 per minute. The two results agree well with each other within the experimental error. The mean of the two results is in very satisfactory agreement with the mean of the values obtained by Brown and Mitchell. These workers used an expansion chamber, and two values were obtained by them from experiment and from the Konopinski-Uhlenbeck extrapolation respectively.

REFERENCES

(1) FEATHER, N. *Phys. Rev.* **35**, 1559 (1930).
(2) SARGENT, B. W. *Proc. Roy. Soc.* A, **139**, 659 (1933).
(3) ALICHANIAN *et al.* *Phys. Z. Sowjet.* **11**, 204 (1937).
(4) CHAMPION, F. C. *Proc. Roy. Soc.* A, **134**, 672 (1932).
(5) FERMI *et al.* *Proc. Roy. Soc.* A, **146**, 483 (1934).
(6) BASCHWITZ, A. *J. Phys. Radium*, **7**, 37 (1936).
(7) NEWSON, H. W. *Phys. Rev.* **51**, 624 (1937).
(8) CHALMERS, J. A. *Proc. Camb. Phil. Soc.* **25**, 331 (1929).
(9) GURNEY, R. W. *Proc. Roy. Soc.* A, **112**, 380 (1926).
(10) HENDERSON, W. J. *Proc. Roy. Soc.* A, **147**, 572 (1934).
(11) HENDERSON, M. C. *Phys. Rev.* **48**, 855 (1935).
(12) KURIE, F. N. D., RICHARDSON, J. R. and PAXTON, H. C. *Phys. Rev.* **49**, 368 (1936).
(13) BROWN, M. V. and MITCHELL, A. C. G. *Phys. Rev.* **50**, 593 (1936).
(14) FEATHER, N. *Proc. Camb. Phil. Soc.* **27**, 430 (1931).
(15) ALICHANIAN *et al.* *Phys. Z. Sowjet.* **10**, 78 (1936).
(16) LECOIN, M. *C.R. Acad. Sci., Paris*, **205**, 171 (1936).
(17) LYMAN, E. M. *Phys. Rev.* **51**, 1 (1937).
(18) LANGER, L. M. and WHITAKER, M. D. *Phys. Rev.* **51**, 713 (1937).
(19) O'CONOR, J. S. *Phys. Rev.* **52**, 303 (1937).
(20) UHLENBECK, G. E. and KONOPINSKI, E. J. *Phys. Rev.* **48**, 7 (1935).

APPENDIX

(1) *Calculation of the upper limit from the absorption curve.* Assuming that

$$y^{\frac{1}{4}} = k\,(x_0 - x),$$

replace $y^{\frac{1}{4}}$ by z and write

$$z = h - k\,(x - \bar{x}), \tag{i}$$

so that

$$x_0 = \bar{x} + \frac{h}{k}.$$

Adding n equations of type (i), one for each point to be used in determining the quartic, we obtain

$$S\,(z) = nh,$$

since

$$S\,(x - \bar{x}) = 0.$$

Adding the n equations, each multiplied by $(x - \bar{x})$, we have

$$S\,[z\,(x - \bar{x})] = -kS\,(x - \bar{x})^2.$$

Therefore $$h = S(z)/n,$$

and $$k = -S[z(x-\bar{x})]/S(x-\bar{x})^2,$$

giving $$x_0 = \bar{x} - \frac{S(z)\times S(x-\bar{x})^2}{nS[z(x-\bar{x})]}.$$

(2) *Calculation of errors.* We shall assume the following results:

(*a*) $\text{var}\, kA = k^2 \,\text{var}\, A$, where k is a constant.

(*b*) $\text{var}\, \bar{A} = \Sigma\,(\text{var}\, A)/n^2$, where the mean $\bar{A}$ is obtained from n values of A.

(*c*) $\text{var}\,(A \pm B) = \text{var}\, A + \text{var}\, B \pm 2\,\text{cov}\, AB$.

(*d*) $\text{var}\, AB = (\bar{A}\bar{B})^2 \left[\frac{\text{var}\, A}{\bar{A}^2} + \frac{\text{var}\, B}{\bar{B}^2} + \frac{2\,\text{cov}\, AB}{\bar{A}\bar{B}}\right]$.

(*e*) $\text{var}\, \frac{A}{B} = \left(\frac{\bar{A}}{\bar{B}}\right)^2 \left[\frac{\text{var}\, A}{\bar{A}^2} + \frac{\text{var}\, B}{\bar{B}^2} - \frac{2\,\text{cov}\, AB}{\bar{A}\bar{B}}\right]$.

(*f*) $\text{var}\, f(x) = \left(\frac{df}{dx}\right)^2 \text{var}\, x$, so that

$\text{var}\, A^n = n^2 A^{2(n-1)}\, \text{var}\, A$.

(*g*) $\text{cov}\,(A, kA) = k\, \text{var}\, A$.

We also assume that the β particles are emitted in a Poisson distribution over successive equal intervals of time, if the source is constant. If the mean number emitted during the interval is m, the probability that x will be emitted is $e^{-m}m^x/x!$, where $x = 0, 1, 2$, etc. For such a distribution the variance is equal to the mean m, and the standard deviation is $m^{\frac{1}{2}}$.

Then if N_1 is the number of counts recorded during a time t with an absorber, b_1 the corresponding background count for time t, and $(N_2 - b_2)$ an estimate of the counts due to the source that would have been recorded in time t with zero absorber, then

$$Y = (N_1 - b_1)/(N_2 - b_2)$$

and $$\text{var}\,(N_1 - b_1) = (N_1 + b_1),$$

so that $$\text{var}\ Y = Y^2 \left[\frac{N_1 + b_1}{(N_1 - b_1)^2} + \frac{N_2 + b_2}{(N_2 - b_2)^2}\right].$$

The standard deviation of Y, that is $(\text{var}\ Y)^{\frac{1}{2}}$, for the absorption measurements is given in column 4 of table 2. For radium E, the decay of which is negligible,

$$Y = (N_1 - b_1)/t$$

and $$\text{var}\ Y = (N_1 + b_1)/t^2.$$

(3) *Calculation of error in the upper limit.* The value of Y_0 is given by

$$\frac{\Sigma \frac{Y}{\text{var}\ Y}}{\Sigma \frac{1}{\text{var}\ Y}},$$

the summation extending over the final horizontal part of the curve. The value of var Y_0 is given by

$$1/\text{var } Y_0 = \Sigma\, 1/\text{var } Y.$$

Then

$$\text{var } y = \text{var } Y + \text{var } Y_0,$$

and we have

$$\text{var } y^{\frac{1}{4}} = \tfrac{1}{16} y^{-\frac{3}{2}} (\text{var } y)$$

or

$$\text{var } y^{\frac{1}{3}} = \tfrac{1}{9} y^{-\frac{4}{3}} (\text{var } y).$$

Finally, having found the value of var z for each point on the curve, we obtain

$$\text{var } x_0 = \left[\frac{S(x-\bar{x})^2}{n}\right]^2 \text{var}\left[\frac{S(z)}{Sz(x-\bar{x})}\right]$$

$$= x_0{}^2 \left[\frac{\text{var } S(z)}{[S(z)]^2} + \frac{\text{var } S[z(x-\bar{x})]}{[Sz(x-\bar{x})]^2} \quad \frac{2\text{ cov }\{S(z), Sz(x-\bar{x})\}}{S(z) \times Sz(x-\bar{x})}\right].$$

Now

$$\text{var } S(z) = S \text{ var } z,$$

$$\text{var } [Sz(x-\bar{x})] = S[(x-\bar{x})^2 \text{ var } z],$$

$$\text{cov }\{S(z), Sz(x-\bar{x})\} = S \text{ cov } [z, z(x-\bar{x})] = S(x-\bar{x}) \text{ var } z.$$

Hence

$$\text{var } x_0 = x_0{}^2 \left[\frac{S \text{ var } z}{[S(z)]^2} + \frac{S[(x-\bar{x})^2 \text{ var } z]}{[Sz(x-\bar{x})]^2} - \frac{2S(x-\bar{x}) \text{ var } z}{S(z) \times Sz(x-\bar{x})}\right].$$

A NOTE ON THE THEORY OF PHOTOCONDUCTIVITY

By N. F. MOTT, H. H. Wills Physical Laboratory,
University of Bristol

Received 5 *October* 1937. *Read in title* 26 *November* 1937

ABSTRACT. It is shown on theoretical grounds that the primary photoelectric current in solids may be expected to tend to zero as the temperature is lowered; the presence of certain kinds of impurity may however prevent this. The theoretical conclusions are compared with the results of experiment.

---

§ 1. THEORY

According to the modern theory of solids the absorption spectrum of a metal consists of broad bands, a conclusion which is in agreement with experiment. For an insulating crystal, on the other hand, so long as the atoms are at rest, the theory leads one to expect a series of sharp lines leading up to a continuous band. The spectrum is thus similar to that of an atom. This was first shown by Peierls(1). According to him the considerable breadth of the absorption bands of thin films observed in, say, the alkali halides(2), must be ascribed to the thermal or zero-point vibrations.

The reason for the existence of sharp lines is the following: if an electron is removed from an atom or ion of the lattice, an excess positive charge is left behind; we call this a "positive hole". In the field of this positive hole there will be for the electron a series of stationary states with discrete energy, similar to the stationary states of an electron in the field of a proton. Excitation of the electron into these states will give rise to line absorption; removal of the electron right away from the positive hole will give continuous absorption.

It is clear that absorption of light in one of the sharp lines will not give rise to photoconductivity in the crystal, because the electron is not removed from the field of the corresponding positive charge. One could, however, expect photoconductivity in the region of continuous absorption.

Actually the absorption coefficient in the region of characteristic absorption of, for instance, the alkali halides, is very high, of the order 10^6 cm.$^{-1}$, so that the light cannot penetrate more than about 10^{-6} cm. into the crystal. Experiments on the photoconductivity of, for instance, zinc sulphide or silver bromide are carried out in the long-wave-length tail of the absorption band, where the absorption coefficient is much less than this; in this region we must assume that only a small fraction of the total number of atoms is able to take part in the absorption. These may be atoms at the surface of cracks; for polar salts Herzfeld(3) has shown that the work necessary to excite an electron is less at the surface of a crack than for ions in the body of the crystal. They may also be impurity atoms in solid solution.

In the work of Pohl(2) and his school on coloured alkali-halide crystals, it is probable that an electron replacing a negative ion in the lattice is responsible for the absorption.

The same conclusion holds for the absorption as before; a line absorption, corresponding to transitions in which the electron is not separated from its positive charge, will lie to the long-wave-length side of the absorption band which corresponds to a freeing of the electron. Such a line absorption is, for instance, observed(4) in potassium iodide containing traces of silver iodide. In the case of absorption due to random impurities and cracks, we should expect a continuous band made up of a series of fairly sharp lines superimposed. As regards photo-conductivity, however, the same conclusion holds; that in the long-wave-length edge of the absorption band the light cannot release electrons directly.

It is of course possible that the thermal agitation of the lattice may remove the excited electron from the neighbourhood of the corresponding positive charge before it has time to fall back into the normal state. Suppose that the work necessary to free the electron from the excited state is W; then the probability per time dt that an electron will be released may be taken to be

$$Be^{-W/kT}\,dt,$$

with B of the order of magnitude of the frequency of the atomic vibrations, and thus about $5\cdot10^{12}$ sec.$^{-1}$ The probability per time dt that an excited electron will drop back to the normal state may be written

$$A\,dt$$

with A of the order 10^8 sec.$^{-1}$ Then the probability η that an electron will escape from its positive hole before it drops back into its original state is given by

$$\eta=\frac{1}{1+(A/B)\,e^{W/kT}}.$$

This function is plotted against temperature in the figure, and is seen to drop rapidly with decreasing temperature.

If $A/B=2\times10^{-5}$, the drop takes place at a temperature

$$\frac{W}{k}\Big/\log_e(5\times10^4),\text{ which }\doteqdot 0\cdot09W/k.$$

Thus if the drop takes place at room temperature, W will be about $\frac{1}{4}$ ev.

In any experiment which measures the primary photoelectric current, the current will be proportional to η. We thus reach the conclusion that, when illumination is towards the red end of the absorption region, the current per absorbed quantum must always tend to zero as the temperature is lowered.

This conclusion can be avoided in one case. It may be that all or part of the absorption investigated is due to negatively charged impurities, that is to say, to extra electrons trapped in the lattice in some way, and contributing an excess negative charge to their immediate neighbourhood. In that case no positive hole is formed when the electron is freed, and possibly no stationary state exists except the normal one, as in the hydrogen negative ion. Then illumination at the red end of the spectrum will excite the electron directly into the conduction band, so that it is free to move away.

For polar crystals this conclusion must be accepted with some reserve, for a reason similar to that discussed by Gurney and Mott(5) in a recent paper. In order to simplify the discussion let us consider a polar crystal in which the dielectric constant κ is entirely due to the displacement of the positive and negative ions from their mean positions. At a large distance r from the centre, therefore, the field is $-e/\kappa r^2$, and the polarization

$$P=\frac{1}{4\pi}\left(1-\frac{1}{\kappa}\right)\frac{e}{r^2};$$

the ions are displaced from their mean positions by distances $\pm P/Ne$, where N is the number of ions per unit volume.

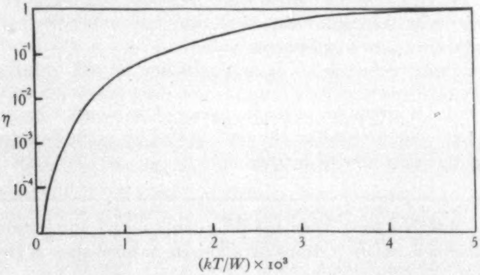

Figure 1. Electrons released per absorbed quantum, as a function of temperature.

Now the time taken by an ion to move from its normal position to its displaced position will be of the order of the period of the residual rays of the crystal, say 10^{-12} sec., which is long compared with the period of visible light. Thus, by the Franck-Condon principle, in considering the optical transitions of an electron trapped at the centre, we must consider the electron as moving in the field due to the ions at rest in their displaced positions. This field near the centre will depend on the structure of the crystal and will not be discussed here; but at large distances r it is simply the difference between the fields e/r^2 in free space and $e/\kappa r^2$ in the medium, and is thus

$$-\frac{e}{r^2}\left(1-\frac{1}{\kappa}\right).$$

If then we think of the electron as being moved quickly away from the centre, it will find itself in a field of potential energy

$$-\frac{e^2}{r}\left(1-\frac{1}{\kappa}\right) \qquad \text{......(1).}$$

This is of the same form as the field due to a positive charge, and there will therefore be excited states for an electron in this field. Hence in this case also illumination in the long-wave limit of the absorption band does not free an electron directly.

On the other hand the field represented by equation (1) is due entirely to the distortion of the lattice by the electron; in a time of the order of 10^{-12} sec. after the electron is excited, the neighbouring ions will move into new positions of equilibrium. It is possible that the heat released in this process is enough to release the electron from the centre where it is trapped. In what follows we shall see that there is some evidence that electrons can in fact be released from negatively charged centres at low temperatures.

Finally, we must add that if electrons are released from colloidal particles of metal, we do not expect any temperature dependence of η (cf. Pohl[(2)], p. 20).

§ 2. COMPARISON WITH EXPERIMENT

Alkali halides. Photoconductivity has been investigated mainly in crystals containing *F* centres. An *F* centre is probably an electron replacing a halogen negative ion in the lattice; a neighbourhood including an *F* centre is thus electrically neutral. We expect, therefore, a sharp drop in the photoconductivity as the temperature is lowered below a certain point. Such a drop, by a factor at least 10^3, is observed at about $-150°$ C. in potassium chloride for example[(2)].

Electrons released from *F* centres are trapped again to form *F′* centres, a second type of centre having an absorption spectrum further in the red. The quantum yield of the transition $F \rightarrow F'$ shows, as we should expect, the same temperature dependence as the primary photoelectric current[(2)]. According to Pohl an *F′* centre is an electron trapped at a point where there is already an *F* centre, in other words two electrons replacing a negative ion; it is therefore negatively charged. We are thus able to understand the fact reported by Pohl[(2)] that as the temperature is lowered the quantum yield of the transition $F' \rightarrow F$ retains its initial value.

Silver halides. Silver bromide is normally an insulator at low temperatures. If it is irradiated with 10^{12} quanta per cm^3, it afterwards shows electronic conductivity in the dark like a semi-conductor. This excited state is destroyed by high temperatures.

In discussing photoconductivity of silver salts, then, we must distinguish between, on the one hand, ions on the surface of cracks, etc., which give electrically neutral centres from which an electron can be released, and metastable centres where an electron is trapped in some way, giving presumably negatively charged centres.

Photoconductivity in silver halides has been investigated by Toy and Harrison[(6)]. In annealed crystals they found, as we expect, a marked drop in the current as the temperature is lowered to liquid air temperature. In unannealed crystals no drop was found, and the results obtained were not reproducible. This may be due to electrons in the negatively charged metastable positions.

These ideas may be applied to some recent results of Berg and Mendelssohn[(7)] on the sensitivity of photographic emulsions at liquid hydrogen temperatures. They find that the sensitivity of a blue-sensitive emulsion drops to 7 per cent of its value at room temperature, that of a panchromatic emulsion in filtered red light to 0·02 per cent. It is, of course, by no means certain that all of this fall in sensitivity is due to a decrease in the number of electrons released by the light. However, we can only understand the presence of any sensitivity at all at the temperature of liquid hydrogen by postulating that some of the electrons released by the blue light are in negatively charged centres. We can thus understand the much greater drop in the sensitivity of the dye-sensitized emulsion; an electron can only be released from the electrically neutral adsorbed dye molecule with the help of a quantum of radiation.

Results similar to those of Berg and Mendelssohn have been obtained by Ungar(8) who finds that with many sensitizers (eosin, pinachrom violet) the red sensitivity disappears entirely at −180°. For pinacyanol, on the other hand, the drop is not much greater than for the blue sensitivity.

Other crystals. In both diamond and in zinc blend Lenz(9) has found a large drop in the photoelectric current between the temperature of the room and that of liquid air. It has, however, been suggested(10) that the drop is due to the setting up of space charge, which should be more stable at low temperatures. Dr A. L. Reimann has, however, informed me that he has carried out experiments in zinc blend by using flash illumination and thus avoiding the setting up of space charge; he has found that the photo-induced current drops by a factor 40 between the temperature of the room and that of liquid air.*

REFERENCES

(1) PEIERLS. *Ann. Phys., Lpz.*, **13**, 905 (1932).
(2) POHL. *Proc. Phys. Soc.* **49** (extra part), pp. 3, 13, 17 and figure 12*a* (1937).
(3) HERZFELD. *Z. Phys. Chem.* **105**, 329 (1923).
(4) HILSCH. *Proc. Phys. Soc.* **49** (extra part), p. 40 (1937).
(5) GURNEY and MOTT. *Proc. Phys. Soc.* **49** (extra part), p. 32 (1937).
(6) TOY and HARRISON. *Proc. Roy. Soc.* A, **127**, 613 (1930).
(7) BERG and MENDELSSOHN. *Proc. Phys. Soc.* **49** (extra part), p. 38 (1937).
(8) UNGAR. *Z. Phys.* **106**, 322 (1937).
(9) LENZ. *Ann. Phys., Lpz.*, **77**, 449 (1925).
(10) HUGHES and DU BRIDGE. *Photoelectric Phenomena*, p. 309 (1932).

---

* I am indebted to Dr Reimann for permission to refer to his unpublished results.

THE SPECTRUM OF MANGANESE HYDRIDE, MnH

By R. W. B. PEARSE, Ph.D., Lecturer in Physics, Imperial College, London, S.W. 7 and A. G. GAYDON, Ph.D., Beit Scientific Research Scholar, Imperial College, S.W. 7

Received 13 *November* 1937. *Read in title* 11 *February* 1938

ABSTRACT. A discharge tube suitable for the excitation of band spectra of the hydrides of refractory metals which do not appear well in a vacuum arc, is described. The spectrum of manganese hydride, MnH, is described; bands have been observed in the red, yellow-green, green, blue, and blue-violet regions of the spectrum. Vibrational quantum numbers are assigned to the bands. The spectrum of MnH is briefly discussed in relation to the spectra of CaH, CrH, FeH, CoH, NiH, CuH, and ZnH.

---

§ 1. INTRODUCTION

In a previous brief publication(1) we have reported the occurrence of the spectrum of manganese hydride in a high-tension arc in a flame of burning hydrogen, and in a discharge-tube source. We have now greatly improved the design of the discharge tube and have been able to photograph the spectrum under higher dispersion. The present communication describes the new tube and gives a more detailed account of the spectrum.

§ 2. EXPERIMENTAL

The high-tension arc. In our earlier investigations of the spectra of the hydrides of the metals chromium(2), manganese, iron, cobalt and nickel(3), we used as source a high-tension arc between electrodes of the metal in a flame of hydrogen burning in air. The arc was maintained by a 5000-v. transformer with an output of 7½ kva. The hydrogen was burnt in a Meker burner with all the air-holes closed. A rapid flow of hydrogen from a commercial cylinder was used, the flame being about 10 in. in height. The burner itself served as the lower electrode, the discharge taking place from a piece of the metal, of dimensions about 5 mm. cube, which stood on a graphite cylinder 1 cm. in diameter resting on the grid of the burner; the optimum length of this cylinder varied with the metal in use, being longer for more refractory metals, but was of the order 2 cm. A long graphite rod projecting into the flame from above was used for the upper electrode, the distance between the two electrodes being about 2 cm.

This source proved capable of producing the hydrides of manganese, chromium, cobalt, and nickel, but for high-dispersion photographs exposures of several hours were necessary, during which the source required constant attention and consumed rather a lot of hydrogen. For manganese and nickel the oxide bands lie in the same region of the spectrum as the hydride bands, and at times these were strongly developed in the outer part of the flame and tended to mask the hydride bands. Moreover, at atmospheric pressure the line spectrum of the metal was rather strongly produced.

We have also tried to obtain the spectra of the hydrides of the transition elements in other sources. The usual type of arc in hydrogen at reduced pressure has proved unsuccessful, the spectrum of nickel hydride failing to appear at all in this source. A hollow cathode of the Schuler type also failed to produce the hydride bands of manganese or nickel, even when run very hot so that the line spectrum of the metal was strongly displayed and the vapour pressure was such that the metal was quickly driven from the cathode.

The necessary conditions for producing the hydride bands strongly appeared to be that there should be a fairly high partial pressure of the metallic vapour mixed with the hydrogen and a high current density of electrons of moderate velocity; in other words, they were essentially positive column conditions. An attempt was therefore made to design a discharge tube which fulfilled these requirements.

The discharge tube. The chief difficulty in using manganese in a discharge tube is the high temperature necessary to produce sufficient vapour pressure of the metal. All materials of which the tube can conveniently be made become too soft at this temperature to withstand evacuation. After various trials the design shown in figure 1 (*a*) was adopted. A wide pyrex tube T, about 70 cm. long and $3\frac{1}{2}$ cm. in external diameter, with a glass window W at one end and fitted with two large aluminium electrodes E_1, E_2, formed the main discharge tube, which was capable of carrying a large current. In the middle of this large tube a small quartz tube Q, whose shape is shown in figure 1 (*b*), formed a constriction in the positive column of the discharge. It was supported by two disks of high-melting-point steel which fitted closely to the quartz and also into the large tube; the steel disks were held together by two thin threaded steel rods. The quartz tube was about 6 cm. long and was of 10 mm. internal bore at the ends and from 3 to 5 mm. bore at the constriction. The high current-density of the discharge produced intense local heating and vaporized some of the metal, which was placed in a small depression in the middle of the capillary. The quartz, not having to stand any mechanical strain or maintain the vacuum, could be heated much more strongly than is normally possible with a discharge tube. The metal reacted to some extent with the quartz, but the product of the reaction formed a surface film which protected the rest of the tube for some time; in any case the quartz tube could easily be replaced.

The electrode E_1, nearer to the window, consisted of a piece of sheet aluminium bent into a cylinder about 10 cm. long and 3 cm. in diameter. It was supported by a steel rod screwed into it, this rod being sheathed by a length of glass tubing which was sealed into a side tube with red sealing wax. Light from the capillary of the quartz tube Q thus passed through the hollow aluminium electrode to the window. The electrode E_2, at the other end, consisted of a length of aluminium rod supported on a piece of stout tungsten wire sealed through a pyrex tube which passed through a large rubber stopper fitting into the end of the discharge tube; by removing this stopper the quartz capillary could be slid out and refilled with the metal under investigation. The whole discharge tube was placed in a wooden trough full of water, two lead weights, cast to a suitable shape, being used to sink it. The discharge was maintained by a 5000-v., 7½-kva. transformer. A slow flow of hydrogen from a commercial cylinder was passed through the tube when in use, this serving to sweep out any impurities baked out of the quartz or metal by the intense heat.

A piece of metallic manganese, in size about 2 mm. cube, was placed in the centre tube. Visual observation showed that the green system of MnH bands previously observed in the flame was strongly developed as soon as the manganese began to vaporize. The current through the tube and the pressure of hydrogen were regulated so as to bring out the bands as strongly as possible. The pressure of hydrogen was a few millimetres of mercury. As the pressure was raised the potential-drop along the capillary increased, and when this became of the same order as the cathode fall at a steel surface the current passed through the steel frame and formed an additional anode and cathode. At lower pressures the discharge passed through the capillary, which became white-hot. Moderate pressures of hydrogen seemed best for producing the hydride bands, the line spectrum of manganese being brought out strongly if the pressure was too low.

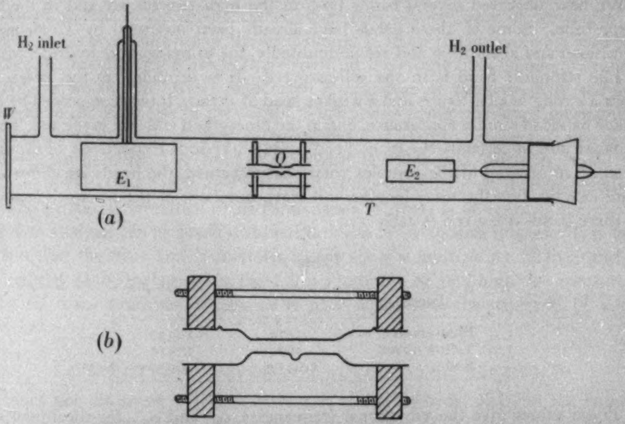

Figure 1. Diagram of the discharge tube. (*a*) General assembly; (*b*) central part drawn to larger scale.

It will be observed that the discharge tube is of robust construction and requires no elaborate glass blowing. All the parts are of simple design and may easily be replaced separately without complete dismantling of the tube. The manganese-hydride spectrum obtained in the tube was photographed in the second order of a 20-ft. concave grating, with dispersion 1·9 A./mm.; it was found that satisfactory plates could be obtained in from five to thirty minutes. The tube thus compares very favourably with the high-tension arc, for which exposures of several hours were necessary on the first order of the 20-ft. grating. The spectrum was also much cleaner, being free from oxide bands and showing less continuum at the red end. The secondary spectrum of hydrogen is present on most of our plates but this was not a serious objection for work at high dispersion. These lines could easily be identified by a comparison spectrum; they declare their origin, moreover, by their lack of sharpness due to Doppler broadening.

§ 3. DESCRIPTION OF THE SPECTRUM

We have observed several bands both in the high-tension arc and in the discharge tube. Some of these bands have already been observed by T. Heimer(4) in emission and absorption and are undoubtedly due to manganese hydride, MnH.

The strongest band is in the yellow-green. It is degraded to the violet and shows a strong head at $\lambda 5677$ and a weaker head at $\lambda 5720$. It is accompanied by two weaker bands of similar appearance, one in the blue-green and one in the red. These bands are almost certainly the (0, 0), (1, 0) and (0, 1) bands respectively of the same system. On account of the complex rotational structure, the heads are difficult to locate exactly, but the wave-lengths and wave-numbers of the stronger heads of the three bands are given in table 1:

Table 1

Band	λ	ν
Blue-green	5172	19330
Yellow-green	5677	17610
Red	6237	16030

These values give the vibrational frequencies, ω_0' and ω_0'', for the initial and final electronic states as 1720 and 1580 cm^{-1}. Values of these constants for neighbouring elements of the periodic table are presented together in table 2 for comparison:

Table 2

Hydride	ω_0'	ω_0''
CaH(5)	1333	1299
MnH	1720	1580
NiH	1493	(1900)*
CuH(6)	1611	1866
ZnH(7)	1824†	1552
ZnH$^+$(8)	1337	1832

* Calculated from the molecular constants *B* and *D*. † Own measurements from heads.

There is also a strong band in the blue. This is degraded to the red and shows heads at $\lambda 4741$ and $\lambda 4794$; it is presumably the (0, 0) band of another system. Five strong branches stretch towards the red from this band, and have a spacing which suggests that they are of *P* form. The appearance of the band strongly suggests the presence of *Q* branches, and from the occurrence of the five *P* branches it seems that the electronic states involved probably have a multiplicity of five. Until the rotational analysis is complete it is impossible to state the electronic transition definitely, but it is quite likely to be either $^5\Pi \rightarrow {}^5\Sigma$ or $^5\Sigma \rightarrow {}^5\Pi$. We have already⁽²⁾ briefly discussed the likely electronic states of MnH and either of these transitions seems quite probable on a priori grounds.

There is also a much more open type of band in the blue-violet; the appearance of this structure is best seen from the plate. The band is degraded to the red, but no head has been observed. The strong lines fall into five branches, but these are very erratic and are probably strongly perturbed. These branches close up towards the violet, so that in the region λ4480, where they become weak or are absent, the separation between the lines of the same branch is about 16 cm^{-1}, which would seem to indicate that the origin lies in this region. If the strong lines belong to branches of *P* form we should expect to observe *R* branches of approximately the same strength on the other side of the origin. Some strong manganese lines unfortunately make observations difficult in this region, but it is hard to believe that five strong branches do lie here. The band is somewhat of an enigma, but it is hoped that analyses of the other bands may ultimately throw some light on its interpretation.

The rotational structure of all these bands of MnH is of unusual complexity, and if an analysis can be made it should prove to be of unusual interest. It is fairly certain that the blue and blue-violet bands show a multiplicity of five, and the multiplicity of the yellow-green band also appears to be very high; we are thus led to expect many branches of unusual form in addition to the strong *P*, *Q*, and *R* branches.

§4. SPECTRA OF HYDRIDES OF RELATED ELEMENTS

Since our discovery of the spectrum of nickel hydride, NiH, in the flame of hydrogen containing nickel carbonyl vapour, spectra of the diatomic hydrides of several related elements have been obtained.

With chromium we have observed a band in the region λ3600–3700 which we attribute to CrH. It was obtained with the high-tension arc-in-flame source described in the introduction. Bands attributed to cobalt hydride have been observed by A. Heimer⁽⁹⁾ at Stockholm. The (0, 0) band is in the region λ4492 and is degraded to the red. A band at λ4288 attributed to iron hydride, FeH, has also been reported by A. Heimer⁽¹⁰⁾. The band is designated $^1\Sigma \rightarrow {}^1\Sigma$ in this report, but this is presumably a misprint, for FeH, having an odd number of electrons, must show an even multiplicity.

These elements of the third period of the periodic table all show roughly the same binding energy and stability when they form diatomic hydrides. These elements, and also zinc in the next row, in their unexcited states all have the electronic configuration $1s^2\,2s^2\,2p^6\,3s^2\,3p^6\,3d^n\,4s^2$, where *n* takes the values 0, 4, 5, 6, 7, 8, and 10 for the elements calcium, chromium, manganese, iron, cobalt, nickel, and zinc respectively. The configuration $3d^9\,4s^2$ in the series belongs to copper, but in this case it is not the normal state, for one of the 4*s* electrons falls back into the *d* shell giving $3d^{10}\,4s$; this configuration puts copper with the monovalent elements of group I, but excitation to $3d^{9}\,4s^{2}$ would bring copper into the series we have been considering and so it should show relationship with iron, cobalt, and nickel. Thus it seems likely that for these elements the binding with the hydrogen atom is due chiefly to the electrons in the 4*s* shell and that the unfilled 3*d* shell is relatively unimportant apart from its effect on the multiplicity of the spectral terms. The molecular constants for some of these hydrides have not been calculated yet, so a quantitative comparison of the binding forces cannot be made at present, but if such a comparison could be made it might well increase our knowledge of the general problem of the binding forces in diatomic molecules.

§5. DESCRIPTION OF PLATES

Plate 1. (*a*) and (*b*) are the spectrum of MnH as obtained in the high-tension arc in hydrogen flame and photographed on a glass prism spectrograph with an exposure of 20 min.; (*c*) is an enlargement of the blue band of the same spectrum; (*d*) is an enlargement of the yellow-green band.

Plate 2 shows the spectrum of MnH as obtained in the discharge tube, photographed in the second order of a 20-ft concave grating, with an exposure of 18 min. (*a*) and (*b*) are the violet band, and (*c*), (*d*) and (*e*) the blue band. In (*e*) the five strong branches which are probably of *P* form are indicated.

REFERENCES

(1) Pearse, R. W. B. and Gaydon, A. G. *Nature, Lond.*, **139**, 590 (1937).
(2) Gaydon, A. G. and Pearse, R. W. B. *Nature, Lond.*, **140**, 110 (1937).
(3) Gaydon, A. G. and Pearse, R. W. B. *Proc. Roy. Soc.* A, **148**, 312 (1935).
(4) Heimer, T. *Naturwissenschaften*, **24**, 521 (1936).
(5) Grundström, B. *Z. Phys.* **69**, 235 (1931).
(6) Frerichs, R. *Z. Phys.* **20**, 170 (1923).
(7) Hulthén, E. *C.R. Acad. Sci., Paris*, **173**, 524 (1921).
(8) Bengtsson, E. and Grundström, B. *Z. Phys.* **57**, 648 (1930).
(9) Heimer, A. *Naturwissenschaften*, **24**, 413 (1936).
(10) Heimer, A. *Naturwissenschaften*, **24**, 491 (1936).

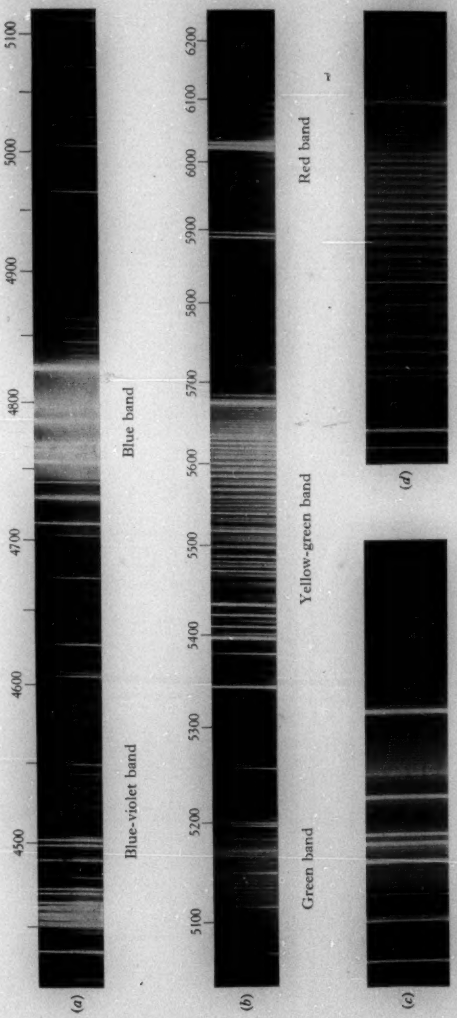
(a)
(b)
(c)
(d)
Blue-violet band
Blue band
Green band
Yellow-green band
Red band
4500
4600
4700
4800
4900
5000
5100
5100
5200
5300
5400
5500
5600
5700
5800
5900
6000
6100
6200

Plate 1. The spectrum of MnH as obtained in the high-tension arc.

PHYSICAL SOC. VOL. 50, PT. 2 (R. W. B. PEARSE AND A. G. GAYDON)

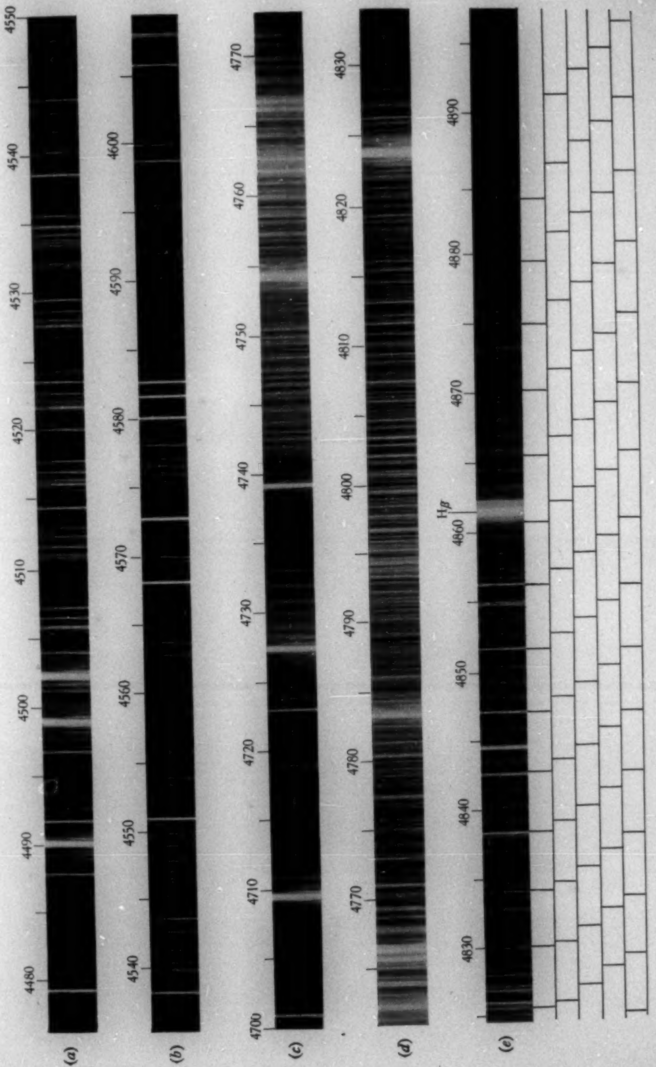

Plate 2. Spectrum of MnH as obtained in the discharge tube.

To face page 206

THE SPARKING POTENTIAL OF MERCURY VAPOUR

By F. LLEWELLYN JONES, M.A., D.Phil.

AND

W. R. GALLOWAY, B.Sc., University College, Swansea

Received 19 *April* 1937, *in revised form* 17 *November* 1937.
Read in title 28 *January* 1938

ABSTRACT. The sparking potential of mercury vapour between parallel electrodes previously degassed at about 750° C. was measured throughout a wide range of vapour densities, and the influence of the material of the cathode on the sparking potential was examined. The sparking potential was found to be almost a linear function of ρd from about 500 to 5000 V. where ρ, d are the density of the vapour and the distance between the electrodes, respectively. The minimum sparking potential was measured for a nickel cathode, a steel cathode, and when the cathode was covered with a film of mercury; and the potentials were found to be 400, 380, and 305 V. respectively.

§1. INTRODUCTION

The measurements of the sparking potential of pure monatomic gases is of interest in the general theory of the conduction of electricity in gases owing to the relative simplicity of the molecule in its reaction with the colliding electrons. Further, it appears to be a general rule that, except in the case of helium, the minimum sparking potential increases with the atomic number of the gas, and that the corresponding value of pd decreases, where p is the pressure of the gas and d is the distance between the electrodes. This paper describes experiments carried out with mercury vapour in order to find whether this gas has the same general electrical properties as the noble gases in spite of its lower ionization potential. The measurements were extended to pressures of one atmosphere because high pressure mercury vapour discharges have recently found industrial application. Consequently it is of interest to find whether any change in the nature of the primary ionization process is indicated by the sparking-potential curve. For instance, the presence of minute traces of impurity in certain monatomic gases containing a high concentration of metastable atoms causes marked changes in the slope of the sparking curve when the relative importance of the different processes of ionization changes(1).

Again, if the nature of the cathode surface plays a predominant role in the maintenance of a discharge current however small, whether as a result of the bombardment of positive ions or of metastable atoms or to the incidence of radiation from the current, then the sparking potential will depend on the work function of the cathode surface, and it should have different values with different cathode surfaces. In many previous investigations, particularly with the permanent gases, the measurements have been found to be almost independent of the nature of the cathode surface, but this conclusion is of doubtful validity owing to the neglect of the complete out-gassing of the cathode. Gas layers on the cathode probably make all metals behave as if they have the same work function, and it is therefore improbable that any difference would be observed for different metals if they had layers of the same gas on their surfaces.

§2. DESCRIPTION OF THE APPARATUS

The type of discharge tube used is illustrated in figure 1. The electrodes consisted of disks 3·8 cm. in diameter and about 1 mm. thick, having their edges bevelled to avoid sharp points. One electrode was made of nickel and the other of Staybrite steel. They were highly polished and, together with the tungsten wires for the seals, they were heated in vacuo at a temperature of about 750° C. for many hours before they were fixed in the tube. The distance between the electrodes was 2·55 mm. and the ratio of the diameter to the distance apart was about 15, so that the field between them could be regarded as uniform(2).

When the tube was complete it was maintained at a temperature of 400° C. for some days while it was continuously evacuated with a diffusion pump and the usual liquid-air traps.

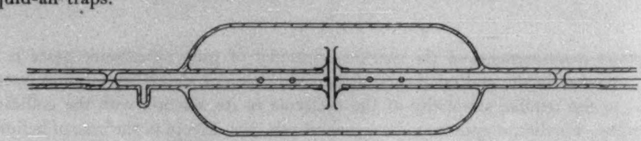

Figure 1.

In order to raise the density of the mercury vapour to any desired value the tube was placed inside an electric furnace. The temperature inside was indicated by a mercury thermometer so placed that its bulb was as near as possible to the electrodes when the discharge tube was in position. The whole of the tube, including the seals, was maintained at the same temperature, while the discharge itself was observed through a window. This was made of steel tube 1 cm. in diameter screwed into the wall of the furnace; and it contained a short glass rod extending perpendicularly from the discharge tube to the outer case of the furnace, and the small space around the rod was tightly packed with asbestos. It was found that this method of conducting the light from the spark involved the minimum cooling of the part of the tube opposite the window.

Up to 500 V. the high-tension supply was derived from a battery of small accumulators, but for higher potentials up to 6000 V. the supply was obtained by rectifying and smoothing adequately the output from a step-up transformer. The potential difference across the electrodes was measured by means of a milliammeter in series with a 4-MΩ resistance, and also by means of an electrostatic voltmeter.

§3. EXPERIMENTAL PROCEDURE

In some experiments the spark was detected by an electrometer method in which the total charge passed between the electrodes was exceedingly small, but it was found that the same results were obtained by a simpler method—that of observing the glow when there was a resistance of 16 MΩ. in series with the tube.

The vapour pressures of the mercury at the various temperatures T were obtained from tables$^{(3)}$, and the curves were drawn to show the variation of the sparking potential V with the pressure p. Initial experiments revealed that the curves taken while the temperature of the tube was rising did not coincide with those obtained while the temperature was falling. This was due to a small lag between the thermometer reading and the actual temperature of the discharge tube. Thus, when the temperature was rising the thermometer was slightly warmer than the vapour, and when the temperature was falling the thermometer was slightly cooler than the vapour. The method adopted in order to obtain the temperature of the vapour corresponding to the potential V was as follows. It was assumed that the temperature lag was the same whether the tube was warming up or cooling down (and any error introduced in this way is not serious); then for any given sparking potential the corresponding temperature of the vapour was obtained by taking the mean of the two temperatures recorded during the heating and cooling. A very large number of runs were made with many different tubes over a period of some months, and all the results obtained by this method were found to be the same within the experimental error. This was greatest at the highest temperature and it was then about 3 per cent.

§4. THE MINIMUM SPARKING POTENTIAL

The measurement of the minimum sparking potential is of interest because in this region any errors in the determination of the gas pressure are of no account, consequently changes in the sparking potential due to changes in the cathode surface are more easily seen. During the preliminary measurements it was noticed that the minimum was about 80 volts lower when the temperature was rising than when it was falling. This difference could not of course be attributed to any change of pressure during the rise and fall of the temperature, and it was found that the lower minimum was the same whatever metal was used as cathode. Further, the difference was only obtained under certain conditions, and those were conditions under which it was expected that mercury would be condensed on the electrodes; for example when the cold tube was heated from room temperature to about 180° C. a film of mercury was seen to condense on the electrodes. On the other hand, when it was certain that the mercury would be all evaporated from the electrode surfaces the lower value of the minimum sparking potential was not obtained. The lowest value of the minimum sparking potential must therefore be attributed to the observed film of mercury condensed on the cathode surface. This film could be removed simply by heating the glass tube near the electrodes with a blow-lamp. Moreover, if the tube was heated first to 360° C. and then allowed to cool to about

180° C. the electrodes were slightly warmer than the glass and no film was observed to condense; the electrodes remained bright. Tubes which had been in use for some time were treated in this way, and the electrodes were also heated by passing a discharge between them before sparking curves in the region of the minimum were taken. Further, new tubes were constructed from which all mercury was excluded during the out-gassing process by means of liquid-air traps, and the sparking potentials were measured immediately after the pure mercury had been introduced and the tube sealed off. After a number of measurements made in this way, the highest reproducible value of the minimum sparking potential thus obtained was taken as the value for the clean electrode. These values* were: 400 V. for the nickel

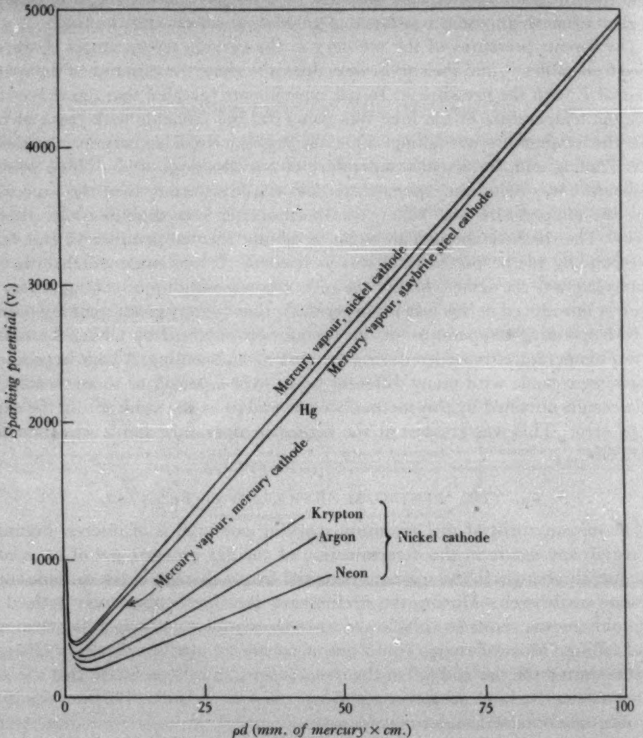

Figure 2.

---

* A preliminary account of these results was published in *Nature*(4) in December 1936.

cathode, and 380 v. for the Staybrite steel cathode. By warming up the cold discharge tube to about 180° c. the electrodes were covered with a film of mercury, and with each electrode in turn as cathode the minimum sparking potential was found to be 305 v.

§5. DISCUSSION OF THE RESULTS

The correct spark parameter is the product of the distance d between the electrodes and the density ρ of the vapour. As the temperature of the vapour rises both the density and the mean energy of agitation of the atoms increases. However, even at 360° c. the mean energy of the atoms is so small compared with that of the electrons that any effect on the ionization can be neglected. The parameter here adopted is the product of d and the pressure p at which a permanent gas at a temperature 15° c. would have the same density as the mercury vapour at a temperature T° c. This pressure is easily found from the saturation vapour pressure of the mercury by multiplying by $(273+15)/(273+T)$, assuming that association is negligible. This parameter then facilitates comparison of the sparking curves for mercury with those published for the permanent gases. The V, pd curves for nickel and steel cathodes are given in figure 2, from which it can be seen that V is practically a linear function of pd from about 500 to 5000 v. The value of pd at the minimum was 1·2 while at the highest vapour density used pd was 100 and V was nearly 5000 v.

For comparison the sparking curves for the noble gases near the minimum potentials are also given in figure 2, and for these we are indebted to Dr S. P. MacCallum. It can then be seen that mercury vapour has the same general sparking characteristics as these gases, in that the minimum sparking potential increases and the corresponding value of pd decreases as the atomic number of the gas increases; except in the case of helium.

The various values of the minimum sparking potential for mercury show that they are characteristic of the metal of which the cathode is made only if it has been out-gassed. This dependence of the minimum on the cathode surface affords definite evidence in support of the view that the cathode plays an important role as a source of electrons in maintaining a discharge current.

§6. ACKNOWLEDGEMENTS

We wish to express our best thanks to the Department of Scientific and Industrial Research for a grant made to one of us (W. R. G.) during these investigations, and to Prof. E. J. Evans for extending to us the facilities of his laboratory.

Note added in proof. Since this paper was communicated, values of the minimum sparking potential of mercury vapour have been published by R. Grigorovici(5). There is general agreement between his results and ours, but for a clean iron cathode he found a minimum potential of 520 v., and with the cathode covered with mercury a potential of 330 v. was obtained. These compare with the lower values of 380 v.

and 305 v. respectively which were given by us⁽⁴⁾. Grigorovici considered that his higher values were due to the incomplete degassing of the electrodes in his experiments, but it appears to us that the difference might be partly due to nonuniformity of the electric field between those electrodes. It is well known that the sparking potential of the monatomic gases varies considerably with the ratio of the diameter of the electrodes to their distance apart when this ratio is less than 10. If the ratio is too low the sparking potential is raised in order to make good the loss of ionization due to the diffusion of the electrons into weaker parts of the field. Because this diffusion is very marked in monatomic gases the value of 15 was adopted for the ratio in our experiments.

REFERENCES

(1) Penning, F. M. and Addinck, C. C. J. *Physica*, **1**, 1007 (1934).
(2) MacCallum, S. P. and Klatzow, L. *Phil. Mag.* **17**, 291 (1934).
(3) *International Critical Tables*, **3**, 206.
(4) Jones, F. Llewellyn and Galloway, W. R. *Nature, Lond.*, **138**, 973 (1936).
(5) Grigorovici, R. *Bull. Soc. Roumaine Phys.* **38**, No 68, p. 7 (1937).

A NOTE ON NUCLEAR SELECTION RULES

By C. D. ELLIS, F.R.S.

Received 29 *October* 1937. *Read in title* 26 *November* 1937

ABSTRACT. Experiments have been made to determine the intensity of a γ ray of 3·2 MV., suspected to be emitted by ThC″–Th.Pb, by comparing the number of recoil protons from deuterium with those due to the well known γ ray of 2·62 MV. It appears most probable that between one and three quanta are emitted in every hundred disintegrations. This result is shown to lend support to the view that it is practicable to assign to the various nuclear states experimental spin values which can be used consistently in different sets of selection rules.

§ 1. THE NUCLEAR SELECTION RULES

In the present state of theory there are two important nuclear selection rules, one governing transitions of an excited nucleus, the other the disintegration of a nucleus with the formation of the product nucleus in one of its excited states. Both of these rules are expressed by assigning spin values to the various states and relating the probability of a given change to, in addition to other factors, the change of spin occurring in the process. The present note deals with the criteria which determine the probability of radiative changes of an excited nucleus. There are good theoretical grounds for considering such changes to be permitted as involve a spin-change of either 1 unit, 2 units, or zero, zero to zero being forbidden. A direct experimental method for determining whether the spin-change is 1 unit (for a dipole transition) or 2 units or zero (for a quadripole transition) is provided by observation of the internal conversion coefficient, which is always greater for a quadripole transition. In this way it is possible to assign a set of relative spins to the various excited states of a nucleus. To take a particular case, the level-system of Th.Pb is shown in the figure(1) with the spin-values, the energies of the states, and the relative excitations that arise from the disintegration ThC″ → Th.Pb. It should be mentioned that these spin-values not only account for the formation and transitions of Th.Pb but also form part of a consistent scheme covering all the four bodies ThC, ThC′, ThC″ and Th.Pb. It was a matter therefore of some importance when various workers obtained indications of the emission of a γ ray of about 3·2 MV. corresponding to the transition from the uppermost to the lowest level, since in this case the spin-change of 3 units should forbid the transition or at least make it extremely improbable.

§ 2. PREVIOUS INVESTIGATIONS

The first indications of this γ ray were obtained by Chadwick, Blackett and Occhialini(2) when they were investigating with a cloud chamber the production of positron-electron pairs from lead by the γ rays of ThC″. They observed a few tracks having energy slightly too high to be associated with the main 2·62-MV. γ ray X, but while suggesting the possibility that these were due to the 3·2 MV. γ ray they yet pointed out that errors of measurement or unrecognized deflections of the tracks might have been responsible.

Alichanow, Alichanian and Kosodaew(3) analysed the energies of the electrons liberated from lead, using semicircular magnetic focusing and counters. Their main curve could be accounted for by the known γ rays, but beyond the tail of the spectrum due to the 2·62-MV. γ ray they found a small hump in the region of 3·2 MV. The effect seemed to be very slight and only of the magnitude of possible probability-fluctuations.

Simons and Zuber(4), although they are careful not to overstate their result, appear to have obtained indications that this γ ray is considerably more intense. They used a cloud chamber containing in turn argon and methyl iodide to investigate the production of positron-electron pairs, and they concluded that "if it be assumed that all the pairs of total energy greater than 2·0 MV. arise from this radiation, then it follows that there may be 0·12 ± 0·06 quanta of this higher energy per quantum of the lower energy (2·63 MV.)".

There seems little doubt that this 3·2-MV. γ ray has been detected, but the data as to its intensity are unsatisfactory. Since it is just this point that has such an important bearing on the applicability of the nuclear selection rules, it seemed worth while to attempt to obtain additional information. The results of the present experiment, while compatible with a weak intensity, render it improbable that the number of quanta of the 3·2-MV. γ ray is more than about 2 per cent of the 2·62-MV. γ ray.

§ 3. THE PRESENT EXPERIMENTS

The method of investigation chosen was to use the disintegration of the deuteron. It is well known that γ rays of energy greater than about 2·2 MV. lead to the disintegration of this nucleus, the proton and the neutron sharing approximately the excess energy. Thus the 2·62-MV. γ ray of ThC″ gives recoil protons of about 0·2 MV. energy and these can be recorded by means of a suitable ionization chamber attached to a linear amplifier. The 3·2-MV. γ ray should give recoil protons of about 0·5 MV., that is kicks of more than twice the size. In addition, since in this region the probability of disintegration increases with the excess energy, the method should be more sensitive to the γ ray of higher frequency. Certain factors had to be considered in the design of the ionization chamber. In deuterium at atmospheric pressure the ranges of the two types of recoil protons would be about 1·4 and 3·8 cm., and unless the linear dimensions of the ionization chamber were large compared to these there would be a high probability of a proton hitting the side of the chamber before it had completed its full range. There are many disadvantages in using a very large chamber, so it was decided to fill the chamber with a mixture of 40 per cent of deuterium and 60 per cent of carbon dioxide, which has about the stopping power of air. In this mixture the ranges are approximately 3·3 and 8·6 mm. The collecting electrode was in the form of a plane grid of diameter 6 cm.

arranged midway between two plane electrodes also of 6 cm. diameter, and each electrode was at a distance of 3 cm. from the grid. This electrode system defining a cylinder 6 cm. in diameter and 6 cm. long was contained in an earthed brass box 12 cm. in diameter and 10 cm. long. With 4000 V. applied between both extreme electrodes and the grid there was an approximately uniform collecting field of 1300 V./cm.

A radiothorium source of 2·7 millicuries was placed at a distance of 16 cm. from the centre of the ionization chamber and surrounded with lead, the thickness of which in different experiments was varied between 1 and 3 cm. The number of ions corresponding to a given size of kick had been previously determined by using α particles of known range. The size of the proton kicks due to the 2·62-MV. γ ray were found to correspond to an energy of 0·24 MV. with an uncertainty of about 20 per cent, and this is in rough agreement with previously known data. The number of such kicks observed in different experiments was consistent with the various degrees of filtering of the γ rays, and the total number agreed approximately with that calculated from the cross-section of the deuteron.

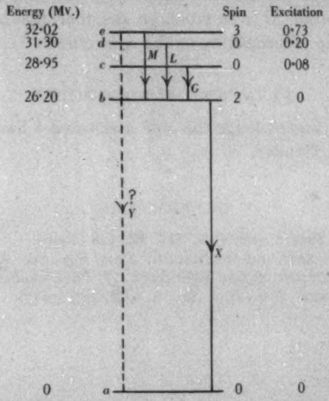

The overall amplification of the recording system was varied several times, but in each experiment a careful search was made for kicks of the size to be expected from a 3·2-MV. γ ray. Observations were made for a total time of 4 hours, during which 400 disintegrations due to the 2·62-MV. γ ray occurred, and the natural effect with the source removed was also measured for an equal period of 4 hours. In a region ± 10 per cent on either side of the size expected from the 3·2-MV. γ ray there were 29 kicks without the source and 33 with the source. Taking a wider range of ± 20 per cent there were 50 kicks without and 56 with the source. These figures are sufficient to make it very improbable that the 3·2-MV. γ ray has 5 per cent of the intensity of the 2·62-MV. γ ray, for in that case, when account is taken of the greater probability of absorption and small correcting factors there should have been about 29 extra kicks. Considering this experiment and the other evidence as a whole we may conclude that it is most probable that between 1 and 3 quanta of the harder γ ray are emitted for every 100 quanta of the main 2·62-MV. γ ray.

Reference to the figure will show that there is a γ ray M of energy 0·58 MV. which is due to a transition also starting from the uppermost level. Since its intensity, in quanta, is 0·7 of that of the 2·62-MV. γ ray, we can conclude that it is about fifty times more intense than the 3·2-MV. γ ray which is also associated with the same initial level. The probability of a transition will involve, among other factors, the frequency of the radiation emitted, in the sense of rendering more probable the emission of the higher frequency. That in spite of this the intensity of the permitted transition M is so much greater than that of the forbidden one Y is a strong proof of the practicability of the spin criteria.

§ 4. ACKNOWLEDGEMENT

It is a pleasure to acknowledge the able assistance I have had in these experiments from Mr R. D. Gander.

REFERENCES

(1) Oppenheimer. *Proc. Camb. Phil. Soc.* **32**, 328 (1936).
(2) Chadwick, Blackett and Occhialini. *Proc. Roy. Soc.* A, **144**, 235 (1934).
(3) Alichanow, Alichanian and Kosodaew. *J. Phys. Radium*, **7**, 163 (1936).
(4) Simons and Zuber. *Proc. Roy. Soc.* A, **159**, 383 (1937).

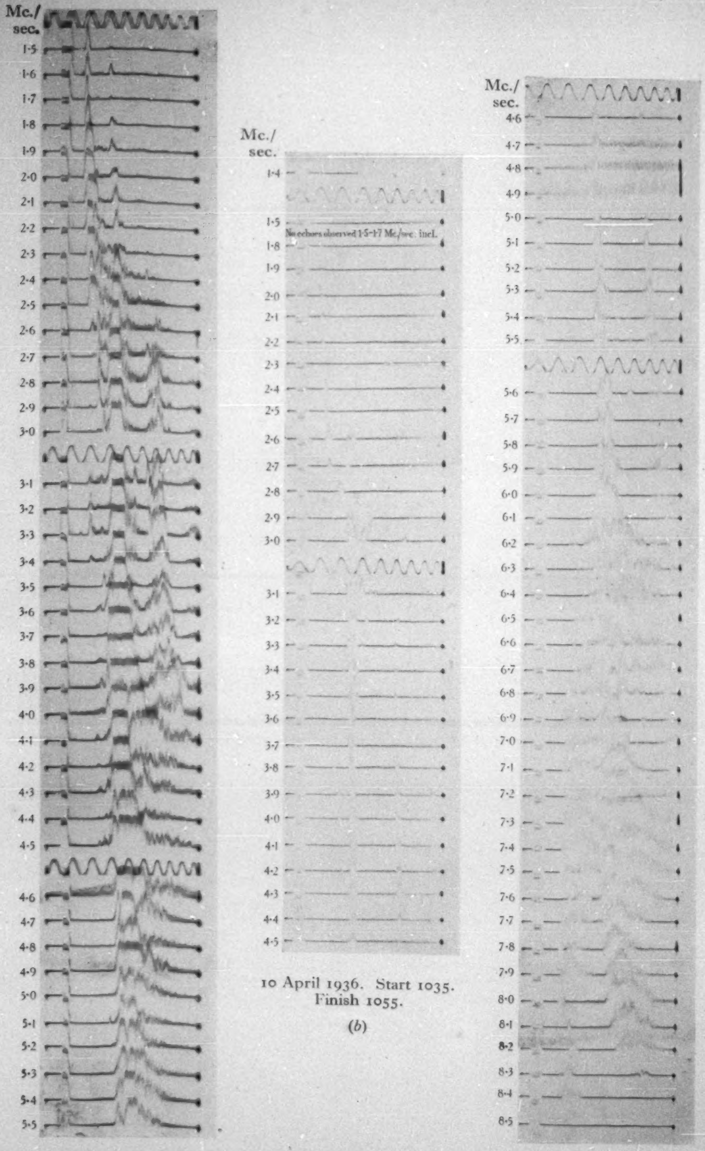

7 February 1936.
(*a*)

10 April 1936. Start 1035.
Finish 1055.
(*b*)

10 April 1936.
(*c*)

Plate 1.

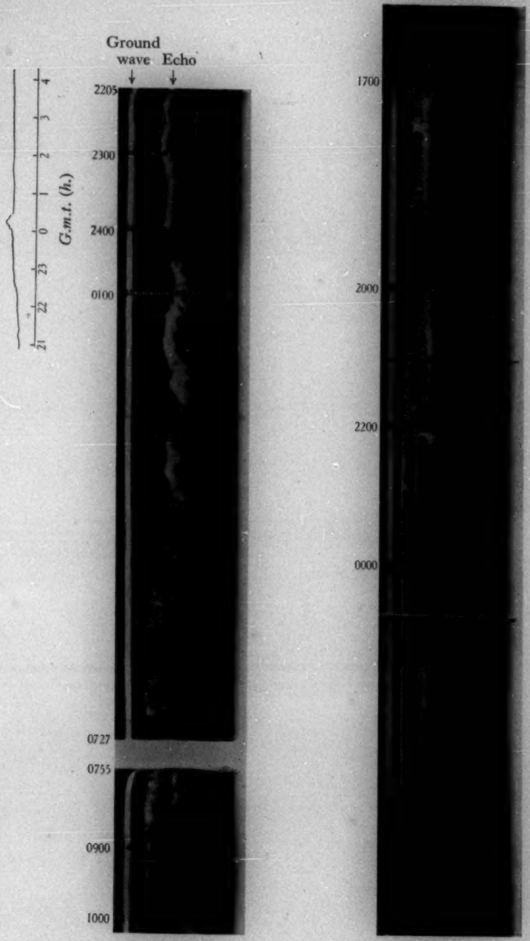
Ground wave
Echo
G.m.t. (h.)
4
3
2
1
0
23
22
21
2205
2300
2400
0100
0727
0755
0900
1000
1700
2000
2200
0000

21/22 January 1936.
(*d*)

9/10 June 1936.
(*e*)

Plate 2.

To face page 217

HIGH-LATITUDE RADIO OBSERVATIONS

By A. B. WHATMAN, B.A., Royal Corps of Signals

AND

R. A. HAMILTON, B.A., Harmsworth Scholar,
Merton College, Oxford

Received 10 *September* 1937. *Read in title* 28 *January* 1938

ABSTRACT. Observations were made on the ionosphere for nearly a year at 80° 23′ N., 19° 31′ E. It was found that at local noon the E region was present throughout the winter except on a few days which were magnetically disturbed. The electron-density in this region is at a minimum at midwinter and a maximum at midsummer. The F_1 region is observed at noon only during the summer months with maximum electron-density at midsummer. The annual variation of maximum ionization in the F_2 region is irregular and not very great, but the electron-density is at a maximum in spring and in late autumn. The diurnal variation of electron-density in the F_2 region is more marked in the dark period, with a day to night ratio of 2·3 : 1, than in the summer solstice period when the ratio is 1·5 : 1. This latter figure which is also the ratio for the E and F_1 region is in fair agreement with the ratio of 1·63 : 1 deduced theoretically on the assumption that the ionizing power is proportional to the altitude of the sun. In all cases the minimum is near midnight with maxima before and after noon and a subminimum near noon.

The effect of magnetic storms is to increase the electron-density in the absorbing region below the E region and, in the summer, to reduce markedly the electron-density in the F_2 region. Reflections from the persistent E region persist to very high frequencies especially between 1200 and 1800 G.m.t.

An intense E region, with a high reflection coefficient, occurs at all seasons during magnetically quiet conditions, and occurs almost solely between 1400 and 2300 G.m.t.

No special conditions in the ionosphere obtain when the aurora is overhead, and absorption is not usually markedly increased under such conditions.

§ 1. INTRODUCTION

The Oxford University Arctic Expedition, 1935–1936, to North-East Land provided an opportunity for carrying out research on the ionosphere, the special interest of working in such a high latitude being that during the winter for 127 days at sea-level the sun is below the horizon, and therefore during this period each region in the upper atmosphere is cut off from the direct effect of ultraviolet light and uncharged corpuscular radiation, except for such radiation as has already passed through lower regions of the atmosphere. Further, North-East Land is to the north of the zone of maximum auroral frequency. The only ionospheric observations previously made north of this zone were those of de Bruine at Angmagssalik during the polar year 1932–1933.

The expedition was given generous support by the Royal Society, by Oxford

University, the Royal Geographical Society, and other Societies. With the help of Prof. E. V. Appleton and of officers of the Radio Research Station at Slough, and with the benefit of the results (then unpublished) of the British Expedition to Tromsö during the international polar year, the following programme was drawn up, with a view to collaborating with the Union Radio Scientifique Internationale, so that the best results might be obtained: (*a*) a $\{P', f\}$* observation at local noon every day; (*b*) a $\{P', f\}$ observation at each hour of the international days fixed by the Union Radio Scientifique Internationale; (*c*) continuous $\{P', t\}$† recording as often as possible (on 2·6 Mc./sec. during the summer, and on 1·0 Mc./sec. during the dark period); (*d*) a number of $\{P', f\}$ observations during strong magnetic storms; and (*e*) $\{P', f\}$ observations on the solar eclipse on 19 June 1936, in accordance with the programme arranged by a subcommission of the Union Radio Scientifique Internationale.

Owing to the difficulty of transporting sufficient petrol, the number of $\{P', t\}$ records was limited to two observations per fortnight—on the two days preceding each international day—and continuously for a week at each of the equinoxes. Unfortunately it was not possible to take a self-recording magnetograph, and although we converted the Benndorf self-registering electrometer into a magnetograph it was not very sensitive, and it worked for only part of the season. Instead of (*d*), therefore, observations were made during clear days when the aurora was visible directly overhead. Further, owing to the unexpectedly high critical frequencies obtained, we were forced to economize in oscillograph recording paper by making observations only every 2 hr., instead of every hour, during international days. Otherwise the programme was carried out as planned, from 30 August 1935 to 13 August 1936. The results of the observations on the solar eclipse have been published elsewhere(1).

§ 2. EQUIPMENT, ETC.

The base hut in which the research was carried out was established on a rocky promontory in Brandy Bay at 80° 23′ N., 19° 31′ E.

The Breit and Tuve pulse method was used. The power was supplied by a 1-kVA., 230-v., 50-c./sec. alternator, driven by a 2-b.h.p. Petter engine, which was governed and provided with a heavy flywheel that reduced the cyclic variation to 1 in 250. A frequency-meter provided a check on the supply frequency. Interference-suppression devices were fitted to the ignition, and commutator and slip-ring devices to the alternator.

The transmitter, similar to that used by Ratcliffe and White(2), was housed in a small hut about 80 yd. from the main base hut, and was in telephonic communication with it. Its power was 75 w.

The aerials were horizontal dipoles with twin wire feeds. The aerials proper, as opposed to the feeders, were cut to resonate at 3·0 Mc./sec., but the feeders themselves were cut to suit the topography of the site. Thus, the feeders for the sending aerial were about 25 ft. long, and those for the receiving aerial were about 60 ft. long. No attempt was made at impedance-matching for any particular frequency, and there probably was not much frequency-discrimination in the combined system. The aerials were each supported on three 30-ft. masts, and the central dip in each span was about 5 ft. The effective height was very low. The ground underneath consisted of boulders and sheets of rock. At a distance of less than a quarter of a mile there was a 1000-ft. cliff, rising to a mountain 1500 ft. high.

---

* $\{P', f\}$ refers to a curve plotted to show the relation between the equivalent path P' followed by the atmospheric waves, and the frequency f.

† $\{P', t\}$ refers to a curve plotted to show the relation between the equivalent path P' followed by the atmospheric waves, and the time t.

The receiver was in the main base hut. It was almost the same as that used at the Radio Research Station at Slough(3).

For a $\{P', f\}$ observation the frequency of the transmitter was increased in steps of 0·1 Mc./sec. from 0·8 Mc./sec. up to the frequency on which echoes were no longer received. Coil-changes were made four times, so that it took about 20 min. to complete a record, and frequently on occasions of high critical frequency (necessitating changing the recording paper in the camera) it might take half an hour to complete the record. This was a considerable disadvantage, as frequently the conditions were changing with great rapidity. The length of the time base corresponded to an equivalent height of 700 to 1000 km. The camera was in the dark room, the lens and shutter being fixed in the wall which separated the two rooms. The drum was controlled from the living room, and for the $\{P', t\}$ records was driven by a clock, so that the paper-speed was about 4 cm. per hour.

The angle of dip of the earth's field was 82·5°, and the total field $0·53 \pm 0·02$ gauss, corresponding to a gyrofrequency of 1·49 Mc./sec.

The only difficulties encountered were with the insulation during the summer thaw and with the thyratron, which frequently did not strike within half an hour of switching-on, when the temperature was below zero Fahrenheit. We used, therefore, always to keep a warm-jacketed thyratron in the base hut, and on being substituted for the cold one it would strike at once.

§ 3. RESULTS

General results. It might be expected that at a latitude where the sun is below the horizon for 4½ months during the winter and above it for 4½ months during the summer the conditions in the ionosphere might be very different from those obtaining in lower latitudes. In general, however, the same ionized regions are observed in North-East Land as elsewhere. The E region which is observed almost always at noon is of three types: (1) The normal E, returning an undistorted echo which shows group retardation near the critical frequency, and does not reflect energy emitted at higher frequencies; (2) intense E, with a very high reflection coefficient, giving echoes up to the seventh order or more; and (3) persistent E, with a small reflection coefficient giving a sharp echo which shows no group retardation at its critical frequency, but is partially reflecting to pulses of a higher frequency.

An F region is always present: F_1 is absent in the winter, and F_2 absent only during very disturbed conditions in the summer, when F_1 is present. Very occasionally a distinct G region is visible above F_2.

Reflections from the low D region, observed by Mitra and Syam(4), were not observed. On 19 March 1936, at local noon, an echo was observed at an equivalent height of 55 km. on 2·8 Mc./sec. This is the only occasion on which an echo was observed below 85 km., and echoes below 95 km. were rare. In addition, echoes of an irregular type are liable to be seen in great numbers at random heights at any time and on any frequency.

It is not easy to define exactly these three different types of E region, but on examining the $\{P', f\}$ or $\{P', t\}$ records there is never any doubt as to which class an echo belongs. The normal E region has a reflection coefficient of the order of 0·1 to 0·2, the echoes show slight group retardation near the critical frequency and are not visible on higher frequencies: intense E region has a reflection coefficient of the order of 0·7 to 0·8 and usually persists as a partial reflector on frequencies above the critical frequency with a reflection coefficient which decreases as the frequency increases. Persistent E region has a reflection coefficient of the order of 0·1 or 0·2 below its critical frequency, but above it it has so small a reflection coefficient that though the first echo is at the saturation level there is no trace of a second echo; in other words, the reflection coefficient is not greater than 0·01.

It must be emphasized that the difficulties encountered in analysing the records are very great, especially in winter, and it is necessary to state here the criteria used in determining the critical frequencies. It often happens that after a few observations, 0·1 Mc./sec. apart, of a sharp single E echo, an echo is obtained which has apparently been reflected from a region higher than E, yet is not a definite F echo. This frequency is denoted by f^*E°. There may then be some pictures with only a single E echo, and some with echoes from greater equivalent heights, and a frequency is eventually reached on which an F echo is observed and continues on all higher frequencies. This has been taken as fE°. In the summer on the critical frequency thus determined by the appearance of F (rather than by the appearance of an echo above E), the E echo shows group retardation. It is thus the lowest frequency which will penetrate all ionized regions below the F regions. In the winter the E echo (of the α-E type) does not show group retardation and persists beyond this frequency as a partial reflection.

The determination of fF_1° presents no real difficulty. It is the frequency on which the $\{h', f\}$ curve shows group retardation, or bends over horizontally as echoes are received from a uniform height from the F_2 region.

In winter the echoes received from the F_2 region are very scattered and stratified: the lower edge of the echo on the oscillograph is sharply defined and its equivalent height varies regularly with frequency, but energy is received for a considerable time afterwards so that the total width of the reflected pulse is equivalent to 100 km. or more. (*a*) in plate 1 is a reproduction of part of the local noon $\{P', f\}$ record of 7 February 1936, and it illustrates the diffuse nature of the echoes received during the dark period. It illustrates too a phenomenon which is sometimes observed, the gradual increase of the width of the echo with frequency and a sudden decrease in the energy received on a certain frequency, in this case 4·2 Mc./sec., suggesting the presence of a region for which this is the critical frequency, and yet the lower edge of the echo is continuous from one frequency step to the next.* Sometimes there is no doubt as to the value of fF_2° owing to group retardation, but usually the echoes continue to weaken and increase slightly in equivalent heights as the frequency increases, and disappear without any group retardation or sudden energy-loss for either the ordinary or the extraordinary ray. In the absence of any sure indication of a critical frequency we have been forced to take the highest frequency on which sensible echoes are obtained as $fF_2^\times$, and to take fF_2° as 0·8 Mc./sec. less than $fF_2^\times$. The critical values thus determined are of the same order as those determined at the same time of year when there is no doubt as to the critical frequency. It may be remarked, therefore, that whereas in the summer the pronounced group retardation ensures that the value of fF_2° shall be quite independent of the power of the transmitter, one would hesitate to say that the same is strictly true on many winter days.

On several days when the ordinary and extraordinary rays show group retardation, echoes continue regularly beyond $fF_2^\times$ at an equivalent height slightly greater than F_2. This has been taken to be a spur on F_2, but it must be mentioned that this spur reflects only the extraordinary ray, never the ordinary. Very occasionally the height-separation is greater, and the upper region is more in the nature of an F_3 region than a spur on F_2.

The contrast between the scattered winter echoes as at (*a*) in plate 1 and the sharp clean echoes in the summer as at (*b*) in plate 1 is very striking. The cleaning up begins to be noticeable at noon a few days after the first sunrise.

On most occasions some echoes were received from the region between the E region and the F region. These echoes are only very rarely regular enough to be said to be reflected from an E_2 region, and we refer to all echoes received from this intermediate region as J echoes. Sometimes echoes were received from all heights above the E region, so that on the oscillograph pattern the E, J, and F echoes are all joined. J echoes are most commonly seen on frequencies above and within 1·0 Mc./sec. of fE°. They almost always occur as partial reflections, rarely as from a totally reflecting layer.

Rather of the same nature, but distinct from them in their occurrence, are what we call the ***polar echoes***. These are first seen on a high frequency and continue irregularly sometimes to a frequency greater than $fF_2^\times$ and sometimes so strongly as to obscure the F region. These echoes are shown at (*c*) in plate 1 below the F echoes, beginning at about 6·5 Mc./sec. and continuing to 8·4 Mc./sec. Sometimes the equivalent height h' of one of these echoes varied rapidly with time so that the echo could be seen moving about on the oscillograph screen. As a rule, however, h' was constant for a given frequency, but the amplitude of the echo changed rapidly and h' varied erratically from one frequency to the next. The polar echoes occur at any equivalent height between 100 and 250 km., and sometimes at greater equivalent heights, and are distinct from the ordinary J echoes in that no echoes are obtained from these heights over the frequency range lying between fE° and about 5·5 Mc./sec., the frequency at which the polar echoes generally first appear.

---

* In the reproduction, the frequency of the calibrator was 1500 c./sec., so that the distance between each wave is equivalent to 100 km. equivalent height.

Local noon observations. The monthly means of the heights and critical frequencies for the E, F_1 and F_2 layers are plotted in figure 1, with the locus of the earth's shadow at local noon, and those for the critical frequencies are plotted in figure 2 with the monthly means at Tromsö for the same period, kindly sent to us by Dr Harang.

No distinction has been made between ordinary E and persistent E: in the winter the E region is always of the persistent E type, and in the summer is nearly always the normal E. On a few occasions both types are present at the same time. During the intermediate period when the E region is sometimes of one and sometimes of the other type, there is no tendency for one type to be either higher or more densely ionized than the other.

Figure 1 shows that the equivalent height of the E region is greater in winter than in summer, averaging 123 km. in December and 102 km. in June. This is to be expected on the assumption that the ionization is due to rectilinear radiation from the sun. Both the equivalent heights and the critical frequencies are more variable from day to day in the winter than in the summer. There is no discontinuity in the critical values at the time when the earth's shadow reaches the E layer at noon, or at any other time. The critical frequency follows an inverse curve with a maximum at midsummer and a minimum at midwinter. The f^*E° curve is rather similar, but more irregular, and with the maximum and minimum occurring earlier.

The Tromsö curve for fE° is not continuous throughout the winter, for an E echo was never obtained there during undisturbed conditions when the sun was below the horizon. It should be noted that a similar result was obtained at Tromsö during the polar year three years previously, and near a sunspot minimum.

The F_1 region was observed on three isolated occasions during September but was not observed during the winter until 21 March. It was present at noon on 7 days at the end of March, was absent from 1 to 7 April and was nearly always present after 8 April. It is very interesting to note that the F_1 region was not observed at Tromsö until 2 May: it is difficult to understand why it should be formed 6 weeks earlier than this at a station some 700 miles further north. It is true that the days are then longer at North-East Land than at Tromsö: nevertheless the ionizing factor which is proportional to $\int \sin h\, dt$ integrated from sunrise to noon, is greater at Tromsö. fF_1° is a maximum at midsummer and, as in the case of fE°, the critical values in the main follow a $\sin^{\frac{1}{4}} h$ curve, where h is the sun's altitude at noon.[*]

The fluctuations from day to day of fF_2° are very large, especially during the winter. The monthly means do not give a smooth curve, but it is clear that there are

---

[*] See p. 226.

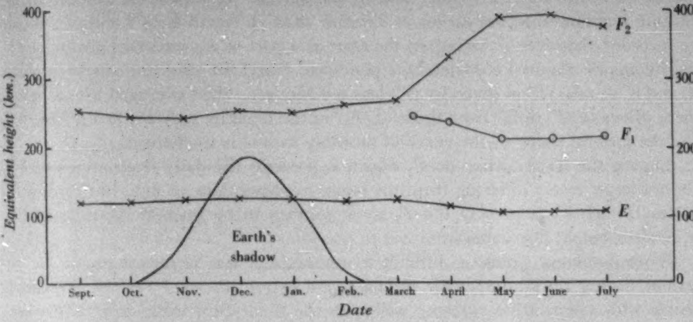

Figure 1.

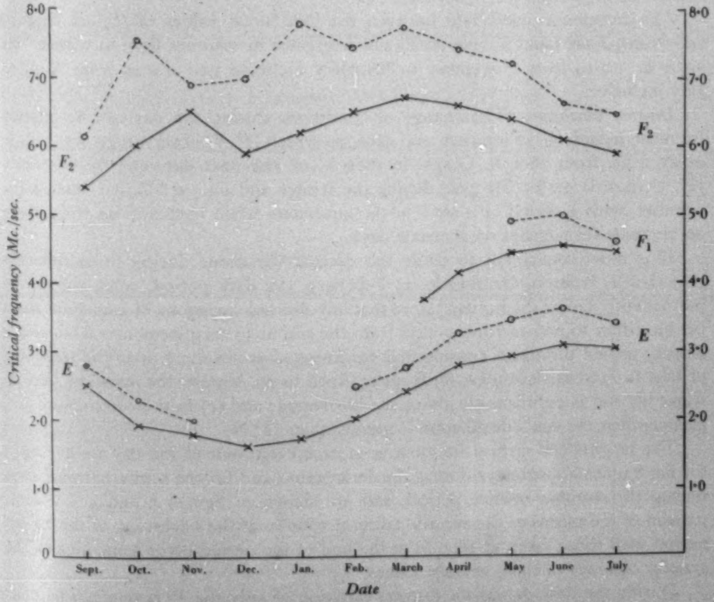

Figure 2. ○------○ Tromsö; ×——× North-East Land.

ionization maxima in November and in the spring. It should be noted that the autumn maximum occurs earlier at Tromsö than at North-East Land. It should be recorded that even if we regard the spur as a part of F_2, and take always as $fF^{\times}$ the frequency required completely to penetrate F and the spur and anything above it, and if we take fF° as given by $fF^{\times}$ less 0·8 Mc./sec., then averaged over a month these values of fF° differ from those of fF_2° in the table by only 0·1 to 0·3 Mc./sec., and the general shape of the curve of monthly means is unchanged.

During the winter when no F_1 region is present, the daily fluctuations of $h'F_2$ are not large, rarely differing from the mean by more than 30 km., but during the summer when F_1 is present the F_2 layer appears to be pushed upwards and its equivalent height fluctuates from 200 to 600 km.

A phenomenon which is difficult to understand was observed on twelve occasions during the summer: the ordinary and extraordinary F_1 echoes are clearly visible with a separation agreeing well with the theoretical value of 0·76 Mc./sec., but besides them a weak but very clear echo can be distinguished and traced on all frequencies, behaving exactly as the ordinary component but with a critical value smaller by only from 0·4 to 0·5 Mc./sec.

The correlation coefficient between the local noon values of fF_2° at Tromsö and North-East Land is very small and is greater in summer than in winter. Its value is +0·19 from November to February inclusive and +0·29 from April to July inclusive.

Diurnal variations. The change of conditions during the day can be studied from the records of 22 international days, on which $\{P', f\}$ observations were made every 2 hr. from 1600 h. G.m.t. to 1600 h. on the next day, and from seventy $\{P', t\}$ records on 2·0 Mc./sec. during the winter and on 3·0 Mc./sec. during the summer, with a period of a week at the equinoxes when observations were made on alternate frequencies on alternate days.

It is most convenient to study the diurnal variations during three different periods: (*a*) from 19 October to 25 February, the dark period, when the sun is permanently below the horizontal, so that any diurnal variations of ionization must be due either to non-rectilinear rays from the sun or to rectilinear rays which have already passed through a considerable thickness of atmosphere or to the transport of ions from lower latitudes; (*b*) from 15 April to 29 August, the sunshine period, when the sun is permanently above the horizontal; and (*c*) in the summer-solstice period when the sun's declination is greater than 18° N.

The heights and critical frequencies at each even hour of the day are averaged for the 8 international days during the dark period and for the 6 international days during the summer-solstice period, and are shown in figures 3 and 4. A comparison of the means of the records taken at 1600 h. at the beginning of the 24-hr. period with those taken at 1600 h. at the end of the period gives some idea of the general accuracy of these average values.

During the dark period the diurnal variation of only the F_2 region can be considered because, though E echoes are very frequently received, the critical frequency of the E region is, except near noon, usually below the absorption level, so that it

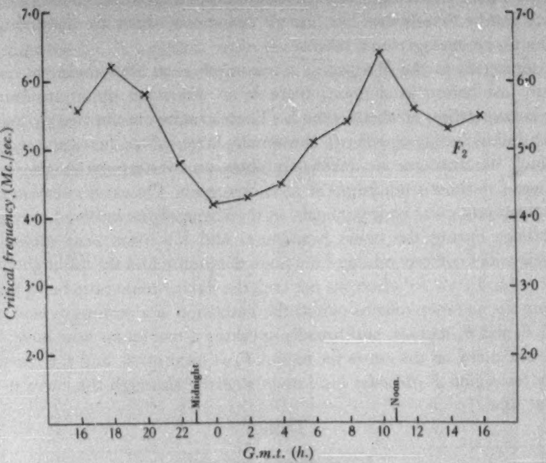

Figure 3. Dark period.

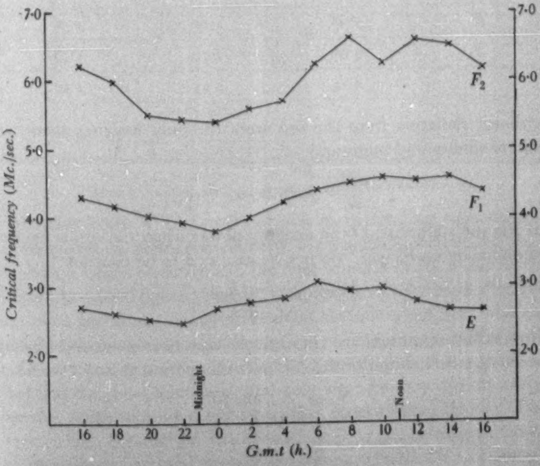

Figure 4. Summer solstice period.

has already been penetrated when echoes are first received. Sometimes the critical frequency can be determined but, except near noon, there are not enough determinations for an average to be taken.

The ionization in the F region is a minimum soon after midnight, rising to a maximum just before local noon: there is an afternoon minimum rising to an evening concentration at about 1800 h. These results are not merely the effect of averaging and including one or two abnormally large values, for of the eight records from which the averages are taken, six show an evening maximum at 1800 or 2000 h. and five show a minimum at 1200 or 1400 h. On every occasion the curve of diurnal variation was approximately of the shape of the curve of averages, with high readings during the hours near noon and low ones near midnight. The electron-densities corresponding to the noon maximum and the midnight minimum are $7{\cdot}6 \times 10^5$ and $3{\cdot}3 \times 10^5$ electrons per cm.^{3}, the day-to-night ratio being thus 2·3:1.

During the summer-solstice period the ionization is a minimum near midnight in the E, F_1 and F_2 regions, and broadly speaking a maximum near noon. There is one very low point on the curve for region F_2 at local noon, and the maximum on the curve for region E precedes local noon slightly, although the curve is very flat about that time.

Table 1

Layer	N (10^5 electrons per cm.^{3})		Ratio of maximum to minimum
	Max.	Min.	
E	1·68	1·12	1·50
F_1	3·96	2·70	1·47
F_2	8·15	5·45	1·50

If rectilinear radiation from the sun were the only ionizing agent we should have at the maximum and minimum

$$\frac{dN}{dt} = Q \sin h - \alpha N^2 = 0,$$

where h is the sun's altitude, Q the ionizing power when the sun is overhead, and α the recombination coefficient. So if α be assumed to be constant

$$\frac{N_{\text{max.}}}{N_{\text{min.}}} = \sqrt{\frac{\sin h_{\text{max.}}}{\sin h_{\text{min.}}}}.$$

The maximum and minimum are respectively very near noon and midnight, and taking the average declination of the sun over this period as $20\tfrac{1}{2}^\circ$, we have

$$\frac{N_{\text{max.}}}{N_{\text{min.}}} \simeq \sqrt{\frac{\sin 30^\circ}{\sin 11^\circ}}$$
$$\simeq 1{\cdot}63.$$

This theoretical value is greater than the value actually obtained. This is what we should expect, however, for the heating and rarefaction of the atmosphere during the day and the cooling and contraction during the night would tend to reduce the day-to-night ratio of electron-density. It will be seen that the electron-density at midday during the dark period, when the sun is below the horizontal (as much as 14° below the horizontal at midwinter), is greater than at midnight during the summer solstice.

In contrast with these results it must be pointed out that at Tromsö during the polar year the region F_2 critical frequency was actually greater at midnight than at midday during the period of the midnight sun(5).

Magnetic disturbances. To determine the time of day at which magnetic disturbances occurred most frequently, the magnetograms were examined and the number of times when a magnetic storm occurred during each period of 1 hr. between two successive hours was counted. As was mentioned above, the magnetograph was by no means sensitive and the criterion of a storm is merely qualitative, but the resulting curve, figure 5, leaves little doubt that the most disturbed period is between 0500 and 0900 G.m.t., while there is a minimum near local noon and a small maximum between 1600 and 1900 G.m.t. This is the result of analysing the records of the whole year, but during the autumn and winter it was the latter period that was the most disturbed, and only after January did the early morning period become much more disturbed than any other time of the day. The number of days from which the analysis has been made is 122. The magnetic conditions at local noon were described qualitatively and compared with Dr L. Harang's qualitative description of the conditions at Tromsö. The agreement is quite good: the condition of quiet at one station usually corresponds to quiet or small disturbance

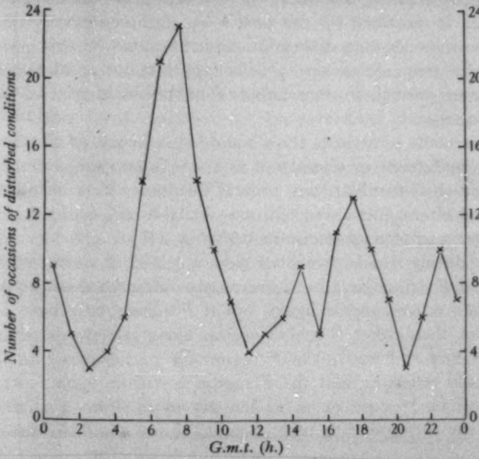

Figure 5. Times of occurrences of magnetic disturbances.

at the other, and so on, and on only 4 days out of the 121 on which comparisons have been made were the magnetic conditions very different. We feel reasonably justified, therefore, in referring to the magnetic conditions at Tromsö on days when we have no magnetic record available.

Direct comparison between ionosphere conditions and magnetic data. On no occasion was it found impossible to obtain any reflections at all, as reported elsewhere, though on 2 April 1936 at local noon only a few echoes were obtained near 7·0 Mc./sec. $\{P', f\}$ observations were made every 2 hr. after local noon on this day to examine the rate at which conditions returned to normal. The absorption limit—that is, the frequency on which echoes are first observed—fell slowly, and by 1900 G.m.t., $8\frac{1}{2}$ hr. after local noon, the first echo from the E region was received on 2·5 Mc./sec. It remained for the next 6 hr. until observations ceased, though even this is above the average absorption-limit frequency at this period of day and year. The critical frequencies were a trifle high but not at all abnormal, and the layer-heights were normal, so we conclude that the storm affected only the region below the E region.

The $\{P', t\}$ records sometimes show a sudden cessation of all echoes—probably a sudden commencement of absorption as there is no group retardation and the frequency is much lower than any critical frequency ever recorded. On every occasion for which magnetic records are available the sudden absorption was accompanied by a sudden magnetic disturbance. If we consider only periods of less than 1 hr. during which no echoes were received, it can be stated that when persistent E and F echoes have been previously obtained, then the echo pattern is unchanged when echoes appear again, but if F echoes only have been observed before cessation, then either F echoes appear alone afterwards, or else a weak E region appears first and masks the F region for perhaps half an hour, when it becomes partially reflecting and the F region is visible again. (*d*) in plate 2, a $\{P', t\}$ record on 2·0 Mc./sec. on 21/22 January 1936, shows a sudden cessation at midnight and the corresponding magnetogram shows a sudden disturbance at the same time.

On twenty-one occasions at local noon—and these were all between September and February inclusive—the critical frequency of the E region could not be determined, as the F region was visible on the lowest frequency on which echoes were observed. On only one of these was the absorption frequency above the average, so that on twenty occasions the ionization of the E region was unusually small. On these occasions as a rule the magnetic conditions were disturbed, usually stormy, and at 10 h. (M.E.T.) at Tromsö on these days there is usually a no-echo condition. Further, on these days, the critical frequency of F_2 region at North-East Land is almost always considerably below the average.

Direct examination of the equivalent heights and critical frequencies on days classified as quiet and stormy respectively shows that there is no tendency at any season for $h'E$, fE°, $h'F_1$, or $h'F_2$ (in winter) to adopt, on either class of day, values above or below the general average, but that fF_2° is almost always above the average on quiet days and is always below the average on stormy days. fF_1° shows a small but definite tendency in the same direction.

The effect of a very big storm during the summer is to cause $h'F_2$ to become very large and fF_2° to become low, so much so that at times the F_2 echoes cannot be seen, indicating either that the layer is so high that the echoes are beyond the end of the time base, or else that the critical frequency has fallen below that of the F_1 region. Frequently too the echoes are very weak, with the E echoes appearing first normally at about the usual frequency (about 1·6 Mc./sec.) but with a no-echo condition on frequencies from about 3·3 to 4·5 Mc./sec.

The fact that maximum ionization is reduced during magnetic storms is important, for it is contrary to expectation. It means that ions, instead of being produced, are either lost during a discharge or are redistributed throughout a greater volume because of the lowering of density accompanying the thermal expansion of the atmosphere.

Persistent E. One of the most striking features of this phenomenon is the manner in which strong undistorted partial reflections persist to a high frequency. The highest frequency on which echoes are detected from the persistent E region is referred to in this communication as the *persistence frequency*. Persistent E occurs only during magnetically quiet periods.

There is no marked seasonal variation, but the diurnal variation is very marked. If we adopt, and extend, the convention used by the British Polar Year Expedition at Tromsö and give a weight 1 to all occasions when the persistence frequency is between 2·6 and 5·2 Mc./sec., a weight 2 when the persistence frequency is between 5·2 and 7·8 and a weight 3 for higher persistence frequencies and add the results for every even hour of the day, we obtain the values shown in table 2.

Table 2

G.m.t.	Total	G.m.t.	Total	G.m.t.	Total
1600	21	0200	5	1000	4
1800	20	0400	3	1200	14
2000	12	0600	5	1400	18
2200	6	0800	4	1600[2]	22
0000	7				

The figures are derived from the 286 international-day records, with twenty-two records at each of the hours. Persistence frequencies greater than 8·0 Mc./sec. were observed on fourteen occasions, all between 1200 and 1800 h. inclusive.

Aurora. Owing to shortage of personnel and the almost persistent cloudiness, insufficient observations were made between 0000 and 0700 h. to determine the time of maximum frequency of the aurora. The auroral arcs and bands were predominately in the south, but sometimes a weak corona was visible overhead, and occasionally bands from the south passed overhead and set in the north. A number of $\{P', f\}$ observations were made when aurora was visible overhead or soon afterwards. There is no feature common to all the records, and evidently the effects of aurorae can be very different. On some occasions the absorption frequency is higher than normal, but on no occasion did the no-echo condition obtain. The only generalizations that can be made are (1) that the F region seems always to be quite normal, and (2) that conditions change very rapidly in the course of a few minutes, so that one record would be very different from another taken 10 min. later.

Results of the {*P′*, *t*} *records.* The diurnal variation of the electron-densities cannot be directly studied from the {*P′*, *t*} records, but the probability of penetrating certain regions with 2·0 Mc./sec. in the winter and with 3·0 Mc./sec. during the summer can be calculated. Figures 6 and 7 represent the results of the 2·0-Mc./sec. {*P′*, *t*} records during the dark period, and of the 3·0-Mc./sec. records during the sunshine period. The lower curve represents the percentage probability that the lowest echo is reflected from the *E* region, i.e. that *h′* is less than 130 km.,

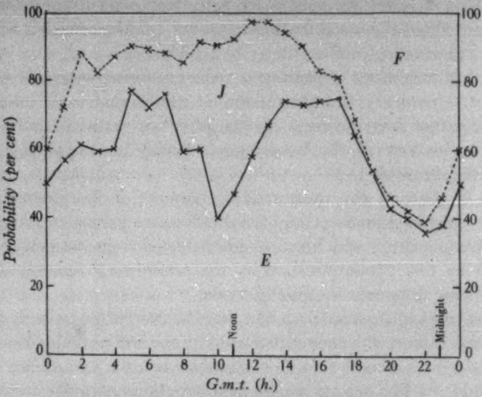

Figure 6. Dark period, 20 Mc./sec.

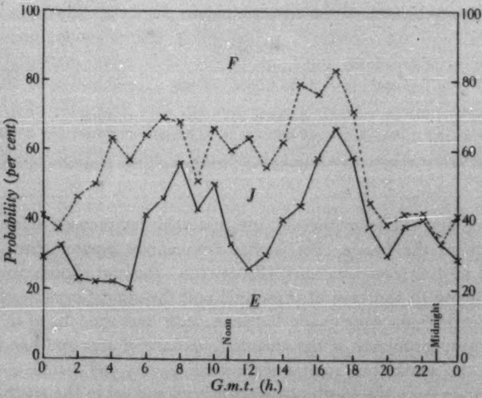

Figure 7. Sunshine period, 30 Mc./sec.

and the dotted line is the probability of the lowest echo being reflected from either the *E* or the *J* region, i.e. of *h′* being less than 180 km., so that the distance between the curves is the probability that the lowest echo is a *J* echo, and the distance above the dotted curve is the probability that the lowest echo is an *F* echo. The curves are not dissimilar to the curves showing the diurnal variations of the critical frequency, with a night minimum and a daytime maximum with a subminimum near midday. It can be seen too that the *J* echoes are very rare near midnight, a fact which suggests that the diurnal variation of ionization in this intermediate region is greater than that in the *E* region.

Intense E. Table 3 shows the number of times intense *E* was observed on the {*P′*, *t*} records at each hour of the day. The total number of observations at each hour is about 70, so that intense *E* occurs on nearly 20 per cent of the occasions at 1600 h. The evening maximum is very pronounced, and intense *E* is rarely observed from 0000 to 1200 h. In eleven months it was observed only once at local noon. It seems to be more common near the equinoxes than near the solstices, but the number of observations is not really great enough for this to be stated definitely. Intense *E* does not begin very suddenly, but the reflection coefficient seems to grow quickly and then to decrease slowly as in the reproduction of the 3·0 Mc./sec. {*P′*, *t*} record of 9/10 June 1936 at (*e*) in plate 2. Intense *E* occurs only in magnetically quiet conditions.

Table 3

G.m.t.	Number of occurrences	G.m.t.	Number of occurrences	G.m.t.	Number of occurrences
1	2	9	1	17	11
2	1	10	0	18	8
3	0	11	—	19	9
4	0	12	1	20	6
5	0	13	1	21	8
6	0	14	4	22	6
7	1	15	3	23	2
8	0	16	13	0	1

Irregular echoes. The polar echoes were observed strongly on 30 of the 294 local-noon records, and weakly on many more. Irregular echoes similar to the polar echoes but visible on all frequencies occurred on 35 local-noon observations. Neither type tends to occur at any special time of day, and both are most common during October, November, December and January, though they occur also in the summer. These echoes occur in all conditions of magnetic activity.

It seems that during these times the maximum ionization in the intermediate region between *E* and *F* is very little less than in the *E* layer, and that these random echoes are returned from ion-clouds or ion-concentrations where the ionization is greater than the normal. Since these echoes occur in the winter as well as in the summer, it seems that the clouds must be formed perhaps by local ionization caused by a burst of charged particles from the sun, or possibly from ion-clouds formed by meteors as suggested by Skellet and observed by several observers(6). If the former is the real cause it is surprising that there is no correlation between the occurrence of polar echoes and the magnetic conditions: if the latter it is not easy to see why the echoes should be observed to such an extent in high latitudes.

In the past many echoes have been observed for which a satisfactory explanation is difficult to find, so we do not hestitate here to record that on twenty-three occasions we obtained photographs—54 photographs in all—of echoes with equivalent heights between 500 and 640 km. on frequencies between 1·4 and 2·3 Mc./sec., and once on frequencies between 2·8 and 3·4 Mc./sec. Sometimes an *E* echo is visible at the same time and sometimes not. No special magnetic conditions are favourable to the reception of these echoes. We believe them to be genuine echoes for (1) they have the appearance of echoes, definite and sharp with a break in the time base line, showing that they are in synchronism with the pulse for the 20 cycles of the a.-c. supply during the exposure of $\frac{2}{5}$ sec.; (2) we were very far from any disturbing source other than in our own a.-c. supply; and (3) the slightness of the variation of equivalent height makes it unlikely that they are caused by a spot on the commutator or some other local periodic disturbance.

At times conditions are changing very rapidly, so that the echo pattern has changed very noticeably during the period of about 2 min. during the change of an inductance at the receiver. Only one of the days on which this was marked was stormy: usually magnetic conditions were quiet or slightly disturbed.

Many great-circle communication routes between important centres pass through Arctic regions, and if direct wireless communication between these places is to be reliable, it will be necessary to understand the various changes taking place in this part of the ionosphere and to predict the times and frequencies at which conditions will be best for communication. During the winter, conditions in the ionosphere are very erratic though the absorption is low. Communication is difficult at all seasons during periods of strong magnetic activity.

§ 4. ACKNOWLEDGEMENTS

We wish to express our sincere thanks for the invaluable help and advice given to us by Prof. E. V. Appleton, by Mr R. Naismith and other officers of the Radio Research Station at Slough, and by Dr Leiv Harang of the auroral observatory, Tromsö, who has kindly provided us with relevant data from Tromsö and given us permission to refer to them. We wish also to thank the Department of Scientific and Industrial Research for the loan of the receiver; Prof. Townsend, in whose laboratory most of the apparatus was made; the many British firms which supplied us with apparatus either free or at reduced prices; and the Royal Society and other learned bodies, without whose moral and financial help the expedition could not have taken place.

REFERENCES

(1) Whatman and Hamilton. *Nature, Lond.*, **139**, 69 (1937).
(2) Ratcliffe and White. *Proc. Phys. Soc.* **45**, 399 (1933).
(3) Appleton, Naismith and Ingram. *Philos. Trans.* A, **236**, 201 (1937).
(4) Mitra and Syam. *Nature, Lond.*, **123**, 953 (1935).
(5) Appleton, Naismith and Ingram. *Philos. Trans.* **236**, 218 (1937).
(6) Mitra, Syam and Ghose. *Nature, Lond.*, **133**, 533 (1933).

THE DIURNAL VARIATION OF THE IONOSPHERIC ABSORPTION OF WIRELESS WAVES

By J. E. BEST, Ph.D. and J. A. RATCLIFFE, M.A.

Received 4 *September* 1937. *Read in title* 28 *January* 1938

ABSTRACT. Experimental determinations of the reflection coefficient of wireless waves reflected from the *F* region of the ionosphere are described. The afternoon variation of the reflection coefficient was investigated on several days between June and December 1936. Days with a quiet ionospheric behaviour were chosen, and the tests made in choosing such days are described. The results can be explained on the assumption that the absorption occurs in the lower portion of a simple *E* region of the type considered by Chapman. It is shown that the recombination coefficient must be independent of the pressure at heights above 110 km. at least, and that it must have a value not less than 10^{-8}. It is pointed out that this value does not fit in with the usually accepted theory. The absorption measurements are shown to be in agreement with Martyn's(11) suggestion that the collisional frequency for electrons in the neighbourhood of the *E* region is given by assuming that the value at a height of 90 ± 5 km. is 10^6 per second and that the scale-height of the atmosphere is 9 km.

---

§1. INTRODUCTION

This paper is concerned with the absorption of waves reflected from the *F* region of the ionosphere at vertical incidence. It has previously been shown(1) that, except under conditions of marked group retardation in region *F*, the absorption of these waves is determined by their passage through the *E* region, and in this paper we attempt to make deductions about the structure of the *E* region from observations on the amplitude of the *F*-region echoes. The observations recorded were made on occasions when the *E*-region behaviour was quiet, and our criteria for quiet conditions are described in § 2. The object of the experiment was to investigate the variation of the *E*-region absorption (of *F*-region echoes) with the sun's zenith angle throughout the afternoon, and to see how far the behaviour on quiet days could be explained on the simplest possible picture of the *E* region.

The experiments and experimental results are described in § 2. In § 3 a theoretical investigation is made of the way in which the absorption of *F*-region echoes would vary with the sun's zenith angle on the simplest possible assumption that all the absorption occurs in an *E* region of the type suggested by Chapman(5). In § 4 the conclusions are compared with the experimental results, and in § 5 it is suggested that deductions can be made about the processes of electron-loss in the *E* region.

The experiments are in some ways similar to those described by Prof. Appleton in his Bakerian Lecture(3) to the Royal Society, in which the seasonal variation of midday absorption was studied. Appleton discusses this seasonal variation of absorption in terms of the sun's zenith angle and comes to conclusions similar to those outlined here, with one exception mentioned in § 4.

§2. EXPERIMENTAL ARRANGEMENTS AND RESULTS

The observations were made at Cambridge, during the second half of 1936, with a Breit and Tuve pulse transmitter and a receiver about 1 mile apart. The transmitter frequency could be varied by a remote control from the receiver. A cathode-ray oscillograph was used in conjunction with a time sweep, in the usual way, and was observed visually.

For the absorption-measurements a fixed frequency was used on any one day, and was selected as follows. Before a day's experiments were started the curve relating equivalent path P' to frequency f was examined, and a frequency was selected which gave reflections from the F region with no magneto-ionic splitting due to region F_1. A typical $\{P', f\}$ curve is shown in figure 1 and the frequency selected corresponded to the point marked f. During the afternoon the F region alters so that the $\{P', f\}$ curve drifts to the left, and the fixed frequency corresponds in turn to points more and more to the right of the line f–f'. Near the point g there occurs considerable splitting of the echo, and retardation of one component due to the F_1 region. The absorption produced by this retardation will be discussed later. Since the frequency on which observations were made was chosen afresh each

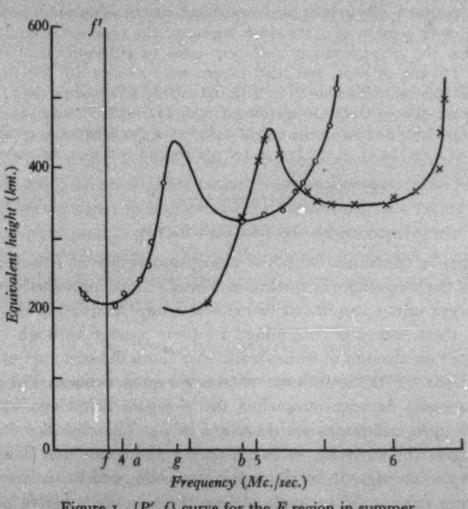

Figure 1. $\{P', f\}$ curve for the F region in summer.

day it was not the same at different times of the year: it varied from 4·2 Mc./sec. in June to 3·2 Mc./sec. in December. Measurements of intensity were made by noting the reading of a calibrated gain-control required to bring the echo-amplitude to a given mark on the oscillograph screen. This sufficed for the measurement of relative amplitude, so that the variation of reflection coefficient with time of day could be determined. From time to time the amplitude of the ground wave was measured in the same way to make sure that the transmitter had not changed. Towards sunset, when the amplitude was greater, it was possible to obtain absolute values for the reflection coefficient by comparing the first and second reflections, and then the values obtained earlier in the day could be converted into absolute values also.

The amplitude measurements were made by averaging through intervals of 5 min. In order to determine the extent to which two such averages are significantly different, two sets of amplitude observations, separated by about half an hour, were taken in the afternoon, when the echo-amplitude was increasing. In each set amplitudes were observed every 5 sec. for a period of 10 min. The means were 2·28 and 3·33 respectively and the standard deviations 0·12 and 0·175; it follows that the standard deviation for the difference of the means was 0·21. The condition for a significant difference between the two means is that it should be greater than twice its standard deviation and this is clearly satisfied by the data. It may be deduced that two means separated by 10 per cent are just significantly different. In the routine amplitude measurements the averages were not obtained with the same precision, but differences of 50 per cent or more may be taken as real differences of the same order.

At intervals of 30 min. an observation was made of the penetration of the E region; this observation took usually about 10 min. In the earlier of our observations the two threshold frequencies at which (*a*) F-region echoes first appeared, and (*b*) E-region echoes disappeared, both with increasing frequency, were observed, and a day's observations were not used unless both these frequencies behaved smoothly and regularly throughout the day. We have given reasons elsewhere^(2)^ for supposing that these conditions represent what may be considered as quiet ionospheric behaviour. Later in the year conditions were made even more stringent and a detailed $\{P', f\}$ curve was taken in the neighbourhood of the E penetration frequency every 30 min.

These $\{P', f\}$ curves on quiet days exhibited ledges on the E region such as Halliday(4) has observed. It was noticed that the occurrence of very weak traces of abnormal ionization in the E region, producing but very small variations in penetration frequency, in general rendered these ledges unobservable. Only those days were later classed as quiet for which these ledges appeared to vary smoothly and regularly throughout the day. We are fairly satisfied that, with one exception (16 July), the early observations would have been classed as quiet on this basis. On one occasion (6 November) a single persistent layer of weak abnormal ionization at a height of 100 km. was observed which did not correspond to the vanishing or obscuring of the ledges. Here the criterion was insufficient to exclude a case in which an abnormal influence was undoubtedly present. The care described here in the classification of days was taken because results for even slightly disturbed days were found to be very different from those for quiet days, as will be shown later when we discuss the results for 6 November.

Except that observations of *E*-region penetration, each occupying about 10 min., were made at intervals of 30 min., measurements of amplitude were obtained continuously throughout the period from midday to sunset. The absorption-measurements were stopped in the evening when the reflection coefficient became so great that its difference from unity could not be measured, and the *E*-penetration measurements were stopped when the frequency approached the broadcasting band.

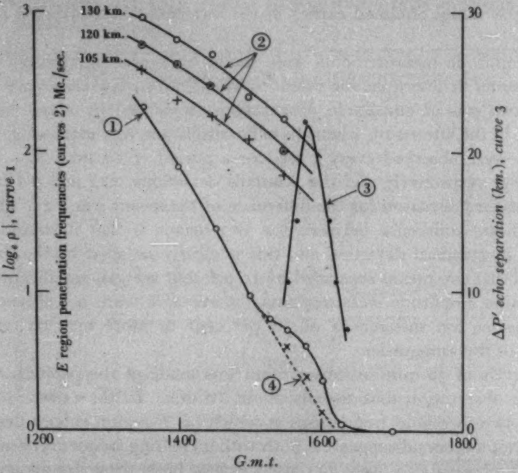

Figure 2. Results on 30 November 1936. Frequency, 3·22 Mc./sec.

Although experiments were started on a large number of days the results were not used, for the purposes of this paper, unless throughout the day the *E*-region behaviour satisfied the condition of quietness previously explained. This limits the results to 12 days, distributed fairly evenly throughout the interval between 5 June and 2 December 1936.

The results of a typical day's experiments are given in figure 2, which shows the observed reflection coefficient (1) and the *E*-region penetration frequencies (2), each as a function of time of day.* Each point on the curve (1) represents the mean of about 20 observations taken during a period of 5 min. The curve (3) also shows the amount of the observed separation due to splitting of the F-region echo. This splitting arises from retardation in the F_1 region and corresponds to the portion a–b of the $\{P', f\}$ curve shown in figure 1. The intensity-measurements were made on the more retarded echo (ordinary wave), and a correction was made in the following way to estimate the corresponding absorption in the F_1 region. It was assumed that the path-difference between the two echoes was entirely due to group retardation in the F_1 region, and that the extra absorption would be given by

---

* The *E* region on this occasion showed three penetration frequencies corresponding to equivalent heights of about 105, 120, and 130 km. The three penetration frequencies are shown in the figure.

$$\Delta(\log\rho) = -\frac{\nu}{2c}\Delta P',$$

where ρ is the reflection coefficient, $\Delta P'$ is the group retardation, and ν is the collisional frequency in the F_1 region(1). The value 3×10^3 per second was taken for ν, and the absorption then calculated was used to correct the observed reflection coefficient as shown in curve (1) of figure 2. The corrected portion of the curve is marked (4). The fact that it appears to be a smooth prolongation of the uncorrected portion of curve (1) indicates in the first place that the hump in the observed curve is in fact due to F_1-region retardation, and in the second place that the value chosen for ν is roughly correct.

§ 3. THEORETICAL CONSIDERATIONS

In the following discussion:

c is the velocity of light,
e the charge on the electron (e.s.u.),
h the distance above the ground,
H the earth's magnetic field,
H_L the vertical component of the earth's magnetic field,
H the scale height of the atmosphere,
I the number of electrons produced per cm.³ per second by an ionizing agency,
κ the absorption coefficient,
m the mass of the electron,
N the number of electrons per cm.³, and p the pulsatance of the wave,
$p_H = \mathrm{H}e/mc$ and is the gyromagnetic pulsatance,
$p_L = \mathrm{H}_L e/mc$ and is the longitudinal gyromagnetic pulsatance equal to $1{\cdot}21\times2\pi.10^6$,
$p_0 = \sqrt{(4\pi Ne^2/m)}$ and is the penetration pulsatance for a region with maximum electron-density N,
$x = h/H$ and is the height measured in terms of the scale height of the atmosphere,
α is the recombination coefficient,
β the attachment coefficient,
θ the angle between the vertical and the earth's magnetic field,
μ the refractive index,
ν the collisional frequency of the electrons,

ν_0 the value of ν at the ground, and ν_m the value of ν at the level of maximum ionization.

ρ is the reflection coefficient of the wave, equal to $\exp(-2\int\kappa dh)$ where the integral is taken over the path of the wave in the ionosphere,

ρ is the density of the atmosphere and χ the sun's zenith angle.

In attempting to explain the absorption-measurements we shall assume that all the absorption occurs in the E region.* We shall also assume that the E region is produced by the incidence of a monochromatic ionizing radiation on an atmosphere with an exponential gradient of density (i.e. a homogeneous isothermal atmosphere) and that the loss of electrons is due entirely to a recombination process, so that the rate of loss is proportional to N^2. The coefficient of recombination will be assumed to be constant throughout the region. This type of E region has been discussed by Chapman(5) and we shall call it a *Chapman region*. In the type of atmosphere which we have assumed the frequency of collision between electrons and molecules will vary exponentially with height.

In calculating the total absorption of a wave reflected from the F region we start with the expression(6)

$$\kappa = \frac{1}{2c}\frac{4\pi e^2}{m}\frac{N\nu}{(p \pm p_L)^2+\nu^2}\frac{1}{\mu}.$$

We next assume that the value of μ for the wave as it passes through the E region is approximately unity, since the wave-frequency concerned was always sufficiently large compared with the penetration frequency of the E region. The absorption coefficient for the ordinary wave at any height is now seen to be given by

$$\kappa \propto \frac{N\nu}{(p+p_L)^2+\nu^2} \qquad \text{......(1).}$$

We shall investigate the variation of the numerator and the denominator of this expression separately. Let us assume first that the ionization is in equilibrium with the ionizing agency so that we have

$$N \propto \sqrt{\frac{I}{\alpha}}.$$

From Chapman's analysis we have

$$I = B\exp\{-x - C\sec\chi\exp(-x)\},$$

where B and C are constants.

We have assumed an exponential variation of the collisional frequency, so that we have also $\nu = \nu_0\exp(-x)$. These assumptions give

$$N\nu = \nu_0\sqrt{\frac{B}{\alpha}}\exp\left\{-\frac{3x}{2} - \frac{C\sec\chi}{2}\exp(-x)\right\}.$$

This expression for the numerator in equation (1) has a maximum at a distance x' below the ionization maximum, where $\exp(x') = 3$, corresponding to a distance $1{\cdot}1H$ below the ionization maximum. The forms of the ionization curve and of the curve for $N\nu$ are shown in figure 3.

---

* It is assumed that the correction mentioned in § 2 has been made for F_1-region absorption.

In integration through the absorbing region to calculate the total absorption, the most important contributions will arise from those regions near the maximum for $N\nu$ and if, at these places, $(p+p_L)^2 \gg \nu^2$ then the variation of ν in the denominator of (1) can be neglected.

We can show that this approximation is legitimate by considering the fact, stressed by Appleton[(7)], that the measurements of penetration frequency show the propagation at the E-region maximum to be quasi-transverse in character, so that $(\sin^2\theta/2\cos\theta)\,p_H \gg \nu$ at these levels. This gives $\nu \ll 6\cdot5\times10^5$ at the E-region maximum, and hence $\nu \ll 1\cdot95\times10^6$ at the level of maximum $N\nu$. For the waves used in the present absorption-measurements p is of the order of $2\cdot5\times10^7$ per second, and it appears certain that $(p+p_L)^2 \gg \nu^2$ at the height considered. We therefore replace

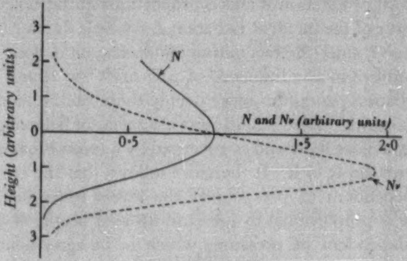

Figure 3

$$\frac{N\nu}{(p+p_L)^2+\nu^2}$$

by

$$\frac{N\nu}{(p+p_L)^2}$$

in expression (1).

We are now in a position to integrate the absorption of a wave in going right through the E region and returning after reflection from the F region and we have

$$-\tfrac{1}{2}\log\rho = \int_0^\infty \kappa\, dh$$

$$= \frac{1}{2c}\frac{4\pi e^2}{m(p+p_L)^2}\int_0^\infty N\nu\, dh$$

$$= \frac{1}{2c}\frac{4\pi e^2}{m(p+p_L)^2}\nu_0\sqrt{\frac{B}{\alpha}}\int_0^\infty \exp\left\{-\frac{3}{2}\frac{h}{H}-\frac{C\sec\chi}{2}\exp\left(\frac{-h}{H}\right)\right\}dh \quad \text{......(2).}$$

$$= \frac{1\cdot25}{c}\frac{4\pi e^2}{m(p+p_L)^2}H\nu_0\sqrt{\frac{B}{\alpha}}\left(\frac{\cos\chi}{C}\right)^{1\cdot5} \quad \text{......(3).*}$$

---

* See Appendix

This expression shows that the integrated absorption varies with the sun's zenith angle in such a way that

$$-\log \rho \propto (\cos \chi)^{1\cdot5} \qquad \text{......(4).}$$

It is next of interest to calculate expressions for the total absorption in the cases where electrons are lost either (*a*) by attachment to neutral molecules, or by (*b*) recombination, the recombination coefficient α varying proportionally to the molecular density.* It is first to be noted that in each of these cases no maximum of ionization density could be formed by any radiation whose ionizing power decreased as it passed through the medium. This has previously been pointed out by Appleton & Naismith(8) for case (*a*). It is equally true for case (*b*), as can be seen by noting that the rate of production of ions is proportional to the molecular density ρ and to the ionizing power of the incident radiation I, whereas the rate of loss of electrons is proportional to ρN^2, since the recombination coefficient is itself proportional to ρ. Hence, under equilibrium conditions $\rho I \propto \rho N^2$ or $N^2 \propto I$, and since I decreases steadily as the radiation penetrates more deeply there can be no maximum in N.

Appleton & Naismith(8) have recently given reasons for believing that the E region is produced by ultraviolet light and is governed by a recombination process, so that the above arguments apply to it. It therefore follows that the coefficient of recombination α is independent of pressure at the levels concerned. It is generally supposed(9) that α is proportional to pressure up to a height of about 80 km. and then becomes independent of pressure, which is in agreement with the above deduction.

If maxima of ionization are observed considerably lower down, either they must be due to ionizing agencies whose ionizing power does not decrease as they penetrate (e.g. corpuscles), or the limiting pressure at which the recombination coefficient has usually been supposed to become constant must be considerably in error.

Returning now to the calculation of total absorption in the case where electron-loss is either by attachment or by recombination with α proportional to density, we notice that, although a maximum of ionization cannot occur in either of these cases, there will be a maximum in the value of $N\nu$ so that, for the reasons given in the discussion of equation (1), there will be a level at which the absorption is a maximum and the absorption coefficient integrated to infinity will be finite.

If we now assume that the ionization maximum occurs in a region where α is independent of density but that the absorption occurs a little lower down, where the processes of electron-loss are assumed to be either attachment, or recombination with α proportional to pressure (the increasing pressure will make both these processes more likely lower down), we can perform calculations similar to those given earlier in this section. We shall not give the calculations in detail but merely outline them first for the case of attachment and then for that of recombination.

---

* Theories of recombination based on three-body processes require α to be proportional to pressure, and for an isothermal atmosphere this is the same as being proportional to density.

Attachment. $I=\beta p N$ for equilibrium

hence
$$N=\frac{I}{\beta p}$$
$$=\frac{B\exp\{-x-C\sec\chi\exp(-x)\}}{\beta p_0\exp(-x)}$$

and
$$N\nu=\frac{B\nu_0}{\beta p_0}\exp\{-x-C\sec\chi\exp(-x)\}.$$

Hence
$$-\log\rho\propto\cos\chi \qquad \text{......(5)*}.$$

Recombination with α proportional to density (and pressure). For this case we may write $\alpha=ap$.

Then for equilibrium $I=apN^2$.

Therefore
$$N=\sqrt{\frac{I}{ap}}=\sqrt{\frac{B\exp\{-x-C\sec\chi\exp(-x)\}}{ap_0\exp(-x)}}$$

and
$$N\nu\propto\exp\left\{-x-\frac{C\sec\chi}{2}\exp(-x)\right\},$$

which leads to
$$-\log\rho\propto\cos\chi \qquad \text{......(6)*}.$$

Equation (3) is left in a form involving the unknown intensity of the ionizing radiation. It is shown in the appendix that it is possible to transform it into the expression
$$-\tfrac{1}{2}\log\rho=\frac{2\cdot06}{c}\frac{p_0^2}{(p+p_L)^2}H\nu_m \qquad \text{......(7)},$$

which involves the penetration frequency p_0 and other quantities which may be taken as known. As we have already pointed out, the assumption leading to expressions (5) and (6) do not explain the formation of the ionization maximum; it is therefore not possible to turn equations (5) and (6) into a form involving the penetration frequency of the region.

§ 4. COMPARISON BETWEEN THEORY AND EXPERIMENT

We have calculated the magnitude of the absorption coefficient as a function of the sun's zenith angle on the assumption that there is always equilibrium between the electron-production and dissipation processes. At first sight we should not expect equilibrium except near midday, but we shall nevertheless test whether the total absorption is proportional to some power of $\cos\chi$, in accordance with equations (3), (5) and (6), by plotting the observed values of $\log\log\rho$ against $\log\cos\chi$. The results are shown in figure 4, which represents 12 days between June and December 1936. The closeness with which the observed points lie on straight lines shows that the observed values of $\log\rho$ are proportional to some power of $\cos\chi$ and, if we exclude 16 July and 6 November, it appears that the power is very close to 1·5 as given by equation (3). We have mentioned in § 2 that the $\{P', f\}$ observations give some reason for rejecting both these days. It thus seems that the diurnal variation of absorption can be explained on the assumption that α in the absorbing region is independent of pressure and that the ionization is at each instant in equilibrium

---

* See Appendix.

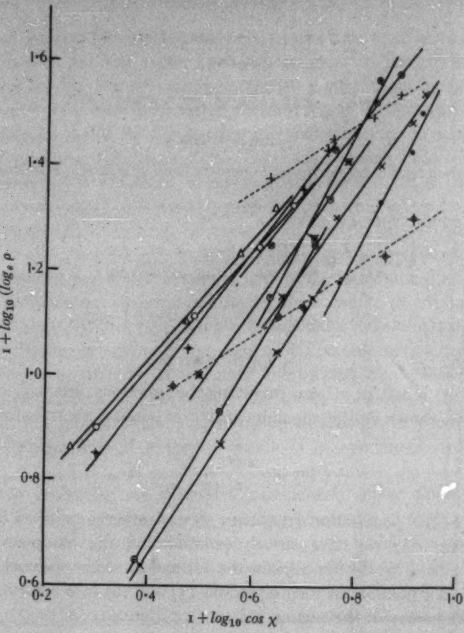

Figure 4

Symbols in figure 4	Date (1936)	Frequency (Mc./sec.)	Mean slope of curve
•	5 June	4·16	2·0
×	8 June	4·16	1·4
⊙	13 July	3·75	1·9
+	16 July	3·95	0·65
⊗	17 July	3·95	1·35
⊕	13 October	4·14	1·7
✕	16 October	3·36	1·5
○	21 October	3·30	1·1
△	28 October	3·45	1·15
✦	6 November	3·45	0·7
⊠	30 November	3·22	1·45
✚	2 December	3·22	1·25

Mean slope excluding 16 July and 6 November: 1·48.

with the ionizing agency. We shall discuss the significance of this equilibrium in the next section.

If the electrons were lost in the absorbing region by a process of electron-capture, or by recombination with α proportional to pressure, equations (5) and (6) show that we should expect $\log \rho$ to be proportional to $\cos \chi$ so that the slope of the lines in figure 3 would be 1 instead of 1·5. If, further, the ionization lagged behind the ionizing agency, we should expect an even slower variation of $\log \rho$ with $\cos \chi$. It appears from the experimental results that we must discard both these possibilities.

In his Bakerian Lecture to the Royal Society, Prof. Appleton(3) described experiments in which the absorption of a wave of frequency 4 Mc./sec. was measured at midday throughout a period of 2 years. He compared the absorption with the corresponding value of the sun's zenith angle and found during the summer months that $\log \rho$ was approximately proportional to $(\cos \chi)^{\frac{3}{2}}$. In comparing the ratio of the summer to the winter noon values of $\log \rho$ he found, however, a marked disagreement with the simple theory. He considered that this discrepancy might possibly be due either to the influence of region-F_1 absorption in winter, or to the absorbing influence of a stratum below region E in which ν was not negligible in comparison with p, so that the variation of attenuation with change of χ was not so rapid as it is in the case of region E. Our diurnal curves for quiet days, however, appear to fit the $(\cos \chi)^{\frac{3}{2}}$ law both in summer and in winter, and it is difficult to reconcile the two results.

We have seen that equation (3) gives the right form of variation with the sun's zenith angle, so we now turn to equation (7), which is derived from equation (3), and consider whether the observed absolute value of the reflection coefficient agrees with our knowledge of the magnitude of the other quantities. We shall take the results of figure 2, which give, at 1400 G.m.t.

$$\log \rho = -1{\cdot}85,$$

$$p_0 = 2\pi \times 2{\cdot}75 \times 10^6 \text{ sec.}^{-1},$$

$$p = 2\pi \times 3{\cdot}22 \times 10^6 \text{ sec.}^{-1},$$

and hence, from equation (7) $H\nu_m = 3{\cdot}5 \times 10^{10}$ cm./sec. In this calculation we have taken the greatest of the three penetration frequencies which were observed on this occasion; the equivalent height of the corresponding region was about 130 km.* To see whether the calculated value of $H\nu_m$ is reasonable we take Martyn and Pulley's(10) suggested values for the E region, viz.: $H = 9{\cdot}05$ km. and $\nu = 3 \times 10^5$ sec.$^{-1}$, giving $H\nu_m = 27 \times 10^{10}$ cm./sec. This appears to be too large, and would lead to a value of $\rho = e^{-14\cdot3}$, which is much too small. It is interesting to see what result we get if we take the simple theory as correct and use the observed value of ρ to give a value of ν_m assuming that $H = 9$ km. in the E region. We then arrive at the value $\nu_m = 3{\cdot}9 \times 10^4$ per second, considerably lower than Martyn and Pulley's value. This is the value at the level of maximum ionization, around 130 km. If we adopt a previous suggestion of Martyn(11), that $\nu = 10^6$ at 90 km., then with $H = 9$ km.

---

* The heights here quoted cannot be measured more accurately than within about ± 5 km., partly on account of instrumental inaccuracy and partly on account of group retardation in the E region.

we should have $\nu = 1{\cdot}2 \times 10^4$ at 130 km. which is not very different from our value. The value given here is also in agreement with some values given in his Cambridge Ph.D. thesis (not published) by F. T. Farmer, who used the group-retardation method previously described^(1) and obtained a mean value of $\nu = 10^4$ sec.$^{-1}$ at a height of 130 km. We consider that a value of about 2×10^4 cannot be far wrong at 130 km.

In comparing this value of ν with that suggested by other workers for the *E* region we first draw attention to the fact that, if $H = 9$ km. near the *E* region, the value of ν is changing rapidly with height in this neighbourhood, so that it is important to specify the exact height when quoting a value for ν. We have mentioned that our value applies to a height of about 130 km., the level of maximum ionization at midday in midwinter; calculation and observation show that the level of maximum ionization at midday in summer is about 120 km., and 5×10^4 is the appropriate value for the collisional frequency. We have previously mentioned that the level of maximum absorption is at a distance $1{\cdot}1H$ below the level of maximum ionization, so that the values of ν at this level would be $4{\cdot}5 \times 10^4$ in winter and $1{\cdot}5 \times 10^5$ in summer. When we remember that the value 3×10^5 given by Martyn and Pulley^(10) as "the mean value at the level of the *E* region" is based on absorption measurements, so that it represents the lower portion of the *E* region, it does not seem to be in serious conflict with the values given above.

§ 5. CONCLUSIONS

It appears to be possible to explain the experimental results regarding the absorption of waves, reflected under quiet conditions from the *F* region, by assuming that when the waves are not retarded by being near *F*-region critical frequencies, the absorption takes place in an *E* region which is of the Chapman form, i.e. a region in which the electrons are produced by homogeneous electromagnetic radiation incident from the sun, and the electron dissipation process is one of recombination with α independent of the pressure. This supposition requires that α must remain independent of the pressure down to levels about 12 km. below the *E*-region maximum.

An important point in the explanation outlined above is that the ionization throughout the absorbing region appears to be in approximate equilibrium with the ionizing agency over quite a large portion of the day. This means that in the equation

$$\frac{dN}{dt} = I - \alpha N^2$$

both I and αN^2 are large compared with dN/dt. Taking the values calculated from the observed absorption curves for 1600 G.m.t. in winter, and assuming that the appropriate value of N is that which would be calculated for the level of maximum $N\nu$, i.e. $1{\cdot}1H$ below the level of maximum N, we find that α must be at least 10^{-8}. This value is considerably larger than that, 2×10^{-10}, calculated by Chapman^(13) for recombination between electrons and positive ions at those pressures for which α is independent of pressure.

We have arrived at this same conclusion from a study of the diurnal variation of *E*-region penetration frequencies⁽²⁾; in that connexion the conclusion is valid only for the level of maximum ionization in the *E* region, but the present work shows it to be true lower down. The same deduction has been made for the level of the *E*-region maximum by Prof. Appleton in his recent Bakerian Lecture⁽³⁾.

In connexion with the results recorded in this paper it is interesting to recall an observation made by F. W. G. White⁽¹²⁾, who pointed out that in the afternoon and evening the absorption of waves decreases more rapidly than would have been deduced from a simple Chapman region. The reason for this is now seen to be that he was considering a Chapman region with too small a value of α, arrived at by observations on the nocturnal decay of the ionization maximum. We have given reasons elsewhere⁽²⁾ for supposing that the value of α in the daytime is greater than at night.

§6. ACKNOWLEDGEMENTS

In conclusion we wish to record our very great indebtedness to our colleagues who gave valuable help with the observations. Our thanks are due especially to Dr F. T. Farmer, and also to Mr K. G. Budden and Mr K. Weekes.

APPENDIX

We here take up some mathematical points referred to in the body of the paper.

(i) For the Chapman region given by

$$N=\sqrt{\frac{B}{\alpha}}\exp\left\{-\frac{x}{2}-\frac{C\sec\chi}{2}\exp(-x)\right\},$$

the maximum of ionization occurs at a height x_m given by

$$\exp(x_m)=C\sec\chi \qquad \text{......}(a),$$

and the maximum value of N at this level is

$$N_m=\sqrt{\frac{B\exp(-\frac{1}{2})}{\alpha(C\sec\chi)^{\frac{1}{2}}}} \qquad \text{......}(b).$$

(ii) Equation (2) involves the integral

$$\int_0^\infty \exp\left\{-\frac{3}{2}\frac{h}{H}-\frac{C\sec\chi}{2}\exp\left(-\frac{h}{H}\right)\right\}dh.$$

Write $\frac{h}{H}=x$ and we have

$$H\int_0^\infty \exp(-x)\exp\left\{-\frac{C\sec\chi}{2}\exp(-x)\right\}\exp\left(-\frac{x}{2}\right)dx.$$

Now write $\frac{1}{2}C\sec\chi=k$ and $Z=\sqrt{k}\exp(-\frac{1}{2}x)$, and the integral becomes

$$H\int_{z=\sqrt{k}}^{z=0}\frac{Z^2}{k}\exp(-Z^2)\left(-\frac{2}{\sqrt{k}}\right)dZ$$

$$=Hk^{-\frac{3}{2}}\left[Z\exp(-Z^2)-\int\exp(-Z^2)\,dZ\right]_{Z=\sqrt{k}}^{Z=0} \qquad \text{......}(c).$$

Now x_m is known to be of the order of 12 so that, from equation (*a*),

$$C \sec \chi = 2k \fallingdotseq e^{12};$$

hence

$$\sqrt{k} \fallingdotseq 280.$$

The first term in equation (*c*) is thus approximately zero at both limits; the second term is the error-function integral taken between the limits 0 and 280, which, from tables such as those given by Jeans in his *Dynamical Theory of Gases*, are seen to be effectively the limits 0 and ∞ which give the value $\sqrt{\pi}/2$. The integral is therefore equal to

$$\tfrac{1}{2}\sqrt{\pi} H \left(\frac{2}{C \sec \chi}\right)^{1\cdot 5} = 2\cdot 5 H \left(\frac{\cos \chi}{C}\right)^{1\cdot 5},$$

which leads to equation (3).

(iii) If in equation (3) we substitute the value of N_m as given by (*b*) and then convert to the penetration frequency p_0 as given by

$$p_0^2 = 4\pi N_m e^2/m,$$

and also substitute

$$\nu_m = \nu_0 \exp(-x_m) = \frac{\nu_0}{C \sec \chi}$$

from (*a*), we obtain

$$\frac{1\cdot 25 \exp(\frac{1}{2})}{c} \frac{p_0^2}{(p+p_L)^2} H\nu_m = \frac{2\cdot 06}{c} \frac{p_0^2}{(p+p_L)^2} H\nu_m,$$

which is equation (7).

(iv) Expressions (5) and (6) involve the integral

$$\int_0^\infty \exp\{-x-k\exp(-x)\}\, dx,$$

where

$$k = C \sec \chi.$$

This integral is

$$-\frac{1}{k}\Big[\exp\{-k\exp(-x)\}\Big]_0^\infty \fallingdotseq \frac{1}{k} = \frac{\cos \chi}{C},$$

when k is large.

REFERENCES

(1) Farmer and Ratcliffe. *Proc. Roy. Soc.* A, **151**, 370 (1935).
(2) Best, Farmer and Ratcliffe. *Proc. Roy. Soc.* A, **164**, 96 (1938).
(3) Appleton. *Proc. Roy. Soc.* A, **162**, 451 (1937).
(4) Halliday. *Proc. Phys. Soc.* **48**, 421 (1936).
(5) Chapman. *Proc. Phys. Soc.* **43**, 26 (1931).
(6) Booker. *Proc. Roy. Soc.* A, **150**, 283 (1935) (see equation (41)).
(7) Appleton. *Proc. Phys. Soc.* **45**, 208 (1933).
(8) Appleton and Naismith. *Proc. Roy. Soc.* A, **150**, 685 (1935).
(9) Pedersen. *Propagation of Radio Waves* (Copenhagen), Fig. V. 3, p. 55 (1927).
(10) Martyn and Pulley. *Proc. Roy. Soc.* A, **154**, 463 (1936).
(11) Martyn. *Proc. Phys. Soc.* **47**, 323 (1935).
(12) White. *Proc. Phys. Soc.* **46**, 91 (1934).
(13) Chapman. *Proc. Roy. Soc.* A, **132**, 353 (1931).

A COMPARISON OF THE MIXED-POWDER AND SUBSTITUTION METHODS IN THE QUANTITATIVE EVALUATION OF X-RAY REFLECTIONS FROM CRYSTALLINE POWDERS

By J. C. M. BRENTANO, D.Sc.
Physics Department, University of Manchester

Received 19 *October* 1937. *Read in title* 26 *November* 1937

ABSTRACT. The conditions determining the quantitative measurement of X-ray reflections by the substitution and by the mixed powder methods are compared with regard to the evaluation of atomic scattering factors. The paper is supplementary to a paper by Brindley and Spiers; it contributes particularly to the discussion of particle-size, of extinction, and of differential absorption. A method is indicated for determining the presence of differential absorption and so avoiding errors which may arise from that cause when the mixed-powder method is applied to coarse particles. Techniques are described relating to the substitution and to the mixed-powder methods. Attention is drawn to a technique in which the mixed-powder and substitution methods are used conjointly.

---

§ 1. INTRODUCTION

Messrs Brindley and Spiers have kindly given me the opportunity of reading the MS. of their paper on "The measurement of the intensities of X-ray reflections from crystalline powders in absolute units"(13), the main subject of which is a comparison of the merits of the mixed-powder and of the substitution methods, and invite me to set out in a separate note those points on which my own experience leads to additional remarks. I gladly fall in line with this proposal in order that the two papers may conjointly provide an account of the technique which we have found effective in our work.

The more general aspects concerning the quantitative evaluation of intensities of X-ray reflections from powders have been dealt with by me in a short paper(1) related to some work of Schäfer. I may be allowed to refer to this paper so as to avoid repetition; Brindley and Spiers also discuss these points in so far as they are more directly connected with the comparison of the two methods and come to largely similar conclusions. Any difference in our views does not concern these more general aspects, but rather the practical application of different techniques. These points are perhaps best represented by reference to the successive development of the methods.

§ 2. GENERAL SURVEY

The first comprehensive discussion of the experimental conditions affecting intensity measurements was given with the classical measurements of the intensities of X-ray reflections from single rock-salt crystals by Bragg, James and Bosanquet (reference to the various papers can be found in Bragg⁽²⁾), when two points arose requiring particular attention. One was the establishing of the correct relation between the incident and the reflected beam having regard to absorption, the other was the correct allowance for the extinction effects which arise when the crystal units or crystallites composing the mosaic crystal exceed a certain size. With the aim of eliminating such errors the writer resorted to extremely fine powders constituted of such small particles that the maximum size of the crystallites imposed by the particle-size fell below the limit at which extinction effects arise. By using powders instead of single crystals the intensities of reflections became much weaker, and while in the experiments of Bragg, James and Bosanquet a direct comparison of the intensities of the incident and reflected beams could be made by means of a sensitive ionization method, with the much weaker reflections from powders a direct comparison did not seem practical. We therefore did not attempt to obtain absolute values of atomic scattering factors, but limited the problem to comparative measurements, a procedure which was generally adopted in later work. At first, we made use of a standard powder which could be inserted in the direct beam for given intervals of time, so that its reflections could be used as a measure of its intensity. The evaluation of the atomic scattering factors does then still require the allotment of the correct absorption coefficients to the powder specimens. We abandoned, therefore, this method in favour of the mixed-powder method⁽³⁾, in which fine powders of the substances to be compared are mixed in a known weight-ratio, when the same absorption coefficient, which does not require to be known explicitly, applies to the reflections from both substances, provided the powders are so fine that the absorption in the individual particle has a negligible effect on the reflected intensity. This it has when the particle-size is chosen so as to eliminate extinction effects and the required condition was therefore satisfied in our measurements⁽¹⁰⁾. Glocker and Schäfer⁽⁴⁾ applied the mixed-powder method to coarser powders, assuming that the particles were constituted of sufficiently small crystallites to avoid extinction errors, without giving consideration, however, to the fact that the assumption of a common absorption coefficient no longer held good and that any difference in the absorption coefficients of the substances affects the reflected intensities. An error arises then, owing to the fact that in a coarse powder mixture the X-rays reflected from particles of both one and the other substance travel on the average for a predominant part of their path in that substance. For the convenience of the present discussion we call this effect the "differential absorption effect". Schäfer in a subsequent paper⁽⁵⁾ has discussed in detail the errors involved.* Bradley⁽⁶⁾ has avoided the necessity of preparing fine powders by alloying the elements to be compared. Coarse particles of the alloy can then be used. The method is restricted to the comparison of those elements which can be alloyed to form crystallites with a common lattice and other limitations are imposed, but it eliminates in a very elegant way the extinction and absorption errors of coarse particles. Brindley and Spiers⁽⁷⁾ avoid the effects of differential absorption (not those of extinction) encountered with large particles, by resorting to separate layers and exposing them in succession, in which case, as we have indicated above, the absorption coefficient for each layer must be known. They give a detailed analysis of this procedure which originally they called "the method of separate layers". With the fine particles satisfying the condition of negligible extinction used in our work, the differential absorption effect does not arise, as the limitation imposed in order to avoid extinction restricts the size of the particle more than is required for avoiding absorption. In increasing the accuracy of measurement the writer, in collaboration with Baxter, was, however, faced with a particular source of error resulting from the superposition of lines on background steps and on other lines(11, 12). Such superpositions occur with the reflection lines of one single substance; they increase in number, however, with the number of lines and are thus reduced when the reflections of the two substances are recorded separately.

---

* See also reference (10).

The writer was thus also induced to resume the separate recording of the reflections from the two substances placed alternately in the camera, a procedure for which we used the term "substitution method", a term adopted in their recent paper also by Brindley and Spiers. Their work was entirely independent of ours and had also different aims, as they were primarily interested in separating the layers so as to avoid the necessity of preparing fine particles and intimate mixtures of powders, while we were mainly concerned with obtaining separate records of the lines and background steps of the two substances so as to avoid superpositions.

It will be seen from this survey that the development of intensity-measurements is not in the direction of evolving one general method, but rather of developing a number of specialized techniques adapted to particular conditions. In fact, so long as we are unable to prepare in a general way particles of controlled sizes or particles constituted of small crystallites and to introduce into the calculation sufficiently accurate values for the absorption coefficients, only limited groups of substances are accessible to intensity-measurements, and separate consideration has to be given to each individual case.

A few specific points may be discussed, having regard in the first place to the evaluation of atomic or unit-cell scattering factors. Such determinations require the elimination of any influence of the particular habitus of the reflecting crystallites, i.e. of extinction effects and also of all effects of absorption.

§ 3. PRIMARY EXTINCTION

Primary extinction becomes appreciable for crystallites, the term being used in the sense of the extension of a regular lattice block, exceeding 100 or 1000 atom layers according to the atomic weights of the elements constituting the crystals. This corresponds to magnitudes of the crystallites of the order of $5 \cdot 10^{-5}$ or $5 \cdot 10^{-4}$ mm. Such small crystallites may be secured either by actually reducing the size of the particles to these limits or with coarser powders if the particles are adequately subdivided into smaller crystal units. In our experience such a state of subdivision cannot be presumed to exist, and while a large mosaic crystal is generally subdivided into much smaller crystallites we are not justified in assuming that the size of such crystallites decreases at the rate at which the overall size of the crystal particles becomes smaller, the habitus of the crystallites being rather not to break into smaller units after a certain limit is reached.

To quote two typical instances the writer observed for rocksalt and for copper, which can be taken as representatives of the soft, imperfect and of the ductile types of crystals and for which it might be expected that the breaking up of particles into very small crystallites will most readily take place, quite appreciable extinction effects even after violent mechanical action, so long as the particles themselves exceeded the limits above which the individual crystallites would give extinction effects. This indicates that the individual crystallite was of the same order of magnitude as the crystal particle. Similar observations were made by other experimenters.

We certainly do not wish to say that coarser particles of a powder are never subdivided into such small crystallites as to be free from extinction, but it appears that such a condition cannot be presumed to exist without having actually been ascertained for each particular powder. Such a verification can be carried out in two ways: either by determining the intensities of a number of lines and comparing these with the normal intensity-distribution of the substance and so revealing extinction effects by systematic differences of the intensity-distribution (such an evaluation requires that the scattering properties and temperature factors of the substance shall be already well known), or by comparing the relative intensities of the lines with those obtained from a preparation of the same substance known to be so fine as to be free from extinction. In this case a fine powder must actually be available.

§4. ABSORPTION AND SECONDARY EXTINCTION

Absorption coefficients have been determined experimentally for a number of substances; in a more general way they can be derived from expressions established by Jönsson(8). Brindley and Spiers, in advocating the use of the substitution method, suggest obtaining the necessary absorption coefficients of the substances constituting the separate layers from Jönsson's expressions. Comparing the absorption coefficients so derived with experimental values so far as such data are available, for instance the values collected in Compton and Allison's book(9), the agreement is far from uniform; we do not feel sure, therefore, whether these expressions can be considered as sufficiently reliable until they have found a fuller theoretical basis. Any uncertainty on this point should not, however, constitute an objection against the substitution method, as it can be safely assumed that within a short time sufficient experimental material will be available either to confirm or to modify Jönsson's expressions and so to make definite values available. A difficulty of a different kind appears, however, in applying these data. The intensity of the X-ray beam is reduced more than by normal absorption when it encounters crystallites oriented at a reflection angle with regard to the beam. Such a secondary extinction effect appears as an addition to the coefficient of true photoelectric absorption. For the case of a fine powder with crystallites oriented at random this entails an addition to the normal absorption which is of comparatively little significance. The effect becomes much more important, however, for coarser powders, in which the individual crystallites even when small are arranged as a mosaic approximately parallel one to another. The addition to the normal absorption coefficient introduced by secondary extinction deserves then closer attention, as it is peculiar to each individual powder and assumes different values for different reflections. Further, in our experience some binding or spacing material must in general be added to the powder, which besides fixing the powder in its holder has the important function of preventing preferential orientation, which occurs when the powder is pressed in the frame or cavity in which it is held. This binding material adds to the absorption, particularly with substances of small atomic weight. Brindley and Spiers do not discuss the effects of secondary extinction and of the binding material on the absorption coefficient. There are certainly instances when they do not arise, namely, with hard particles constituted of small crystallites arranged in a micro-crystalline random orientation, which cannot be affected by outside agents. Secondary extinction is then small, and a binding material can be dispensed with. In general, however, the addition of a binding material seems necessary and the modification of the normal absorption coefficient introduced by it and by the secondary extinction effect of mosaics must be taken into account when the substitution method is being used.

§ 5. THE TWO METHODS COMPARED

Comparing the merits of the substitution and the mixed-powder methods, we may say that the most prominent advantage of the first seems to be that it can be applied to coarse particles, its disadvantage that it requires explicit knowledge of the numerical values of the absorption coefficients of the powders.

From what we have discussed in §§ 3 and 4, it will be seen that correct values of scattering factors can only be obtained if errors due to extinction and to preferential orientation are eliminated. The practical way for ascertaining that this condition is satisfied requires that the substances shall be available in a state of fine powder, either for using such a powder in the actual determination, or for providing the means of verifying by comparison that for the particular substance larger blocks are sufficiently subdivided and oriented at random. The substitution method does not, therefore, make accessible to quantitative evaluation of scattering factors the large number of substances of which no fine powders can be prepared; it can be applied to the limited group of coarse powders or aggregates from such substances for which it can be ascertained that they are constituted of sufficiently small crystallites and that these are oriented at random and not in the pattern of a more or less regular mosaic.

We tend, therefore, to view the problem of determining scattering factors or making absolute intensity-measurements in the first place as a problem of preparing sufficiently finely subdivided powders, and consider that powder methods should be used for accurate quantitative measurements only when such powders are available. In previous papers we have indicated the means by which fine powders can be obtained; we found that they could be prepared by chemical processes of precipitation or of reduction but not by the mechanical action of crushing or grinding.

§ 6. POINTS OF TECHNIQUE

A few remarks may be made regarding points of technique which, in individual cases, may weigh in deciding in favour of one or the other method.

As regards the substitution method, it will be seen in each individual case whether sufficiently reliable absorption coefficients for the particular substances and wave-lengths are available and whether such values apply to the actual powder layer. Here we may indicate a method whereby one difficulty, encountered with our original design of powder-holder and also with the powder-holder described by Brindley and Spiers—that the powder must be mixed with binding material affecting the absorption coefficient or firmly pressed in a holder and so subjected to preferential orientation—can be eliminated by exposing it to X-rays behind a celluloid window or in a narrow celluloid tube, according to the type of camera used, the only essential condition being that the two powders to be compared should be placed behind windows giving equal absorption.

Regarding the method of mixed powders a limitation is imposed by requiring substances in the state of fine powders, but the preparation of an intimate mixture of particles of two substances presents no serious difficulty if a brittle spacing or mixing substance is used, in the way described by us elsewhere. In this connection it should be mentioned that there exists a definite criterion for ascertaining whether the particles of a mixed powder are sufficiently small or sufficiently well mixed. This consists in taking records from the mixture for two wave-lengths so chosen that the X-rays suffer widely different absorption, while avoiding those wave-length ranges for which the scattered intensities are much affected by anomalous dispersion. When the relative intensities of the reflections from the two constituents of the powder are then compared, any differential absorption error is distinctly shown by a change in the relative intensities of the lines obtained for the two wave-lengths. No equally direct test is available for deciding whether absorption coefficients have been correctly assessed or whether extinction effects have occurred.*

To illustrate the point by reference to the experiments quoted by Brindley and Spiers, it fully conforms with expectation that with the coarse particles errors of differential absorption should occur; at the same time we are not sure whether part of the deficiencies observed is not due to extinction. That mechanically prepared copper powders show marked extinction effects has been observed by the writer in the case of mixed layers of mechanically pulverized and chemically precipitated copper with nickel, any differential absorption effect being in these conditions small owing to the small difference in the absorption coefficients. The actual correct assessment of extinction by comparison of the intensities of reflection for varying orders or angles requires a very detailed knowledge of the change of scattering with angle and of the temperature factor.

---

* It should be noted—a point which does perhaps not appear so clearly from the discussion in § 5 of Brindley and Spiers's paper—that for the substances and wave-lengths generally used extinction sets a smaller limit to the permissible size of the crystallites than differential absorption sets to the size of the particles. When the crystallites are constrained by the particle size, the limitation set to the extension of the particles in view of extinction will thus also eliminate differential absorption. The converse relation cannot in general be assumed to hold good.

When the mixed-powder method is used for larger particles it should be noted that any differential absorption effect very largely depends on the relative absorption coefficients of the two substances and disappears when the linear absorption coefficient is the same(10). Such effects can thus be greatly reduced by choosing substances with nearly equal absorption coefficients. This technique makes it possible in selected cases to apply the mixture method to very coarse particles if such measurements are justified when regard is had to extinction.

In our experiments we had used aluminium as a comparison substance; owing to the small scattering factor of the aluminium atom comparatively large crystallites are free from appreciable extinction and so we can obtain strong aluminium re-reflections without much interference from extinction effects. Brindley and Spiers now recommend aluminium for general use. It should be noted, however, that we were able to use aluminium because our particles complied with the criterion of negligible extinction and therefore, *a fortiori*, were sufficiently small not to give rise to any errors of differential absorption; the reason why we preferred it was, in the first place, that it has no absorption edges in the range of wave-lengths usually used and introduces therefore no appreciable anomalous dispersion and no absorption steps.* Such effects need, however, only be considered in measurements of a high accuracy. Outside of such requirements, when it is desired to avoid differential absorption effects of larger particles it is preferable to choose a substance which has nearly the same absorption coefficient as the substance to be investigated, among the range of oxides and chemically reduced metal powders which are available in the state of sufficiently fine subdivision.

§7. OTHER DEVELOPMENTS

I take the title chosen by Brindley and Spiers for their paper as signifying that quantitative measurements of scattering factors are the subject under discussion. It is for this reason that I have dealt with these in the foregoing notes. Brindley and Spiers remark, however, that in previous papers I impose an unwarranted restriction by assuming beforehand that extinction effects should be avoided. The points in my papers to which these remarks apply are concerned as is the present discussion, with the measurement of scattering factors, and I think that for such measurements superpositions with extraneous effects should be excluded. There is certainly, however, a wide field for the substitution method outside of this particular domain;

---

* The aluminium used in our experiments was chemically prepared aluminium powder obtained from Kahlbaum; the ordinary aluminium powders prepared by mechanical processes are not suitable. Brindley and Spiers, experimenting at first with such powders, found that they were unsuitable and in a discussion expressed surprise that I could use aluminium powder for intensity-measurements until they obtained a sample of an aluminium powder from the same source. The point illustrates clearly the great importance of using suitable powders.

in fact while Brindley and Spiers developed and discussed the substitution method as a means of avoiding the necessity of preparing fine particles and intimate mixtures for the comparative determination of scattering factors, I myself at an earlier stage did not pursue the use of the method for determining scattering factors owing to the difficulty of assessing correct values for the effective absorption coefficients. I took it up again after having developed the method of mixed powders to meet problems which arose in connection with this method and as an auxiliary to it.

Two applications are here of particular interest. One is the comparison of corresponding reflections from different preparations of the same substance, when by comparing the shape and intensity of lines from preparation of different fineness we can ascertain whether the required state of subdivision has been attained. Instances of too imperfect powder particles or of vanishing size-distribution can so be found. In such comparisons, where both powders are constituted of the same substance, the correct assessment of the absorption coefficient is immaterial, so long as the same proportion of binding material is used in each case and the particles are sufficiently small in all the powers to avoid the occurrence of a differential absorption effect between this binding material and the particles. By using for one of the powders particles constituted of sufficiently large crystallites, we can obtain lines the width of which is only determined by factors other than the condition of the crystallites and thus distinguish any goniometer broadening from the broadening due to the imperfection of the crystallites. Another application is the use of the substitution method for obtaining separate records and the exact relative location of lines and background steps which on the record from the mixed powder are in too close proximity to be easily evaluated⁽¹²⁾. It is possible to determine from such separate records whether actual superposition has taken place, and in some cases to correct for superpositions from the intensity-distribution determined for each line. It is for this reason that the goniometer described in another paper⁽¹¹⁾ has been so designed that the two patterns of lines obtained by the substitution method are recorded under conditions securing as accurately as possible their correct relative position, this is done by taking the two records on adjacent strips of the same film held throughout in a rigid position with respect to the slit system of the goniometer.

In conclusion, attention may be drawn to one merit of the substitution method which has not been mentioned in the paper by Brindley and Spiers, namely, that in comparison with records from the mixed powders the lines stand out of the background more strongly. This does not reduce the interference of background steps we have discussed in other papers, as the whole of the powder instead of one part only contributes to one group of lines and to the regularly reflected part of the background, but it helps to make the lines more easily measurable.

We wish by no means to present the distinction between the two methods as a case of superiority of one over the other, and if we lay more weight than Brindley and Spiers on the precautions which have to be taken when the substitution method is applied to measurements with large particles, this is because we believe that the substitution method, by eliminating differential absorption, does not in itself eliminate other more subtle errors which account for many faulty investigations associated with coarse powders, a point with which Messrs Brindley and Spiers will probably agree, but which should perhaps be stressed in the interests of those less familiar with the intricacies of intensity-measurements of X-ray reflections.

§8. ACKNOWLEDGEMENT

I wish to thank Prof. W. L. Bragg, F.R.S., for the interest taken in the preparation of this paper.

REFERENCES

(1) Brentano, J. C. M. *Z. Phys.* **99**, 65 (1936).
(2) Bragg, W. L., Darwin, C. G. and James, R. W. *Phil. Mag.* **1**, 897 (1926).
(3) Brentano, J. C. M. *Phil. Mag.* **4**, 620 (1927); **6**, 178 (1928).
(4) Glocker, R. and Schäfer, K. *Z. Phys.* **73**, 289 (1932).
(5) Schäfer, K. *Z. Phys.* **86**, 738 (1933).
(6) Bradley, A. J. and Hope, R. A. H. *Proc. Roy. Soc.* A, **136**, 272 (1932).
(7) Brindley, G. W. and Spiers, F. W. *Proc. Leeds Phil. Lit. Soc.* **3**, 4 and 73 (1935).
(8) Jönsson, E. Thesis, Uppsala (1928).
(9) Compton, A. H. and Allison, S. K. *X-rays in Theory and Experiment* (1935). London.
(10) Brentano, J. C. M. *Proc. Phys. Soc.* **47**, 932 (1935).
(11) Brentano, J. C. M. *Proc. Phys. Soc.* **49**, 61 (1937).
(12) Baxter, A. and Brentano, J. C. M. *Phil. Mag.* **24**, 473 (1937).
(13) Brindley, G. W. and Spiers, F. W. *Proc. Phys. Soc.* **50**, 17 (1938).

SENSITIVITY OF PHOTOGRAPHIC PLATES IN THE REGION 2500–2000 A.

By A. HUNTER, Ph.D. and R. W. B. PEARSE, Ph.D.,
Physics Department, Imperial College of Science and Technology

Received 24 *November* 1937. *Read in title* 11 *February* 1938

ABSTRACT. The effect of sensitizing photographic emulsions for the wave-length region 2500 to 2000 A. by bathing them in fluorescent substances before exposure, or by decreasing their gelatin content, is examined experimentally. The characteristics of seventeen different types of plates are compared by a simple method of sensitometry in which the plates are given stepped exposures to the γ bands of nitric oxide under reproducible conditions. Direct density-comparisons made by visual estimation are then sufficient to give the information as to relative sensitivities which is most likely to be required by the practical spectroscopist. Apart from the Ilford Q2 plate, which has special characteristics that are fully discussed, it is found that a measurable record can be obtained with the least possible exposure on an ordinary plate. In this sense, therefore, the methods of sensitization at present available do not have the effect which is generally ascribed to them. Their main use is for increasing contrast and saturation density, not threshold sensitivity. A table gives the relative threshold exposure times needed for the different plates at various wave-lengths, and spectrograms on representative plates are reproduced.

§1. INTRODUCTION

Having had occasion recently to photograph spectra of low intensity in the region 2500 to 2000 A., we were surprised to find that more satisfactory results could be obtained with ordinary plates than with plates recommended as having much higher ultra-violet sensitivity. This paper presents the results of experiments made with a view of clearing up this apparently anomalous behaviour. The point of view throughout is that of the practical spectroscopist who wishes to photograph a spectrum in this region of the ultra-violet.

It is well known that the sensitivity of an ordinary photographic emulsion begins to fall rapidly just below 2500 A., and is very low at 2000 A. In the Schumann region the sensitivity becomes negligibly small. This fall is due, not to an intrinsic failure of the short-wave radiation to render developable the silver salts used in the emulsion, but to an increasingly strong absorption of the radiation by the gelatin of the emulsion. Thus in the Schumann region the halide grains are still photochemically active, but they are so completely screened by an opaque layer of gelatin that the emulsion is useless for photography. To radiation of wave-lengths 2500 to 2000 A. the gelatin is not so opaque, and the effect is accordingly not so pronounced: an ordinary plate is still serviceable at 2500 A. and can be made to yield traces at 2000 A. Nevertheless, the results obtainable in this region are unsatisfactory in

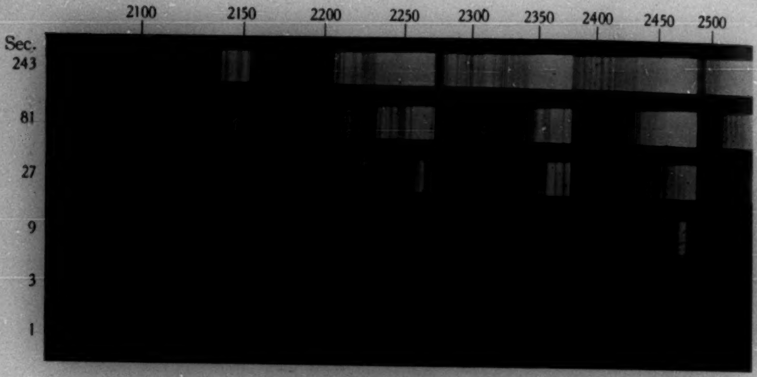
2100
2150
2200
2250
2300
2350
2400
2450
2500
Sec.
243
81
27
9
3
1

(3) Hilger Schumann plate.

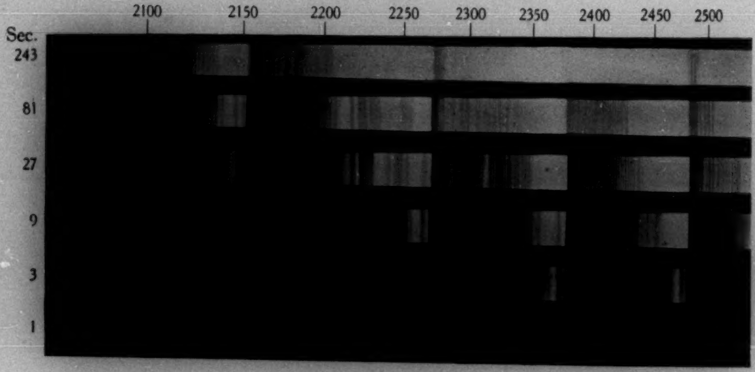
2100
2150
2200
2250
2300
2350
2400
2450
2500
Sec.
243
81
27
9
3
1

(4) Ilford *Q2* plate.

Plate 2.

comparison with those in the near ultra-violet, and many attempts have been made to combat the fall in sensitivity. These attempts are based on the assumption, obviously made with considerable *a priori* justification, that the photographic technique which has succeeded in vacuum spectroscopy will also be effective in increasing sensitivity in the region 2500 to 2000 A. It is in fact commonly stated that this is indeed so(1,2). Uncritical acceptance of such assertions without careful examination of their exact meaning, however, is, we believe, a source of widespread disappointment among spectroscopists, to whom this region is of great importance.

§2. TYPES OF SENSITIZATION IN PRESENT USE

In the Schumann region the loss of sensitivity mentioned above is commonly overcome in two ways. For the region 2500 to 2000 A., too, the preparation of specially sensitive plates, whether in the laboratory or in the factory, is based on one of these methods.

(1) It may be arranged that the radiation shall have to pass through as little gelatin as possible before encountering the silver halide. Examples of this method are:

(*a*) the original Schumann plates(3), in which no gelatin is used;

(*b*) the commercial Schumann plates (Hilger and Agfa), in which the gelatin-content of the emulsion is greatly reduced as compared with an ordinary emulsion;

(*c*) the Duclaux-Jeantet plates(4), in which the gelatin of an ordinary plate is removed by solution in sulphuric acid;

(*d*) the Ilford Q plates(5) in which a rock-garden effect is produced by the manufacturing process, the silver halide grains being concentrated on the surface of the gelatin.

(2) An ordinary plate may be bathed in a fluorescent substance which can convert the short waves into radiation able to penetrate the gelatin. Substances commonly used are:

(*a*) mineral oils(6) and greases(7);

(*b*) sodium salicylate(8);

(*c*) anthracene(9);

(*d*) commercial sensitizers, such as those used on special ultra-violet plates marketed by Eastman* and Agfa†.

In view of our disappointing experience with certain of the more usual of these devices for sensitizing, we decided to make a thorough test of plates representing each type.

§3. EXPERIMENTAL PROCEDURE

The method of testing is in essence as follows. Each plate was exposed to ultra-violet light (2500 to 2000 A.) under standard reproducible conditions. It was then processed according to the manufacturer's recommendations. Finally, a direct comparison was made, wave-length by wave-length, between the densities produced in this way on the several plates. The following discussion of the procedure adopted may perhaps be of interest.

---

* Di-hydro-collidine, ethyl carboxylic ester.

† Messrs Agfa Photo, Ltd., inform us that the nature of the Agfa sensitizer is a manufacturing secret.

Since the variation of plate-sensitivity with wave-length is so marked in this region, direct exposure to a source emitting radiation of a mixture of wave-lengths is useless. For the same reason the use of a monochromatic source would not yield enough information: a series of such sources would be necessary. The most satisfactory method is to disperse a mixture of wave-lengths into a spectrum, expose the different plates to this spectrum, and then make density-comparisons between the plates at corresponding points along the spectrograms. The spectrum used may consist of lines, bands, or a continuum. Of these, a band spectrum is to be preferred, since, unlike both a line spectrum and a continuum, it will usually exhibit a considerable range of intensity in a short range of wave-lengths; and, unlike a continuum, it will serve as its own wave-length scale. As for the source, arcs and sparks are not so easy to control as discharge tubes. After some trials with other sources, we finally decided on a heavy-current discharge tube(10), through which passed a slow stream of air. This provides a steady source of the γ bands of nitric oxide, which extend throughout the region 2500 to 2000 A.; see plate 1. The bands are characterized by strong, well-defined heads, with long branches slowly degraded in the direction of shorter wave-lengths. The range of intensity thus available makes this band system particularly suitable for comparison of plate characteristics in the ultra-violet. The tube was run from a 7-kva. transformer delivering 5000 V. In order to obtain the required densities with manageably long exposures, the current through the tube was reduced to 0·15 amp., representing a current-density in the discharge of about 0·4 amp./cm.^{2} Such a current-density is easily obtainable in the small discharge tubes to be found in most spectroscopic laboratories. It was found that the current could be kept constant to within 1 per cent indefinitely.

As spectrograph, the Hilger E2 medium quartz instrument was used with a slit-width of 0·02 mm. The region 2500 to 2000 A. occupies 9 cm. at the focus of this instrument, and the mean practical resolving-power (purity) is 15,000. On plates measuring 11 × 5 cm., six exposures could be made without using any part of the emulsion within 1 cm. of an edge. It was found necessary to confine exposures in this way to the central regions of the plate for two reasons. Where the processing involved bathing the plate in acetone, the emulsion tended to separate from the glass for several millimetres all round the edge. More important still, in certain of the plates tested, notably the Schumann and Q plates, fogging was nearly always much greater at the edges than in the middle of the plate. Both effects, of course, render accurate comparison of densities near the edges impossible. Another important precaution, whose neglect in the early stages led to trouble, may be mentioned here. The exit aperture of the spectrograph had to be reduced in width to the minimum required, otherwise light scattered inside the instrument during one exposure encroached both on the exposed strip of the previous exposure and on the unexposed strip intended for the next. This would result in a spurious sensitization due to pre-fogging, which could not conveniently be allowed for.

Table 1

Plate			Processing		
Name	Sensitizer		Bathed in	Developed in	Time (sec.)
1. Imperial ordinary	None		—	MQ at 20° c.	120
2. Ilford Paget Half-tone*	None		—	Process developer ID 13	120
3. Hilger Schumann	Method 1 (*b*)		—	Schumann developer	30
4. Agfa Schumann	"		—	"	30
5. Duclaux-Jeantet	Method 1 (*c*)		—	MQ at 20° c.	120
6. Ilford Q1†	Method 1 (*d*)		—	"	120
7. Ilford Q2†	"		—	MQ + 400 per cent excess KBr	120
8. Imperial ordinary‡	Commercial kerosene	Method 2 (*a*)	Benzene	MQ at 20° c.	120
9. " ‡	Medicinal paraffin		"	"	120
10. "	White vaseline		"	"	120
11. "	Yellow vaseline		"	"	120
12. "	Apiezon M grease		"	"	120
13. "	Sodium salicylate	Method 2 (*b*)	Alcohol	"	120
14. "	Anthracene	Method 2 (*c*)	"	"	120
15. Ilford S.R. panchromatic	"		"	"	300
16. Eastman ultra-violet	Dihydrocollidine, ethyl carboxylic ester	Method 2 (*d*)	Acetone	"	120
17. Agfa ultra-violet§	Unknown		"	"	120

* This plate was originally marketed as the Ilford Special Ultra-violet plate.

† Through the kindness of Dr O. Bloch, of Messrs Ilford, Ltd., we were enabled to test certain forms of Q plates other than those marketed as Q1 and Q2, for instance plates with heavier coatings of the same emulsions, with faster types of emulsion, and with Q emulsions incorporating an ultra-violet-sensitizing dye. From our point of view, however, none of these represents an improvement over the Q2 plate.

‡ Several brands of commercial kerosene and of medicinal paraffin were tried. Their sensitizing effects, however, did not vary significantly.

§ See second footnote, p. 257.

Each of the plates under test was exposed to a constant intensity of radiation for time-intervals of 1, 3, 9, 27, 81 and 243 sec. The plates used and the processing to which they were subjected are listed in table 1. In order to approximate as closely as possible to actual conditions of use, development was confined to the methods recommended by the manufacturers, even though higher densities could be obtained by modifying those recommendations. When possible (as for example when several different sensitizers were used on the same type of emulsion) batches of plates were developed together. Control exposures on ordinary plates were taken at frequent intervals. Subsequent comparisons never revealed visible differences of density between corresponding bands on such plates.

It will be seen that the apparatus required for this method of sensitometry need not be complicated: a low-power transformer operating a simple discharge tube with a slow air-leak provides the source, and a small quartz spectrograph might well be used for taking the photographs. Comparison spectrograms are obtained quite quickly, and the result of most interest can be seen by direct inspection of the finished plates. Thus although we have tested only a few of the plates available for this region of the spectrum, it should be possible for anyone interested in other emulsions to set up the necessary apparatus and have qualitative results within a few hours. Once the records have been obtained, of course, quantitative results can be derived from them, if desired, by suitable photometric methods.

§4. DISCUSSION OF RESULTS

It is important to realize that many of the terms used to specify the properties of an emulsion for photography in the visible and near ultra-violet regions are of little significance in the region 2500 to 2000 A. Since, in general, the $\{D, \log E\}$ curves for an emulsion at these wave-lengths have no straight portions of any considerable length(11), such terms as "inertia", "contrast", and "speed" must be considered as having their conventional meanings only in a very general sense. There is no reason, however, why these terms should not be used if they are redefined, not in terms of characteristic curves, but in accordance with their practical significance to the spectroscopist.

In most cases, especially where the source is weak, the spectroscopist wishes first (*a*) to obtain a measurable record of the spectrum with the least possible exposure, and then (*b*) to reproduce, as a range of perceptible density-differences, the intensity-differences present in the actual spectrum.

We shall define the *sensitivity* of an emulsion at any wave-length in accordance with (*a*) above: one plate will be said to be more sensitive than another when the minimum exposure (intensity × time) necessary to produce a measurable record on the first at the given wave-length is less than the corresponding quantity for the second. Different observers will, no doubt, have different views on what constitutes a measurable record; but these differences will be so small in relation to the actual sensitivity-differences present in the various plates that no confusion is likely to occur. Similarly, the *contrast* of an emulsion at any wave-length will be defined in accordance with (*b*) above: one plate will be said to be capable of showing more contrast than another when it will record a greater range of perceptible density-differences between a minimum observable density and saturation.

Our results show that

(*a′*) no plate tested, except the Ilford Q2 plate, gives more blackening for small values of exposure than does an ordinary plate. That is to say, an ordinary plate is at least as sensitive (according to the definition above) as the sensitized plates, with this one exception. Usually it is more sensitive.

(*b′*) the sensitized plates, on the other hand, are capable of showing more intensity-contrast than ordinary plates, that is they have a bigger saturation density. This increased density, however, is obtained only by prolonging exposure beyond that which is needed to reach saturation with ordinary plates.

The conclusion (*a′*) above is contrary to the generally accepted ideas on the performance of plates of the Schumann type and sensitized plates in this region. In table 2 are given the numerical results which justify it. They are arranged in the way which, it is hoped, will prove most useful to the spectroscopist who wants to select the emulsion that will record radiation of a given wave-length in the shortest possible time. The numbers given in the table, wave-length by wave-length, against a given plate represent minimum exposure times needed to produce measurable records on that plate. The figures at each wave-length are in all cases relative to an ordinary plate as 1, the irrelevant intensity-differences in the nitric oxide spectrum being thus eliminated. Each number was obtained by dividing the

Table 2. *Minimum exposure times needed to produce measurable records on various plates at different wave-lengths*

Wave-length (A.) / Plate*	2500	2400	2300	2200	2100	2000
1. Imperial ordinary	1	1	1	1	1	1
2. Paget ½-tone	7	6	5	5	3	2
3. Hilger Schumann	9	9	4	3	2	1·5
4. Agfa Schumann	9	3	2	1·5	1·3	1
5. Duclaux-Jeantet	3	2	1·5	1	1	1
6. Q1	18	15	12	9	9	6
7. Q2	1	0·7	0·5	0·3	0·2	0·1
8. Ordinary + kerosene	1	1·5	3	3	2	1
9. Ordinary + paraffin	9	14	9	7	4	3
10. Ordinary + white vaseline	2	1·5	2	2·5	1·5	2
11. Ordinary + yellow vaseline	3	2	2	2	2	2
12. Ordinary + apiezon M	9	24	24	15	6	3
13. Ordinary + sodium salicylate	2	2	2	2	2	2
14. Ordinary + anthracene	3	4	3	3	3	3
15. Panchromatic + anthracene	7	5	7	9	27	> 27
16. Eastman ultra-violet	3	2	3	4	3	3
17. Agfa ultra-violet	2	2	3	4	6	6

* For a full description of the plates used and the processing to which they were subjected, see table 1. The numeration is the same in both tables.

minimum exposure time needed for the test plate by that needed for the ordinary plate. Interpolation by eye was sometimes necessary, since there is a factor of 3 between the stepped exposures. The numbers given are means obtained from two complete batches of test plates. It will be seen that the only emulsion giving numbers less than 1 is the Ilford Q2, though some of the other plates are as good as ordinary plates at some wave-lengths.

These results can also be seen from plates 1 and 2, which will also serve to illustrate our conclusion (*b′*) above. The plates reproduce the 6-step logarithmic exposures made as described earlier on (1) an Imperial ordinary plate, (2) an Imperial ordinary plate sensitized with kerosene, (3) a Hilger Schumann plate, and (4) an Ilford Q2 plate. This selection is fairly representative of the plates tested.

Confining our attention first to one particular band-head, say that at λ2370, we find that in the 1-sec. exposures it appears with about equal intensities on the ordinary and the Q2 plates; it is less prominent on the oiled plate and almost invisible on the Schumann plate. The λ2270 band appears in 1 sec. on the Q2 plate only. In 3 sec. it appears on the ordinary also, but not until the 9-sec. strip is reached does the oiled or Schumann plate show it. The minimum exposure needed to record the λ2160 band is 3 sec. for the Q2, 9 sec. for the ordinary, and 27 sec. each for the oiled and the Schumann plates. For the detection of a weak spectrum, then, the Q2 is as good as an ordinary plate at λ2500 and becomes increasingly better towards λ2000. The oiled and Schumann plates—and these are representative of all the others—never reach the same sensitivity as the ordinary, though they tend towards it at the shorter wave-lengths.

On the other hand, if we now consider the way in which the density of a given band increases with exposure time, the other effect, (*b′*) above, of the so-called sensitization becomes apparent. The λ2370 band, for example, increases its density steadily with time, but not so rapidly on the ordinary plate as on the others. Although on the Schumann plate it is weaker at the start it rapidly strengthens until in the 27-sec. exposure the blackening at the head is greater than on the ordinary plate. Nevertheless farther along the band, where the lines are intrinsically weak, the ordinary plate still holds the advantage. It is this which makes the bands on the ordinary plate appear long and of relatively uniform intensity, whilst on the Schumann plate they seem to be shorter and to comprise lines of a greater range of intensity. Further in the ultra-violet the effect is much more pronounced. On the ordinary plate the λ2160 band-head has reached a density which, though low, is nevertheless a maximum, in 27 sec. The oiled plate does not even show the band till exposed for 27 sec., but then it goes on, as the exposure time increases, to densities which no amount of over-exposing would produce on an ordinary plate. If the spectrum to be photographed has intensity to spare, and a negative with strong contrast is required, the oiled plate, the Schumann plate, the Q plates, in fact all the "specially sensitive ultra-violet plates", will give high densities when exposed long enough.

The apparently anomalous results mentioned at the beginning of the paper can now be explained. A plate is commonly said to be under-exposed when the density is small, or the negative looks thin. This view of the matter, inherited from experience in the visible and near ultra-violet, leads to inflated ideals and correspondingly disappointing results in the region 2500 to 2000 A. A more useful criterion would be that a plate is over-exposed when the range of intensities of interest is carried over the shoulder of the $\{D, \log E\}$ curve to the nearly horizontal portion. This maximum density for an ordinary emulsion at $\lambda 2300$, say, is so quickly reached that there is a tendency to over-expose enormously in a vain attempt to raise it. Meanwhile, of course, visible and near-ultra-violet radiation scattered in the spectrograph proceed to fog the plate. In addition—and this is more serious—increasing the exposure time brings up the density of the weaker part of the spectrum to that of the stronger, and therefore destroys what little contrast there is. In absorption, for example, weak bands may be entirely lost owing to this effect, whilst in emission, bands of very different intrinsic intensity may appear of equal and uniform strength throughout. While this contrast can be restored by oiling the plate and giving the same exposure as before, it can also be restored in a measure simply by exposing less. Better still, a Q2 plate can be used and a much greater latitude can be obtained without loss either of sensitivity or of maximum density.

Much of the previous sensitometry in this region has been done with sources giving line spectra. The tendency here is to over-expose excessively at the centres of the lines. Under these conditions, the increase of maximum attainable density produced by oiling a plate appears as a spurious increase of sensitivity. No doubt the oiled plate will, as the saying is, "go down further" than the untreated one: certain lines in the far ultra-violet will be strengthened by the process. But a careful examination will show that others, weaker but still visible on the ordinary plate, are removed entirely by oiling. This effect may, of course, be a desirable result in some circumstances. An arc spectrum photographed on Q1 plates, for instance, appears beautifully clean, with fine lines standing out well from a clear background. Nevertheless, the background is clear only because weak lines which would have appeared on an ordinary plate do not appear on the Q1 plate. It is often remarked, for example, that the nitric-oxide bands, which appear in spectrograms of the copper arc on ordinary plates, are not so commonly noticed on similar spectrograms on Schumann plates.

If we leave aside for the moment the Q2 emulsion, the conclusions to be drawn are these. If the intensity of the spectrum to be recorded is low, then oiling is worse than useless, in the sense that it will increase exposure time: the photograph should be taken on an untreated ordinary plate. The price paid will be poor contrast, resulting from a low saturation density. If, on the other hand, the intensity of the source is higher, and the intensity-distribution in its spectrum is of interest, then densities and therefore contrast-values unobtainable on an untreated ordinary plate can be obtained by what is called "sensitizing" it, or by using plates of the Schumann type. The price here will be either the loss of the weaker parts of the spectrum or the necessity for longer exposures. If a Q2 plate is used, however, neither short exposure time nor, within limits, final density need be sacrificed. The price here, however, is that the spectrogram is apt to appear veiled, and that the mechanical properties of the emulsion film are poor, handling being almost as deleterious to a Q2 plate as to a Schumann plate.

In conclusion, it might perhaps not be out of place to emphasize that the authors do not find, as has sometimes been implied, that ultra-violet sensitive plates are of no use in the region 2500 to 2000 A., nor that ordinary plates are just as effective for all purposes. It has been shown that it cannot be assumed that oiling an ordinary plate will automatically improve its performance: in many cases quite the opposite will be achieved. Nor is it true that a plate of the Schumann type is always more sensitive than an ordinary plate: frequently it requires longer exposures to reach a given density. Each problem must be considered on its merits, the advantages and disadvantages of each type of emulsion must be weighed, and a plate must be chosen whose performance most nearly fulfils the requirements.

REFERENCES

(1) Hopfield and Appleyard. *J. Opt. Soc. Amer.* **22**, 488 (1932).
(2) Weichmann. *Z. wiss. Phot.* **34**, 140 (1935).
(3) Schumann. *Astrophys. J.* **3**, 220 and 387 (1896).
(4) Duclaux and Jeantet. *J. Phys. Radium*, **2**, 156 (1921).
(5) Ilford Limited. *J. Sci. Instrum.* **12**, 333 (1935).
(6) Harrison. *J. Opt. Sci. Amer.* **11**, 113 (1925).
(7) Beach. *Nature, Lond.*, **123**, 166 (1929).
(8) Tien Kiu. *C.R. Acad. Sci., Paris*, **201**, 1348 (1935).
(9) Helmick. *J. Opt. Soc. Amer.* **9**, 521 (1924).
(10) Hunter and Pearse. *J. Sci. Instrum.* **13**, 403 (1936).
(11) Johnson and Hancock. *J. Sci. Instrum.* **10**, 339 (1933).

MONOCHROMATORS FOR PURPOSES OF IRRADIATION

By J. W. PERRY, Computing Department, Adam Hilger Ltd.

Demonstrated 7 *May* 1937. *Manuscript received* 26 *May* 1937

ABSTRACT. The conditions for a large output of energy by monochromators are analysed and expressed in a convenient form. Description is given of a new type of monochromator for large output, which may be single or double, with glass or quartz optical work. An instrument constant is proposed as a measure of the output-capacity of monochromators.

---

§ 1. INTRODUCTION

Monochromators, in their function of providing approximately homogeneous light from a given heterogeneous radiation, are often desired to possess the to some extent incompatible attributes of high output-capacity and high purifying-power. As these two properties are frequently in conflict, cases arise in which the emphasis falls on the one or the other and we here are more particularly concerned with the case in which major importance is attached to output, while purity and the suitability of the instrument in other respects are required to fulfil subsidiary conditions imposed by the particular purpose in view. Monochromators adapted to such conditions may be single or double monochromators. They are largely employed for purposes of irradiation, for instance of substances under investigation for photochemical or biological change, and are here termed *irradiation monochromators*.

The capacity of a monochromator to receive and deliver high radiation energy depends upon several contributory factors as may be seen from a brief analysis of this property. Let the slit of the instrument be illuminated from a source of radiation having a continuous spectrum, and the illumination on the slit be $(\delta E)_\lambda$ watts per mm.^{2} per steradian for the wave-length interval λ to $(\lambda+\delta\lambda)$ under consideration. Consider the light-flux Φ passing an element of area of the slit, of height δy and width δx (assumed great enough to prevent diffraction effects) and admitted to the dispersing system by the collimating lens. The distance of the lens from the slit is f_1 and an area A of it is utilized. Then the flux Φ will be given by

$$\delta\Phi=(\delta E)_\lambda \frac{A}{f_1^2}\,\delta x\,\delta y.$$

δx is determined by

$$\delta x=f_1\frac{dI_0}{d\lambda}\,\delta\lambda,$$

where, assuming the passage of light in the prism system reversed, I_0 is the angle of refraction on emergence from the system for the direction of the collimator axis.

If then T_λ be the transmission factor of the system for wave-length λ, the corresponding flux $\delta\Phi'$ finally delivered at the exit slit can be expressed in the form

$$\delta\Phi' = P_\lambda\,(\delta E)_\lambda,$$

where

$$P_\lambda = T_\lambda\, A\, \frac{\delta y}{f_1}\, \frac{dI_0}{d\lambda}\, \delta\lambda.$$

The quantity P_λ, since it determines what part of the given energy-distribution at the slit is capable of being utilized, represents what may be termed the output capacity of the monochromator for wave-length λ, as distinguished from the inherent character of the incident illumination represented by $(\delta E)_\lambda$ and the selective effect of adjustment of the exit slit. It bears a direct and obvious relation to the Smith-Helmholtz constant for the instrument. The capacity of the monochromator to receive and deliver radiant energy is thus shown to be proportional to the area of the aperture, the angular subtense of the slit-length at the collimating lens, and the angular dispersion, in addition to the obvious transmission factor T. This factor corrects for losses due to reflection and absorption in the whole system, of which in these respects the prism system accounts for considerably the major part.

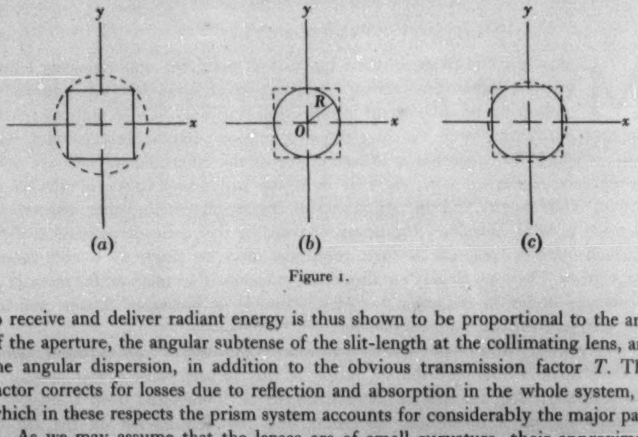

Figure 1.

As we may assume that the lenses are of small curvature, their approximate contribution to factor T is very simply determined. The usual expression for prismatic transmission does not, however, when dispersion takes place and in the presence of absorption, give a satisfactory value for T_λ, except as applying to a particular element of area of the aperture. The aperture of the instrument, out of consideration for transmission and for other reasons, is often limited, as in (*c*), figure 1, partly by the prism or prisms and partly by the collimator objective. The extreme cases to which (*c*) is an approximate mean are depicted in (*a*) and (*b*) in figure 1, and in the following the transmission for case (*c*) will for the purpose of an approximation be assumed to be an exact mean of the transmissions for these extreme cases.

Let the x-axis intersect the collimator axis and lie in the plane of a principal section of the prism system and let the radius OR of the (circular) collimator aperture with centre O be r and let the angle xOR be θ.

Let us further define as follows for wave-length λ the relevant quantities dependent on wave-length. Let L stand for $d\Phi_\lambda/d\sigma$, the superficial density of the flux Φ_λ for a wave-length interval, $\delta\lambda$, in the region of wave-length λ, and per unit cross-sectional area σ in the beam emerging from the collimator; let F be the total transmission factor obtained with Fresnel's formulae, and applied to correct the reflection losses for the whole dispersing prism system; let τ be the fractional transmission per unit length for the material of the dispersing prisms; and let l, a function of x, be the linear light path through the prisms system.

Then for cases (a) and (b) respectively,

$$l = ax + b = ar\cos\theta + b,$$

where a and b are easily determined constants and the zero of θ is chosen so that a is positive. If x_+ and x_- are the limiting positive and negative values of x respectively, and the limiting values of y for case (a) are $\pm Y$, the flux incident on the prism system will be for cases (a) and (b):

$$\Phi_a = 2Y(x_+ - x_-)L,$$
$$\Phi_b = \pi r^2 L.$$

The flux Φ' finally transmitted will be

$$\Phi_a' = 2YL\,F\tau^b \int_{x_-}^{x_+} \tau^{ax}\,dx,$$

$$\Phi_b' = 2r^2L\,F\tau^b \int_0^\pi \tau^{ar\cos\theta} \sin^2\theta\,d\theta.$$

By introducing the variable z, such that

$$z = \tfrac{1}{2}a(x_+ - x_-)\log_e \tau = ar\log_e \tau,$$

where, be it noted, the natural-logarithmic extinction coefficient $\log_e \tau$ is employed for convenience instead of the usually recorded decadic extinction coefficient, and by dividing by the corresponding value of Φ and integrating, the transmission factor T is obtained for the two cases in the convenient forms;

$$T_a = \frac{\sinh z}{z}\tau^b F,$$

$$T_b = \frac{2I_1(z)}{z}\tau^b F.$$

I_1 here denotes the modified Bessel function of the first kind and first order.

For the mean case (c) the transmission factor T_c will then be given by

$$T_c = \left(\frac{\sinh z}{2z} + \frac{I_1(z)}{z}\right)\tau^b F.$$

As the constant b is the mean path-length when $x = 0$, and the expression within the bracket is always in excess of unity, the relative transmission for full aperture is always greater than the transmission for the mean path-length b. When the absorption is negligible the absorption factors reduce, of course, to unity and the factor T becomes equivalent to F. This completes the analysis of the output capacity of the instrument. The resulting conditions for a high P factor have been studied in the instruments introduced as irradiation monochromators and described in the following section.

§ 2. DESCRIPTION OF INSTRUMENTS

The novel features of the irradiation monochromators of Messrs Adam Hilger, Ltd., designed by the writer, will now be described. The instruments may take the form of single or double monochromators, and may have optical work of glass or quartz. In each case continuous adjustment of the wave-length with constant focusing is effected throughout the available range by single-hand adjustment of a rotating divided drum and screw.

The double monochromator is constructed in two tiers as shown in the lower half of figure 2. When the instrument is used as a single monochromator, the light in the upper tier proceeds to a slit at S_2' instead of being reflected downwards to slit S_2 by prism Q_1. L_1 and L_2 are respectively the entrance and exit lenses of the upper half of the instrument, each being single aspherical lenses corrected for the immediate neighbourhood of their optical axes. L_1 is fixed in definite relation to the slit S_1, while L_2 is mounted on a platform A which may rotate about the centre O_1 but is constrained by rollers bb, which are mounted on a table D rotating about centre O_2. The straight edge c, rigidly connected with platform A, makes permanent contact against the rollers bb. This straight edge is parallel to a line joining the centres O_1 and O_2. The centre O_2 is defined by a carefully ground circular fitting in a carriage B, the position of which along a straight slide in the direction uu is controlled by the drum F and screw E, whole revolutions of the drum being indicated by a counter.

Light entering by the slit S_1 traverses the lens L_1 and the prism P_1, which is fixed, and falling on L_2 is imaged in the form of a spectrum in the focal curve kk. When, for the single monochromator, prism Q_1 is absent, its place is taken by a plane parallel compensating block. Slit S_2', which is at a fixed distance from centre O_2 and is mounted on the rotating platform D, lies in the focal curve kk and thus selects a certain wave-length band for subsequent utilization. By rotation of the drum F, the position of (i) the lens L_2, (ii) the carriage along the slide, and (iii) the slit S_2' in its rotation about O_1 and O_2, may be readjusted for different wave-length settings, while constant focusing is retained at the slit S_2', as will be seen below.

In the double monochromator, the slit S_2' is absent and the light, reflected into the corresponding slit S_2 by the prism Q_1, is received again by the prism Q_2 and is delivered to the lower half of the instrument, of which the optical work is geometrically similar to that in the upper half. The lens L_3 is attached to the same platform D as lens L_2, and the prism P_2 and lens L_4 occupy positions at the lower level corresponding to their counterparts in the upper. The slit S_3 thus selects, after a

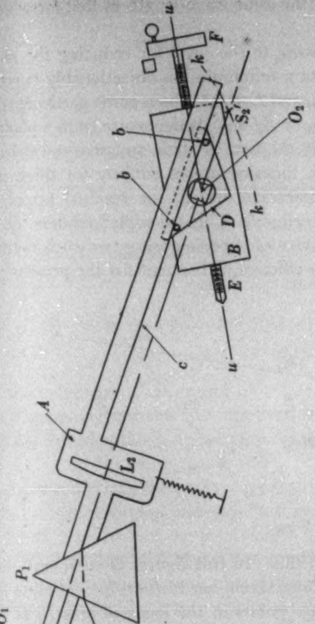
u
F
k
S_2'
O_2
b
b
D
B
E
k
u
c
A
L_2
P_1
O_1
L_1
S_1

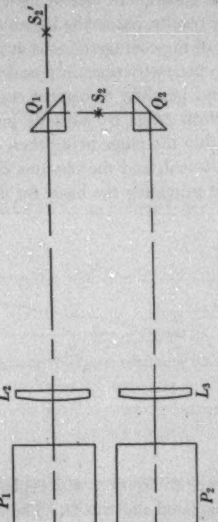
S_2'
Q_1
S_2
Q_2
L_2
L_3
P_1
P_2
L_1
L_4
S_1
S_3

Figure 2. Diagrammatic view of double monochromator.

further stage of purification, light of the same wave-length as that for which slit S_2 is set.

Under normal circumstances, owing to the need for reducing the number of lenses and consequent loss of light to a minimum, an objectionably curved image inevitably results, but as the lenses L_2 and L_3 rotate about some particular point O_1, the locus of the conjugate focus at S_2 or S_2' and its departure from a plane are not subject to the restrictions imposed by the laws of static systems, and it has in fact been found possible to correct such focusing errors entirely for three points in the spectrum range by suitable geometrical design, the residual errors at other points within the range being then negligible. This principle* renders the rotating lens adjustment, and the obvious device of superimposing two such mechanisms, capable of providing the basis for an efficient instrument for the present purpose.

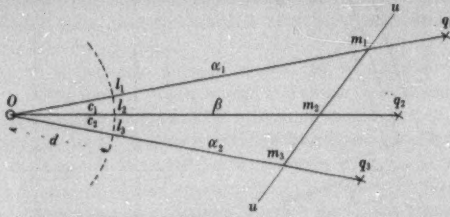

Figure 3.

Reference to figure 3 will explain this. In this figure, O represents the fixed centre designated above as O_1. The construction has further, in relation to figure 1, the following signification: l_1, l_2, l_3 are points in the locus of lens L_2 at constant distance d from O; m_1, m_2, m_3 are points corresponding respectively to l_1, l_2, l_3 in the locus of O_2; q_1, q_2, q_3 are similarly corresponding points in the locus of S_2'; C_1 and C_2 are the angles q_1Oq_2 and q_2Oq_3 respectively.

It will be clear from the above, and by reference to figure 2, that if the slit S_2' is at a constant optical distance from the centre O_2, the variations of the radial distance of O_2 from O_1 must, in order that compensation of variations of the focal distance may be obtained, be equal to these variations. Let the said constant distance O_2S_2', equal in general to the segment mq in figure 3, be denoted by e, and let the distance from the lens L_2 to focus S_2' be as follows:

$$l_1q_1 = \alpha_1 + e,$$

$$l_2q_2 = \beta + e,$$

$$l_3q_3 = \alpha_2 + e.$$

Then the radii vectors Om_1, Om_2, Om_3 will be $(\alpha_1 + d)$ $(\beta + d)$ and $(\alpha_2 + d)$ respectively. The condition that the locus uu may be rectilinear is then equivalent to the stipulation that the angle $m_1m_2q_2$ as calculated from triangles Om_1m_2 and Om_2m_3

---

* Patented by Adam Hilger, Ltd.; a British patent specification 374429.

shall have equal values for these two cases. By simple trigonometry this condition gives

$$\frac{\operatorname{cosec} C_1}{\alpha_1'+d'}+\frac{\operatorname{cosec} C_2}{\alpha_2'+d'}=\frac{\cot C_1+\cot C_2}{d'+1},$$

where α_1', α_2' and d' are written for α_1/β, α_2/β and d/β respectively. With slight rearrangement and some reduction this gives an equation for the determination of d' to secure the required condition as follows:

$$Ad'^2+Bd'+C=0,$$

where

$$\begin{aligned} A&=(\tan \tfrac{1}{2}C_1+\tan \tfrac{1}{2}C_2),\\ B&=\{(\alpha_1'+\alpha_2')(\tan \tfrac{1}{2}C_1+\tan \tfrac{1}{2}C_2)\\ &\qquad +(1-\alpha_1')\operatorname{cosec} C_1+(1-\alpha_2')\operatorname{cosec} C_2\},\\ C&=\{\alpha_1'\alpha_2'(\tan \tfrac{1}{2}C_1+\tan \tfrac{1}{2}C_2)\\ &\qquad +\alpha_2'(1-\alpha_1')\operatorname{cosec} C_1+\alpha_1'(1-\alpha_2')\operatorname{cosec} C_2\}. \end{aligned}$$

Of the values for d' so found only one, having a value appreciably less than unity, is generally suitable for application in the present case, on account of mechanical considerations. Its employment results in sharp focusing being obtained at the slit S_2' at the points q_1, q_2 and q_3. The errors of focusing at intermediate points measured axially then follow approximately a cubic relation, being of opposite sign for the segments q_1q_2 and q_2q_3, and amount at maxima to small quantities of the order of $\pm 4\times 10^{-4}$ of the focal length of the lens L.

In the calculation of d, if e is not constant, owing for example to the presence of some denser medium with dispersion such as prism Q_1, corrections in the variations of the focal distance should of course be made for this, and likewise it is possible to adjust d so that instead of the locus for the points m_1 being linear, any required departure from linearity at the points considered may be obtained.

The mechanical design of the instrument has been carefully considered. The instrument is housed in a massive casting and remains in permanent adjustment. The lenses are all of aperture diameter 12·7 cm. and of mean focal length 56 cm. The prisms are 11·7 cm. high and have a face-length of 13·0 cm.

As materials, crystalline quartz, glass, and fused quartz are contemplated, but although large pieces of fused quartz may occasionally be available, the absorption per unit length of such material in the requisite dimensions has for the shorter wave-lengths been found to be greater than that of the usual, smaller, first-quality specimens, and the applications of this material are therefore correspondingly restricted. The glass employed is a light flint glass, so that the farthest possible transmission into the near ultra-violet commensurate with reasonable dispersion may be secured. The lines in the mercury spectrum at 365 mμ. may in fact be seen with this glass system in train. In order that these materials may be employed in the same basic mechanical construction, and on account of their differing refractive indices, the angles of the prisms P_1 and P_2 differ for the various materials, being 60° for fused quartz, and 54° 17′ for crystalline quartz and for glass.

The linear carriage-travel measures approximately 236 mm. from wave-length 202 to 795 mμ. for each of the quartz systems, and 78 mm. from wave-length 397 to 795 mμ. for the glass system. Settings can be made accurately by division to 0·01 mm. throughout this range; this corresponds in wave-length to 1 angstrom or less (the approximate wave-length accuracy for all wave-lengths less than about 6000 A.) throughout the spectrum. Calibration tables are supplied with the instrument to connect drum-reading and wave-length. The local inverse dispersion in mμ./mm. at the exit slit is given in figure 4 in the form of curves for the various materials when the instrument is used as double monochromator. For the single monochromators the dispersion-reciprocal would be twice that indicated by the curves.

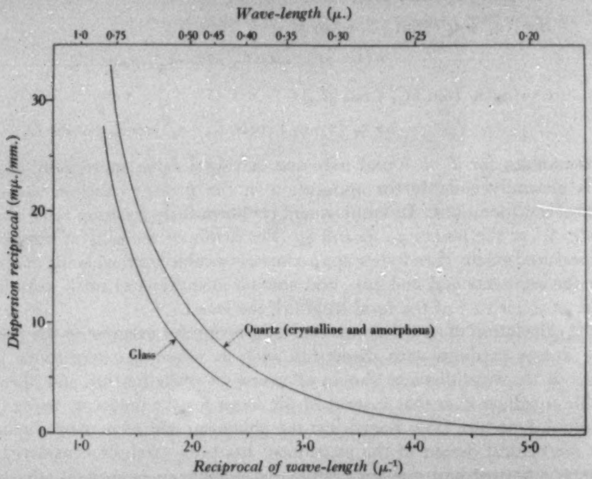

Figure 4. Dispersion reciprocal for double monochromators.

Provision is also made for converting the instrument into a quartz spectrograph, not by compromise on the optical design of the monochromator but by utilizing the external mechanical construction of the instrument, which lends itself to housing the optical work of a medium-sized spectrograph having lenses of approximately the same focal lengths as those of the monochromator. The optical work of the latter is in fact mounted in such a manner that it may be removed, interchanged for the smaller spectrograph optical work (the collimating and camera lens of which have apertures of 51 mm.), and accurately replaced when desired without need for readjustment. The end cover of the instrument together with the prism Q_1 is removed in this case and a spectrograph camera back takes its place.

APPENDIX

It is the object of the present note to propose, for the property referred to above as output capacity, an approximate and convenient measure which may reasonably be expected to be included in the specification of a monochromator and would be of immediate service to the user of such instruments. As has been indicated in the foregoing sections, the complete expression for the output capacity P_λ for wave-length λ, wave-length interval $\delta\lambda$, and slit-length y, takes the following form:

$$P_\lambda = T_\lambda A \frac{y}{f_1} \frac{dI_0}{d\lambda} \delta\lambda.$$

The implied presence of the absorption factor in the factor T_λ causes an unnecessary complication for the present purposes, owing principally to its variability, but this may be eliminated by considering practically absorptionless regions of the spectrum. The remaining factors are all strictly relevant and form together an easily determined constant for such instruments if definite conventional values be assigned to the variables λ, $\delta\lambda$ and y. Accordingly let λ be 546·1 mμ. (mercury green radiation), while $\delta\lambda = 1$ mμ. and $\delta y = 1$ mm. The output capacity constant, here denoted by P, which is of the dimensions L^2, then becomes numerically determined by

$$P = T \frac{A}{f_1} \Delta I_0,$$

where the millimetre is the unit of length and ΔI_0 is the angular dispersion of the system for 1 mμ. at 546·1 mμ. for reversed passage. In most cases the direction of passage will not appreciably affect the value of ΔI_0, and a simple calculation, assuming minimum deviation for wave-length 546·1 mμ., will generally suffice.

It is now proposed that this constant should be stated for all monochromators for which output capacity is of importance, and it is hoped that some agreement may be arrived at on this question among the makers and users of such instruments.

The practical value of this constant may be seen from the following considerations. Given a monochromator of known P and an incandescent source of known emission m ergs per second per mm.^{2} per steradian per mμ. at wave-length 546·1 mμ. in the direction of the collimator axis, imaged by a condensing lens on the monochromator entrance slit, then apart from losses in the condensing lens, the approximate available output at the exit slit is given by simple multiplication roundly as mP ergs per mμ. per second per mm. of slit-length. By a knowledge of this quantity the suitability of the instrument for various purposes can be directly judged.

The complete expression proposed for P will now be given explicitly in a simplified form, in which we allow for reflecting mirror surfaces and assume the component lenses to be of small curvature and the dispersing prisms to be simple and all of the same angle, all such parts making air contact at each surface.

$$P=\frac{1}{n}\frac{dn}{d\lambda}\frac{Ak\tan I_0}{f_1}T,$$

where

$$T=\frac{1}{2}\left[\prod_{i=1}^{k}\left\{\frac{\sin^2 2I}{\sin^2(I+I')}\right\}_i+\prod_{i=1}^{k}\left\{\frac{\sin^2 2I}{\sin^2(I+I')\cos^2(I-I')}\right\}_i\right]\left[\prod_{i=1}^{j}\left\{\frac{4n}{(n+1)^2}\right\}_i\right]\prod_{i=1}^{l}R_i.$$

This applies to prisms at minimum deviation and is in a form suitable for logarithmic calculation. In other cases equivalent forms should be used, based on the definition of P.

In this expression λ is the wave-length in mμ., n the refractive index of the denser medium at each refraction, A the utilized area of the collimating lens, and f_1 the distance from the slit to the collimating lens. I, I' are the angles of incidence and refraction respectively at dispersing prism surfaces, and R is the reflection factor at any mirror surfaces included in a given system. The products extend over all the surfaces, respectively k, j and l in number, of (i) the dispersing surfaces obliquely inclined to the incident light, (ii) the dioptric surfaces (lenses and reflecting prisms) normal thereto and (iii) any catoptric surfaces. All instrument-dimensions are in millimetres. The values of the constant P for the instruments above described are as given in the following table.

Material	Single monochromator	Double monochromator
Crystalline quartz	$7{\cdot}2 . 10^{-4}$	$9{\cdot}8 . 10^{-4}$
Glass	$14{\cdot}5 . 10^{-4}$	$18{\cdot}9 . 10^{-4}$
Fused quartz	$7{\cdot}6 . 10^{-4}$	$11{\cdot}3 . 10^{-4}$

ON THE EVALUATION OF SOME HEXAGONAL STRUCTURE FACTORS

By C. A. BEEVERS and H. LIPSON, University of Manchester

Received 23 *September* 1937

ABSTRACT. The formulae $\Sigma \cos h\alpha . \cos (k-i)\beta$, $\Sigma \cos h\alpha . \sin (k-i)\beta$, $\Sigma \sin h\alpha . \cos (k-i)\beta$, $\Sigma \sin h\alpha . \sin (k-i)\beta$, which are very useful in calculating the intensities of X-ray reflection from hexagonal crystals have been tabulated for various values of h and k. In these formulae α and β are the semi-sum and semi-difference of the hexagonal co-ordinates x and y.

§1. INTRODUCTION

The utility of contoured graphs of the structure factors involving only two indices has been pointed out by Bragg(1) and a discussion of the formulae involved(2) showed that it is quite practicable to prepare general sets of such graphs, provided too many reflections are not required.

Those of the graphs which contain elements of pattern which are repeated a number of times can be obtained by graphical construction, but in the cases of higher symmetry *P* 4*b*, *P* 4*m*, *C* 3*m*, *H* 3*m*, *C* 6*m*, the only available method seems to be to evaluate the function at specific points in the projection and to find the contours by interpolation. Thus one has first to evaluate the figure fields—arrays of numbers giving the value of the structure factor over a network of points. The drawing of the contours from these numbers involves a great deal of further work, particularly if diagrams have to be prepared for reproduction. It occurred to the writers that it would be well worth while to prepare the figure fields themselves for reproduction, and an attempt has been made to gauge the relative values of the two methods of representation.

The purpose of structure-factor charts is two-fold: firstly, an investigator will require the value of the structure factor at any point, and secondly, he will require to know how to move the position of an atom in order to change the value of its contribution in any particular way. For quite general points in the area it is obvious that the contoured graphs are better for both purposes. But if we need consider only those points in the unit cell for which the structure factor has been computed in the preparation of the graphs, it is obviously easier to read off the value from a figure field than to interpolate between two contours. Since, moreover, the contoured graphs would involve a quite considerable loss of accuracy in drawing and reproduction, the authors have been led to prepare sets of figure fields. If required, the contoured graphs can be prepared from these by individual workers, who will then know the accuracy with which the graphs are drawn. The limitation of the atomic positions to sixtieth parts of the unit cell (as in the tables to be described) is quite immaterial in the early stages of the analysis of a crystal, although further processes may be necessary towards the end of a structure determination.

§ 2. SCOPE OF THE PRESENT WORK

The utility of the structure-factor fields increases with the complexity of the formula, and is therefore most pronounced in the plane groups based on the hexagonal lattice. For the plane groups *C* 3*m*, *H* 3*m*, *C* 6*m*, only three formulae are involved, namely

$$\Sigma \cos h\alpha \cos (k-i)\, \beta,$$

$$\Sigma \cos h\alpha \sin (k-i)\, \beta$$

and

$$\Sigma \sin h\alpha \cos (k-i)\, \beta,$$

where

$$\alpha = \tfrac{1}{2}(x+y), \quad \beta = \tfrac{1}{2}(x-y).$$

Although it does not occur in the plane groups the formula

$$\Sigma \sin h\alpha \sin (k-i)\, \beta$$

has also been evaluated (see § 7), and these computations have been made for the following indices:

(*h*	*k*)						
1	0	1	1				
2	0	2	1	2	2		
3	0	3	1	3	2	3	3
4	0	4	1	4	2	4	3
5	0	5	1	5	2		
6	0						

Further, the computation of

$$\Sigma \cos h\alpha \cos (k-i)\, \beta$$

for orders going up to $h=11$ has also been carried out.* For these high orders, of course, the accuracy for interpolated points is much lower, but nevertheless the charts are exceedingly useful in the determination of structure.

§ 3. METHOD OF COMPUTATION

The evaluation was effected by the aid of the strips prepared by the authors(3) for Fourier synthesis, in the following way. Consider the formula

$$\Sigma \cos h\alpha \sin (k-i)\, \beta,$$

and take the case $h=3$, $k=1$, $i=\bar{4}$. We have to evaluate

$$\cos 3\alpha \sin 5\beta - \cos \alpha \sin 7\beta + \cos 4\alpha \sin 2\beta.$$

For a given value of α this can be evaluated for all values of β by adding three sine strips with amplitude $\cos 3\alpha$, index 5; amplitude $-\cos \alpha$, index 7; amplitude

---

* By Miss M. A. S. Ross and one of the authors.

$\cos 4\alpha$, index 2. Moreover the values of $\cos 3\alpha$, $-\cos\alpha$, $\cos 4\alpha$ are merely the numbers on the strips $100\,C\,3$, $\overline{100}\,C\,1$, $100\,C\,4$, respectively. (Since the strips have been printed only to an amplitude 99, those for amplitude 100 had to be written by hand.) The range of α or β can be extended from the 90° limit of the strips to 180° by reversal of the appropriate strips.

The calculation may also be effected along lines of equal β, the same principles being used. In order to provide an adequate check all the calculations have been done in both ways.

The area covered by the calculations is given by $0<\alpha<180°$, $0<\beta<90°$. The relation of this area to the unit cell is shown in figure 1 by the singly shaded area. For $C\,6m$, the plane group of highest symmetry, this covers three times the area necessary, which is shown doubly shaded in figure 1, but the points outside this area can be brought into it by reflection in the symmetry lines of the plane group, which are the lines in figure 1.

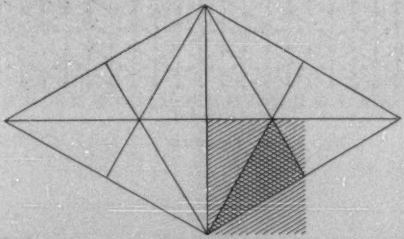

Figure 1. Symmetry lines of the plane group $C\,6m$, showing the unique area.

The lines of constant α and constant β after reflection to within the unique area, are shown in figure 2. The intersections of these lines show that a quarter of the points are calculated three times, and the remainder once. This fact affords a very effective check on the general features of the diagram.

In the case of the plane groups $C\,3m$ and $H\,3m$ the unique area is twice the doubly shaded area of figure 1. The structure factors in these cases, however, have A and B parts, and when the formulae for these parts are considered separately the doubly shaded area of figure 1 proves to be sufficient, as is shown below.

The A part of the structure factors for both $C\,3m$ and $H\,3m$ is the cos.cos formula which has already been dealt with. The B parts are cos.sin and sin.cos. The cos.sin formula has lines of symmetry and antisymmetry as shown in figure 3*a*, and the sin.cos formula has these lines as shown in figure 3*b*. Thus if we are prepared to reflect into the unique area, with a change of sign if necessary, then this area is sufficient for the representation of the formulae.

The planes having h and k divisible by a common factor n were not calculated themselves but were obtained from the appropriate plane of lower order by taking every nth point. Further, the following fact was utilized as a check whenever possible: If $h-k=3n$, $k-i=3(k+n)$ and $i-h=-3(k+2n)$. Since all these quantities are multiples of 3, the figure field is more highly symmetrical than the

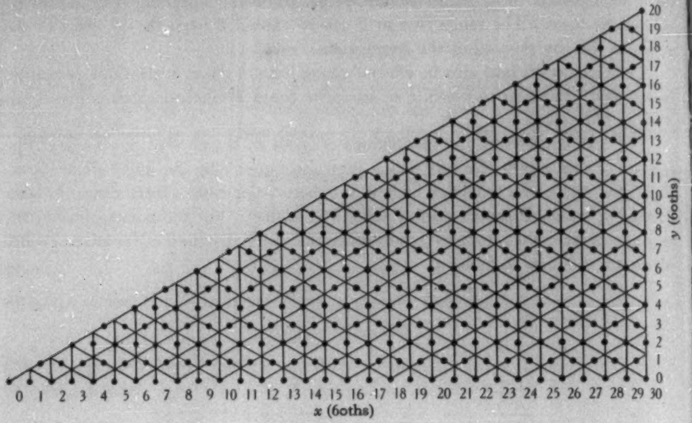
0 1 2 3 4 5 6 7 8 9 10 11 12 13 14 15 16 17 18 19 20 21 22 23 24 25 26 27 28 29 30
x (60ths)
0 1 2 3 4 5 6 7 8 9 10 11 12 13 14 15 16 17 18 19 20
y (60ths)

Figure 2*a*.

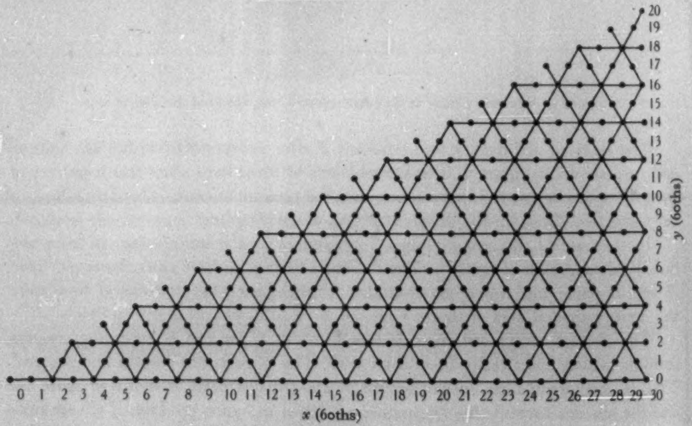
0 1 2 3 4 5 6 7 8 9 10 11 12 13 14 15 16 17 18 19 20 21 22 23 24 25 26 27 28 29 30
x (60ths)
0 1 2 3 4 5 6 7 8 9 10 11 12 13 14 15 16 17 18 19 20
y (60ths)

Figure 2*b*.

Figure 2. Lines of constant α, figure 2*a*, and constant β, figure 2*b*, after reflection into the unique area.

general figure field, and it can be derived from the figure field for the plane $(n, k+n, -k-2n)$. For example, the figure field for $(41\bar{5})$ can be derived from $(12\bar{3})$

by interchanging α and β in the latter and then reading off every third line of the field for constant β, and remembering that this changes the formula cos.sin into sin.cos and vice versa.

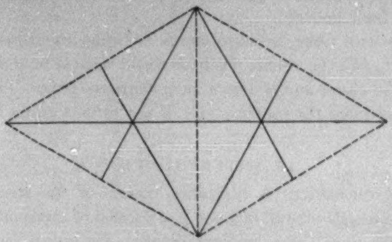

Figure 3*a*.

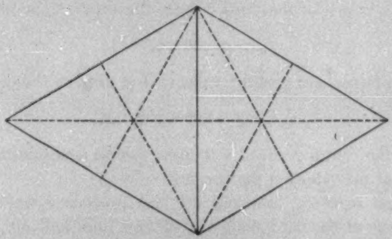

Figure 3*b*.

Figure 3. Lines of symmetry and antisymmetry (shown as broken lines) in $\Sigma \cos h\alpha . \sin (k-i) \beta$, figure 3*a*, and in $\Sigma \sin h\alpha . \cos (k-i) \beta$, figure 3*b*.

§ 4. LIMITS OF INDICES AND PROBABLE ACCURACY

The foregoing process results in the evaluation of the structure factors at intervals of 6° of x and y. This sets a limit to the indices which can be used, for obviously we cannot determine the direction of a shift of co-ordinates if there are not enough points calculated to determine the surface uniquely. The problem is similar to that of resolving-power in Fourier projection.

Owing to rounding-off errors, the final totals are not always correct to one unit, but they are considered to be practically all within $1\frac{1}{2}$ units of the true values.

§ 5. PRACTICAL DETAILS

The figure fields have been reproduced on an Ormig duplicator. The transfers for the duplicating machine were typed in a hexagonal array* covering the unique area. Positive values are in blue and negative ones in red. The co-ordinates in

---

* Owing to the relation between the vertical and horizontal spacings of the typewriter used, the angle between the hexagonal axes is actually 121° instead of 120°.

60ths of the unit cell are indicated in green opposite the lines of numbers in the direction of the axes. An example of a field is given in table 1, in which the foregoing colours are represented respectively by Roman figures, Roman figures with lines above, and Italic figures.

If a structure with three or more atoms is being investigated it is probably more convenient to plot the atomic positions to the nearest 60th of the cell-edge on a net which fits the charts and is drawn on transparent paper. The paper can then be laid on the charts and the contributions of the various atoms can be read off.

§6. INTERPOLATION

If, for a final calculation of intensities, values of the structure factors are required at finer intervals than 6° in x and y, a process of interpolation can be used. For 3° intervals we want values midway between the points given in the tables. If we assume that the equation to the curve connecting four regularly spaced points having values a, b, c, d is of the third degree, the value at the midpoint of b and c is

$$\tfrac{1}{16}(-a+9b+9c-d).$$

For 2° intervals a formula to give the value at one-third of the distance from b to c would be

$$\tfrac{1}{81}(-5a+60b+30c-4d),$$

and the value at the centre point of a triangle can be found accurately enough by taking the mean of the values at the corners.

For the highest accuracy, however, the best procedure would probably be to make cross-sections of the field along the various lines and prepare graphically a closer figure field over the area in question. The accuracy with which this can be done is highest for the planes of lower order, but it is believed that an accuracy of about 8 units is possible even in the highest orders of the present tables.

§7. APPLICATION TO THREE-DIMENSIONAL STRUCTURE FACTORS

Although the figure fields were originally prepared for use only with $hki0$ intensities, it was found that in some space groups they are of great help in calculating general intensities. They are so when the formula is of the type

$$\left\{\Sigma \begin{matrix}\cos\\ \sin\end{matrix} h\alpha \begin{matrix}\cos\\ \sin\end{matrix} (k-i)\,\beta\right\} \begin{matrix}\cos\\ \sin\end{matrix} lz.$$

In order to make the figure fields more nearly comprehensive, therefore, the function $\Sigma \sin h\alpha \sin (k-i)\,\beta$ has also been evaluated, though it does not occur in the plane groups. Moreover, some of the formulae which are not of this type can be expanded in order to allow of the use of the figure fields. For instance the formula for the B part of the space group no. 149, $C\,3m1$ can be expressed as

$$\cos lz\,.\,\Sigma \sin h\alpha\,.\cos (k-i)\,\beta + \sin lz\,.\,\Sigma \cos h\alpha\,.\cos (k-i)\,\beta,$$

which can be computed fairly quickly from tables of $\cos lz$ and $\sin lz$ and the structure factor fields.

Table 1. $\Sigma \cos h\alpha \sin (k-l)\beta$ (3 2 5 0)

																																																										39		*40* $\overline{261}$	20
																																																							37		*38* $\overline{210}$		$\overline{243}$		19
																																																				35		*36* $\overline{095}$		$\overline{152}$		$\overline{193}$		$\overline{207}$	18
																																																	33		*34* 011		$\overline{034}$		$\overline{080}$		$\overline{121}$		$\overline{143}$		17
																																														31		*32* 049		044		022		$\overline{009}$		$\overline{042}$		$\overline{065}$		$\overline{075}$	16
																																													30 000		036		056		062		049		032		013		001		*y* 15
																																										$\overline{099}$		$\overline{045}$		008		052		079		088		086		078		068		065	14
																																							$\overline{187}$		$\overline{144}$		$\overline{088}$		$\overline{026}$		031		075		103		117		118		115		111		13
																																				$\overline{213}$		$\overline{205}$		$\overline{172}$		$\overline{119}$		$\overline{057}$		005		059		098		122		133		134		132		131	12
																																	$\overline{168}$		$\overline{194}$		$\overline{196}$		$\overline{174}$		$\overline{131}$		$\overline{076}$		$\overline{017}$		038		081		110		123		126		126		123		11
																														$\overline{087}$		$\overline{125}$		$\overline{151}$		$\overline{160}$		$\overline{149}$		$\overline{118}$		$\overline{074}$		$\overline{024}$		022		062		087		098		099		094		089		087	10
																											$\overline{017}$		$\overline{045}$		$\overline{073}$		$\overline{095}$		$\overline{105}$		$\overline{101}$		$\overline{083}$		$\overline{051}$		$\overline{014}$		021		049		066		069		063		051		038		031		9
																								007		005		$\overline{007}$		$\overline{021}$		$\overline{035}$		$\overline{043}$		$\overline{041}$		$\overline{030}$		$\overline{010}$		014		036		050		053		046		028		005		$\overline{018}$		$\overline{035}$		$\overline{041}$	8
																					$\overline{017}$		002		015		020		022		020		019		021		029		041		053		063		064		055		035		005		$\overline{031}$		$\overline{065}$		$\overline{093}$		$\overline{108}$		7
																		$\overline{059}$		$\overline{037}$		$\overline{011}$		013		033		048		059		068		074		083		090		095		095		087		069		038		$\overline{003}$		$\overline{049}$		$\overline{095}$		$\overline{135}$		$\overline{161}$		$\overline{171}$	6
															$\overline{087}$		$\overline{075}$		$\overline{054}$		$\overline{026}$		004		032		057		077		094		108		118		125		127		123		111		087		051		005		$\overline{047}$		$\overline{101}$		$\overline{150}$		$\overline{186}$		$\overline{207}$		5
												$\overline{083}$		$\overline{086}$		$\overline{080}$		$\overline{063}$		$\overline{040}$		$\overline{010}$		021		050		076		099		118		130		140		142		139		125		101		066		021		$\overline{031}$		$\overline{086}$		$\overline{139}$		$\overline{181}$		$\overline{209}$		$\overline{219}$	4
									$\overline{053}$		$\overline{067}$		$\overline{076}$		$\overline{074}$		$\overline{064}$		$\overline{046}$		$\overline{021}$		006		034		061		084		104		120		130		135		133		123		103		074		036		$\overline{010}$		$\overline{059}$		$\overline{107}$		$\overline{149}$		$\overline{181}$		$\overline{198}$		3
						$\overline{021}$		$\overline{034}$		$\overline{046}$		$\overline{054}$		$\overline{056}$		$\overline{051}$		$\overline{041}$		$\overline{025}$		$\overline{005}$		016		038		056		074		088		098		104		105		099		087		067		040		008		$\overline{029}$		$\overline{065}$		$\overline{099}$		$\overline{127}$		$\overline{146}$		$\overline{151}$	2
			$\overline{003}$		$\overline{009}$		$\overline{015}$		$\overline{022}$		$\overline{027}$		$\overline{029}$		$\overline{029}$		$\overline{026}$		$\overline{018}$		$\overline{008}$		004		015		026		037		044		052		055		056		056		050		043		029		013		$\overline{006}$		$\overline{025}$		$\overline{045}$		$\overline{062}$		$\overline{074}$		$\overline{081}$		1
000		000		000		000		000		000		000		000		000		000		000		000		000		000		000		000		000		000		000		000		000		000		000		000		000		000		000		000		000		000		000	0
0		1		2		3		4		5		6		7		8		9		10		11		12		13		14		15		16		17		18		19		20		21		22		23		24		25		26		27		28		29		30	

x (60ths)

§ 8. APPLICATION TO DOUBLE FOURIER SYNTHESIS

The figure fields for the $\Sigma \cos h\alpha . \cos (k-i) \beta$ formula constitute the functions which have to be multiplied by the F of the plane and then added in a process of double Fourier synthesis in a hexagonal crystal. Supposing the process to have been carried out, therefore, the figure fields are exceedingly useful as an indication of the contribution of individual planes to the total synthesis. If the effect of a change of sign of one plane is required, all that has to be done is to add to the synthesis the correct fraction of the figure field.

§ 9. SUPPLY OF COPIES

Workers who would find a set of these tables useful should write to the authors at the University of Manchester, Physical Laboratories. About sixty copies have been made in all, and at the time of sending in this paper twenty-seven sets have already been supplied to various laboratories.

§ 10. ACKNOWLEDGEMENTS

The authors wish to thank Miss Ross (Edinburgh) and Messrs Goldschmidt and Hardy (Manchester) for help in the computations, Miss M. Siddall for help in the typing, and Dr L. J. Comrie for some very helpful advice. One of us (H. L.) was in receipt of a grant from the Department of Scientific and Industrial Research when this work was being done. The authors owe a great debt to Prof. Bragg for his continued interest and encouragement.

REFERENCES

(1) Bragg, W. L. *Nature, Lond.*, **138**, 362 (1936).
(2) Bragg, W. L. and Lipson, H. *Z. Kristallogr.* **95**, 323 (1936).
(3) Lipson, H. and Beevers, C. A. *Proc. Phys. Soc.* **48**, 772 (1936).

DISSOCIATION ENERGY OF THE CN MOLECULE

By R. SCHMID, L. GERÖ and J. ZEMPLÉN

Received 30 *October* 1937. *Read in title* 25 *February* 1938

ABSTRACT. The perturbations observed on the vibrational levels of the B $^2\Sigma$ state of CN must be caused by intersections with levels of a $^2\Pi$ state as established by the widening of the spin doublets of the B $^2\Sigma$ state, i.e. by the simultaneous but inequal shifting of the spin-doublet components and by the decay of the perturbations with decreasing rotational quantum numbers, leaving the rotationless states unaffected. The perturbing state must be identical with the known A $^2\Pi$ state of CN, as proved by the observed positions of the perturbed places in the CN level scheme.

In this way the vibrational set of the A $^2\Pi$ state becomes observable up to the 30th sublevel, where the vibrational convergence is already very marked. A short extrapolation fixes the convergence limit at about 60500 ± 1000 cm.$^{-1}$ above the ground state X $^2\Sigma$ ($v=0, J=0$) of CN. A comparison of the positions of vibrational levels of the X $^2\Sigma$ and A $^2\Pi$ states shows that the convergence limit of the former should lie in the neighbourhood of the latter; the B $^2\Sigma$ state converges to about 65500 ± 1000 cm.$^{-1}$

On this basis the correlation between C+N and CN levels is found as follows: A $^2\Pi_{\text{convergence}} \rightarrow \text{C}\,(^3\text{P}) + \text{N}\,(^2\text{P}) = 60500 \pm 1000$ cm.$^{-1}$ and B $^2\Sigma_{\text{convergence}} \rightarrow \text{C}\,(^5\text{S}) + \text{N}\,(^4\text{S}) = 65500 \pm 1000$ cm.$^{-1}$ This could then be verified by the observation of intensity drops at energy values where the other C+N term combinations fall. Thus for the dissociation energy of the CN molecule into tetravalent C (^{5}S) and trivalent N (^{4}S) atoms one gets 8·09 e.v. in very good agreement with calculations made on the basis of $\text{CO}\,(\text{X}\,^1\Sigma) + 11\cdot06 \text{ e.v.} \rightarrow \text{C}\,(^5\text{S}) + \text{O}\,(^3\text{P})$.

§ 1. INTRODUCTION

Until recently the dissociation energy of CN could be obtained by calculation only. Usually it was computed on the basis of the dissociation energy of CO in conjunction with thermochemical data, such as the heat of combustion and heat of dissociation of cyanogen (C_2N_2), etc. The chief obstacle to any direct determination in this case lies in the chemical instability of the CN molecule; this is the reason why absorption continua could not be observed and why electron impact methods could not be employed. Even in such cases, however, dissociation limits may often be obtained successfully from perturbation data. The method consists of finding convergence limits of diatomic molecular states by means of perturbations caused by the converging states on other states of the molecule.

The importance of finding the converging set of vibrational states of a molecular term for the purpose of the determination of dissociation limits requires no further argument. Unfortunately the vibrational states which are close enough to each other, and, therefore, to the convergence limit, are often of very high energy; and on account of the Boltzmann factor the probability of transitions to or from them is very seldom high enough to allow their observation as actual electronic bands. Yet, the closer and higher these states are situated, the more easily may it happen that their sets of rotational levels cross over those of other states having vibrational quantum numbers low enough to give rise to direct observation of bands, in which, under favourable conditions, the courses of those intersections will be observed as perturbations. If the perturbations are numerous and extensive enough, there is always a possibility of deriving the correct positions of the perturbing states from the perturbation data (shifts, doublings, intensity anomalies, etc.). Thus the search for perturbations may be considered as most important in the search for dissociation limits.

§2. PERTURBATIONS OF THE CN STATES

Perturbations in the CN bands have been known almost as long as the CN spectrum itself. This spectrum consists of two band systems only, involving three different electronic states. The lowest and highest states are the X $^2\Sigma$ and the B $^2\Sigma$ respectively, the A $^2\Pi$ being situated between them in the energy diagram. It was supposed(1) that the perturbations observed in the violet (B $^2\Sigma \rightarrow$ X $^2\Sigma$) CN bands are caused by the overcrossing of the X $^2\Sigma$ ($v=11$) level by the A $^2\Pi$ ($v=6$) level, and this supposition was afterwards verified(2) by observations in the red A $^2\Pi \rightarrow$ X $^2\Sigma$ bands having v equal to 6 for the upper state, where the reverse perturbation could be observed. Although this perturbation has been very well studied, the others, which are numerous and are observed in the bands of the violet system, have not been thoroughly investigated hitherto.

In the B $^2\Sigma \rightarrow$ X $^2\Sigma$ system of CN one distinguishes between the prominent violet bands and tail bands. While rotational analysis and wave-number measurements for the tail bands have been given by Jenkins(3), for the former no analysis, in the modern sense, extending to all observed vibrational and rotational states has been published for the prominent bands. This is an obvious lack, as in the search for perturbations the exact knowledge of the precise positions of as many levels as possible is extremely important. While early investigators(4) of the violet system merely indicated in their wave-length tables the places where perturbations occur, Birge(5) gave a graph of the perturbations observed in the $2 \rightarrow 2$ violet band, in terms of a numbering, however, which starts from the band head and must be corrected by about 30 units to give the current numbering. However valuable the available data on the violet-band perturbations may be, it was felt necessary to obtain new spectrograms, as the simultaneous inspection of a number of plates greatly increases the probability of detecting all the perturbations. For this purpose a 220-V. d.c. arc was passed between pure carbon electrodes in air and photographed with exposures from 2 min. to 16 hr. in the first and second orders of a 6-m. concave grating (30,000 lines/in.) coated with Hochheim metal on the reflecting surface. This source gives the prominent violet CN bands. To obtain the tail bands, however, the much more complicated excitation with active nitrogen would have been used; by the extreme kindness and courtesy of Prof. F. A. Jenkins, however, we had the privilege of using his own pictures.

While we were trying to systematize the perturbations in the B $^2\Sigma \rightarrow$ X $^2\Sigma$ CN system from a general standpoint, it became more and more apparent that all the perturbations with the exception of two, namely that of the B $^2\Sigma$ ($v=14$) level at the 8th rotational sublevel and that of the B $^2\Sigma$ ($v=15$) level around the 22nd sublevel, could be explained by intersections of the B $^2\Sigma$ vibrational levels with a $^2\Pi$ state. This is proved (i) by the general finding that the perturbations present themselves as widenings of the spin doublets of the $^2\Sigma$ state by unequal shifts of both components of the ρ-type doublets, and (ii) by the observation that also in bands where the overcrossing happens at very low rotational quantum numbers, the doublet width—amounting sometimes to 1–2 wave-number units at the place of crossing—decreases very rapidly to zero with decreasing rotational quantum number, leaving the positions of the rotationless states unaffected (as proved by the entirely regular vibrational scheme of the band system). In theoretical papers on perturbations⁽⁶⁾ it has been shown that the overcrossing of two $^2\Sigma$ states may not affect the doublet width and should cause a shift of the whole set of rotational sublevels, and also of their zero line. The observed kind of perturbation is predicted for intersections of states having $\Delta\Lambda = 1$, and since in the case of CN the perturbed one is a $^2\Sigma$ state the perturbing must be a $^2\Pi$.

Once a $^2\Pi$ state is established as the cause of the more prominent perturbations, it seems natural to connect this with the already known A $^2\Pi$ state of CN. How this supposition was indeed verified may be seen in figure 1, which shows the run of the rotational sets of the vibrational levels of B $^2\Sigma$ and A $^2\Pi$ against the abscissa $J(J+1)$. If one makes the entirely acceptable supposition that the coefficient D in the energy term $DJ^2(J+1)^2$ has nearly the same value for all three CN states, the graphs of the rotational energy in that coordinate system could be substituted with sufficient accuracy by straight lines having slopes equal to the numerical values of the rotational constants B_v. For the sake of simplicity, doublet states are represented by their mean value only.

For the B $^2\Sigma$ state the B_v values are obtained from Jenkins's rotational analysis. The places where the $^2\Pi$-type perturbations occur are marked with circles. The lowest three runs of B $^2\Sigma$ are known up to very high rotational quantum numbers from the spectrum of the arc, which is hot enough for the appearance of band-lines up to $J=100$ and more; in this region the perturbation affects mostly one line only. In the higher vibrational sets of B $^2\Sigma$, however, one often finds more affected lines; we have marked this by doubling the corresponding length of the B runs. This difference in appearance of perturbations at low- and high-lying sets would indeed be expected, because in the crossings by high rotational quantum numbers the two intersecting sets have only very few states with nearly the same energy, while in the crossings with smaller J values the subsequent rotational states remain in the vicinity of each other for more members, and thus the critical interval is much broader. In some bands one finds the unusually wide splitting along the whole length, which shows the rotational set of the perturbing state to run apparently just below the perturbed one, etc. All these features help, of course, to construct the right positions and slopes of the perturbing states.

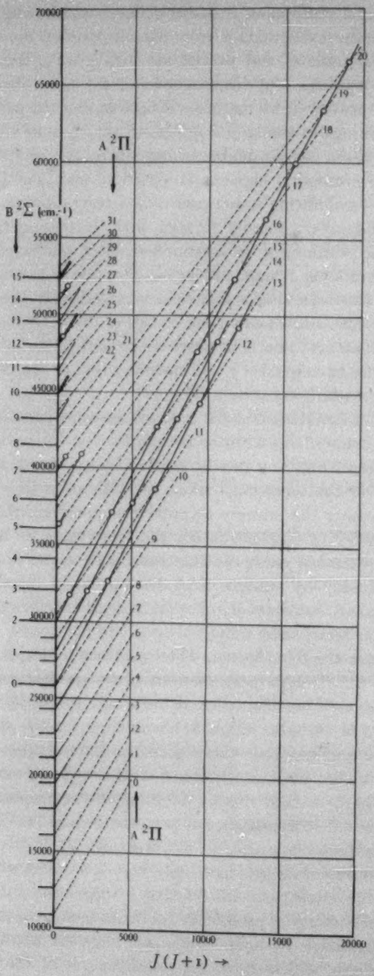
70000
65000
60000
55000
50000
45000
40000
35000
30000
25000
20000
15000
10000
0
5000
10000
15000
20000
B ²Σ (cm.⁻¹)
A ²Π
A ²Π
0
1
2
3
4
5
6
7
8
9
10
11
12
13
14
15
0
1
2
3
4
5
6
7
8
9
10
11
12
13
14
15
16
17
18
19
20
21
22
23
24
25
26
27
28
29
30
31
J (J+1) →

Figure 1.

The deepest-lying A $^2\Pi$ levels in figure 1 have been observed and analysed directly in the CN red bands⁽²⁾. The lengths of the parts observed directly by rotational fine-structure analysis are drawn by full lines. They are of course very short on account of the low effective emission temperature of the source (active nitrogen). The highest three and deepest four vibrational levels of the $^2\Pi$ state are known only by band-head measurement. It involves only an extrapolation of three steps to arrive right to the position of the first (lowest-lying) perturbation on the B $^2\Sigma$ state, and from there, reasonably decreasing the distances between consecutive vibrational sets and diminishing the slope of the rotational runs, one can go forward from step to step, aided repeatedly by the positions of the perturbations. In advancing up to the 30th vibrational set of the $^2\Pi$ state one finds the original vibrational frequency and rotational constant considerably decreased—a sign of the closeness of the convergence limit.

§ 3. CONVERGENCE LIMITS FOR THE CN LEVELS

As we advance from $v=0$ up to $v=30$ for the $^2\Pi$ state, it is found that the decreasing of the distance between two consecutive vibrational states (indicated commonly by ωx in the formula $G(v)=\omega v-\omega x v^2$) must be increased from its original value of 13 cm.$^{-1}$ to about 18 cm.$^{-1}$, a very reasonable amount with respect to the length of the vibrational set, for which the $G(v)$ formula should be completed with further terms containing higher exponents of v, of course. As for the position of the convergence limit one has to proceed by further increasing this decrement, and since the law of this process is at present unknown, at first glance one may believe the result to be very arbitrary. However, a checking up shows this not to be the case; it is found that by assuming the $G(v)$ function to be first as cubic, then of fourth, fifth degree, etc. in respect of v, one gets values for the convergence limit within an interval not exceeding at most 1000–1500 wave-number units. An upper limit is given by the progress observed in the last ωx values, which would reach the last ΔG value within about 20 steps, thus fixing $v_{\max} < 50$.

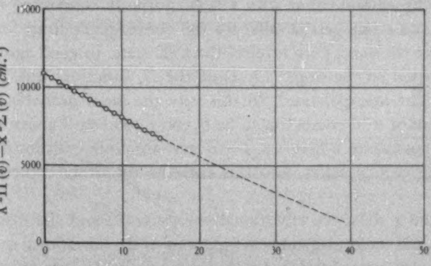

Figure 2.

Some kind of control to the convergence of the $G(v)$ values is afforded by the B_v values of the $^2\Pi$ state, as these should show a convergence to zero at just the same v where $G(v)$ reaches its maximum. By trial one finds the most probable position of the A $^2\Pi$ convergence limit to be about 60500 cm.$^{-1}$ above the CN ground state, with a probable accuracy of ± 1000 cm.$^{-1}$, and $v_{\max}=47$.

A comparison of the vibrational sets of the X $^2\Sigma$ and A $^2\Pi$ states shows that their convergence limits should lie very near together. This is strongly suggested by figure 2, where the term-differences A $^2\Pi(v) - $ X $^2\Sigma(v)$ are drawn as ordinates against the common v's as abscissae. One finds that the observed differences fall along a nearly straight line, which seems to cut the v-axis just in the region where the $v_{\max}$ for A $^2\Pi$ should lie. In a previous paper(7) insufficient attention was paid to the relative position of the X $^2\Sigma$ and A $^2\Pi$ levels; this resulted in the incorrect conclusion that beyond the intersection of the two potential curves, these two states may converge to limits differing in energy more than 0·5 e.v., an error now corrected. In the same paper, in an effort to get the dissociation products of the CN molecule, the Rydberg extrapolation method was used to obtain the convergence limit of the B $^2\Sigma$ state. Now it turns out that this method yields too low a value. This fact was definitely established by computations on the a' $^3\Sigma$ state of CO, where the positions of about 40 vibrational levels, from the first up to just below the convergence limit, are well known(8). Fortunately, in the case of the B $^2\Sigma$ state of CN the value of ωx increases within the observable 15 steps from 21 cm.$^{-1}$ to about 28 cm.$^{-1}$, thus making the extrapolation rather short and keeping the error between narrow limits. By extrapolation with a $G(v)$ formula containing members up to the third power in v one gets a value for the convergence limit for B $^2\Sigma$ of about 39700 cm.$^{-1}$ above the $v=0, J=0$ level of the B $^2\Sigma$ state, in good agreement with the computations based on the slope (i.e. α) of the B_v function, this, too, being large enough for a short extrapolation. In this way the most probable position of the convergence limit of B $^2\Sigma$ comes out to be 65500 ± 1000 cm.$^{-1}$ above the CN ground state, since the position of B $^2\Sigma$ $(v=0, J=0)$ level amounts to 25800 cm.$^{-1}$, i.e. it is the highest of all three CN states, and this corrects the other error in the previous paper(7).

Figures 3 and 4 show the vibrational energy $G(v)$ and the rotational constant B_v for the three CN molecular states as functions of the vibrational quantum number v. The dotted parts are obtained by the most probable extrapolation mentioned above, and by the requirement that $G(v)$ should arrive at its maximum at just the same v where B_v becomes zero.

§ 4. CORRELATION OF THE CONVERGENCE LIMITS WITH ATOMIC LEVELS

The conclusion, established entirely experimentally, that the convergence limits of the CN states are as close-lying as about 5000 ± 1000 cm.$^{-1}$, i.e. 0·6 e.v., may serve as a basis for the determination of the correct correlation with the levels of the separate atoms.

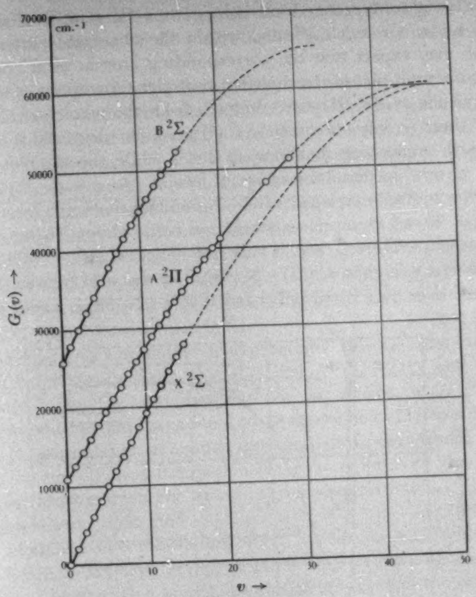

Figure 3.

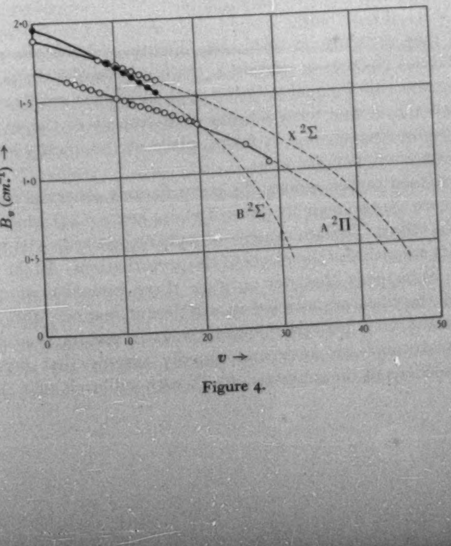

Figure 4.

Since the lower convergence limit belongs to a ${}^2\Pi$ state in which the doublet width seems to be not much affected within the observable interval from $v=0$ to $v=11$, one may expect that the corresponding atomic term combination will consist of atomic multiplet terms showing multiplet separations of about the same order of magnitude as the ${}^2\Pi$ state. Indeed, from the whole set of the atomic C and N terms there is only one, namely C (^{3}P), which may fulfil this requirement, its overall width amounting to about 40 cm.$^{-1}$, while the doublet separation of A ${}^2\Pi$ is about 50 cm.$^{-1}$ in the observed set of levels.

If one wishes to find now a pair of C + N combinations, the lower combination having the C as ^{3}P and the upper combination being about 0·6–0·7 e.v. above the lower, to give rise to a ${}^2\Sigma$ level, there is only one choice: C (^{3}P) + N (^{2}P) for the lower and, at some 0·63 e.v. higher, C (^{5}S) + N (^{4}S). The distance between the two other possible combinations: C (^{3}P) + N (^{2}D) and C (^{3}P) + N (^{2}P) is about twice as large, and thus they may certainly be ruled out. Figure 5 shows the potential energy curves of the three CN states in relation to the C + N levels; the potential function assumed is Morse's with *D* equal to 60500 cm.$^{-1}$ and 39700 cm.$^{-1}$ respectively.

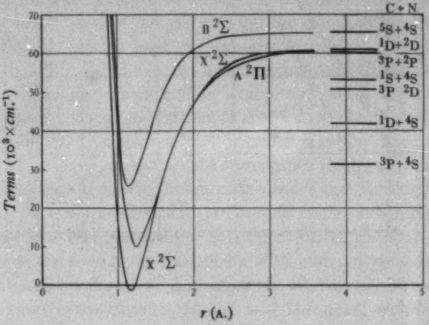

Figure 5.

Having fixed the atomic term scheme with respect to the molecular ground state, one has to investigate what is taking place at the energy values where the other atomic term combinations occur.

As was mentioned earlier, among the perturbations observed in the vibrational levels of B ${}^2\Sigma$, there are two (namely those of $v=14$ and $v=15$) which differ in many respects from the others. The latter cases—already recognized as ${}^2\Pi$ perturbations—show no intensity anomalies at the places of the perturbations. In the two anomalous cases, however, it happens that not only are there intensity anomalies but also the positions of the lines are affected in a different manner, the ρ-type doublet widths sometimes varying in a very rhapsodic way. In seeking reasons for these two anomalous perturbations one may undoubtedly assume that perhaps they are caused by intersections of the sublevels of B ${}^2\Sigma$ with sublevels of X ${}^2\Sigma$, for instance.

The low-lying B levels are indeed overcrossed frequently by higher-lying X levels still in the observable region of the violet bands, but there is no sign of any perturbation.

The place of the higher-lying anomalous perturbation is the $v=15$ level of the B $^2\Sigma$ state, in the neighbourhood of the 22nd rotational sublevel, at a height of about 53400 cm^{-1} or 6·6 e.v. above the ground state. While the R (20) line of the 15 → 15 violet band has normal intensity, R (21) is increased abnormally; R (22) is normal again, but R (23) is very weak; R (24), R (25) and R (26) have normal intensity but R (27) is very weak, and beyond these no more lines are observed. Further, while the 15 → 15 band is relatively intense, there is no trace of the 16 → 16 band or of others with $v \geqq 16$. All this seems to correlate to the fact that the atomic term combination C (^{1}S) + N (^{4}S) lies just at this height, thus indicating as an interpretation a perturbation in the vicinity of a predissociation limit, such as is observed among others in the CO Third Positive bands(8).

For the lower-lying anomalous perturbations ($v=14$) the findings in the 14 → 14 violet band are, in short, that the lines R (8), R (11), and P (10), P (13) show anomalous intensities and irregular doublet widths, while the other lines before, between and beyond these seem to be unaffected. This phenomenon takes place in the CN level-scheme at about 51000 cm^{-1} above the ground state, and this suggests as an interpretation an interaction of the $v=14$ level of B $^2\Sigma$ with some other level (or levels) arising from the atomic term combination C (^{3}P) + N (^{2}D), the position of which is at 50900 cm^{-1}

The next atomic term combination, which has not played a role in this scheme of CN dissociation, is C (^{1}D) + N (^{4}S) at 41900 cm^{-1} A band of the violet system, having the upper level at this height, would fall however in the crowded spectral region where the heads or the tails occur, and must escape reliable observation.

The lowest combination C (^{3}P) + N (^{4}S) is situated at 31700 cm^{-1} The two lower states (X $^2\Sigma$ and A $^2\Pi$) of CN have their highest vibrational levels just below this energy value; the B $^2\Sigma$ state has its fourth level ($v=3$) at this height. Now on spectrograms taken with an arc as source one often finds that bands of the violet system with initial vibrational quantum number $v' \geqq 3$ do not appear with an intensity comparable to that of bands with $v'=0$, 1 and 2. For instance on our plates (taken with a d.c. arc in ordinary atmospheric air) one finds the R branches of the B $^2\Sigma \rightarrow$ X $^2\Sigma$ bands, 0 → 0, 1 → 1 and 2 → 2 at high rotational quantum numbers (up to $J=100$ and more) placed in characteristic groups, namely three pairs of lines due to the spin doubling of the $^2\Sigma$ states, always with almost equal intensity, while there is no trace of a 3 → 3 band. In view of the very considerable intensity of the bands with $v'=2$ one would not expect the sudden drop for bands with $v'=3$. Of course by excitation with active nitrogen this does not hold at all. As for interpretation, it seems probable that the levels arising from the combination C (^{3}P) + N (^{4}S) may cause a predissociation at the B $^2\Sigma$ ($v=3$) level. In this case the border line of the predissociation should cut the $v=2$ run at very high quantum numbers only, a case already met in the N_2 spectrum(9).

§5. DISSOCIATION ENERGY OF CN

The correlation of C+N atomic levels to the convergence and predissociation limits of CN fixes the distance of the lowest atomic combination C (^{3}P)+N (^{4}S) in respect to the x $^2\Sigma$ ($v=0$, $J=0$) ground state of CN at about 31700 cm.$^{-1}$ or 3·91 e.v.; in the usual way this value would be called the energy of dissociation. However, as has been pointed out⁽⁸⁾ in the case of carbon compounds, it seems to be more reasonable to restrict this name to the energy necessary to split the molecule into a tetravalent carbon and a trivalent nitrogen atom: C (^{5}S)+N (^{4}S). This level lies at about 65500 cm.$^{-1}$ or 8·09 e.v., and thus the dissociation energy of CN should be given by this value.

We have arrived at the value of *D* (CN) in this paper on an entirely experimental basis, and it is interesting to know that it agrees very well with the calculated one. This calculation is based partly on thermochemical cycles fixing the difference of dissociation energies of CO and CN at about 70 kcal. or 3·05 e.v., and on the value of the dissociation energy of CO itself, which latter should be obtained by spectroscopic (or electron-impact) experiments. As has been shown⁽⁸⁾, the spectroscopic and electron-impact results concerning the dissociation phenomena of CO (and also the corresponding results on CO_2, which are entirely connected with those on CO) may be interpreted without any contradiction only on the basis of a correlation of C+O levels to the CO states fixing the combination C (^{5}S)+O (^{3}P) in respect to the x $^1\Sigma$ ($v=0$, $J=0$) ground state of CO at the height of 11·06 e.v., a value called by us the dissociation energy of CO. Thus the calculated value of *D* (CN) is equal to $11{\cdot}06-3{\cdot}05=8{\cdot}01$ e.v.

In a forthcoming paper it will be shown that all the observed dissociation phenomena in carbonic compounds (electron impact, light absorption, etc.) could be interpreted in the simplest and easiest way, and without any contradiction, by dissociation into C (^{5}S) atoms.

§6. ACKNOWLEDGEMENTS

This paper has been completed in the spectroscopic laboratory of the Physical Institute of the Royal Hungarian University for Technical and Economic Sciences, Budapest, directed by Prof. B. Pogány. The authors wish to express their deepest gratitude to the Council for Natural Sciences and the Széchenyi Society for their material aid, and especially to Prof. F. A. Jenkins of the University of California, for his kindness in lending to the authors his precious spectrograms of the CN tail bands.

REFERENCES

(1) Rosenthal, J. E. and Jenkins, F. A. *Proc. Nat. Acad. Sci., Wash.*, **15**, 381 (1929).
(2) Jenkins, F. A., Roots, Y. K. and Mulliken, R. S. *Phys. Rev.* **39**, 16 (1932).
(3) Jenkins, F. A. *Phys. Rev.* **31**, 539 (1928).
(4) Uhler, H. S. and Patterson, R. A. *Astrophys. J.* **42**, 434 (1915).
(5) Birge, R. T. *Report on Molecular Spectra in Gases, Bull. Nat. Res. Coun., Wash.*, No. 57, **11** (Part 3), 68 (1926). [For figure see p. 90.]
(6) Dieke, G. H. *Phys. Rev.* **47**, 870 (1935), for example.
(7) Schmid, R. *Z. Phys.* **99**, 562 (1936).
(8) Schmid, R. and Gerö, L. *Z. Phys.* **105**, 36 (1937); **106**, 205 (1937); *Z. phys. Chemie*, (B), **36**, 105 (1937).
(9) Schmid, R. and Gerö, L. *Z. Phys.* **104**, 724 (1937).

NOTE ON THE WHISPERING GALLERY OF ST PAUL'S CATHEDRAL, LONDON

By A. E. BATE, Ph.D., M.Sc., F.Inst.P., Northern Polytechnic

Received 12 *December* 1937. *Read* 28 *January* 1938

ABSTRACT. The apparent disagreement between Rayleigh's deduction and those of Raman concerning the whispering-gallery phenomenon is shown to depend on the fact that Raman used a sustained source which gave rise to interference, whereas Rayleigh dealt with a whisper projected in one direction. Further, it is shown that, whereas Rayleigh attributed the success with a whisper to the fact that it is composed of high frequencies, low frequencies are projected equally well, and that actually the success attained with a whisper is due to its low intensity, which does not give rise to audible echoes. Explanations are offered of the circumferential and radial alternations of sound mentioned by Raman and Sutherland.

§ 1. INTRODUCTION

Sabine(1) referred to a whispering gallery as one so shaped that faint sounds can be heard at extraordinary distances, as a result either of focusing or of the creeping (as Rayleigh(2) termed it) of sound waves round a curved wall. The phenomenon in those buildings in which focusing occurs requires no explanation, and is usually apparent at one region only, the focus; but the galleries of the second category, that in St Paul's being the classic example, still await complete explanation.

The gallery in St Paul's runs round the inside of the dome and overhangs to the extent of some 1·5 m. An iron railing about 1·25 m. in height is on the inner side of the gallery, and the side of the dome forms the outer boundary; a low stone seat runs round the side of the dome. The dome itself is, of course, high above the gallery. A guide, whispering near the wall of the gallery, can be heard easily by a person seated at any point of the circumference. A whisper is more effective than a shout.

Airy(3) suggested that the dome overhead acted as a concave reflector, but Rayleigh(4) pointed out that this explanation is untenable, for in these circumstances the sound, after reflection, would be focused on to the section of the gallery opposite the source, whereas the sound is more or less evenly distributed round the gallery. "The whisper seems to creep round the gallery horizontally, not necessarily along the shorter arc, but rather along that arc towards which the whisperer faces."

§2. RECENT OBSERVATIONS

More recently Raman and Sutherland(5) have detected radial and circumferential variations in the intensity of the sound in the gallery, and state that "The circumferential fluctuations of intensity might be interpreted as being, at least in part, due to the stationary interference of waves which meet after passing in opposite directions round the gallery. But the radial fluctuations are less easily explained, and must be regarded as fundamental in any satisfactory theory of the whispering gallery."(6)

Raman(7) has since shown that the waves do run round the walls as Rayleigh had suggested. He did this by tapping a point on the circumference, timing ten echoes and deducing the velocity on the assumption that the sound travelled round the walls, the values obtained agreed with that of sound in the open air to within 1 per cent. The experiment was performed in several galleries in India, some of which had not been suspected of possessing whispering-gallery properties until he pointed them out.

The writer, by permission of the authorities of St Paul's Cathedral, was able to carry out some experiments in the whispering gallery after it had been closed to the public. The frequencies used ranged from 256 to 6000 c./sec., the sources of sound being heavy tuning forks capable of vibrating for a considerable time. They were held in turn at different distances from the wall, and in every case the sound was heard by observers close to the wall, but the positions of the radial and circumferential alternations varied with frequency and with the distance of source from the wall. It should be remembered that the maximum distance of the source from the wall was about 1·5 m.

§3. EXPLANATION OF THE PHENOMENON

The fact that the low frequencies travelled round the gallery is of particular interest, for a whisper is composed of high-frequency sounds, and to this fact, in part, the phenomenon has been attributed. Actually the success attained with a whisper appears to be due to the fact that the open-air range of whispered sounds is small, and that the sound traversing a diameter would be imperceptible at the side opposite to the source, and would not interfere with the circumferential waves.

The sound which is heard is that which travels round the wall by successive reflections along short chords. This sound suffers very little absorption at the hard smooth wall during reflection, so that the main energy-loss would appear to be due to the divergence of the sound. This, however, is minimized by the reinforcement of incident and reflected waves which combine to produce waves with fronts travelling at right angles to the wall.* At the wall they are in phase, but at a short distance from it (the distance depending on the frequency) they are out of phase, and approximate silence will result. A little farther away from the wall the waves will be in phase again, but with a diminished intensity.

---

* Compare this with the observations of Scott-Russell (B.A. report 1844) on water waves. He found that when the waves were incident on a vertical wall in deep water at an angle of incidence greater than about 75°, the waves were not reflected but passed along the wall, the wave-front being at right angles to the wall.

The existence of these waves may be shown by sprinkling the floor of a small model with lycopodium powder and passing a vertical electric spark of suitable intensity near the wall.(8) (The wave-length of the sound from the spark is probably of the order of one or two centimetres.) The powder is ranged into short ridges at right angles to the wall, which indicates progressive waves near the wall, for if sparks are passed on an open plate, the powder is ranged in continuous circular ridges with the spark as centre; the rings are thus at right angles to the direction of the air-vibration. The distance between the ridges or striae diminishes with intensity.

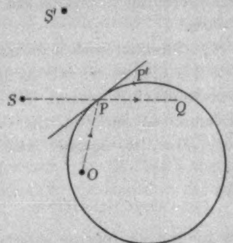

Plan of gallery. O, source; S, image of O at P; S', image of O at P'.

The formation of the waves can be explained by the method of images.(8, 9, 10) Let the circle represent the plan of the gallery; if O be the source of sound and OP a particular ray of sound, the tangent through P represents the plane mirror which reflects OP to PQ, S being the image for the reflected ray which arrives at the point P. The two sources of sound O and S project a narrow beam midway between and at right angles to OS. The actual portion of this beam in the neighbourhood of P is that inside the circle. For an adjacent point P', the image will be S'; thus there is a series of moving images each of which combines with the primary source to form waves with the wave-front at right angles to the circumference. This wave-front will be narrow, for the incident and reflected waves will be in phase only at the circumference.

At a small distance from it they will be out of phase, and approximate silence will result. Farther still, i.e. nearer the centre, the waves will be in phase again, and give rise to audible sound, an effect observed by Raman and Sutherland.

For the more remote parts of the circumference the primary and secondary images will be responsible for the propagation. At a particular point the sound may arrive in two different beams moving in the same direction round the gallery but with different path-lengths. Whether these are in phase or not at that point determines the intensity of the sound, and thus arises the circumferential variation in intensity.

§4. THEORY APPLICABLE TO CONTINUOUS SOUNDS

Another theory suggests(5) that this variation may be caused by interference between the two sets of waves which leave the source and pass round the gallery in opposite directions to meet. This, however, is unlikely in a whispering gallery, for the overlap of different syllables at all points except that opposite the source would make the words indistinguishable. Besides, the whisper seems to creep round the gallery in the direction the speaker faces.(2)

If the whisper is replaced by a source of sound this theory will hold, and the circumferential variations will be definite, whereas with a whisper they are not. This probably explains the disagreement between Rayleigh and Raman—in fact, the latter states that the circumferential variations are most marked at the side of the gallery opposite to the source.

Raman and Sutherland experimented with a miniature gallery composed of a complete circular reflector with a Galton whistle as source; they found that the circumferential variations were uniformly spaced. When, however, a semicircular reflector was used with the source at one end, the variations were found to be unevenly spaced, being more crowded together near the end of the diameter opposite the source.

§5. CONCLUSIONS

The conditions necessary for the whispering gallery effects are (i) a hard wall for good reflection, (ii) a source of sound of sufficiently low intensity to suffer no appreciable reflection from the opposite side of the gallery, and (iii) a source near the wall and directed so that the angle of incidence is large.

REFERENCES

(1) Sabine. *Collected Papers on Acoustics*, p. 261.
(2) Rayleigh. *Sound*, **2**, 127.
(3) Airy. *On Sound*, 145 (1871).
(4) Rayleigh. *Scientific Papers*, **5**, 171.
(5) Raman and Sutherland. *Proc. Roy. Soc.* A, **100**, 424 (1921).
(6) Raman and Sutherland. *Nature, Lond.*, **108**, 42 (1921).
(7) Raman. *Proc. Indian Ass. Cult. Sci.* **7**, 159 (1921–2).
(8) Bate. *Proc. Phys. Soc.* **48**, 178 (1936).
(9) Barton and Killy. *Phil. Mag.* **24**, 728 (1912).
(10) Marsh and Nottage. *Proc. Phys. Soc.* **23**, 264 (1911).

DISCUSSION

Sir Charles V. Boys. It seems to me that some photographs* which I took in the year 1892 might have some interest. The two to which I particularly refer were taken with a view to obtaining ocular evidence on the effect of a single wave front,

---

* Reproduced by Larmor, *Memoir and Scientific Correspondence of Sir George Stokes*, Vol. II, pp. 341–343.

(1) when this is so much inclined to a reflecting surface as to give perfect reflection, (2) when it is nearly perpendicular to the reflecting surface, and (3) when the two actions (1) and (2) are merged. There is no question here of the low intensity of a whisper nor of sustained vibrations, but the single wave of compression when nearly perpendicular to the reflecting surfaces converges upon it and swallows all the energy of any reflection, becoming denser and travelling more quickly.

Dr G. SUTHERLAND. Prof. Raman and I never really had an opportunity of being at St Paul's long enough on end to investigate the matter thoroughly, and I am very glad the author has carried the matter further in this way. What does he make of Sabine's contention that the effectiveness of St Paul's is partly due to the fact that the sides are slightly inclined inwards?

AUTHOR'S REPLY. I am much indebted to Sir Charles Boys for lending me the original lantern slide showing the phenomenon he refers to. The fact that a wave front which at first is really normal to the reflecting surface finally becomes normal in the vicinity of that surface agrees with the note at the foot of page 294.

In answer to Dr Sutherland: if a beam of sound is initially horizontal and strikes a sloping surface in which the normal at the point of incidence is depressed, the beam will be reflected downwards. In St Paul's the concave inclination is very slight, and has the effect of keeping the sound in the gallery. The floor, of course, assists this.

THE VARIATION OF VOLTAGE-DISTRIBUTION AND OF ELECTRON TRANSIT TIME IN THE SPACE-CHARGE-LIMITED PLANAR DIODE

By R. COCKBURN, M.Sc., A.Inst.P., West Ham Municipal College

Communicated by Dr D. Owen, 8 *October* 1937. *Read* 28 *January* 1938

ABSTRACT. In an earlier paper the solutions for the voltage-distribution and electron transit time in a planar diode were restricted to the case of temperature limitation. In this present paper the case of space-charge limitation is dealt with. Langmuir's equations for the voltage-distribution are put into a more convenient form, and expressions are then derived to show the dependence on emission current of the interelectrode current, the cathode field, and the electron transit time for any normal values of emission velocities.

§ 1. INTRODUCTION

In recent years considerable attention has been paid to the conditions existing in the interelectrode spaces of the thermionic valve, and several papers have been published in which the behaviour of simplified models under the action of alternating voltages has been treated mathematically(1, 2, 3, 4). They have all shown the importance of the electron transit time in determining the behaviour of a valve when alternating voltages are applied. When, as is usual, these voltages are small, the transit time differs only slightly from its value under static conditions, and this can therefore be used as a close approximation.

In an earlier paper(5) the author has examined mathematically the variation of static transit time in the temperature-limited plane diode. The general solution for the voltage-distribution was derived from the differential equation of motion, and the effect of initial velocities was treated by assuming that all the electrons were emitted with the same velocity u_0, given by

$$u_0 = \left(\frac{\pi k\theta}{2m}\right)^{\frac{1}{2}}$$

instead of being emitted with the Maxwell distribution. This approximation was shown to be valid as long as the diode remained temperature-limited, that is, for all currents from zero up to that value which just reduced the cathode field to zero. Within these limits it was possible to express in convenient form the variation with current of the voltage-distribution, the cathode field, and the electron transit time, for any normal value of initial velocity. The variation of transit time within these limits is of importance in explaining the cause of electron oscillations(6); and a knowledge of the variation of the cathode field will be necessary in any examination of the upper bend of the {current, voltage} characteristic of the diode, and in the correct interpretation of the Schottky(7) effect in this region.

It is more usual however for a valve to be working in a condition of space-charge limitation. It will be convenient to define at this point the terms to be used in describing the interelectrode conditions in the diode. With a fixed anode voltage V_a the voltage-distribution is determined mainly by the emission current i_e. Thus the diode is *temperature-limited* for any value of interelectrode current i up to the saturation value i_0 which just reduces the cathode field to zero; in this condition the interelectrode current i is equal to the emission current i_e.

For the particular case in which $i=i_0$ the valve is said to be *space-charge-saturated*. Any further increase of i_e causes now only a slight increase in i, and the valve is *space-charge-limited*. The ratio i/i_0 referred to as "degree of saturation" defines the three conditions; thus for space-charge saturation $i/i_0=1$, for temperature limitation $i/i_0<1$, and for space-charge limitation $i/i_0>1$. Figure 1 shows the usual {current, voltage} characteristic of a diode for constant emission current.

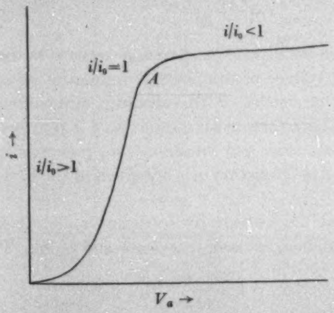

Figure 1. {Current, voltage} characteristic of a diode with constant emission current.

In this case the degree of saturation depends on V_a, which determines i_0. At point A in the region of the upper bend $i/i_0=1$, to the right of this point $i/i_0<1$, and to the left $i/i_0>1$.

The static interelectrode conditions in the space-charge-limited diode have been examined by Langmuir(8) and others(9, 15). Since an initial velocity-distribution is implicit in this condition, the assumption made by the author in the treatment of the temperature-limited condition is no longer valid. Langmuir gives a complete solution for the voltage-distribution for any current greater than the saturation value and for any initial velocities. Owing to his rigorous treatment of the problem, however, it is a somewhat lengthy process to apply his solution to a practical case, and in the present paper Langmuir's results for the voltage-distribution are put into a more convenient form which lends itself to practical application. These results have then been extended to obtain the variation of the cathode field and of the electron transit time. A knowledge of the transit time in the space-charge-limited diode is of particular importance, since it has been shown(1) that the behaviour of a valve is dependent on electron transits not only at ultra-high frequencies but also at the more normal low frequencies. The variation of cathode field is of interest in view of its possible effect on the emission, and on the maintenance of electron oscillations in the magnetron(10).

§2. SUMMARY OF LANGMUIR'S TREATMENT

That part of Langmuir's paper referring to the space-charge-limited diode may be summarized as follows. Assuming that electrons are emitted from the cathode with normal components of velocity having a Maxwell distribution, Langmuir obtains, by integration of Poisson's equation between proper limits, a numerical relation between the variables ξ and η, where

$$\xi = 2\,(x - x_m)\left[\frac{2\pi^3 e^2 i^2 m}{k^3\theta^3}\right]^{\frac{1}{4}} \qquad \text{......(1)}$$

and

$$\eta = \frac{e\,(V - V_m)}{k\theta} \qquad \text{......(2).}$$

Where x and V are the distance and voltage relative to the cathode, x_m and V_m give the position and voltage of the plane of minimum potential, i is the current passing between the electrodes, θ the absolute temperature, k the Boltzmann constant, and e and m have their usual meanings. ξ is positive when reckoned from potential minimum to anode, and negative from potential minimum to cathode. Langmuir's values of ξ as a function of η are given in the first three columns of the table.

Denoting values at the cathode by subscript 1 and reckoning distances and potentials from the cathode, we note that $x_1 = 0$ and $V_1 = 0$. Then

$$V = \frac{\theta}{11{,}600}(\eta - \eta_1) \qquad \text{......(3),}$$

$$(\xi - \xi_1) = 9{\cdot}180 \times 10^5 . \theta^{-\frac{3}{4}} i^{\frac{1}{2}} . x \qquad \text{......(4),}$$

numerical values having been substituted for the constants.* Further it may be shown that

$$\eta_1 = \log_e\left(\frac{i_e}{i}\right) \qquad \text{......(5),}$$

where i_e (Langmuir's i_0) is the total emission current. Equations (3), (4) and (5) together with the tables of ξ enable the voltage-distribution to be computed for given values of θ, i and i_e. Thus these latter having been selected, the value of $-\xi_1$ as a function of η_1, given by equation (5), is substituted in equation (4) and the ξ for a given x is obtained. The corresponding η substituted in equation (3) gives the required V_x.

Langmuir also gives as an approximate equation for the current

$$i = \frac{1}{9\pi}\sqrt{\frac{2e}{m}} . \frac{(V - V_m)^{\frac{3}{2}}}{(x - x_m)^2}\left(1 + 2{\cdot}66\eta^{-\frac{1}{2}}\right) \qquad \text{......(6).}$$

---

* Langmuir, using the electrostatic system for which the dielectric constant $\kappa = 1$, has omitted it from his equations.

Table. $-\xi$, $+\xi$, $\frac{d\eta}{d\xi}$ and τ as functions of η

η	$-\xi$	$+\xi$	$-\frac{d\xi}{d\eta}$	τ
0·05	0·4281	0·4657	0·2448	0·4240
0·10	0·5941	0·6693	0·3605	0·5827
0·15	0·7167	0·8296	0·4564	0·6967
0·20	0·8170	0·9674	0·5426	0·7874
0·25	0·9028	1·0909	0·6230	0·8630
0·30	0·9785	1·2042	0·6997	0·9282
0·35	1·0464	1·3098	0·7740	0·9854
0·40	1·1081	1·4092	0·8465	1·0361
0·45	1·1648	1·5035	0·9177	1·0818
0·50	1·2173	1·5936	0·9881	1·1233
0·60	1·3120	1·7636	1·1280	1·1959
0·7	1·3956	1·9224	1·2676	1·2578
0·8	1·4704	2·0725	1·4084	1·3113
0·9	1·5380	2·2154	1·5513	1·3582
1·0	1·5996	2·3522	1·6972	1·3996
1·1	1·6561	2·4839	1·8467	1·4366
1·2	1·7081	2·6110	2·0004	1·4697
1·4	1·8009	2·8539	2·3223	1·5267
1·6	1·8813	3·0842	2·6673	1·5739
1·8	1·9515	3·3040	3·0391	1·6134
2·0	2·0134	3·5151	3·4418	1·6469
2·2	2·0681	3·7187	3·8796	1·6755
2·4	2·1168	3·9158	4·3571	1·7000
2·6	2·1602	4·1071	4·8789	1·7213
2·8	2·1990	4·2934	5·4503	1·7397
3·0	2·2338	4·4750	6·0769	1·7558
3·2	2·2650	4·6524	6·7651	1·7698
3·4	2·2930	4·8261	7·5216	1·7821
3·6	2·3183	4·9963	8·3540	1·7929
3·8	2·3410	5·1634	9·2705	1·8024
4·0	2·3615	5·3274	10·2801	1·8108
4·5	2·4044	5·7259	13·2815	1·8279
5·0	2·4376	6·1098	17·1193	1·8406
5·5	2·4634	6·4811	22·0344	1·8500
6·0	2·4834	6·8416	28·3352	1·8570
6·5	2·4990	7·1924	36·4170	1·8622
7·0	2·5112	7·5345	46·7876	1·8662
7·5	2·5206	7·8690	60·0982	1·8692
8·0	2·5280	8·1963	77·1851	1·8714
9·0	2·5382	8·8323	127·289	1·8745
10·0	2·5444	9·4465	209·88	1·8762
11·0	2·5481	10·0417	346·03	1·8772
12·0	2·5504	10·6204	570·53	1·8778
13·0	2·5518	11·1845	940·65	1·8781
14·0	2·5526	11·7355	1550·9	1·8783
15·0	2·5531	12·2747	2557·0	1·8785
16·0	2·5534	12·8032	4215·7	1·8786
18·0	2·5537	13·8313	11460	—
20·0	2·5538	14·8260	31150	—
25	2·5539	17·1931	—	—
30	—	19·4253	—	—
35	—	21·5522	—	—
40	—	23·5939	—	—
45	—	25·5643	—	—
50	—	27·4740	—	—
60	—	31·141	—	—
70	—	34·642	—	—
80	—	38·007	—	—
90	—	41·258	—	—
100	—	44·412	—	—
150	—	59·086	—	—
200	—	72·479	—	—
300	—	96·877	—	—
400	—	119·185	—	—
500	—	140·068	—	—
600	—	159·885	—	—
700	—	178·861	—	—
800	—	197·146	—	—
900	—	214·850	—	—
1000	2·5539	232·054	∞	1·8786

In this equation, i, i_e, and θ are known; η_1 and hence ξ_1 are found as before, and V_m and x_m are obtained by putting $\eta=\eta_m=0$, and $\xi=\xi_m=0$ in equations (4) and (5). Then for a given value of V, and hence of η, the corresponding value of x is found from equation (6). It will be seen that although equations (3), (4) and (5) contain the complete solution for the voltage-distribution, they are somewhat inflexible in form, and it is not easy to appreciate the correspondence of different sets of numerical results.

§3. TRANSFORMATION OF THE LANGMUIR EQUATIONS

Consider a pair of plane parallel electrodes separated a distance x_a, with the anode at a potential V_a relative to the cathode, and let the cathode emit a current i_e with an average velocity of emission u_0, where

$$u_0=\left(\frac{\pi k\theta}{2m}\right)^{\frac{1}{2}},$$

or, in terms of voltage,

$$V_0=\frac{\pi}{4}.\frac{k}{e}.\theta \qquad \text{......(7).}$$

The current i, equal to i_s, which will pass between the electrodes when $V_0=0$ and $(dV/dx)_{x=0}=0$ is given by

$$(i)_{V_0=0,\ dV/dx=0\,|\,x=0}=i_s=\frac{\kappa}{9\pi}\sqrt{\frac{2e}{m}}.\frac{V_a^{\frac{3}{2}}}{x_a^2} \qquad \text{......(8).}$$

For the special case in which $V=V_a$ and $x=x_a$, equation (6) becomes

$$\frac{i}{i_s}=\frac{(1-V_m/V_a)^{\frac{3}{2}}}{(1-x_m/x_a)^2}\left\{1+3\left(\frac{V_0/V_a}{1-V_m/V_a}\right)^{\frac{1}{2}}\right\} \qquad \text{......(6a).}$$

It is interesting to note that when the cathode field is zero and $V_m=0$, $x_m=0$, then this equation coincides with one which was derived by entirely different treatment in the author's earlier paper(5) and may be put in the form

$$(i)_{dV/dx=0\,|\,x=0}=i_0=i_s\left\{1+3\left(\frac{V_0}{V_a}\right)^{\frac{1}{2}}\right\} \qquad \text{......(6b).}$$

Now since i_0 can be obtained by measurement whereas i_s can only be obtained by calculation, it is of advantage to use i/i_0 as a parameter rather than the i/i_s of the earlier paper. Equation (6b) gives i_0/i_s correct to within 1 per cent when $V_0/V_a<0{\cdot}01$, which is sufficient for all practical purposes.

Substituting V_0 and i_0 from equations (7), (8) and (6b) in equations (3) and (4) we obtain

$$\frac{V}{V_a}=\frac{4}{\pi}\frac{V_0}{V_a}(\eta-\eta_1) \qquad \text{......(3a),}$$

$$\frac{x}{x_a}=\frac{3}{\pi}\left\{\left(\frac{V_0}{V_a}\right)^{\frac{3}{4}}\left(1+3\frac{V_0}{V_a}^{\frac{1}{2}}\right)^{-\frac{1}{2}}\right\}.\left(\frac{i}{i_0}\right)^{-\frac{1}{2}}(\xi-\xi_1) \qquad \text{......(4a).}$$

Equations (3*a*) and (4*a*) together with

$$\eta_1 = \log_e \frac{i_e}{i} \qquad \text{......(5)}$$

enable the voltage-distribution V/V_a as a function of x/x_0 to be easily obtained for given values of i_e, i/i_0 and V_0.

The position and voltage of the plane of minimum potential are obtained by putting $\eta = \eta_m = 0$ and $\xi = \xi_m = 0$. Thus

$$\frac{V_m}{V_a} = -\frac{4}{\pi} \cdot \frac{V_0}{V_a} \cdot \eta_1 \qquad \text{......(3}b\text{),}$$

$$\frac{x_m}{x_a} = -\frac{3}{\pi} \left\{ \left(\frac{V_0}{V_a}\right)^{\frac{3}{4}} \cdot \left(1 + 3\,\frac{V_0^{\frac{1}{2}}}{V_a}\right)^{-\frac{1}{2}} \right\} \left(\frac{i}{i_0}\right)^{-\frac{1}{2}} \xi_1 \qquad \text{......(4}b\text{).}$$

Taking into account the results of the next section, an examination of equations (3*b*) and (4*b*) shows that whereas the voltage of the potential minimum continues to increase logarithmically with increase of emission current, its distance from the cathode tends towards a maximum value dependent on V_0/V_a; and this will not exceed a limiting value given by

$$\left(\frac{x_m}{x_a}\right)_{\text{max.}} \ngtr 2{\cdot}5 \left(\frac{V_0}{V_a}\right)^{\frac{3}{4}} \left(1 + 3\,\frac{V_0^{\frac{1}{2}}}{V_a}\right)^{-\frac{1}{2}} {}^* \qquad \text{......(4}c\text{).}$$

§4. RELATION BETWEEN i/i_0 AND $\log i_e/i$

For a given electrode system i/i_0 depends only on V_0/V_a and i_e/i, and it is possible to obtain a family of curves showing i/i_0 as a function of η_1, equal to $\log_e (i_e/i)$, with V_0/V_a as a parameter, one of the variables being thus eliminated from the equations.

If we put $x = x_a$ and $V = V_a$ in equations (3*a*) and (4*a*) and denote the corresponding values of η and ξ by the subscript *a*, we obtain

$$\eta_a = \frac{\pi}{4\,(V_0/V_a)} + \eta_1 \qquad \text{......(9)}$$

and

$$\sqrt{\frac{i}{i_0}} = \frac{3}{\pi} \left\{ \left(\frac{V_0}{V_a}\right)^{\frac{3}{4}} \left(1 + 3\sqrt{\frac{V_0}{V_a}}\right)^{-\frac{1}{2}} \right\} (\xi_a - \xi_1) \qquad \text{......(10).}$$

These equations enable i/i_0 to be calculated for any value of η_1 and for values of V_0/V_a less than 0·01. Curves for i/i_0 as a function of η_1 for constant values of V_0/V_a are shown in figure 2. By means of these curves we can now determine for given values of i_0 and V_0/V_a the total emission i_e required to give any anode current i, or vice versa; and it should be possible to devise a method, based on these curves, of

---

* This corresponds to the equation of Langmuir and Compton$^{(15)}$, equation (313), which, however, owing to an arithmetical slip makes x_m only one-tenth of its correct value. Their equation should read

$$x_m < 0{\cdot}016\,(1000I)^{-\frac{1}{2}} \left(\frac{T}{1000}\right)^{\frac{3}{4}} \text{cm.}$$

checking the total emission of a valve under normal working conditions without subjecting it to excessive anode voltages.

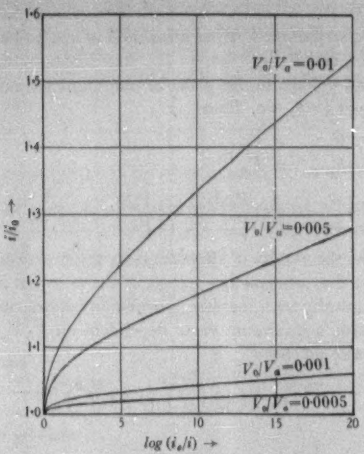

Figure 2. Variation of interelectrode current with emission current.

§ 5. VARIATION OF CATHODE FIELD

The variation of cathode field with current when $i/i_0 < 1$ was given in the earlier paper$^{(5)}$ by an equation of the form

$$\left(\frac{dV}{dx}\right)_{x=0} = \frac{4}{3}\cdot\left(\frac{V_a}{x_a}\right).K,$$

values of K as a function of i/i_0 and V_0/V_a being tabulated.

For the sake of continuity, therefore, an equation of the same form is now derived for the case in which $i/i_0 > 1$. Differentiating equations (3 *a*) and (4 *a*), we obtain

$$\frac{\delta V}{V_a} = \frac{4}{\pi}\frac{V_0}{V_a}\,\delta\eta$$

and
$$\frac{\delta x}{x_a} = \frac{3}{\pi}\left\{\left(\frac{V_0}{V_a}\right)^{\frac{1}{2}}\left(1+3\,\frac{V_0^{\frac{1}{2}}}{V_a}\right)^{-\frac{1}{2}}\right\}\left(\frac{i}{i_0}\right)^{-\frac{1}{2}}\delta\xi,$$

whence
$$\frac{\delta V}{\delta x} = \frac{4}{3}\,\frac{V_a}{x_a}\cdot\left\{\left(\frac{V_0}{V_a}\right)^{\frac{1}{2}}\left(1+3\,\frac{V_0^{\frac{1}{2}}}{V_a}\right)^{\frac{1}{2}}\right\}\left(\frac{i}{i_0}\right)^{\frac{1}{2}}\frac{\delta\eta}{\delta\xi}.$$

Then
$$\left(\frac{dV}{dx}\right)_{x=0} = \frac{4}{3}\,\frac{V_a}{x_a}.K \qquad \text{......(11)},$$

where
$$K = \left[\left\{\left(\frac{V_0}{V_a}\right)^{\frac{1}{2}}\left(1+3\,\frac{V_0^{\frac{1}{2}}}{V_a}\right)^{\frac{1}{2}}\right\}\left(\frac{i}{i_0}\right)^{\frac{1}{2}}\cdot\frac{d\eta}{d\xi}\right]_{\eta_1\xi_1} \qquad \text{......(11 a)}.$$

Values of $d\eta/d\xi$ as a function of η_1 for the region between cathode and potential minimum have been calculated from Langmuir's results,* and are given in column 4 of the table. Since i/i_0 is a function only of V_0/V_a and η_1, K is also a function only of V_0/V_a and of η_1 or i/i_0. In figure 3, therefore, the variation of K with i/i_0 for various values of V_0/V_a is shown in the neighbourhood $i/i_0=1$. The results for cases in which $i/i_0<1$ have been taken from the earlier paper.

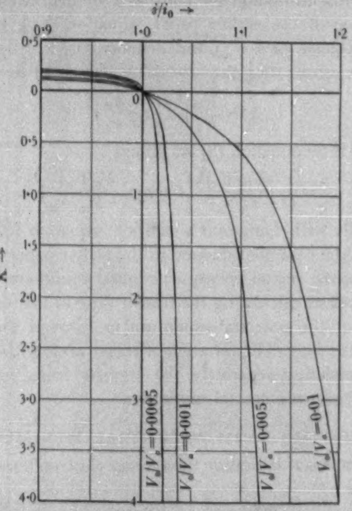

Figure 3. Variation of cathode field with current.

It will be seen that a negative value of cathode field, exceeding the maximum positive field for negligible current, can easily be obtained. Of course in practice i_e/i, and hence i/i_0, is controlled by cathode-temperature, and variation of i/i_0 will therefore be accompanied by some variation of V_0/V_a.

§ 6. THE ELECTRON TRANSIT TIME

When electrons having a Maxwell distribution of velocities move through a retarding field the slower-moving electrons are continually being brought to rest and having their velocity reversed. It can be shown$^{(11)}$, however, that the forward-moving electrons still retain a Maxwell distribution, and it is then easy to prove that the average kinetic energy, and hence the average velocity, of the forward-moving

* Langmuir quotes
$$\frac{d\eta}{d\xi}=\left[e^{\eta}\left(1+P\sqrt{\eta}\right)-\left(1+\frac{2}{\sqrt{\pi}}\sqrt{\eta}\right)\right]^{\frac{1}{2}},$$
where
$$P(\sqrt{\eta})=\operatorname{erf}\sqrt{\eta}=\frac{2}{\pi}\int_0^{\sqrt{\eta}}e^{-\eta}\,\delta\eta.$$

electrons remains constant. This is due to the fact that although the retarding field continually reduces the velocity of all the electrons, the slower-moving ones are being continually filtered out. Thus the average velocity of electrons leaving the potential minimum for the anode is the same as the average velocity V_0 at the cathode, and since the field at the potential minimum is zero, the voltage-distribution up to the anode should correspond with that for a normal saturated diode. Regarding the potential-minimum therefore as a virtual cathode, we can apply the approximate equation of the earlier paper, equation (6*b*), to the virtual diode, provided that the voltage $(V-V_m)$ and distance $(x-x_m)$ be reckoned from the virtual cathode. On substituting the new value of i_s equal to

$$\left(1-\frac{V_m}{V_a}\right)^{\frac{3}{2}}\Big/\left(1-\frac{x_m}{x_a}\right)^2$$

of its value as defined by equation (8) we obtain

$$\frac{i}{i_s}=\frac{(1-V_m/V_a)^{\frac{3}{2}}}{(1-x_m/x_a)^2}\left\{1+3\left(\frac{V_0/V_a}{1-V_m/V_a}\right)^{\frac{1}{2}}\right\},$$

corresponding exactly with Langmuir's solution, equation (6*a*). We are therefore justified in applying the equations derived in the earlier paper for the case of space-charge saturation, to the region between potential minimum and anode; and this course will be adapted in calculating the transit time in this region.

The formation of the potential-minimum in front of the cathode causes an increase in total transit time. The variation of transit time with operating conditions is obtained by considering separately the transits from potential-minimum to anode and from cathode to potential-minimum.

§6·1. TRANSIT TIME FROM POTENTIAL-MINIMUM TO ANODE

It has been shown that at saturation the average electron transit time from cathode to anode is given by

$$T=3\sqrt{\frac{m}{2e}}\cdot\frac{x_a}{V_a^{\frac{1}{2}}}\left\{\frac{1}{(1+V_0/V_a)^{\frac{1}{2}}+2\,(V_0/V_a)^{\frac{1}{2}}}\right\} \qquad \text{......(12).}$$

Equation (12) gives the transit time of an average electron, i.e. one emitted with a velocity of V_0 volts. This differs from the effective average transit time by an amount which is usually negligible in practical examples.

When $i/i_0>1$, a potential-minimum is formed in front of the cathode and, as has been shown above, we may regard the potential-minimum as a virtual cathode emitting electrons with an average velocity V_0 equal to the average velocity at the true cathode. Furthermore we may assume the voltage-distribution between the virtual cathode and anode to correspond to that for a normal saturated diode. Thus equation (12) can be made to give the transit time T_a from potential-minimum to anode merely by changing the origin, and

$$\frac{T_a}{T'}=\frac{3}{2}\left\{\frac{(1-x_m/x_a)}{(1-V_m/V_a+V_0/V_a)^{\frac{1}{2}}+2\,(V_0/V_a)^{\frac{1}{2}}}\right\} \qquad \text{......(13),}$$

where

$$T'=2\sqrt{\frac{m}{2e}}\cdot\frac{x_a}{V_a^{\frac{1}{2}}} \qquad \text{......(13a),}$$

T' has been substituted for convenience and may be regarded as a parameter independent of the conditions of emission. With the help of figure 2, x_m and V_m can be calculated from equations (3*b*) and (4*b*), and equation (13) will then give T_a/T' as a function of i/i_0, or of $\log_e (i_e/i)$, with V_0/V_a as a parameter.

For small values of V_0/V_a and η_1, a convenient approximate formula can be derived. Thus substitution for x_m and V_m from equations (3*b*) and (4*b*) leads after some manipulation to

$$\frac{T_a}{T'}=\frac{3}{2}\left\{\frac{1-\frac{2}{\pi}\cdot\frac{V_0/V_a}{1+2(V_0/V_a)^{\frac{1}{2}}}\eta_1+\frac{3}{\pi}(V_0/V_a)^{\frac{3}{4}}\{1+3(V_0/V_a)^{\frac{1}{2}}\}^{-\frac{1}{2}}(i/i_0)^{-\frac{1}{2}}\xi_1}{(1+V_0/V_a)^{\frac{3}{2}}+2(V_0/V_a)^{\frac{3}{2}}}\right\}, \qquad \text{......(13}b\text{)}$$

when $V_0/V_a < 0{\cdot}01$ and $\eta_1 < 5$, equation (13*b*) is in error by less than 0·5 per cent.

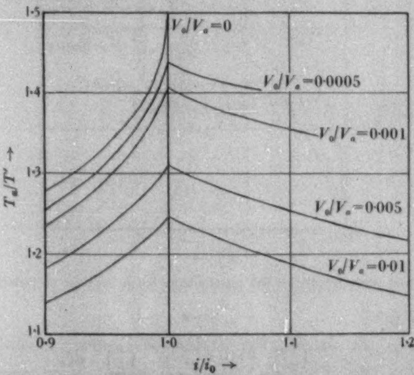

Figure 4. Variation of transit time from potential-minimum to anode.

In figure 4 are shown curves of T_a/T' as a function of i/i_0, for constant values of V_0/V_a; the values for cases in which $i/i_0 < 1$ are from the earlier paper(5). The decrease of T_a/T' with i/i_0 is due partly to the movement away from the cathode of the potential-minimum, and partly to the increase of $-V_m$ causing an increase in the anode voltage relative to the potential-minimum.

§6·2. TRANSIT TIME FROM CATHODE TO POTENTIAL-MINIMUM OF ELECTRONS DESTINED TO REACH THE ANODE

The average transit time T_m from cathode to potential-minimum is here assumed to be the transit time of an average electron, i.e. of an electron which reaches the potential-minimum with a velocity of V_0 volts and which will have left the cathode, therefore, with a velocity of (V_0+V_m) volts. Since we are concerned only with those electrons which actually reach the potential-minimum and hence the anode, this assumption is reasonably correct; although it must be used with reserve if alternating potentials also are present.

If for convenience we consider the potential-minimum as origin, an electron at a point x where the potential is V relative to the new origin will have a velocity u given by

$$\tfrac{1}{2}mu^2 = V_0 e + Ve,$$

but
$$T_m = \int_{0,\,u_0}^{x_m,\,u_m} \frac{dx}{u} = \int_{0,\,0}^{x_m,\,V_m} \sqrt{\frac{m}{2e}}\,.(V+V_0)^{-\frac{1}{2}}\,dx.$$

Now again introducing the parameter T', we find that

$$\frac{T_m}{T'} = \frac{1}{2}\left(\frac{V_a}{V_0}\right)^{\frac{1}{2}} \int_{0,\,0}^{x_m,\,V_m} \frac{dx/x_a}{(1+V/V_0)^{\frac{1}{2}}},$$

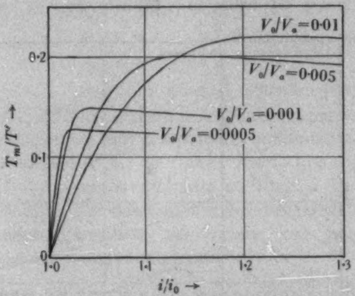

Figure 5. Variation with current of the transit time from cathode to potential-minimum.

but from equation (4*a*)

$$\frac{dx}{x_a} = \frac{3}{\pi}\left\{\left(\frac{V_0}{V_a}\right)^{\frac{3}{4}}\left(1+3\,\frac{V_0^{\frac{1}{2}}}{V_a}\right)^{-\frac{1}{2}}\right\}\left(\frac{i}{i_0}\right)^{-\frac{1}{2}} d\xi,$$

and from equation (3*a*)
$$\frac{V}{V_0} = \frac{4}{\pi}\eta_1,$$

since we are here taking the potential minimum as origin. Finally therefore

$$\frac{T_m}{T'} = \frac{3}{2\pi}\left\{\left(\frac{V_0}{V_a}\right)^{\frac{1}{4}}\left(1+3\,\frac{V_0^{\frac{1}{2}}}{V_a}\right)^{-\frac{1}{2}}\right\}\left(\frac{i}{i_0}\right)^{-\frac{1}{2}} \tau \qquad \text{......(14)},$$

where
$$\tau = f(\eta_1) = \int_{0,\,0}^{\eta_1,\,\xi_1} \frac{d\xi_1}{(4\eta_1/\pi+1)^{\frac{1}{2}}} \qquad \text{......(14a)}.$$

The function τ has been calculated for various values of η_1, and the results are given in column 5 of the table. Equations (14) and (14*a*) therefore give the variation of T_m/T' with i/i_0, or i_s/i, for any value of V_0/V_a. Curves relating T_m/T' with i/i_0 for various values of V_0/V_a are shown in figure 5. It will be seen that for a given value of V_0/V_a, T_m/T' reaches a maximum and then very slowly decreases. This maximum is determined almost entirely by the movement of the potential-minimum. From equation (14) and the tables of τ, an expression for the limiting value of T_m/T' can be obtained. Thus

$$\frac{T_m}{T'} \ngtr 0{\cdot}90 \left(\frac{V_0}{V_a}\right)^{\frac{1}{4}} \left(1+3\,\frac{V_0^{\frac{1}{2}}}{V_a}\right)^{-\frac{1}{4}} {}^{*} \qquad \text{......(14}b\text{).}$$

It is at first surprising that the increase of $-V_m$ with i_e/i, and hence with i/i_0, does not cause a more rapid decrease in T_m/T'. That it does not is due to the fact that for large values of i_e/i the greater part of the potential-drop is concentrated very close to the cathode; for the remainder of the region up to the potential-minimum the field is small and is practically unaffected by the increase of i_e/i. The transit time is therefore mainly affected by the slowly moving electrons in the region of the potential-minimum, where the velocity is not greatly different from V_0. It is due to the neglect of this fact that most earlier approximations for T_m have been too small.

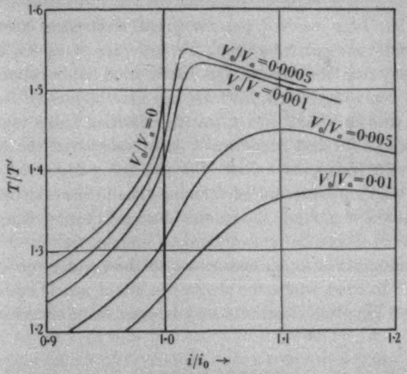

Figure 6. Variation of cathode-anode transit time with current.

The increase of T_m/T' with V_0/V_a is perhaps unexpected, since the average of the electron-velocity will increase with V_0/V_a; it is due to the fact that the position of the potential-minimum also varies with V_0/V_a, and its distance from the cathode increases more rapidly than the velocity.

In figure 6 the results of the last two sections have been combined with those of the earlier paper to show the complete variation of cathode-anode transit time in the planar diode with variation of anode current. It will be seen that the curves for which $i/i_0 < 1$ join smoothly with those for which $i/i_0 > 1$, and this may be regarded

---

* D. O. North(4) gives an expression, equation (14)

$$\frac{\tau_m}{\tau} = \frac{0{\cdot}0016}{x_0}\left(\frac{5V_0}{\log_{10}(I_s/I)}\right)^{\frac{1}{2}}\left(\frac{T}{1000}\right)^{\frac{1}{4}}(1000I)^{-\frac{1}{2}}.$$

This is in error, since it is based on Langmuir and Compton's(15) equation (313). Thus North's inequality of $\tau_m/\tau \ngtr 0{\cdot}04$ for a typical case should be $\tau_m/\tau \ngtr 0{\cdot}4$.

as evidence that the various simplifying assumptions made in each case are applicable within their correct limits to a degree of accuracy sufficient for most purposes.

§7. CONCLUSION

The voltage-distribution, the anode current, the cathode field, and the transit time in a space-charge-limited diode have been derived from the original equations of Langmuir by the use of his tables of ξ. The results have been given in the form of curves having, with the exception of those in figure 2, i/i_0 as the independent variable. Under certain circumstances, however, it might be preferable to use i_s/i_0. In the condition of temperature limitation $i_s/i_0 = i/i_0$; for space-charge limitation, since $i_s/i_0 = (i_s/i)(i/i_0)$, the results can easily be adapted with the help of the curves of figure 2.

The theory has been worked out for plane electrodes, whereas in practice cylindrical electrodes are normally used. For the case of $i/i_0 = 1$, Langmuir(12) has given an exact solution for the voltage-distribution with cylindrical electrodes, initial velocities being neglected; and he has also suggested(8) an approximate solution for the case in which $i/i_0 > 1$, initial velocities being taken into account. Benham(1), Fortescue(13), and McPetrie(14) have calculated the transit time with cylindrical electrodes for $i/i_0 = 1$, initial velocities being neglected. The problem of cylindrical electrodes and finite initial velocities has hitherto defied exact solution. It is however reasonable to apply the results obtained here, qualitatively at least, to those conditions. It should be remembered, of course, that for a thin cathode the effect of initial velocities is much less owing to the greater concentration of field near the cathode. In cases where the electrodes are of nearly equal radii, the conclusions developed for plane electrodes may be used with confidence.

REFERENCES

(1) Benham, W. E. *Phil. Mag.* **9**, 457 (1931).
(2) Johannes Muller. *Hochfrequenztech. u. Elektroakust.* **41**, 156 (1933).
(3) Llewellyn, F. B. *Bell. Syst. Tech. J.* **14**, 632 (1935).
(4) North, D. O. *Proc. Inst. Radio. Engrs, N.Y.*, **24**, 108 (1936).
(5) Cockburn, R. *Proc. Phys. Soc.* **47**, 810 (1935).
(6) Cockburn, R. *Proc. Phys. Soc.* **49**, 38 (1937).
(7) Schottky, W. *Z. Phys.* **15**, 872 (1935).
(8) Langmuir, I. *Phys. Rev.* **21**, 419 (1923).
(9) Epstein. *Ber. dtsch. Phys. Ges.* **21**, 85 (1919).
Fry. *Phys. Rev.* **17**, 441 (1921).
(10) Benham, W. E. *Proc. Phys. Soc.* **47**, 1 (1935).
(11) Thomson, J. J. *Conduction of Electricity through Gases*, p. 363 (1928 ed.).
(12) Langmuir, I. *Phys. Rev.* **2**, 450 (1913).
Langmuir, I. and Blodgett, K. *Phys. Rev.* **22**, 347 (1923).
(13) Fortescue, C. L. *Wireless Engr*, **12**, 310 (1935).
(14) McPetrie, J. S. *Phil. Mag.* **16**, 284 (1933).
(15) Langmuir, I. and Compton, K. T. *Rev. Mod. Phys.* Part II, **3**, 244 (1931).

THE RATE OF VISCOUS FLOW OF METALS: PART 1, TIN

By L. C. TYTE, B.Sc., Ph.D., F.Inst.P., Ballistics Directorate, Research Department, Woolwich

DISCUSSION

Dr **Bruce Chalmers**. Has the author given attention to the question of the purity of the material used, which is usually rather important? Further, tin is a metal in which the crystals readily grow to a large size, and may well be large enough to occupy the whole cross section of the wires used. Etching with ferric chloride solution serves to reveal the size and distribution of the crystals, and I should regard consideration of this point, as well as of the orientations of the crystals, as essential in work of this kind.

The conclusions drawn from figure 6 do not seem to be justified by the apparent accuracy of the points; the curve for 129°, for example, if examined on its own merits, would hardly be regarded as consisting of two straight lines.

I cannot agree with the contention regarding the 19° curves being affected by the $\alpha-\beta$ change, for the change takes place very slowly and is quite obvious. The photographs in figures 12*a* and 12*b* only show that in the latter the fracture took place where there was only one crystal in the cross section; they do not provide any evidence for the suggested $\beta-\gamma$ transition, but might perhaps tell us something about the conditions of strain and temperature necessary for re-crystallization into a single crystal. The same observation applies to the conclusions drawn from figure 15.

The discussion of the incidence of single and double glide appears to be invalidated by the absence of information as to the number and orientations of the crystals present; the effect of crystal boundaries on the stresses required to cause glide has been investigated by various workers, and should be taken into account in any theory based upon the results.

The careful and ingenious work described in this paper would be of greater value if it had been carried out under better defined conditions, and I think that a study of papers by Andrade, by Hanson and his collaborators, and by myself, appearing in the *Proceedings of the Royal Society* and the *Journal of the Institute of Metals* during the last few years, might be of interest to Dr Tyte when he is planning future work.

Author's reply. The problem of distortion of metals has become of increasing interest in recent years, receiving particular impetus by the pioneer work of Carpenter, Taylor and Elam on the production and distortion of metal single crystals. Andrade and his school have done much interesting and valuable work along these lines, adding to our knowledge of the behaviour of single crystals and composite specimens of a few large crystals. However, the older method of attack, viz. that of investigating the properties of polycrystalline specimens, still remains of value. Dr Bruce Chalmer's criticisms appear to be mainly complaints that the methods rightly adopted for the former type of experiment were not applied to the latter.

The experiments described in this paper were carried out in 1928 as part of an investigation of the variation with load and temperature of the velocity of flow of polycrystalline material in the form of wire. As far as I am aware, this investigation is the only one so far carried out on these lines, and the general character of the flow phenomena was naturally the prime object of the research. To this end, the material would appear to be adequately specified by its density and its preliminary treatment, which ensured strictly comparable specimens from experiment to experiment.

Now recrystallization from a few isolated growth centres, resulting in large crystals with orientations different from specimen to specimen, would naturally lead to very irregular behaviour The best reply to Dr Chalmer's suggestion that this growth of large crystals took place in the specimens is offered by the marked regularity of the experimental results, not excepting the experiment at 129° C. Neither this, nor any other experiment, is expected to stand alone as conclusive evidence that the $\{\log_e v, p\}$ curves consist of two straight lines, but the cumulative evidence of the whole series makes this conclusion difficult to avoid.

The $\beta-\gamma$ transition has been fairly widely reported in the literature; if Dr Chalmers is prepared to doubt its occurrence, any remark seems idle.

The specimens being polycrystalline in nature and the elementary grains distributed in a random manner, a discussion of behaviour on general grounds, found on this hypothesis, is perfectly justifiable and the agreement between the calculated and experimental ratios of the constants is unlikely to be fortuitous, confirmation on this point being offered by experiments on lead.

Finally, it may be stated that, although the phenomena have a personal character, as it were, in minor details for each metal investigated, the main conclusions drawn from the experiments on tin have been substantiated by experiments on lead and zinc. Accounts of this further work are shortly to be published.

THE MEASUREMENT IN ABSOLUTE UNITS OF THE INTENSITIES OF X-RAY REFLECTIONS FROM CRYSTALLINE POWDERS

By G. W. BRINDLEY, M.Sc., Ph.D., Mackinnon Student of the Royal Society, Physics Laboratories, University of Leeds

AND

F. W. SPIERS, Ph.D., Physicist, Radium Department, General Infirmary, Leeds

DISCUSSION

The remarks by Dr J. C. M. Brentano printed on page 107 of the present volume relate to the above paper and should have appeared on page 29.

REVIEWS OF BOOKS

A Text Book of Physics, by D. B. Deodhar. Pp. iv + 672. (Allahabad: The Indian Press Ltd., 1937.) Rs. 6.

This is a courageous attempt to include between one pair of covers all the physics which an intermediate student requires, whether classical or modern. In the main it follows familiar lines, and it is divided into five water-tight parts each dealing with one of the branches into which physics is traditionally classified. In each section there has clearly been a definite effort to bring the subject up-to-date, and this is most conspicuously successful in the section on electricity.

The section on sound reads as though the author has himself confused the meaning of temperament with that of scale. Even after we have decided to adopt a pentatonic or diatonic or chromatic scale, or even Bosanquet's 53-tone scale, we have to decide on the exact intonation of each of the tones, and this is what decides the temperament. It is also to be regretted that in such an excellent book, with its real attempt to modernize teaching, there is no attempt to discuss architectural acoustics, a subject which would appear to lend itself rather well to qualitative explanation.

As has been stated above, the section on electricity is quite masterly, and manages to find space for wattmeters, generators, triodes and even the positron and neutron. It is to be hoped that the book will have the success which it deserves.

J. H. A.

Scientific Inference, by Harold Jeffreys, M.A., D.Sc., F.R.S. Reissue with additions. Pp. vii + 272. (Cambridge: at the University Press, 1937.) 10*s*. 6*d*. net.

The additions are not likely to change anyone's opinion of this well-known book. They consist partly of a restatement of the author's main doctrine in the light of criticism directed against it, partly of minor amendments and corrections. But since there may still be some who have not read the book and yet would be interested by it, some brief description of its contents may be desirable.

Jeffreys's fundamental postulate is that knowledge derived from experience can be expressed in propositions each bearing a definite relation (its probability) to the data on which it is based, and that any such probability is either greater than, less than, or equal to any other. On this postulate he bases a logic of that part of physics which consists of numerical laws and mathematical theories and from it he derives rules by which the relative values of such propositions can be ascertained.

Many people believe that Jeffreys has solved completely the fundamental problem of scientific epistemology and that his work is truly epoch making. But that opinion is not universal. Some critics maintain that Jeffreys's conclusions are not logically sound and that his postulate will not bear the weight of the structure he builds on it; most of them have rival logics of their own, based on slightly different definitions of probability. The controversy is not, and probably will never, be ended; my personal opinion is that Jeffreys has the better of the argument, especially in counter-attack. Others simply disbelieve Jeffreys's postulate and all others at all similar to it. Their difference both from Jeffreys and from his critics is so profound that it is impossible to start an argument; Jeffreys naturally ignores them almost completely. But all, whether believers or critics, would agree on the profundity of Jeffreys's thought and on the brilliance of his exposition.

N. R. C.

Introduction to Physiological Optics, by J. P. C. Southall. Pp. x+426. (Oxford: University Press.) 21*s*. net.

This is in many ways a good book. It is attractively produced, and written in a style that is easy to read. Its scope is comprehensive for it includes some very useful chapters on refractive errors and their correction, in addition to discussions of binocular vision, rod-and-cone vision, colour vision and so on. It may certainly be regarded as a valuable reference book, so far as the earlier work on the subject is concerned, but perhaps the contents can be most readily appreciated from the fact that, as the author explains, "the material of the volume has been compiled from a course of lectures given in Columbia University over a long period of years". Possibly because the course had its origins so long ago the book gives the impression, in parts, of being old-fashioned.

Physiological optics is a subject that is very much alive at the present time. There are several important lines of work being developed in various laboratories in the United States and in Europe, lines that show every promise of converging to a point from which we may hope at last to see the whole complicated jigsaw pattern of visual phenomena fitting together to make one complete picture. We might reasonably expect to see some of this activity reflected in the book, but while we are given descriptions of many phenomena, references to recent work are extremely scanty. Nothing is said of the directional sensitivity of the retina observed by Stiles and Crawford, no reference is made to Lythgoe's work on visual acuity, there is no mention of the colour-blindness investigations of Pitt or of Trendelenburg and Schmidt, nothing of the measurements of retinal potentials or of nerve impulses by workers such as Granit, Graham or Hartline, and no reference to adaptation phenomena observed by the binocular method. In some ways perhaps the most surprising omission is that, in a section on colorimetry which includes references to the trichromatic system, colour triangles, transformation of colour co-ordinates from one system to another and so on, no indication is given of the existence of an internationally standardized system of colour specification approved some six years ago by the Commission Internationale de l'Éclairage. From the historical point of view the book is good, but as an up-to-date account of the subject it is far from complete.

W. D. W.

Textbook of Thermodynamics, by Paul S. Epstein. Pp. xii+406. (Chapman and Hall, Ltd.) 17*s*. 6*d*. net.

The authority of Epstein in the field of which this book treats is unquestioned, and the duty of the reviewer is merely to indicate the readers for whom it is intended, and perhaps to point out the features in which it differs from previous books on thermodynamics. As regards the first point, the author himself says that one half is intended for seniors and younger graduate students, whilst the other half is more advanced and could serve as a reference book. Turning then to the scope of the work, we find some new historical matter on the first law, and the usual insistence on the perfect gas. As regards real gases, the author considers that the warnings against the truth of the equation of Van der Waals have been overdone, and that a good word can now be said about it, in order to redress the balance. One other point of interest in his treatment of the fundamentals calls for remark: he postulates, and does not pretend to deduce, the principle of the decrease of internal energy, an attitude which is more honest or less confused than that of most writers on the subject. After the fundamentals have been established, the book deals in turn with applications to solutions and binary systems as well as to surface tension before dealing with Nernst's theorem, which is not entirely divorced from the quantum theory or from statistical mechanics. The degenerate gas is considered and forms an introduction to electronic problems, thence leading to specific heats, thermal radiation and electromagnetic phenomena. The book concludes with two critical chapters, of which the second is particularly valuable.

J. H. A.

Sound Waves, Their Shape and Speed, by DAYTON CLARENCE MILLER. Pp. xii + 164. (The Macmillan Co.) 12*s*. net.

Prof. Miller's phonodeik is well known to students of acoustics. In this comparatively small book, Prof. Miller describes, amongst other experimental work, various uses which have been devised for the phonodeik. That the author has attempted delicate acoustical investigations with a purely mechanical apparatus, consisting, as is well known, of a diaphragm with a mirror attached, shows not only great experimental ingenuity but also considerable courage. Most of us nowadays would demand a microphone, complicated amplifiers and expensive oscillographs for such work. The author's mechanical interests are still further shown in various digressions. The book should be read chiefly because of its historical interest, and also as a record of much patient investigation.

The book includes some hitherto unpublished work on the sound pressures in the neighbourhood of guns, another ingenious instrument, the baroscope, having been invented for this purpose. These experiments were made to determine whether the pressures in the explosion wave were responsible for shell shock. The interesting conclusion is reached that the air pressure acts upon the body much as a squeeze of the hand acts upon the bulb of a scent spray, the hydrostatic pressure in the skull being considerably increased thereby. This conclusion is in agreement with the observation that, in order to produce shock, the pressure pulse besides being of sufficient magnitude must also be of sufficiently long duration.

The book concludes with an account of measurements made to determine the variation of velocity of sound with its intensity, gunfire being used as a source of sound. It is shown that near a gun the velocity of sound can be as high as 2500 ft./sec., but that a few hundred feet away from the gun the velocity has fallen to its normal value.

The book contains a number of interesting photographs. J. E. R. C.

Introduction to Ferromagnetism, by FRANCIS BITTER. Pp. xii + 314. (International Series in Physics. McGraw-Hill Publishing Co., Ltd. London.) 24*s*.

In recent years our knowledge of ferromagnetism has advanced rapidly in several widely divergent directions. New ferromagnetic alloys have been produced with properties that are, from the industrial point of view, greatly superior to those of any of their predecessors, while theories of ferromagnetism have advanced to the stage at which Prof. Bitter can say that "ferromagnetism as such is no longer fundamentally a mystery". Nevertheless the new materials have been discovered almost entirely by purely empirical methods, and we are still far from being able to account for the great range of properties obtainable with modern alloys, although studies of crystal structure and polycrystalline materials have led to important advances in this direction. Prof. Bitter takes the view that the important task for the immediate future is to "build a theory of alloys that will account for their properties about as well as the simple Weiss theory accounts for the magnetic properties of iron", and his book provides a broad survey of the present position of ferromagnetism from this point of view. It therefore includes an account of the theories of Weiss, Heisenberg, and Ising; a treatment of polycrystalline fields; discussions of the relations between magnetization and mechanical deformation, thermal, and electrical phenomena respectively; and a survey of co-operative phenomena (the formation of secondary structures and superlattices) contributed by F. Zwicky. On the purely practical side, there is a long and valuable chapter by T. D. Yensen on the methods of preparation, purification and analysis, which have been found specially valuable for the production of materials of very high permeability, together with a survey of modern industrial materials including alloys of high permeability and magnet steels. There is also an account by W. C. Elmore of the powder technique for the investigation of the magnetic structure of the surfaces of magnetized materials, which is of great interest in connexion with the secondary structures associated with Zwicky's co-operative phenomena. It will be clear that the book puts the reader in touch with all the most progressive branches of the subject, and it has the merit of doing this without overburdening him with unnecessary detail, either theoretical or practical. The treatment is always such as to emphasize the physical basis of the mathematical theories and the points at which pure assumptions are made, while facts which are as yet unexplained are also clearly indicated. The book should prove of great value to many workers in the field between physics and metallurgy, in showing the connexion between their various activities. By revealing to new workers the possibilities of ferromagnetism as a tool for the investigation of the physical condition of alloys, i.e. internal strains and grain structure, it should form a definite contribution towards the study of the theory of metals.

L. H.

Low-Temperature Physics, by M. and B. RUHEMANN of the Physico-Technical Institute, Kharkhov. Pp. x+313. (Cambridge University Press.) 18*s*. net.

Sixty years ago Cailletet liquefied oxygen. At the time this event marked the successful culmination of half a century's unremitting effort to liquefy one of the so-called permanent gases. Faraday had pointed the way in 1823 when he liquefied chlorine, but the path was a stony one which had daunted the spirit of many an investigator. To-day we know that Cailletet's experiment has a greater significance, for it ushered in a new era of low-temperature research, and the volume under review surveys this fascinating field.

The book bears the address of Kharkhov, U.S.S.R. and it is interesting to note that a low-temperature laboratory there is equipped with hydrogen and helium liquefiers.

In their treatment the authors have followed the line of gradual penetration from such macroscopic phenomena as condensation and fusion to processes intimately connected with our concepts of elementary particles, such as give rise to magnetic moment and electrical conductivity. They have given particular attention to fields that have not yet been dealt with in a connected form, such as the subject of crystal structure stable at low temperatures. Considerable stress is laid on the principles of gas-liquefaction and rectification, and this is especially valuable as most of the work in this domain is not to be found within the scope of general physical literature.

The volume is divided into four parts. Part 1 deals with phase equilibrium, covering the topics of gas-liquefaction, the measurement of low temperatures, rectification, and solid-liquid equilibrium. Part 2 is devoted to the solid state and treats of the crystal lattice, the thermal energy of crystals, and Nernst's third law. Part 3 bears the title of orbit and spin. Here are discussed internal degrees of freedom, paramagnetism and magnetic cooling. In part 4 we have the free electron. This covers conductivity at low temperatures and supraconductivity.

Between December, 1935, when the book was written, and May, 1937, when the proofs were corrected, so many new facts came to light and so many papers were published that the authors have found it necessary to add five pages of references to the literature of this period. The book is very clearly written and the authors have rendered a valuable service to all interested in low-temperature physics by collecting and co-ordinating a vast amount of information. The volume will undoubtedly find a place in the library of every department of physics in our colleges as a valuable work of reference.

E. G.

Handbook of British Refrigeration Material 1938. Pp. 177. (The Cold Storage and Produce Review, Empire House, St Martin's le Grand, London.) 5*s.*

The object of the volume under review is to present the range of refrigeration materials that British manufacturers can supply. Although essentially a trade reference guide for the refrigeration industry, it should prove of considerable value to industrial physicists dealing with problems of thermal insulation, instrumental equipment and small refrigeration plants. The book includes a technical section in which the data required in refrigeration work are set out in tabular form. The appearance of this volume is a commendable sign of British enterprise in this field.

E. G.

Alternating Current Electrical Engineering, by PHILIP KEMP. Pp. x + 611. (London: Macmillan and Co.) 15*s.*, 5th edition.

The appearance of a fifth edition of Mr Kemp's text-book on alternating-current engineering is sufficient evidence of its value to a wide circle of readers. Its success is due not so much to novelty of treatment as to the very clear way in which the essentials of the subject are presented, and to a wise selection of the material which has made the book representative of modern practice and has prevented the principles from being buried in a mass of descriptive detail and obsolete material. The 421 illustrations all consist of line drawings showing clearly the principles under discussion. No space is wasted on mere photographs showing external appearances only.

While the book is addressed mainly to students of electrical engineering, it can also be recommended to the many physicists who find it necessary to deal with such things as polyphase power supplies, synchronous and induction motors, transformers, rectifiers, and frequency-changers. At 15*s.* it is very good value.

L. H.

Frontiers of Science, by C. T. CHASE. Pp. xv + 340. (London: The English Universities Press, Ltd.) 12*s.* 6*d.* net.

This is a well-written book dealing with the most recent advances in astronomy, atomic physics, biochemistry and biophysics; some mention is also made of advances in chemistry and medicine. The Astronomer Royal remarks in his introduction: "The author's purpose is to describe what is being done rather than what has already been achieved, and to attempt to show where all this work is leading us."

The book contains 19 whole-page plates; the object of the inclusion of some of these is, however, obscure. It would have been better to include diagrams illustrating specific references in the text: for example on p. 47 an attempt is made to describe the Russell diagram in words—an almost impossible task without an illustration of it. In the chapter on relativity the author follows the general notion that the Michelson-Morley experiment and other attempts to detect ether-drift failed. As Dr C. V. Drysdale pointed out in a discourse before the Physical Society in 1935, this does not represent the facts.

In such a book more might have been said of the important advances made in branches of pure physics other than atomic physics, and in industrial physics; we hope that we may look forward to a further volume from the author's lucid pen covering these topics.

H. R. L.

The Science of Seeing, by MATTHEW LUCKIESH and FRANK K. MOSS. Pp. viii + 548. (London: Macmillan and Co. Ltd., 1937.) 25*s*. net.

The title of this book is the name used by the authors for a very wide field of knowledge which includes numerous topics belonging to about half-a-dozen of the more usually recognized divisions of science; namely, (1) purely physical topics, such as radiation, light sources, instruments, etc.; (2) electrical engineering, such as lighting installations and their maintenance; (3) optical, such as visual acuity, speed of vision and contrast sensitivity, to name only three of the many important topics of physiological optics; (4) pathological, such as long- and short-sightedness, inflammation of the eyes, digestive disorders, etc.; (5) physiological, such as nervous tension, eye-strain, headache, etc.; (6) psychological, such as impression, stimulation, confidence, etc. Thus defined, the science of seeing is, as the authors emphasize, more than a science of vision or a science of light utilization. In dealing with such a comprehensive subject within the limits of some 550 pages, the authors have confined the treatment to matters connected with the more recent knowledge of seeing, and have subordinated or excluded those aspects primarily developed in the relevant sciences named above. Accordingly, the discussions are largely concerned with controllable factors which can contribute to quick, certain and easy seeing, with a view to reducing the handicaps of unsatisfactory seeing conditions. This approach, which is to a large extent novel, cannot but be of great interest to all who are engaged on studies of vision, aids to seeing, or the relations of seeing to human efficiency, progress and welfare. Few, if any, investigators are better qualified to speak on this very wide and important subject than Luckiesh and Moss of the Lighting Research Laboratory of the General Electric Company at Cleveland, Ohio. They are well known both for their numerous papers and previous books on the subject, and also for several of the instruments and devices described in the present volume, such as their brightness meter, their visibility meter and Luckiesh's reflectance gauge. The text is accompanied by 84 tables of numerical data and 143 figures, all of which are well prepared and instructive, and many entirely original. The book ends with a useful bibliography of 184 books, reports and papers, and a good index (14 double-column pages); and a visibility indicator card is provided in a pocket affixed to the back cover.

W. J.

Light, Principles and Experiments, by GEORGE S. MONK. Pp. xi + 477. (New York and London: McGraw Hill, 1937.) 30*s*. net.

We learn from the preface that in the author's many years of teaching optics at the University of Chicago, he has always had to refer his advanced students to several different books for different branches of the subject, for lack of a suitable comprehensive work. The writing of this book is the outcome of that experience—an experience only too common, not only in his own country, but also in ours. Advanced students and their teachers alike will be grateful to Prof. Monk for this very useful and important addition to optical literature, which is both a text-book and a laboratory manual, as its subtitle is evidently intended to indicate. It is for students who have already worked through the equivalent of the Higher Schools or Intermediate Science syllabus of, say, London University, and are proceeding to work of pass or of honours B.Sc. standard. It is the second of the optical works of great merit and importance to come from the same press within a few weeks of one another. The first, Jenkins and White's *Fundamentals of Physical Optics*, with only 24 pages fewer than Monk's book, is devoted entirely to a restricted field, and has already been reviewed (p. 151) in this volume of our *Proceedings*.

The plan of the present work is admirable. In the first part, the text-book of 339 pages, there are (i) eight chapters (99 pages) on geometrical optics, dealing with fundamental concepts, image formation, optical systems apertures, photometry, aberrations, instruments and prisms; (ii) five chapters (150 pages) on those subjects that make up the classical physical optics, namely, the wave nature of light, velocity, interference, diffraction and polarization; (iii) three chapters (73 pages) on subjects that go to form the quantum physical optics, namely, spectra, the interaction of light and material media, and the effects of magnetic and electric fields; and (iv) a chapter (17 pages) on the eye and colour vision. A working knowledge of elementary mathematics including the differential and integral calculus is, of course, assumed, but as far as possible the author treats each topic in such a way that abstract mathematical development is subordinated to discussion of the physical principles involved. To this end, in some cases where the mathematical theory is beyond the scope of the book the results are quoted, while in other cases the derivations are given in appendices. While orthodox methods of presentation are usually adopted, there are several departures from it in novel illustrations and problems; and new advances, such as the recent progress in colorimetry, are discussed as far as the limits of the work allow. Well-chosen problems are set at the ends of chapters and the numerical answers are given at the end of the book.

The second, and much shorter, part of the book, is a laboratory manual (74 pages) consisting of precise working descriptions of twenty-three instructive experiments or groups of experiments. The book closes with a series of eight appendices to the text and to the experimental section, and six tables of useful data. The illustrations are numerous and good, and the index (17 double-column pages) is adequate.

W. J.